To the Graduate Council:

I am submitting herewith a thesis written by He, xiaoling entitled "Hybrid Electric Vehicle Simulation and Evaluation." I have examined the final copy of this thesis for form and content and recommended that it be accepted in partial fulfillment of the requirements for the degree of Master of Science, with a major in Mechanical Engineering.

Jeffery W. Hodgson, Major Professor

We have read this thesis
and recommended its acceptance

Accepted for the Council:

Associate Vice Chancellor and
Dean of The Graduate School

HYBRID ELECTRIC VEHICLE SIMULATION AND EVALUATION

A Thesis
presented for the
Master of Science
Degree
The University of Tennessee, Knoxville

Xiaoling He
August 1997

ACKNOWLEDGMENTS

There are many people to whom I am grateful for making my time at the University of Tennessee, Knoxville so rewarding. I have benefited from knowing the faculty and graduate students in the Department of Mechanical & Aerospace Engineering & Engineering Science in my study for the Master of Science Degree. I am particularly grateful to my advisor, Dr. Jeffrey W. Hodgson, for his guidance and support during the preparation of this thesis. His invaluable advice and sincere academic attitude encouraged me in the process of completing the thesis and will also inspire me in my future work.

I would like to express my appreciation to Dr. William. Hamel and Dr. Roger Parsons, who served as my committee members, for their helpful comments and suggestions on my thesis.

My gratitude also extends to Mr. Matthew Cuddy at the National Renewable Energy Laboratory for his help in understanding ADVISOR, the software which is the basis of my work.

My graduate research has been funded by the Transportation Center of the University of Tennessee, Knoxville. I deeply appreciate their generous financial support for my study and research work.

Lastly, I want to express my deep gratitude to my parents who have encouraged me and led me the way to reach this moment.

ABSTRACT

A model for the Hybrid Electric Vehicle (HEV) simulation has been developed with a specific power control strategy for an electric assist parallel configuration which is adopted by the UT-HEV NEON. A practical way of battery modeling is incorporated into this model. The model was developed on the basis of ADVISOR, which is a HEV simulation model developed at the National Renewable Energy Laboratory with different power control scheme and battery modeling. Some of the component modeling are adopted for the NEON model construction. By using the NEON model, the UT HEV NEON performance has been analyzed by parametric analysis of the vehicle components and power control parameter.

The NEON simulation model implements a power control strategy by throttle position, also it incorporates fundamental features of HEV such as regeneration and regenerative braking. The model can also simulate the vehicle operation as a pure electric vehicle or as a conventional vehicle.

The battery modeling developed yields accurate results without requiring information on the open circuit voltage (Voc) and internal resistance (R), which are generally not readily available.

It is recommended from the simulation results that the APU used for the NEON should have a reduced power capacity in order to achieve the goal of HEV operation for most of the driving condition. The limit for the APU sizing is analyzed in light of the regeneration and ESS assist capability. Besides, the current throttle used should be down sized to about 70% of its current opening for the APU power control. A higher capacity battery would be beneficial in terms of SOC sustaining and extended EV range. Transmission effect on the vehicle regeneration capability and on the vehicle acceleration is analyzed with the two transmissions which have different gear ratio and identical speed and torque map. The choice of the transmission should be made based on the overall performance requirements.

It is further recommended that vehicle tests on a dynamometer and road tests should be conducted for validation of the simulation results.

TABLE OF CONTENTS

CHAPTER	PAGE
1 INTRODUCTION	1
1 Objective	1
2 The Hybrid Electric Vehicle	2
3 HEV Configuration	4
3.1 Series configuration	4
3.2 Parallel configuration	6
4 HEV Power Control	9
5 Component Design Options of HEV	11
5.1 Energy Storage System	12
5.1.1 Battery	12
5.1.2 Flywheel	19
5.1.3 Ultracapacitors	20
5.2 Auxiliary Power Unit	21
5.2.1 Spark ignition engine	21
5.2.2 Diesel engine	21
5.2.3 Gas- turbine engine	22
5.3 Motor/Controller	22
5.4 Transmission System	24
5.5 Other Components	25
5.6 UT-HEV NEON	25
2 VEHICLE MODELING ANALYSIS	27
1 Objective of System Modeling	27
2 Theoretical Analysis	27
2.1 Road load	27
2.2 Propulsion system	29

2.3 ESS__Battery 29
2.3.1 Battery assumptions 30
2.3.2 SOC representation 31
3 Introduction to ADVISOR 32
3.1 Input & Output Module 33
3.2 Parallel Configuration Modeling 33
3.2.1 Power management 33
3.2.2 Simulation model implementation 34
3 NEON SIMULATION MODEL 47
1 Battery Modeling Discussion 47
1.1 Battery Capacity 48
1.2 SOC Algorithm 49
1.2.1 Mass recuperation model 50
1.2.2 Fractional utilization model 50
1.2.3 Other models 52
2 Practical Battery Model 53
2.1 Battery Test 53
2.2 Battery Test Conditions 53
2.3 Test Result Analysis and Model Construction 56
2.3.1 Test verification of Peukert curve 56
2.3.2 Battery V_terminal-I curve under certain SOC 57
2.4 Practical Model and ADVISOR Model Analysis 63
3 The NEON Control Strategy 70
3.1 Power Control Strategy 70
3.1.1 HEV mode power control 71
3.1.2 Conventional model power control 72
3.1.3 Regeneration 73
3.1.4 Regenerative braking 73
3.2 Power Control Module 74
3.2.1 Blockdiagram for P_req>0 76
3.2.2 Blockdiagram for P_req<=0 78
4.Other Revisions to ADVISOR 78

4 NEON SIMULATION 82
1 Introduction 82
2 Validation of the Battery Model 82
2.1 Validation Simulation Analysis 83
2.1.1 Achievable speed and range 90
2.1.2 Power output and battery parameters 90
3 NEON Simulation 91
3.1 NEON Model Parameters 91
3.2 Basic Model for Simulation 91
3.3 Parametric Analysis 93
3.3.1 Regeneration 93
3.3.2 Regenerative braking energy recovery level 99
3.3.3 Comparison for regeneration and regenerative braking effect on SOC and power control 110
3.3.4 Initial SOC value 127
3.3.5 Threshold position effect 127
3.3.6 APU power capacity analysis 134
3.3.7 Transmission effect 147
3.4 EV Range 154
3.5 Maximum Acceleration Effort 159
5 CONCLUSIONS 164
1 NEON Simulation Model Characteristics 164
2 Evaluation and Recommendations from the Simulation Results 165
2.1 APU Power Capacity 165
2.2 Regeneration and Regenerative Braking Effect 165
2.3 Throttle Position Control 165
2.4 Battery 166
2.5 Transmission 166
2.6 Maximum Acceleration 166
2.7 EV range 167
3 Future Work 167
4 Summary 167

References 168

Appendices 172

Vita 196

LIST OF TABLES

TABLE		PAGE
1.1	USABC Criteria for Electric Vehicle Battery Technology	13
1.2	Lead-acid, Nickel-cadmium, Nickel Metal Hydride Batteries	14
1.3	Nickel-Iron Battery Specification	16
1.4	ABB Sodium Sulphur Battery Specification	17
1.5	Projected Lithium Metal Sulfide Battery Characteristics	18
1.6	Expected Specific Energy and Technical Issues for EV battery	19
1.7	Comparison between Ultracapacitor and Lead-acid Batteries	21
3.1	NEON Lead-acid Battery Voc and R from Generalized Formulae	65
3.2	NEON Lead-acid Battery Voc and R from Test Formulae	65
3.3	NEON Battery Data for Simulation	67
3.4	H12N85 Battery Trendline and Generalized Formulae	69
3.5	Error Checking for Generalized and Trendline V_terminal - I Curve for H12N85 Battery	69
4.1	Transmission Comparison	119
4.2	EV Range Simulation Results	123
4.3	Maximum Acceleration Effort Simulation	128
A.1	Generalized and Test Curve Formulae in First Order and Second Order	144
A.2	First Order Formulae Error Checking for NEON Battery V_terminal - I Curve for the Given SOC	145
A.3	Second Order Formulae Error Checking for NEON Battery V_terminal - I Curve for the Given SOC	146

LIST OF FIGURES

FIGURE		PAGE
1.1	HEV Configuration	5
1.2	Parallel Configuration Variation	7
1.3	AC Motor and DC Motor Comparison	23
2.1	Input & Output of *ADVISOR*	33
2.2	PARALLEL Configuration Model of *ADVISOR*	34
2.3	Power Flow Diagram of Parallel Mode in *ADVISOR*	35
2.4	Road Load Module	35
2.5	Transmission Module	37
2.6	Power Train Configuration for APU and Motor in ADVISOR	39
2.7	Torque Coupler Module	39
2.8	Electric Power Request Blockdiagram	43
3.1	Peukert Curve from the Exide Specification	54
3.2	NEON Battery Discharge Current Pattern	55
3.3	NEON Battery Discharge Voltage Pattern	55
3.4	Peukert Curve Comparison	57
3.5	NEON Battery Ah and Wh SOC Comparison	58
3.6	NEON Battery *V_terminal* vs SOC	58
3.7	NEON Battery I vs SOC	59
3.8	V_terminal vs I under certain SOC for NEON Battery	60
3.9	Generalized Curve for NEON Battery	61
3.10	NEON ESS Battery Blockdiagram	61
3.11	Comparison of Battery R from Generalized & Tested Formulae	66
3.12	Comparison of Battery Voc from Generalized & Tested Formulae	66
3.13	*V_terminal - I* curve under SOC for H12N85 Battery	68
3.14	NEON Torque Coupler Configuration	70
3.15	Torque- Speed map of APU and MOTOR of UT-HEV NEON	71
3.16	NEON GEO 1L Engine $T_{APU\_avail}/T_{APU\_max}$ vs TP Map	75
3.17	Linearization of $T_{APU\_avail}/T_{APU\_max}$ vs TP Map for NEON Geo 1L Engine	75
3.18	Torque Coupler Module for P_req>0	77

3.19	TP & Torque block for P_req>0	77
3.20	TP_reset subsystem	79
3.21	Torque Coupler Module P_req<=0	79
3.22	Torque Coupler Module for NEON Simulation	80
3.23	Revised GUI for NEON Parallel model simulation	81
3.24	Parallel Model for UT-HEV NEON	81
4.1	Battery Model Validation Simulation in FUDS Cycle	84
4.2	Battery Model Validation Simulation in HIWAY Cycle	87
4.3	Comparison of Torque Request to APU & ESS vs APU Threshold Torque	92
4.4	Regeneration Effect with NEON Battery for FUDS Cycle	94
4.5	Regeneration Effect with NEON Battery for HIWAY Cycle	96
4.6	Regeneration Effect with H12N85 Battery for FUDS Cycle	100
4.7	Regeneration effect with H12N85 Battery for HIWAY Cycle	102
4.8	Regenerative Braking Effect with NEON Battery for FUDS Cycle	104
4.9	Regenerative Braking Effect with NEON Battery for HIWAY Cycle	107
4.10	Regenerative Braking Effect with H12N85 Battery for FUDS Cycle	111
4.11	Regenerative Braking Effect with H12N85 Battery for HIWAY Cycle	114
4.12	SOC Recovery in Different Control Schemes	117
4.13	Combination of Power and Speed Curves for NEON Battery in FUDS Cycle	119
4.14	Combination of Power and Speed Curves for NEON Battery in HIWAY Cycle	121
4.15	Combination of Power and Speed Curves for H12n85 Battery in FUDS Cycle	123
4.16	Combination of Power and Speed Curves for H12N85 Battery in HIWAY Cycle	125
4.17	SOCinit Effect Comparison for FUDS Cycle	128
4.18	SOCinit Effect Comparison for HIWAY Cycle	129
4.19	Threshold Position Effect of the Throttle for FUDS Cycle	130
4.20	Threshold Position Effect of the Throttle for HIWAY Cycle	132
4.21	Threshold Position Effect on the Torque of APU in FUDS Cycle	135
4.22	Threshold Position Effect on the Torque of APU in HIWAY Cycle	137
4.23	Comparison of Requested and Achievable Speed and Range in Conventional Mode Driving	140
4. 24	APU Power Effect on the Vehicle Performance in FUDS Cycle, with H12N85 HORIZON Battery	141
4.25	APU Power Effect on the Vehicle Performance in HIWAY Cycle, with H12N85 HORIZON Battery	143
4.26	Torque Request and Threshold Torque of APU with Different APU_trq_factors	145

4.27	APU Power Effect on the Vehicle Performance in FUDS Cycle, with NEON Battery	148
4.28	APU Power Effect on the Vehicle Performance in HIWAY Cycle, with NEON Battery	150
4.29	Transmission Comparison for FUDS Cycle	152
4.30	Transmission Comparison for HIWAY Cycle	153
4.31	EV Simulation with NEON Battery for FUDS Cycle	155
4.32	EV Simulation with NEON Battery for HIWAY Cycle	156
4.33	EV Simulation with H12N85 HORIZON Battery for FUDS Cycle	157
4.34	EV Simulation with H12N85 HORIZON Battery for HIWAY Cycle	158
4.35	Maximum Acceleration Effort Simulation in HEV Mode	160
4.36	Maximum Acceleration Effort Simulation in EV Mode	162

LIST OF SYMBOLS

accsry_kw	factor used to define the accessory power load (KW)
A_F	frontal area of the vehicle (m^2)
Ah	battery Ampere-hour capacity
A-model	ADVISOR battery model
APU	auxiliary power unit
APUbool	EV mode simulation control parameter
	1, for HEV and conventional mode
	0, for EV mode
APU_idlespd	APU idle speed (rad/s)
APU_idletrq	APU idle torque (rad/s)
APU_launch_speed	vehicle speed at which APU assist starts (rad/s)
APU_start_speed	prescribed vehicle speed for starting APU assist (rad/s)
CAP	battery capacity (Ah)
C_D	coefficient of aerodynamic drag of the vehicle
C_3	battery capacity at 3-hour discharge rate (Ah)
DOD	battery depth of discharge
E_bty	battery energy (J)
ESS	energy storage system
EV	electric vehicle
F	force applied to the vehicle (N)
F_accel	acceleration force (N)
F_aero	air drag force (N)
F_grade	climbing force due to grade (N)
F_roll	rolling resistance (N)
FUDS	Federal urban driving schedule
g	local acceleration of gravity (m/s^2)
g_1	coefficient of discharge current

gr	gear ratio
$gr_{previous}$	previous gear ratio
gr_mot_ICE	pulley ratio between APU and motor
HEV	hybrid electric vehicle
HEVbool	HEV mode flag
	HEVbool=1, HEV mode
	HEVbool=0, conventional mode
HIWAY	HIGHWAY driving schedule
i	instantaneous current of the battery, charging or discharging (Am)
I	average current of the battery, charging or discharging (Am)
I_k	current of the battery, charging or discharging (Am)
I_3	discharge current at 3-hour rate (Am)
I_{APU}	moment of inertia of APU ($kg.m^2$)
I_battery	battery current (Am)
I_charge	battery charging current (Am)
I_discharge	battery discharging current (Am)
I_mot	motor moment of inertia ($kg.m^2$)
K	Peukert constant
K_0, K_1, K_2	rolling resistance coefficients
key_on	key_on>0 HEV or conventional mode
	key_on=0 ZEV mode
m	mass of the vehicle (kg)
m_{eq}	equivalent mass of the rotating parts of the vehicle (kg)
max_I_con	maximum controller current (Am)
max_P_term	power consumption of battery under maximum controller current (KW)
max_T_mot	maximum motor torque (Nm)
max_ω_mot	maximum motor speed (rad/s)
min_V_con	minimum controller voltage for operation(V)
mot_pktrq_factor	motor peak torque factor
mot_trq_scale	motor torque-speed map scale
M	total equivalent mass of the battery electrolyte and electrodes (g)

ΔM	mass depletion in each constant power run interval of the vehicle (g)
P_accessry,P_a	accessory power consumption of APU (KW)
P_{avail}	power available from APU and motor (KW)
P_{APUa}	power output from APU (KW)
P_{ESS}	power output from ESS (KW)
P_{busr}	power request from motor to battery (KW)
P_{bty_avail}, P_{btya}	power available from battery (KW)
P_in	power input (KW)
P_inertia, P_i	inertia power consumption of APU (KW)
P-model	practical battery model (KW)
P_motor	power request to motor (KW)
P_mot_avail, P_mota	power available from motor (KW)
P_out	power output (KW)
P_req	power request to the torque coupler from transmission (KW)
P_tx	power available from transmission (KW)
P_wh_req	power demanded at the wheel (KW)
r	radius of the wheel (m)
regen	Boolean parameter to determine the condition for regeneration 1, for SOC sustaining with regeneration 0, for SOC depletion without regeneration
regen_level	parameter set for the regenerative braking recovery level control, continuous value from 0 to 1
R	internal resistance of the battery(Ω)
R_charging	internal resistance to charging(Ω)
R_discharging	internal resistance to discharging (Ω)
SOC	battery state of charge
SOChi	prescribed highest SOC level
SOC_init	initial SOC
SOClo	prescribed lowest SOC level
SOC_prev	previous SOC level
T_accessry	torque for accessory load of APU (Nm)
T_avail	torque available from torque coupler (Nm)

T_{APUa}	APU torque output with accessory & inertia load (Nm)
T_{APU_avail}	APU torque output with constraints and accessory & inertia load (Nm)
$T\_{APU\_map\_trq}$	the torque available at certain speed of APU (Nm)
T_{APU_max}	maximum APU torque at given speed (Nm)
$T\_{APU\_threshold}$	APU torque at threshold throttle position (Nm)
$T\_inertia$	inertia torque of APU (Nm)
T_mot	torque request to motor (Nm)
T_mot1	torque request to motor with consideration of motor inertia (Nm)
T_motor	motor torque output (Nm)
T_mot_max	maximum motor torque output under certain speed (Nm)
T_req	torque request to torque coupler (Nm)
T_tx	torque request to transmission from the wheel (Nm)
$T\_tx\_inertia$	transmission inertia torque (Nm)
T_wh	wheel torque available (Nm)
TP	throttle position (%)
TP_init	initial throttle position (%)
$TP\_threshold$	threshold throttle position (%)
V	velocity of the vehicle (V)
Voc	open circuit voltage of the battery (V)
$V\_term, V\_terminal$	terminal voltage of the battery (V)
α	Peukert exponent
η	efficiency of the system
η_e	battery charging efficiency
η_{mot}	efficiency of motor
η_{tx}	efficiency of transmission
ρ	density of ambient air (kg/cm^3)
ω	speed of the wheel (rad/s)
ω_{APU}	APU speed output (rad/s)
ω_max	maximum transmission speed under certain gear ratio (rad/s)
ω_min	minimum transmission speed under certain gear ratio (rad/s)
ω_mot	motor speed request (rad/s)

ω_motor	motor speed output (rad/s)
ω_req	speed request to torque coupler (rad/s)
ω_tx	speed request to the transmission (rad/s)
ω_wh	wheel speed (rad/s)
$\dot{\omega}\_mot$	rotational acceleration of the APU(rad/s^2)

CHAPTER 1

INTRODUCTION

1.Objective

The investigation of the potential of electric vehicles (EV) and hybrid electric vehicles (HEV) as viable transportation options has been of interest for many years. Concerns over atmospheric pollution, petroleum consumption and energy efficiency have promoted intensive studies in the past twenty years to determine electric and hybrid electric vehicle designs and applications which are technically and economically viable.

The evaluation of vehicle performance is of great importance to the development and technical innovation in vehicle design. It provides guidance for the vehicle design to meet the performance criteria and insight into optimization of the design.

The objective of this thesis is to demonstrate the performance characteristics of a hybrid electric vehicle through vehicle simulation. The simulation model is developed from the software ADVISOR, which was implemented by the National Renewable Energy Laboratory, to suit the configuration of the particular vehicle--- UT-HEV NEON. The vehicle performance are evaluated with respect to vehicle acceleration, range, power consumption, battery state of charge (SOC) and other characteristics under different driving conditions. The control strategy is analyzed for the construction of the vehicle power control model, and the battery modeling is emphasized for practical representation of the battery for simulation. The simulation is intended to evaluate the performance of the vehicle and could be a tool for achieving optimal design and improvement of vehicle performance.

2. The Hybrid Electric Vehicle

An electric vehicle (EV) is a vehicle driven by electricity. A hybrid electric vehicle (HEV) refers to a vehicle driven by two different energy sources for power, e.g. an internal combustion engine and an motor. EV has a relatively long history than HEV. The first EV was made in 1873 by R. Davidson of the United Kingdom, when technologies for other types of vehicle had yet to be developed. The vehicle was driven by an iron/zinc primary battery[1], and was built 10 years earlier than the first gasoline fueled vehicle, which was made by Germans Daimler and Benz in 1885. In 1860, a French man, G.Plante, invented secondary lead-acid batteries[2]. In 1881, another Frenchman, G. Trouvje, made the first EV powered by lead-acid batteries. In 1886, an electric bus was put to use in London. By the end of the 19th century, the majority of the vehicles made were EVs.

However, with the remarkable improvement in the performance of internal combustion engine vehicles, electric vehicles had almost vanished from the scene by 1930. Concerns over the performance of battery-powered EVs are vehicle range, acceleration, rechargeability and cost. An EV made by a Belgian in 1899 demonstrated a top speed of 105 km/h, In the 1960s, General Motors(GM) designed a prototype EV powered by high energy density silver/zinc batteries, with a range of 60 km to 120 km per charge. In the 1970s, Japan developed an EV that could run 520 km per charge[1]. The newly developed EV-1 by GM demonstrated high acceleration, i.e. from 0 to 60 mph within 8.5s. The range of EV-1 at normal driving condition is reported to be around 110 ~ 150 km per charging of the battery[17].

Worldwide research activities have been conducted on EVs and HEVs in the past decades. In Japan, US and Europe, government supported programs have been conducted and vehicle demonstrations have been held since 1976.

---

[1] Primary battery: A single discharge type battery. A primary battery cell contains finite quantity of the reactants participating in the reaction; once this amount is consumed (on completion of discharge), a primary battery cell can not be reused.

[2] Secondary battery: A multiple-cycle type battery cell. On completion of cell discharge, a secondary battery cell can be recharged by forcing the electric current through the cell in the reverse direction, which results in the regeneration of the initial reactants from the reaction products. Therefore, electric energy from an external source is accumulated in the form of chemical energy in the cell.

Before a commercialized vehicle could be developed, EV and HEV research declined when the oil crises of 1974 and 1979 faded. In the 1980s, however, environmental concerns revived interest in EVs. Increased vehicle usage and the associated air pollution as well as the greenhouse effect claimed increasing attention and support for the study of EVs and HEVs. In 1988, Los Angeles announced a competition to solicit the production of 10,000 EVs by 1995. In 1990, a rule was adopted by the California Air Resources Board, requiring that a growing percentage of the vehicle sold in California be Zero Emission Vehicle (ZEV), i.e. 2% for 1998, 5% for 2001 and 10% for 2003. The mandate was revised in February,1996 so that the goal is to have 10% of each auto-maker's sales in California by 2003 be ZEV. The worldwide interest in clean air has led the automobile industry to intensify their efforts on EV & HEV programs. Past years have seen great progress in the concept design and research in HEV towards commercialization around year 2000.

So far, EVs have been powered mostly by batteries, although other electric power sources and energy storage devices are under development for EVs and HEVs. These are mainly fuel cells, ultracapacitors and flywheels. Presently, they are not mature enough to power vehicles with satisfactory performance.

The development of EV and HEV are mainly hindered by the technology of the electric energy storage system (ESS). In the case of the battery, problems are associated with:

- low specific power, which means that the peak power, thus acceleration is limited
- low energy storage capacity, which means that the range is limited
- low charging and recharging efficiencies and long charging time
- life cycle
- cost

Given the current technology of batteries, HEVs overcome some of obstacles presented by EVs, and offer the potential for improving the performance of the vehicle. The HEV, which is driven by a dual power sources, has the major advantage over EV in that it would

- allow acceptable acceleration and range performance of the vehicle
- keep the fuel economy and emission level under control
- offer great potential for fuel savings due to load-leveling by electric power system
- be operated using alternative fuels, with maximum fuel efficiency
- minimize the energy loss by means of regenerative braking and reduced vehicle accessory load
- reduce the weight and size of the engine due to the reduced power capacity requirement to the engine
- use a battery pack that can be much smaller compared with EV battery packs

The current technical emphasis on HEV development lies in optimization of the energy storage system, power transmission and control, and low vehicle energy consumption including efficient energy use for accessories, low friction and aero-drag force through structural design and material improvement.

3. HEV Configuration

Hybrid electric vehicles take on two major forms, i.e. series and parallel. Different configurations exhibit different characteristics, require different design and control strategies, and may also be suitable for different applications.

3.1 Series configuration

In a typical series hybrid electric vehicle, as shown in fig.1.1, a generator, which is driven by an internal combustion engine (ICE), recharges the batteries. The three components, ICE, generator, and electric motor, are arranged in series. Series HEVs have no mechanical connections between the ICE and the wheels. Therefore, power is transferred electrically to an electric motor that drives the wheels. The main characteristics of series hybrid configuration are:

- optimal operating point

  The engine/generator can be operated at a fixed point within the engine speed/torque map for the power output, a point which can be selected for high efficiency or for low emissions.

- low efficiency

  Due to the energy conversion between the IC engine and the generator and between the generator and the motor, i.e. mechanical and electrical energy conversion and vise versa, there are inherent energy losses associated with series HEV.

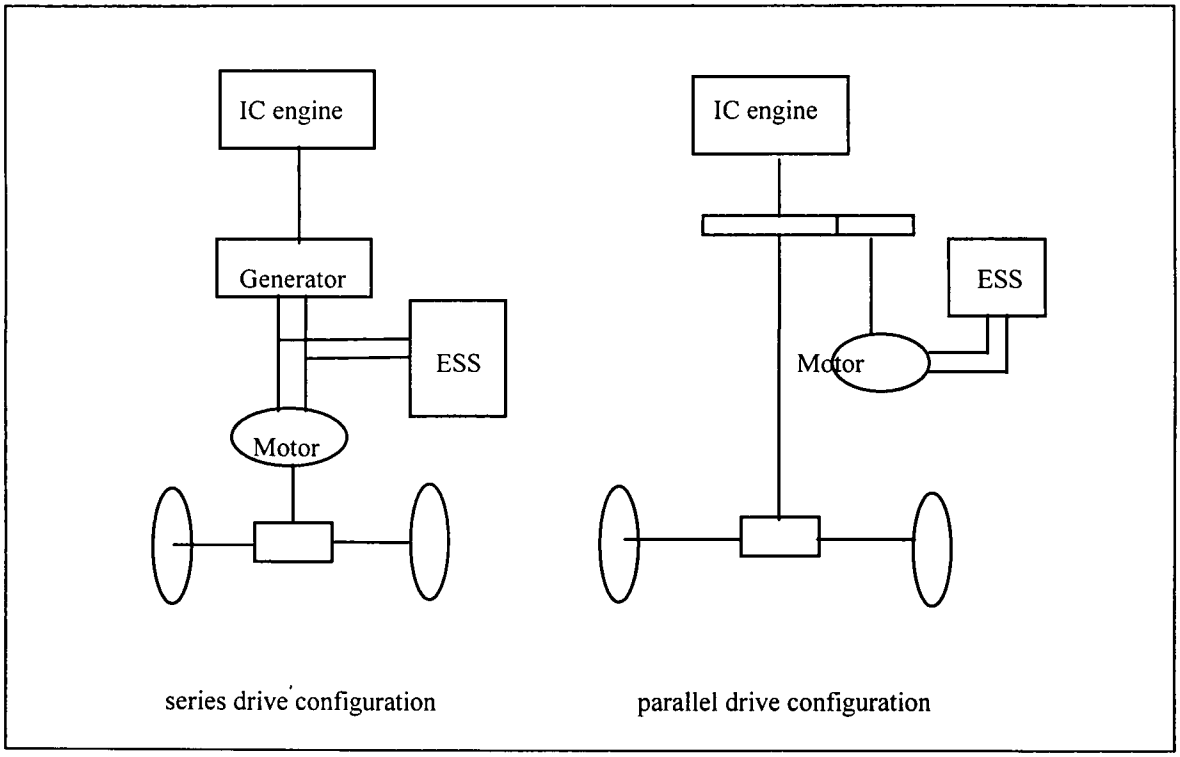


fig.1.1 HEV Configuration

- large power capacity requirement

  As the power transmission is in series, the power capacity of the motor, generator and IC engine are all the same as defined by the maximum wheel load. This restricts the vehicle from applications which demand high power capacity such as large passenger car due to the energy efficiency concern.

- reduced emissions since the engine does not have to idle and can be turned off when not needed

- varieties of options when mounting the engine and vehicle components

The characteristics of series configuration means that its feasible application could be:

- applications requiring a small IC engine and generator

  This is because that the power delivered from the IC engine would be small and the energy losses are limited.

- operation of vehicle in which the combined efficiency of the generator and the electric motor is as good as the efficiency of the conventional gear box.

  This may allow the vehicle to be applied to heavy duty vehicles while still maintaining an acceptable energy efficiency. High efficiency for a series configuration may be achieved by using a high-speed synchronous generator and a permanent magnet motor which has very high magnetic energy density[13].

3.2 Parallel configuration

In parallel hybrid drives, the IC engine and the electric motor are arranged in parallel rather than in series. In this configuration, a generator is not required if the motor can function as a generator for charging the batteries.

Parallel configurations can be designed with variations as shown in fig.1.2. Fig.1.2A is a two shaft configuration in which the driving torque is a combination of the torques from the electric motor and the

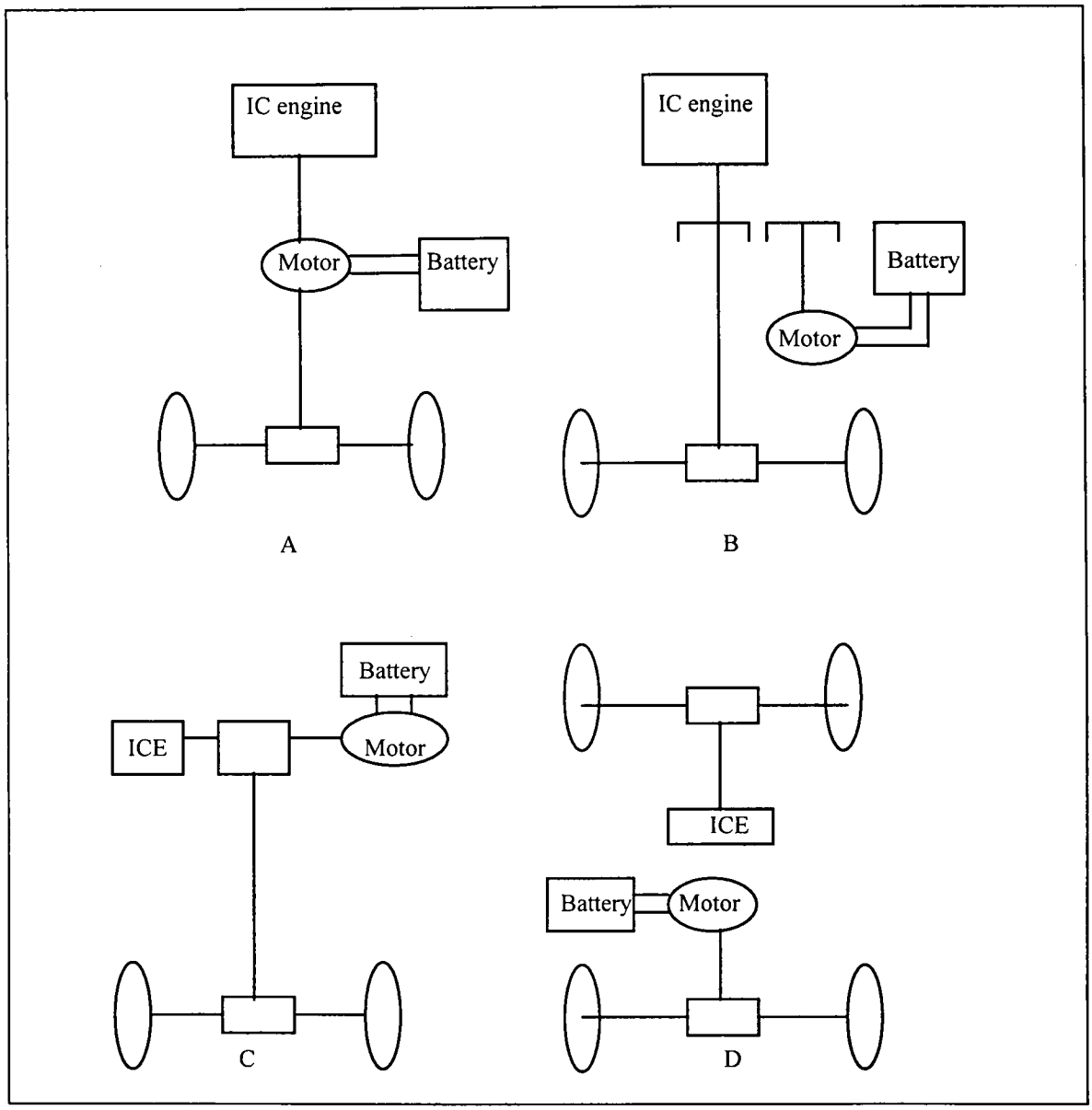


fig.1.2 Parallel Configuration Variation

IC engine. Fig.1.2B is a one shaft design in which torques from both driving units are also combined. The distribution of torque between these two units can be determined by the control strategy in the design stage for the application requirements.

In fig.1.2C, power is generated by combining the two speeds from ESS and IC engine in a differential gear box which is positioned in between the two units. In this case a fixed torque from the two units is generated although speed between the two can be regulated to some extent. The equal torque demand also assumes the limited operating range of the motor and IC engine in terms of their speed and torque distribution because the significant difference between the torque-speed maps of the two units. This is not a desirable feature for traction demanding high torque at low rotation speeds of the motor. The configuration in fig.1.2D is another pattern of parallel drive system although there is no mechanical connection between the driving shafts of the two driving units. Both IC engine and motor are used for driving the wheels, though each assumes different responsibilities. The power for traction is contributed by the two.

The parallel configuration offers several advantages over the series configuration:

- Reduced power capacity requirements

  Since the power required to drive the vehicle is provided by the electric motor and the APU simultaneously, thus it could be divided by designing the IC engine and electric motor to deliver half of the maximum power required each, which means that in the parallel configuration the nominal capacity of these components would be one-half that of the series design.

- increased efficiency, no power losses due to conversion

  Since the power from the APU is utilized directly by the drivetrain through the direct connection between the power unit and the wheels, there is no losses in energy conversion. Also, the elimination of generator helps to reduce the cost and weight of the system.

- flexible power distribution between power sources

By incorporating an appropriate control strategy, the power distribution between the two power sources can be commanded in a way that leads to the overall best performance of the system.

It can be seen that the design of an HEV is more flexible and difficult to implement when compared with conventional vehicles due to the characteristics of the energy storage system and complexity of the control system.

4. HEV Power Control

The proper control strategy is crucial to the overall performance of the vehicle. The characteristics of the components of the vehicle also determines what performance could be achieved. Component design, vehicle configuration and control strategy are interdependent on each other.

The objective of the control strategy is to

- maximize the fuel efficiency
- minimize emissions
- minimize propulsion system cost to keep overall vehicle cost competitive
- maintain the vehicle performance acceptable in terms of acceleration, range, handling, noise etc.

As far as power control of the HEV is concerned, HEV propulsion systems can be classified into different categories based on the roles and the contributions of the APU and the ESS. In parallel modes, the major function of APU and ESS may switch between the primary power source and the auxiliary power source.

The major form of the control strategy for HEVs include:

- *Electric-assist parallel:*

  The electric-assist parallel uses the APU as the primary propulsion component which is mechanically connected to the wheels. The electric motor and batteries provide auxiliary power to increase the total power output. This allows the use of a small APU operated at some optimal region to reduce emissions

by avoiding running the engine at full-throttle position. The electric motor and batteries can be selected with relative small energy and power capacity. They are also available for energy recovering through regenerative braking, which boosts the efficiency in urban driving.

- *APU-assist parallel:*

  The APU-assist parallel uses the electric motor and batteries for the primary propulsion while the APU is turned on only for high speeds, hill climbing, or hard accelerations. The advantage of this control strategy is that most of the energy used is electric energy which would tend to reduce the overall emissions and the amount of fuel used. It also allows the engine's electric starter to be eliminated because the APU is turned on when the vehicle is running. The emission levels, however, may be compromised by the fact that the engine is turned on at the moment of high power demand, so the engine is running rich and gives off more emissions. To reverse this side effect, an electrically heated catalyst can be incorporated to reduce the start-up emissions.

- *Thermostat-series:*

  The thermostat series uses electric energy for operation with the APU providing additional energy for range extending. The batteries' state of charge (SOC) are fluctuating between the high and low set points with the APU and the generator being used to charge the batteries when the SOC drops. The advantage of this series design is that it allows the APU to be operated at a fixed point with optimal emission control and efficiency, which prevents APU from experiencing transient loads. Emissions can be further reduced by adding an electrically heated catalyst to reduce cold-start emissions.

- *Load-level series:*

  The load-level series configuration is designed to match the average power requirement of the vehicle with the power that is produced from APU. The power peaks are provided by batteries, while during the low power periods, the batteries are recharged such that the state of charge of batteries can be maintained around the mid SOC. The advantage is that the battery pack can be made relatively small

with high power capacity, which allows the vehicle weight to be reduced. The APU is operated over a wider range as demanded by power requirements.

As can be seen from the above, there is a wide spectrum control strategies under each configuration option, though the component design dictates to some extent what control strategy should be used.

5. Component Design Options of HEV

An HEV is composed of conventional vehicle components and electric vehicle components. The HEV propulsion system and control strategy determine, to large extent, the design selection of the components. Given the configuration of the propulsion system, different control strategies can result in different vehicle performance.

Major HEV components can be classified as engine related or electric power related.

Electric vehicle components

- electric motor/controller
- electric energy storage system
- system controller
- generator

Engine related components

- power unit
- system controller
- fuel system for power unit

5.1 Energy Storage System (ESS)

Among all the components of the drive system, the ESS in an HEV is a major area of concentration for achieving the desirable performance of the vehicle. Currently three major forms of ESS are under investigation for EV & HEV applications: batteries, ultracapacitors, and flywheels. The different forms of ESS have different characteristics, performance and economies. The development of high-performance, safe and reliable ESS are vital to the commercialization of EVs and HEVs. Requirements for the ESS include energy storage capacity in term of specific energy (Wh/kg), specific power (W/kg), cycle life and cost. The energy storage capacity of ESS limits the range of the vehicle, and power output defines the maximum acceleration achievable and the hill climbing capability. Cycle life, cycle efficiency and cost are important for the battery being considered for application. Currently, EVs & HEVs are mainly limited by the ESS technology, which renders the vehicle not commercially competitive.

5.1.1 Battery

Batteries store and deliver electric energy chemically by initiating and reversing chemical reactions. Batteries are a relatively matured technology compared with high speed flywheels and ultracapacitors. Major secondary battery technologies for near-term and mid-term applications are lead-acid battery, nickel-cadmium battery and nickel metal hydride batteries. For the long term plan, lithium-polymer and lithium-ion are promising technologies.

Some other concerns over battery usage, other than the problems of power and energy capacity, charging efficiency, cost and life cycle, are concerns over gassing and self-discharge. Gassing is a phenomena that occurs when over-charged batteries release hydrogen and oxygen gases as water is decomposed. For a battery to be maintenance free, it is necessary to retard gas liberation. Otherwise, the electrolyte would be depleted prematurely and catastrophic failure would result. Battery self-discharge means that the electrical energy will be discharged over time although there is no external load. This must be controlled within certain range for batteries used for EV.

The major technical specifications for batteries to be used for HEVs established by United States Advanced Battery Consortium (USABC) are listed in Table 1.1[20].

The characteristics required of EV batteries, other than those to ESS in general, are

- safety
- recycleability
- simple maintenance
- rechargeability, and
- no risk to environment

The technical features and the current development of some major battery technologies are briefly introduced below.

Table 1.1 USABC Criteria for Electric Vehicle Battery Technology

	Mid term criteria	*Commercialization criteria*	*Long term creteria*
Price	< $150/kWh	< $150/kWh ($ 75 desired)	*< $ 100 kWh*
Cycle life	600 @ 80% DOD	1,000 @ 80% DOD	*1,000 @ 80% DOD*
		1,600 @ 50% DOD	
		2,670 @ 30% DOD	
Range @ Life (Urban Miles)	100,000	100,000	100,000
Calender Life	5 years	10 years	10 years
Power Density	250 W/L	460 W/L	600 W/L
Energy Density	135 Wh/L	230 Wh/L	300 Wh/L
Specific Power	150~200 W/kg	300 W/kg	400 W/kg
Specific Energy	80~100 Wh/kg	150 Wh/kg	200 Wh/kg
Regenerative Specific Power	75 W/kg	150 W/kg	200 W/kg
End of Life (EOL)	20 % of the norminal	20 % of the norminal	20 % of the norminal
Operating Performance	-30 to +65 0C	-30 to +65 0C	-30 to +65 0C
Normal Charge	6 hrs, 20~100% SOC	6 hrs, 20~100% SOC	3~6 hrs, 20~100% SOC
High Rate Charge	<15 min, 40~80% SOC	<30 min @ 150 W/kg, 20~70% SOC	<15 min, 40~80% SOC
Efficiency at EOL	75%	80%	75%
Off tether Pack Energy Loss	Thermal loss<3.2 W/kWh	3 days: < 10% with no performance loss	Thermal loss<3.2 W/kWh
	(<15% in 48 hrs)	12 days: < cumulative loss < 25% with some	(<15% in 48 hrs)
	Self discharge <15%/48 hrs	performance loss @ extreme temprature limits	Self discharge <15%/month

Source:[20]

5.1.1.1 Lead-acid battery

The lead-acid battery is the most economical battery available. The conventional lead-acid battery is characterized by its limited energy storage capacity and power output. Lead-acid batteries can be made maintenance free. Several new lead-acid battery technologies are being studied, or have been applied to HEVs with increased performance. Table 1.2 gives the specifications for advanced lead-acid battery and other batteries[18][19].

5.1.1.2 Nickel-cadmium battery

The nickel-cadmium battery provide 30 % more specific energy and twice or three times of range than lead-acid batteries. It offers improvements in peak power, range and life. Some problems are that the battery must be fully charged or discharged at regular interval since shallow discharge may degrade the capacity due to the memory effect. Also, deep discharging at low temperatures gives the worst capacity. It is suitable for high temperature operation since the discharge reaction within the battery is an exothermic reaction, which makes the battery temperature exceed the temperature of normal conditions for battery application. The battery must be cooled to 30 ~50 °C before charging, since the charging efficiency is low at high temperature. Therefore certain consideration should be given to the insulation of the battery once it is applied to the vehicle. Nickel-cadmium batteries are not maintenance free as they require a system for regular watering and removal of the hydrogen gas generated during recharging[4].

Table 1.2 Lead-acid, Nickel-cadmium, Nickel Metal Hydride Batteries

	Lead acid	*Nickle Cadium*	*Nickle Metal Hydride*
Energy (Wh/kg)	35(55)	50(60)	70(120)
Power (W/kg)	200(450)	175(200)	150(220)
Life(cycles)	450(2000)	1250(1650)	1500(2200)
Cost ($/kwh)	125(75)	600(110)	540(115)

Note: The above information is derived from following conditions:

1. Wh/kg is measured at C_3 rate. W/kg is for 30 s at 80% depth of discharge;
2. cycles to 80% depth of discharge.

Other disadvantages are that cadmium is a highly toxic material, and the costs of nickel and cadmium are high. Also, nickel (unlike Iron) can not be recycled to be used as battery material[1].

5.1.1.3 Nickel metal hydride battery

Another alkaline battery is the nickel-hydrogen battery. Two types of hydrogen storage can be used: a high-pressure vessel and hydrogen alloy storage. The nickel/metal-hydride (Ni/MH) provides a substitute for cylindrical Ni/Cd cells for general consumers. The Ni/MH battery has a specific energy of 1.5~2 times or that of the lead-acid battery, and the specific power and life cycle are better than that of the conventional lead-acid battery. Ni/MH batteries are also safe to use in light of environmental concerns and they are maintenance free.

The major concern over the application of this battery is the control of the temperature rise when recharging and discharging, the rise in hydrogen pressure accompanying this temperature rise and detecting when the battery is fully charged. Another problem is the degradation of the metal hydride at high temperatures. Methods have been found that over-charging and gassing can be determined by the combination of temperature and aging parameter of the battery. Optimal charging pattern have been derived from tests[2].

Included in Table 1.2 are some specifications for nickel-cadmium and nickel metal hydride batteries. The values indicated in the brackets represents the potential for long term development.

5.1.1.4 Nickel-iron battery

The nickel-iron battery was developed by EPI of the US and Japan. The specifications available are listed in Table 1.3. The battery, like the nickel-cadmium battery, has problems in cost and recycling. It can not be made into a sealed battery because water must be added each time it is charged due to the fact that the water in the electrolyte undergoes electrolysis.

Table 1.3 Nickel-Iron Battery Specification

	EPI Battery	*JAPAN Battery*
Energy (Wh/kg)	56	54
Energy (Wh/L)	136	100
Power (W/kg)	94	
Norminal capacity(Ah)	231	165
Operating voltage (V)	6	1.23

derived from source [1]

5.1.1.5 Nickel-zinc battery

The nickel-zinc battery has a specific energy expected to be 1.5~2 times that of the lead-acid battery. However, the demonstrated service life is only 400 cycles. This is because zinc oxide, a discharge product at the anode, is soluble in the electrolyte. While zinc withstands repeated dissipation and precipitation with discharging and recharging, the shape change and the inactivation of the electrode reduce capacity and battery life. The cost of the battery is about twice that of the pb-acid battery, therefore its cycle life needs to be 1,000 for it to be commercially viable.

5.1.1.6 Sodium-sulfur battery

The NaS battery offers an energy capacity 3 times that of the lead-acid battery. The power output is only moderate, about 1.3 of the lead acid battery's specific power. It also has a long projected life and low projected volume production cost.

The main problem associated with the sodium-sulfur battery is that it requires a high operating temperature, (650~700°F). Heat must be supplied when it is not in use to maintain the battery in a molten state within the encapsulated insulation[4]. This is because if the battery is accidentally cooled, it takes several hours to recover its operating temperature. The battery developed by Asea Brown Boveri (ABB) is listed in Table 1.4.

Problems to be addressed include the durability of the battery under the normal operating temperature heat cycle, reduction of recharging time, proven reliability in mass production, and cost reduction.

Table 1.4 ABB Sodium Sulfur Battery Specification

Model	B120K		
Energy (Wh/kg)	93		
Energy (Wh/L)	134		
Heat loss (W)	70		
Norminal voltage (V)	60	48	24
Min. discharge voltage (V)	56.1	44.9	22.4
Internal resistance (Ohme)	60	38	9.6
Max. discharge current (Am)	250	300	600
Continous discharge current (Am)	160	200	400
Continuous charge current (Am)	80	100	200
Capacity (Ah)	160	200	400

derived from source [1]

5.1.1.7 Lithium battery

Lithium batteries use lithium or its alloy for the anode and use either a polymer, liquid or solid state electrolyte. The cathode of the battery may be MnO_2, carbon, or some other material. Lithium is a very electrochemically active metal, which yields much high electric ion interaction capacity for high discharging and charging currents. This may significantly improve the battery energy and power capacity. The lithium polymer battery is the long term development goal. Some features are briefly described below.

1) Lithium-metal sulfide battery

A lithium-metal sulfide battery of the same weight and volume of a lead-acid battery would double the range and acceleration of the vehicle. The operating temperature is 450°C, which requires the addition of a thermally insulated container to keep the battery hot without external heating source. It is safe for operating and maintenance free with no need for watering, ventilation or gas pumping. Some of the projected characteristics of lithium-metal sulfide battery under development by EPRI are cited in Table 1.5[6].

2) Lithium disulfide battery & lithium polymer battery

Lithium-disulfide batteries use iron sulfide as the cathode instead of sulfur as in the Lithium metal sulfide battery. The disulfide battery promise a specific energy of 3~5 times that of the lead acid battery, and a peak

Table 1.5 Projected Lithium Metal Sulfide Battery Characteristics

Voltage (162 cells, average discharge)	216 V
Energy output (under SAE driving cycle J227a/D)	36 kWh
Power at 80% depth of discharge (30s)	45 kw
Specific energy	72 Wh/kg
Specific Power	89 W/kg
Power/energy ratio	1.24
Cycle life (at 100% DOD/ at 80% DOD	500/1200
Charging/discharging rate	1 hour
Cost	~ lead-acid battery cost

power of 5~7 times that of the lead-acid battery. For the lithium-disulfide battery, problems presented are its life cycle and calendar lifetime[5].

Lithium-polymer batteries have the potential of 3~5 times the specific energy and 3~4 times the specific power of conventional lead-acid batteries. Research show that the lithium polymer battery with optimal graphite yields 320~360 mAh/g capacity. It also has a stable charge/discharge cycling feature, and can easily be manufactured with a variety of polymer material combinations.

Lithium batteries are a far-term battery for EVs and promises an EV range of more than 300 miles in a single charge. One problem with this battery is that the operating temperature of the battery is well above room temperature, therefore thermal management of the battery must be supplied.

5.1.1.8 Other batteries

There are a number of viable, rechargeable batteries being considered for EV usage, such as sodium-nickel chloride and zinc-bromine. Up to now, neither of them are matured enough to satisfy the need for EV applications. Expected improvement of the battery specific energy and problems to be solved for different batteries are summarized in Table 1.6.

Table 1.6 Expected Specific Energy and Technical Issues for EV battery

	Specific Energy	*Specific Power*	*Life*	*Safety*	*Cost*	*Scale up*
Sealed Pb-Acid	45		*			
Ni/Cd	60				**	
Ni/Fe	60				**	
Ni/MH	80		*	*	**	*
Ni/Zn	80		**		**	
Na/S	130				*	
Na/NiCi	120		*		**	
Zn/Br	80	*	*	*	*	
LiAl/FeS	120		*	*	**	*
Lithium	180	*	*	**	**	**
Metal/Air	250	**	**		*	*

Note: Asterisks indicate the increasing difficulty in achieving the goal. Source[1]

5.1.2 Flywheels

Flywheels store energy mechanically in the form of kinetic energy. The flywheel take an electric input to accelerate the rotor up to speed by using the built-in motor, and return the electrical energy by using this same motor as a generator. The kinetic energy stored in flywheels is $T = \frac{1}{2} I \omega^2$, where I is the mass moment of inertia of the wheel and ω is the speed of the wheel. To increase the energy storage, it is necessary to increase the speed, consequently the centrifugal force will increase as a function of M and ω, $F = M*\omega^2*r$, where M is the mass of the flywheel and r is the radius of the flywheel. Since the tensile stress resulting from centrifugal force F must be off-set by the tensile stress in the material, the ideal material for constructing the flywheel rim is one having a high tensile strength and lower density, such as fiberglass/epoxy or kevlar/epoxy, with a much higher tensile strength to density ratio which is about 7 times of that of the normal steel.

Flywheels have great potential for high energy storage and high efficiency for energy recovery. They can have high specific power compared to batteries, 300~6,000 W/kg have been achieved, while their specific energy is very low, with only 7 Wh/kg. Flywheels also have a long life and little degradation with time. For applications in HEVs, safety and containment are major issues to be resolved.

5.1.3 Ultracapacitors

An electric double layer capacitor is an extremely large capacity condenser, which is commonly referred to as an "ultracapacitor". Ultracapacitors store electric energy by accumulating and separating unlike-charges physically, as opposed to batteries which store energy chemically in reversible chemical reactions. Power densities of 2,000 to 4,000 W/kg have been demonstrated [PNGV Program,1994]. They also have relatively high charging/discharging efficiencies, typically over 80%.

Material under study for ultracapacitors include carbon-metal fiber, foamed (aerogel) carbon, carbon particulate with binder, doped conducting polymer films on carbon cloth and mixed metal oxide coatings on metal foil. Research has also been undertaken for electro-chemical capacitors which exhibit even better characteristics over ultracapacitors. Comparisons between lead-acid battery and ultracapacitor parameters are listed in Table 1.7.

Ultracapacitors are ideal for HEVs as load-leveling devices because they have:

- high specific power for acceleration
- high power acceptance during regenerative braking
- excellent cycle life, insensitive to deep and quick discharging
- high cycle efficiency compared with batteries
- easy measurement of state of charge from voltage

These characteristics made ultracapacitors well-suited to load-level a battery or fuel cell. The shortcoming of the ultracapacitor is its relative low energy density--typically 5~10 Wh/kg. Weight and bulk limitations restrict the device to have no more than a few hundred Watt-hours of energy, which is enough to sustain peak-power output for only a few seconds.

Table 1.7 Comparison between Ultracapacitor and Lead-acid Batteries

	Battery	*Ultracapacitor*
Charge time	1~5 hours	0.3 ~ 30 s
Discharge time	0.3 ~ 3 hours	0.3 ~ 30 s
Energy (Wh/kg)	10 ~ 100	1 ~10
Power (W/kg)	<1000	<7,000
Cycle life	1,000	>500,000
Charge/Discharge efficiency	0.7 ~ 0.85	0.85 ~ 0.95

Source [11]

Another obstacle for ultracapacitor application is that the terminal voltage varies significantly with the state of charge of the ultracapacitors.

5.2 Auxiliary Power Unit of HEV

The power unit of a typical HEV includes the electric motor and the auxiliary power unit (APU) which is powered by fuel. APUs for HEVs generally include spark ignition engines, Diesel engines and gas turbine engines. Their characteristics are briefly explained below.

5.2.1 Spark-ignition engine

The spark ignition engine is the most widely used engine for automobiles. It has the most matured technology, also the cost is low. For HEVs, the weaknesses are:

- the emissions and fuel economy are not satisfactory for future standards
- throttling losses, and friction losses lower the efficiency
- limited compression ratio lowers the efficiency

5.2.2 Diesel engine

Diesel engines have been used for heavy-duty applications for many years. They feature

- high efficiency due to no throttling and high compression ratio

- high torque at low speed for heavy duty purpose machine
- heavy No_x emission due to lean operation, and high particulate emissions at high loads due to incomplete combustion

In addition, they are usually heavy and noisy.

5.2.3 Gas-turbine engine

A turbine engine's advantages are:

- it can run on a variety of fuels
- the combustion is complete and clean which results in low emissions
- it is light and simple for design

The disadvantages are

- high cost
- slow response to speed change
- low thermal efficiency at partial load

The selection of the APU would depends on the characteristics of the engine, specific configuration of the vehicle, the power requirement for recharging the ESS, and for the specific driving condition requirements. The APU of a HEV should be compact, efficient, and clean.

5.3 Motor/Controller

The motor and controller are cornerstones of the HEV that allow the vehicle to be propelled by electric energy. In an electric propulsion system, the controller regulates the amount of current and voltage that the electric motor receives through the signal from the accelerator pedal in the vehicle, and controls the electric

energy provided to the motor. The energy recaptured during regenerative braking is also directed through the motor controller into the ESS when the motor functions as a generator.

Electric motors for HEVs can be divided into two major types: AC or DC. The AC category can be further divided into AC induction and AC synchronous (or brushless DC).

DC motors were commonly used for variable speed control in the past, and the controller is simple to implement. AC motors and controllers usually have a higher range of operating efficiency than DC motors, but the controller is more expensive. A typical efficiency map of DC and AC motors is shown in fig.1.3[18]. A comparison shows that:

- AC motors have higher efficiency over a broader range than DC motors. This is more distinct in the low speed and low torque range. This means that for highway cruising with a low torque demand, the AC motor is more efficient.
- The AC motor has a high efficiency than the DC motor at low torque. The DC motor has its highest efficiency at high speed and high torque, a desirable feature for energy recapture through regenerative braking.

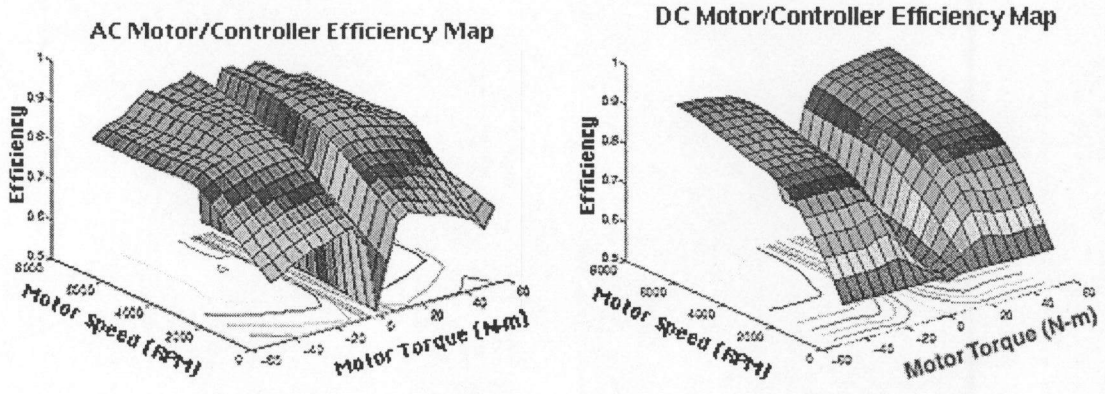


fig.1.3 AC Motor and DC Motor Comparison[18]

For HEV applications, the motor/controller should feature the following:

- high efficiency power control over a wide range of torque and speed
- reduced sizing & weight, low moment of inertia and low cost
- adjustment by acceleration, deceleration and regenerative braking
- high reliability

Problems to be addressed for HEV motor/controllers are:

- finding a solution to motor heating due to regenerative braking
- ensuring the rechargability of the ESS during regenerative braking.

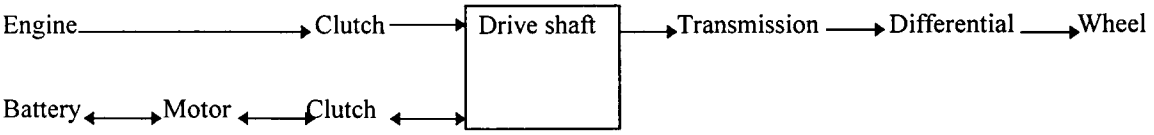
5.4 Transmission system

The transmission design options are essentially the same as that of the conventional vehicle, although the power transmission path is different as shown below. The specific design should be determined in conjunction with the vehicle configuration choice. The major consideration about the choice of transmission is that the gear ratio of the transmission should ensure that the APU and the motor would be operated in a range. Transmission efficiency is also an important factor to be considered.

For series HEV, the configuration would be

Engine ⟶ Generator ⟶ Battery ⟶ Motor ⟶ Transmission ⟶ Differential ⟶ Wheel

For parallel UT HEV NEON, it is:



5.5 Other Components

Other components of concern are body, chassis and accessories. The body style of an HEV may not be significantly different from the conventional vehicle. However, for efficient energy use, the vehicle should be built for reduced aerodynamic drag force, and low friction from the tire, also vehicle weight should be considerably reduced. This means that a light vehicle with less frontal area and low aero-drag coefficient, or the product C_dA, is an optimal design.

The chassis of the vehicle has a major effect on the mass of the vehicle. New materials structural designs are required to reduce the vehicle weight.

5.6 UT-HEV NEON

The University of Tennessee's HEV NEON (UT-HEV NEON) to be analyzed in this thesis is a parallel HEV using ESS-assist power control. This is different from the parallel model established by ADVISOR. The assist strategy of the NEON is based on the throttle position. ESS assist comes when the APU torque has reached the threshold determined by the throttle position. The assist increases as the throttle position is further pressed down. Regeneration for sustaining the battery SOC and regenerative braking for the recovery of the vehicle energy are incorporated in the power control strategy. To simulate the performance of UT-HEV NEON, a particular power control module had to be developed.

The major components of the vehicle are as described below. Specific analysis about the UT-HEV NEON will be made in the later chapters regarding the control strategy, simulation model development and simulation programming file construction.

- Vehicle curb mass — 1360 kg
- Power Control — Parallel, battery assist
- APU — 1.0 L 4-stroke, 3-cylinder Suzuki/Geo engine, modified running on compressed natural gas(CNG). The power rating is 50HP.

- Fuel — CNG
- Motor — Unique Mobility SR180P Brushless DC Permanent Magnet Synchronous Motor, with 32kW at 3,000 RPM as the rated power for continuous operation and 46 kW for intermittent operation. The detailed technical specifications from the manufacturer is as per Appendix 1.
- Motor/controller — CR20-300A Brushless DC Motor Controller
- Battery pack — 16 12 V EXIDE U1-DC9 lead-acid batteries. The terminal voltage for each cell is 12.6 V. The nominal battery terminal voltage is16*12.6=201.6 V. The capacity is 17.3 Ah. The battery capacity specification supplied by the manufacturer is in Appendix 2.
- Transmission — Chrysler A-578, with 5-speed forward and 1 reverse. The transmission gear ratios: gr_1=3.54, gr_2=2.13, gr_3=1.36, gr_4=1.03 and gr_5=0.72.
- Tire — Michelin low rolling resistance tire, with friction coefficient of the rolling resistance f=0.007 and the tire pressure 50psia.
- DC/DC Converter — For charging 12 V system controller battery from main battery pack.

CHAPTER 2

VEHICLE MODELING ANALYSIS

1. Objective of System Modeling

Modeling is an important tool for evaluating vehicle performance. HEVs are different from the conventional vehicles in that they incorporates electric energy storage system for propulsion and results in additional complexity to the analysis and design.

Apart from the concern over the modeling of conventional vehicle components and their interactions, such as road vehicle interaction and engine, motor, transmission interactions, specific concerns for HEV modeling lie in the modeling of the electrical propulsion system and power distribution between the two power sources.

In this chapter, an analysis on vehicle power transmission and battery modeling will be made. The simulation software ADVISOR for HEV analysis running under MATLAB/SIMULINK toolbox will be introduced. Specific concern and conditions for construction of the simulation model in ADVISOR will be analyzed.

2.Theoretical Analysis

2.1 Road load

The power requirements of a vehicle generally include the power for acceleration, hill climbing, and the power to overcome aerodynamic drag force and rolling resistance. It can be calculated as:

driving force:

$$F = F\_aero + F\_roll + F\_accel + F\_grade \quad (2\text{-}1)$$

where

air drag force $$F\_aero = \frac{1}{2}\rho C_D A_F V^2 \quad (2\text{-}1.1)$$

rolling resistance $$F\_roll = mg\cos\theta\,(K_0 + K_1 V + K_2 V^2) \quad (2\text{-}1.2)$$

acceleration force $$F\_accel = (m + m_{eq})a \quad (2\text{-}1.3)$$

force due to grade $$F\_grade = mg\sin\theta \quad (2\text{-}1.4)$$

therefore, the power demand at the wheel would be

$$P\_wh\_req = F\omega r \quad (2\text{-}2)$$

where

ρ density of air

C_D coefficient of aerodynamic drag of the vehicle

A_F frontal area of the vehicle

V velocity of the vehicle

m mass of the vehicle

m_{eq} equivalent mass of the rotating parts

g acceleration of gravity

K_0, K_1, K_2 rolling resistance coefficient

r radius of the wheel

ω speed of the wheel

2.2. Propulsion System

Power is delivered to the wheel through the transmission from the ESS & motor/controller, and/or from the APU. There are power losses in the drivetrain. Therefore, the power output from each component can be associated with the power input to the component by:

$$P\_out = P\_in * \eta \tag{2-3}$$

In the case of a pure EV, power from the ESS is converted from electric power to mechanical power through the transmission and motor. When other energy losses are neglected, the power output from the ESS is

$$P\_ESS = P\_wh\_req / (\eta\_mot * \eta\_tx) \tag{2-4}$$

where

η_mot and η_tx are the efficiencies of the motor and the transmission respectively.

In the case of conventional vehicles, when the power comes from an APU only, and the APU is directly connected to the transmission,

$$P\_APU = P\_wh\_req / \eta\_tx \tag{2-5}$$

For an HEV propelled by power from both the APU and the ESS, the total power is a sum of P_ESS and P_APU. The power distribution is determined by the control strategy adopted for the vehicle. It should be analyzed in light of the control strategies and specific conditions under which the vehicle is driven.

2.3 ESS __Battery

Different modeling approaches are required for modeling different forms of ESS. The UT-HEV NEON uses batteries as the ESS.

2.3.1 Battery Assumption

A general approach is to model the battery as a perfect voltage source with internal resistance. The terminal voltage and current are related by the internal resistance of the battery :

$$V\_terminal = Voc - I*R \quad (2\text{-}6)$$

where $V\_terminal$ terminal voltage (volt)

V_{oc} open circuit voltage of the battery (no load voltage)

R internal resistance of the battery, which can be further represented as R_charging and R_discharging

I current of the battery

The battery open circuit voltage and internal resistance are affected by the electrolyte concentration, degree of discharge of the cell, temperature and other factors. In addition, changes occur due to battery aging, battery cycle pattern (deep or shallow discharging), and chemical reactions taking place inside the battery. The resistance of the battery to charging and discharging is also affected by the polarization effects of the electrode and the electrolyte in the process of the chemical reaction. As a result, the battery terminal voltage would be affected by above factors and the charging and discharging current.

One of the key parameters for representing the battery is to state the battery capacity in term of Ampere-Hour (Ah). It is common practice to state the battery capacity available at a particular discharge rate and battery temperature when the battery is discharged to a particular end-point voltage. For example, the 3-hour rate capacity represents the capacity available when the battery delivers a current that discharges it after 3 hours at 20°C and is normally denoted as C_3. The capacity depends on the current at which it is discharged. The higher the current being taken from the battery, the lower the available battery capacity. The loss in available capacity at higher discharge rates is due to the inability of the cell reaction to keep pace with the demand for current, principally caused by the inability of fresh electrolyte from the bulk of the

cell to quickly replace the depleted electrolyte at the surface of and within the plates. The heat evolution during rapid discharging also causes the losses of capacity. The Ah capacity can be associated with the discharge current in the formula given below:

$$CAP=KI^{\alpha} \tag{2-7}$$

where CAP Ah capacity under current I

I average discharging current

α Peukert exponent

K Peukert constant

This formulation was derived by Peukert in 1897 for lead acid batteries[12]. It provides a good fit to various experimental data. The value of α is between -0.2~-0.7. When α=0, it represents an ideal cell with the capacity not affected by the current. This formula assumes average current for calculation.

2.3.2 SOC representation

The battery state of charge (SOC), and battery depth of discharge (DOD) are parameters used to represent the battery capacity available. One expression for representing the battery depth of discharge[8] is

$$DOD = \frac{\int_0^T I[1+g1(\frac{I}{I3}-1)]dt}{C3} \tag{2-8}$$

where I average discharge current

I_3 discharge current at 3-hour rate

C_3 battery capacity at 3-hour discharge

g_1 coefficient of discharge current

In the case of a battery for which the capacity is not affected by the discharge current, (g_I=0), the above calculation can be simplified as

$$DOD = \frac{\int_0^T Idt}{C3} \tag{2-9}$$

Following the above definition, the battery state of charge (SOC) is defined as

$$SOC = 1 - DOD \tag{2-10}$$

This formulation is based on the 3-hour rate as the standard reference for battery capacity, and is valid under the assumption that the Voc and R are functions of SOC only.

Another way of representing the battery is to use the Peukert theory, in which capacity changes can be reflected through the average current output or input. Therefore, the Peukert capacity is used as the total capacity reserved in battery, and the DOD is calculated as:

$$DOD = \frac{\int_0^T Idt}{KI^{\alpha}} \tag{2-11}$$

Equation (2-11) is the formula used by ADVISOR for the battery simulation.

3. Introduction to ***ADVISOR***

ADVISOR is a simulation model developed at the National Renewable Energy Laboratory (NREL) for HEV simulation. The software is developed under MATLAB and SIMULINK. The Graphical User Interface is implemented for interactive data input and output. Simulation results are plotted and data files for plotting are generated. ADVISOR can simulate the performance of conventional, APU-assist parallel, and series HEV vehicles. The parallel model of ADVISOR is the focus for the following analysis since the component modeling for transmission, motor/controller and the road load effect would be adopted for developing the UT-HEV NEON model.

3.1 Input & Output Modules

The input and output module are illustrated in fig.2.1. Input parameters are determined from the vehicle component information or chosen for the specific vehicle simulation.

3.2 Parallel Configuration Modeling

The parallel configuration is simulated based on the block diagram as shown in fig.2.2. This block is used for the powertrain modeling of the vehicle.

3.2.1 Power management

The modeling of the HEV system is based on the theoretical analysis of power transmission. The parallel mode in ADVISOR is an APU-assist parallel configuration. The power demanded by the road load comes first from the ESS, battery. The APU power assist is started under the condition that the vehicle speed for

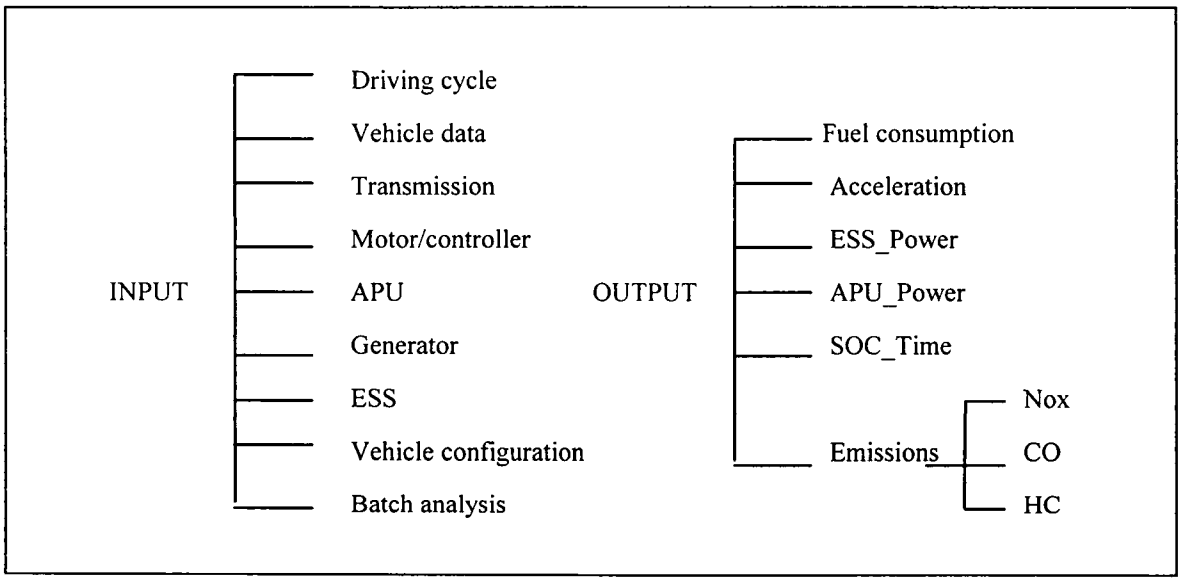


fig.2.1 Input & Output of *ADVISOR*

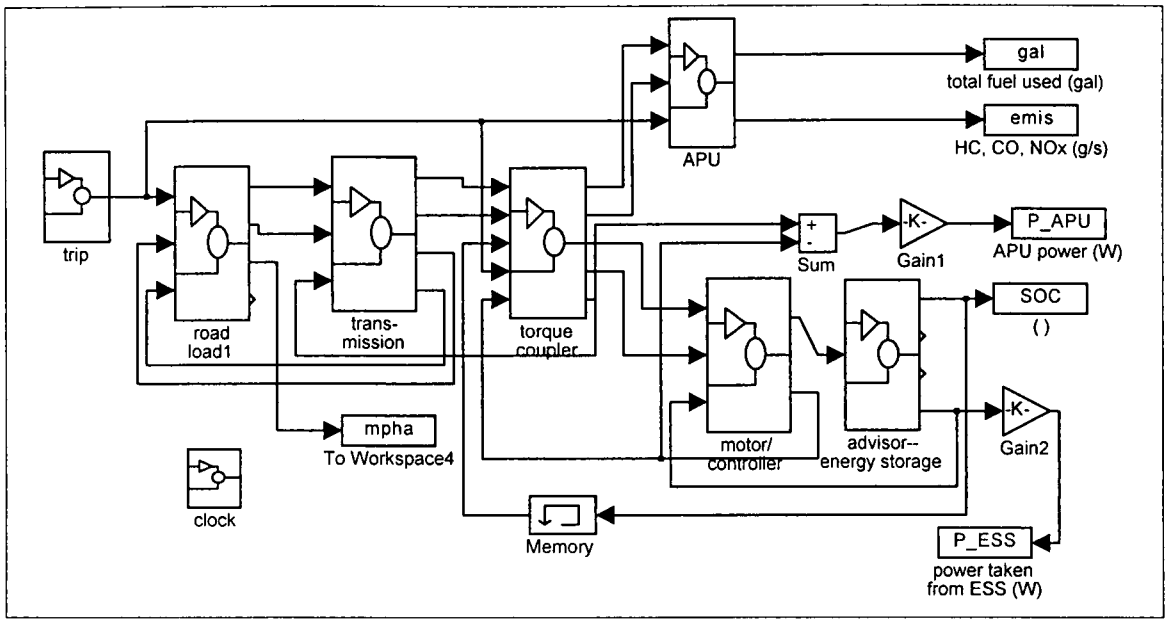


fig 2.2 PARALLEL Configuration Model of *ADVISOR*

starting the APU assist has reached. The APU launching speed is a variable depending on the SOC level and the prescribed vehicle speed for the APU to start. At this speed and above, the APU either provides power or idles, depending on the power demand and the power contribution from the ESS. The power transmission for this parallel configuration is briefly illustrated in fig.2.3.

3.2.2 Simulation model implementation

The block diagrams of the major subsystems are explained below. Input parameters of these models are as per the modeling requirements under MATLAB/SIMULINK.

3.2.2.1 Road load module

The power requirements of the road load as determined by the commanded speed, or driving cycle, are computed as analyzed in section 2.1. The road load module is shown in fig.2.4. The achievable speed and acceleration of the vehicle are calculated as a result of power available from transmission to the wheel.

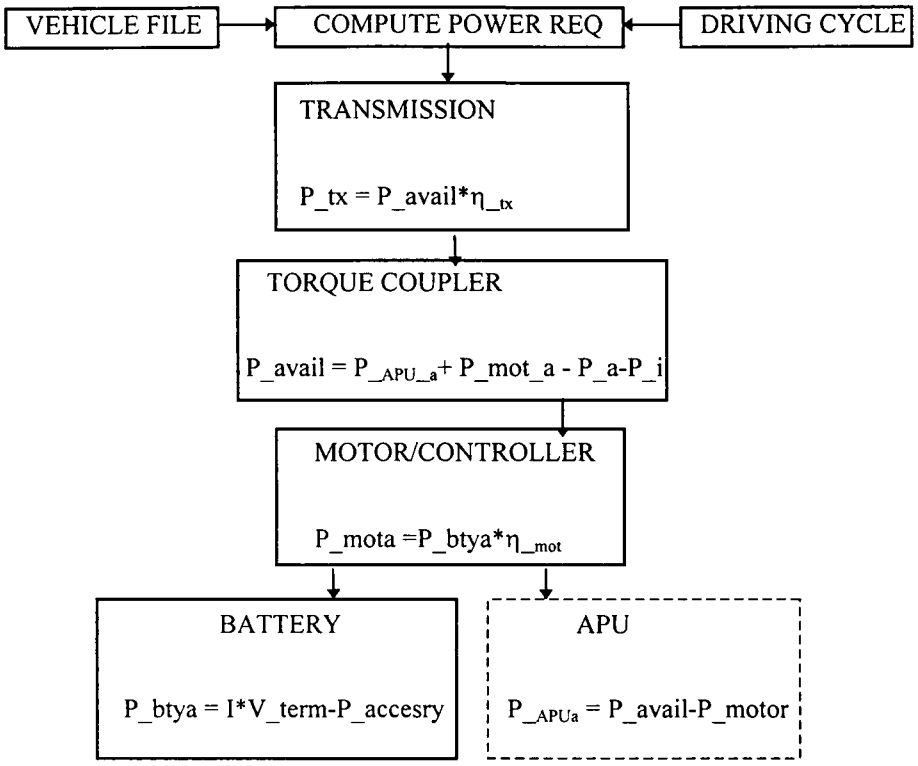


fig. 2.3 Power Flow Diagram of Parallel Mode in *ADVISOR*

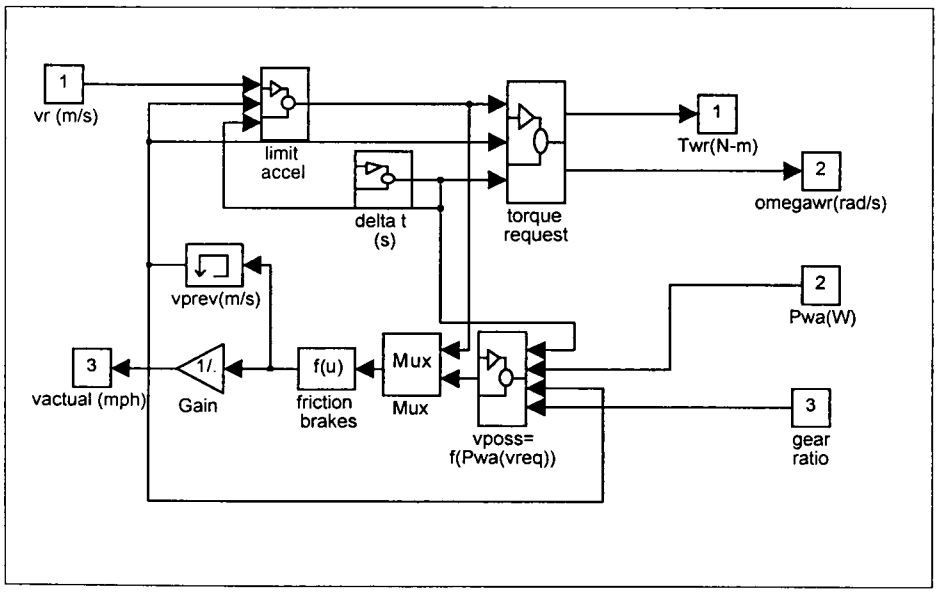


fig.2.4 Road Load Module

In constructing this block, the power analysis is made with following conditions:

- the speed calculation assumes no tire slip, which means that the maximum friction is considered
- the maximum acceleration value is prescribed as g/2, to meet the limit requirement of the SIMULINK module, where $g=9.81 m/s^2$.
- the wheel speed limit is set as 1E20 km/s for simulation purpose, which means that there is no upper practical limit for the speed.

The outputs are requested wheel torque T_wh, wheel speed ω_wh and the actual vehicle speed $V_{\_actual}$.

3.2.2.2 Transmission module

As shown in fig. 2.5, the function of the transmission block is to:

- check the gear ratio, gr, to see if the speed range of the current gear ratio fits the requested speed, so that the proper shift would be made. The shift logic is:

  gr = [ω_tx>ω_max]+{[ω_tx<ω_min]}*(-1)+gr_previous

  therefore

  gr = gr_previous; when ω_min<ω_tx<ω_max

  gr = gr_previous +1; when ω_tx>ω_max

  gr = gr_previous -1; when ω_tx<ω_min

  Here gr is the current gear ratio, and gr_previous is the previous gear ratio. ω_min and ω_max are the minimum and maximum transmission speeds corresponding to the current gear ratio. ω_tx is the requested speed to the transmission. The simulation

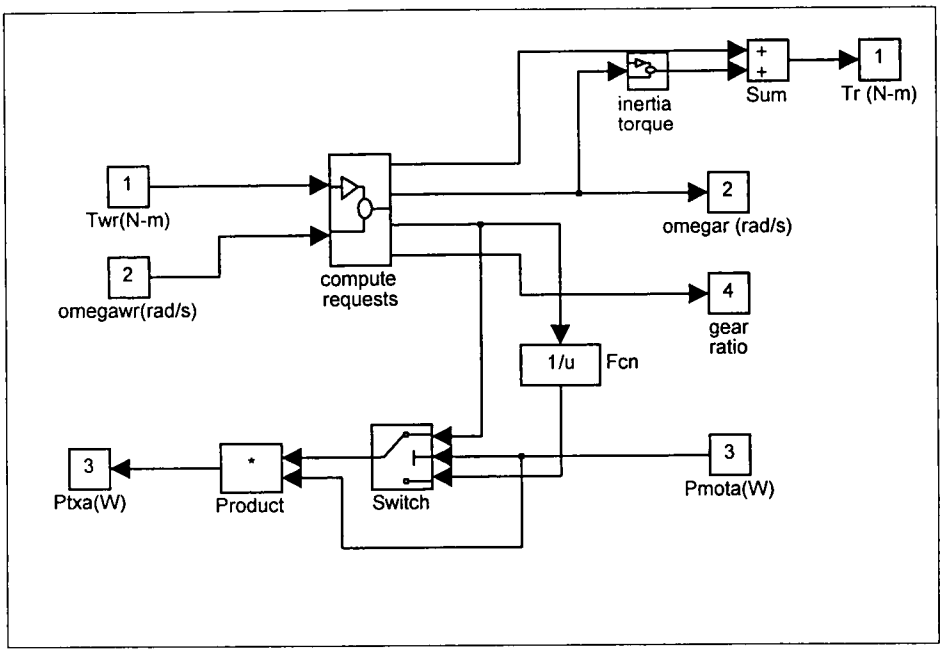


fig.2.5 Transmission Module

- checks the maximum and minimum speed of transmission based on gear ratio
- checks the shift lag to determine the transient torque output during the gear shift

  The shift lag is checked in each prescribed interval during the simulation and the transmission shift delay constant is set at a fixed value in the input information. The torque output is determined as:

- T_tx=T_wh/gr after the shift or before the shift;

  T_tx=0 during the shift

- the gear ratio is used for the torque and speed calculation as per

  T_tx=T_wh/gr ω_tx=ω_wh*gr

- the speed and torque are constrained within the operating range of the transmission through the saturation box, which is the block of SIMULINK for restricting the maximum and minimum values of the parameter concerned.

- the power request is modified to include the inertia torque, by

$$T\_req = T\_tx/\eta\_tx + T\_tx\_inertia \qquad T\_tx>0$$

$$T\_req = T\_tx*\eta\_tx + T\_tx\_inertia \qquad T\_tx<0$$

$$\omega\_req = \omega\_wh*gr$$

$$P\_req = T\_req * \omega\_req$$

P_req is the requested power for achieving the commanded speed. It is used as input to the Torque Coupler module for further power computation.

- the power output is computed by a look-up table which gives the transmission efficiency as a function of transmission speed and torque.

$$P\_tx = P\_avail*\eta\_tx \qquad P\_mot\_avail>0$$

$$P\_tx = P\_avail/\eta\_tx \qquad P\_mot\_avail<0$$

Therefore, the total power demand for achieving the speed is determined. This power comes from both the APU and the ESS as commanded by the torque coupler module, which distributes the power request in accordance with the power control strategy.

3.2.2.3 Torque coupler module

The torque coupler is a computational block for the coupling of power from both the APU and the ESS. It represents the physical transmission of the torques and speeds between the APU and the motor. Its function is to distribute power between the two taking into account the vehicle speed, SOC of ESS, speeds and torques available from the APU and the motor.

In ADVISOR, the physical interpretation for the computation of motor and APU power output is as shown in fig.2.6. The model constructed in ADVISOR for the Torque Coupler is shown in fig.2.7.

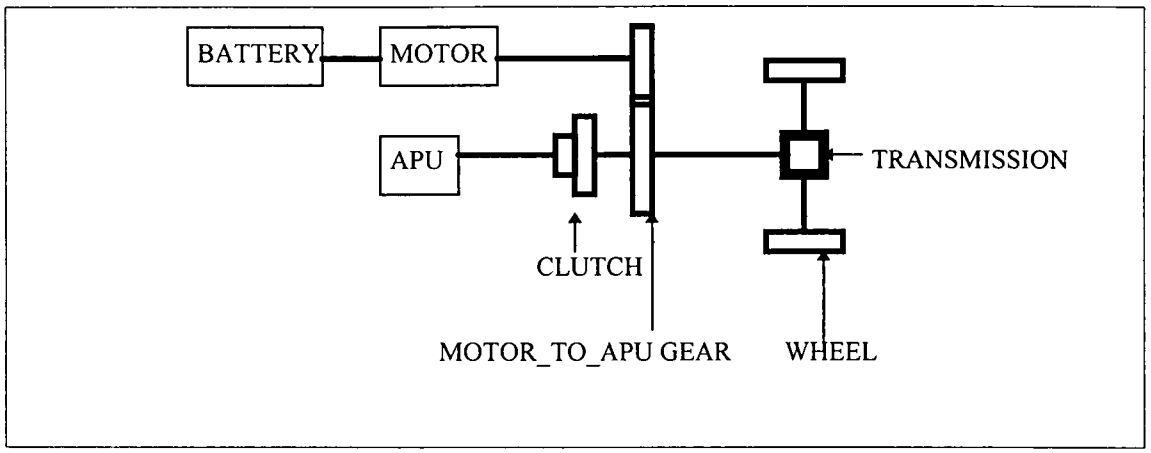


fig. 2.6 Power Train Configuration for APU and Motor in ADVISOR

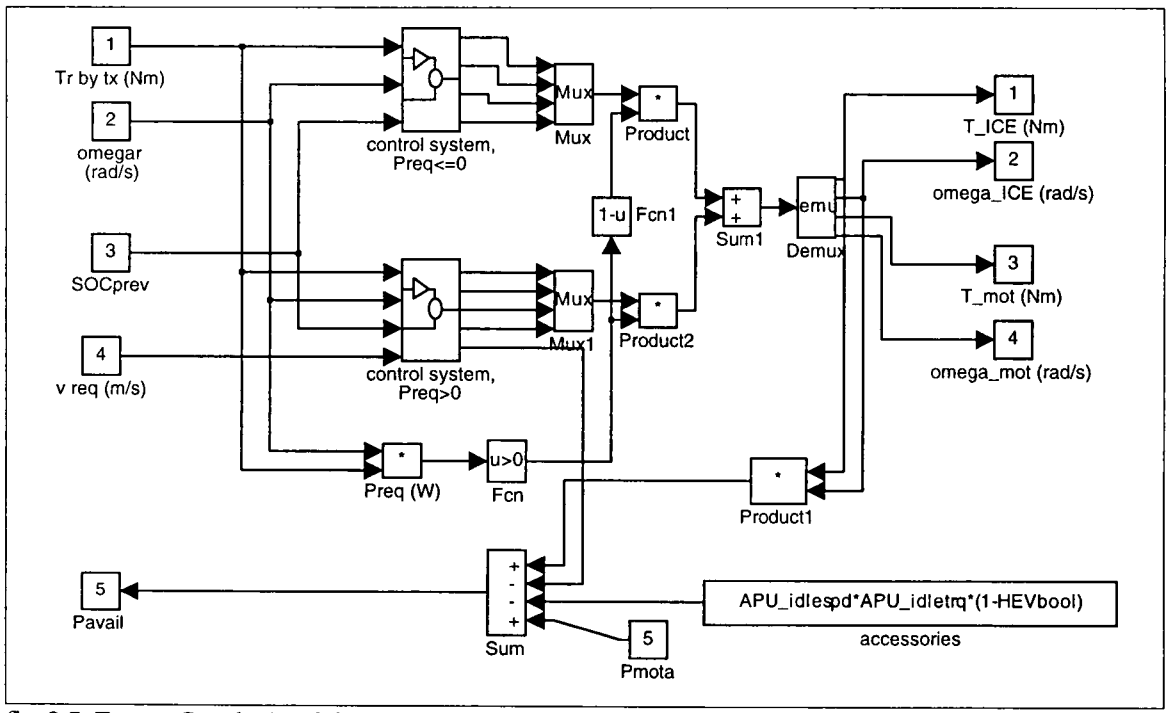


fig. 2.7 Torque Coupler Module

The torque and speed of APU is associated with the torque and speed of the motor by the gear between the APU and the motor.

The torque coupler identifies two conditions of power request from transmission module to determine the output of the APU and the motor, i.e.

- P_req>0 , represents conditions under which the drive wheels requires power;
- P_req<0, represents conditions under which regenerative braking can be invoked.

Case 1: P_req<0

In this case, the APU is either idling with idle torque and idle speed, or the APU is off with zero speed and torque.

The electric motor outputs are determined by:

T_mot=T_req / gr_mot_ICE, ω_mot=ω_req * gr_mot_ICE.

Here gr_mot_ICE is the gear ratio between motor to APU as shown in fig.2.6, it is not the gear ratio of transmission.

Case 2: P_req>0

When the power request is P>0, the torque coupler distributes power between the APU and the motor with certain constraints. These constraints include:

- The APU power is determined first by checking if the prescribed condition has reached for APU-assist, which is determined by SOC level and the prescribed APU launching speed as defined by the following:

$$APU\_launch\_speed = APU\_start\_speed \frac{SOC\_prev - SOC\_lo}{SOC\_hi - SOC\_low} \quad (2\text{-}12)$$

where APU_start_speed is the speed prescribed as an input data for simulation. SOC_hi and SOC_lo are also the prescribed limit of SOC level to prevent battery from over charging and over discharging. APU come for assist when the actual vehicle speed is greater than the APU_launch _speed and the SOC is greater than SOC_lo.

- Achievable APU speed and torque

  The APU speed, $\omega_{\_APU}$, is determined from the requested speed with constraint of the operating speed range of the APU. The APU may be idling. The torque output from the APU, $T_{\_APU}$, is determined in accordance with the requested torque and the available torque under the given APU speed. The APU inertia and accessory load are taken into account in the computation of the APU torque output.

- The motor power output

  The motor speed and torque request is determined by

  $T\_mot=(T_{\_APU}-T_{\_APU\_avail})/gr\_mot\_ICE \qquad \omega\_mot=\omega_{\_APU} * gr\_mot\_ICE$

  Note that $T_{\_APU}$ is the total requested torque with consideration of engine accessories when in the conventional mode. $T_{\_APU\_avail}$ is the torque contributed by APU. Therefore, the rest of the torque required is provided by the motor.

  The total power available from the torque coupler, which means from both the APU and the motor, is the power available from the ESS and the power available from the APU reduced by the APU inertia and accessory power consumption in the conventional mode.

  $P\_avail=T_{\_APU\_avail} * \omega_{\_APU} + P\_mot\_avail - P\_inertia - P\_accessry$

Note that the power distribution strategy used by the ADVISOR is completely different from the one of the UT HEV NEON in that

- the UT-HEV NEON is a ESS assist parallel, which is different from the APU assist parallel of THE ADVISOR model;
- the power distribution of the NEON is determined by the throttle position, not simply by the gear ratio between the APU and the motor;
- Regeneration is not included in the ADVISOR model, but is an important feature of NEON in power control;

Therefore, the Torque Coupler model needs to be developed independently for the NEON simulation. This will be analyzed in Chapter 4.

3.2.2.4 Motor/controller module

In this module, the input parameters, motor torque and motor speed are used for calculation of power output from ESS. Consideration is given to the power consumption by motor inertia and other constraints for the simulation purpose. The power request to the motor is converted into an electric power request. Calculations are as described below.

- The torque and speed requests to the motor/controller are converted into ESS power output with consideration of motor inertia torque requirement,

  $T\_mot1=T\_mot+I\_mot*\dot{\omega}\_mot$

- The electric power request is computed with the constraints of the maximum and minimum motor map torque and speed defined by the specific motor type as well as motor efficiency. The block diagram is shown in fig. 2.8.
- The motor speed is constrained within the maximum motor speed range as

  $\omega\_motor=\omega\_mot$ when $\omega\_mot<max\_\omega\_mot$

  $\omega\_motor=max\_\omega\_mot$ when $\omega\_mot>max\_\omega\_mot$

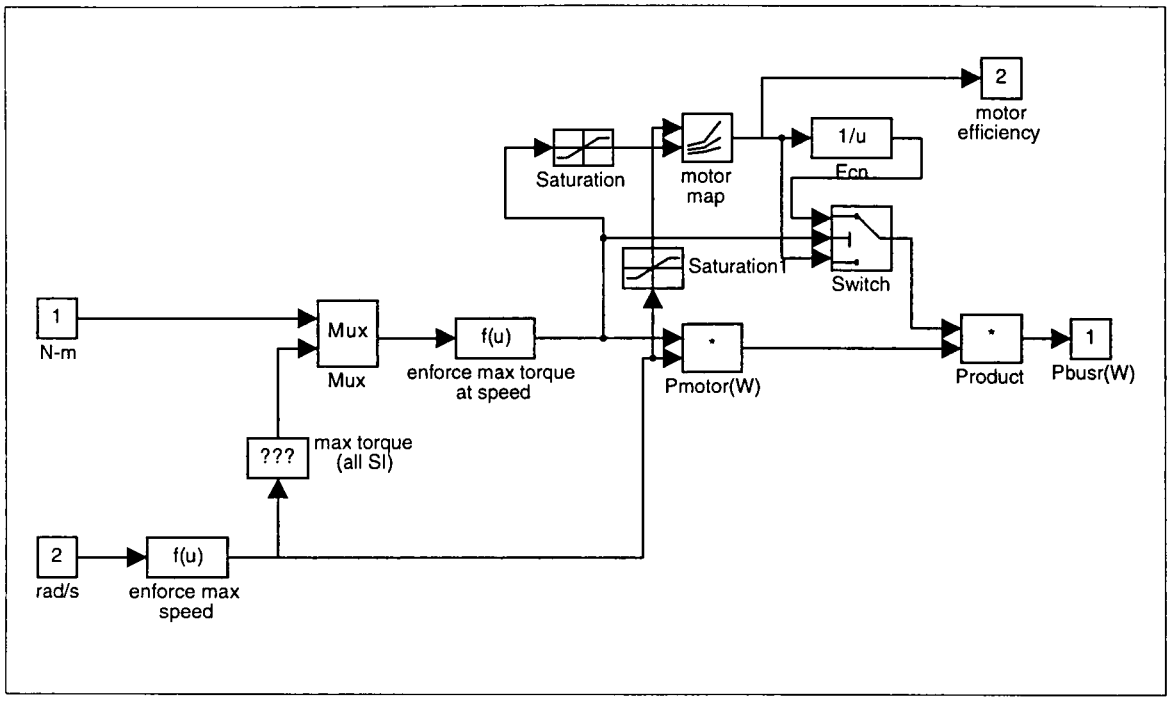


fig. 2.8 Electric Power Request Blockdiagram

- The maximum motor torque allowed under the specified speed is defined by

  T_mot_max=max_T_mot*mot_pktrq_factor*mot_trqscale*HEVbool

  where max_T_mot is the maximum map torque of the motor, mot_pktrq_factor is the motor peak torque factor as defined in the input motor map, and the mot_trqscale is the map scale factor used for the motor speed torque map.

- The torque within the maximum range is confined by

  T_motor= T_mot1+[T_mot_max-T_mot1] *[T_mot1>T_mot_max]

  + [-T_mot_max-T_mot1]*[T_mot1<-T_mot_max]

  therefore:

  T_motor=T_mot_maxwhen T_mot1>T_mot_max

T_motor= -T_mot_max when T_mot1< -T_mot_max

T_motor=T_mot when -T_mot_max < T_mot < T_mot_max

- The maximum power request from motor is computed by

  P_motor=T_motor*ω_motor

- T_motor is saturated by motor torque map's minimum and maximum torque range
- Saturate ω_motor by motor torque map's minimum and maximum speed range
- Find the efficiency in accordance with above speed and torque by a look-up table
- The electric power request is obtained as

  P_busr=P_motor*η_mot when T_motor>0

  P_busr=P_motor/η_mot when T_motor<0

The output of this block, P_busr, is the power request to the battery as a result of the wheel load. This parameter serves as input to the battery model to determine the power available from the battery.

3.2.2.5 Battery modeling

In ADVISOR ESS modeling, the battery output current and terminal voltage are obtained based on the data available on the Voc and R as a function of the SOC. For the purpose of the NEON simulation model construction, this model is reconstructed based on the generalized formula for V_terminal as a function of SOC and I as analyzed in the next chapter. Therefore, a detailed analysis of ADVISOR is not made here.

Some common features of the two battery models would be the calculation of Ah capacity and SOC based on the theory as analyzed before in this chapter, i.e.

$$SOC = SOC\_init - \frac{\int_0^t idt}{KI^{\alpha}} \qquad (2\text{-}13)$$

where I is average current to time t, and i is the instantaneous battery current *I_charge* or *I_discharge*. Therefore:

$$I = \frac{\int_0^t idt}{t} \qquad (2\text{-}14)$$

- the current I is limited to be within max_I=10E30, min_I=101E-5;
- The Ah is checked to be within the range of maximum Ah capacity of the battery, an input data determined from battery specification.
- The battery charging efficiency is considered, which leads to

  I_discharge=I; I>0

  I_charge= $I*\eta_e$; I<0

  where η_e is the battery charging efficiency.

So far, we have analyzed the blockdiagrams contained in ADVISOR parallel model. This parallel model can not be applied to the simulation of UT-HEV NEON. This is because the power control strategy of NEON is ESS assist rather than the APU assist of the ADVISOR model. Besides, the battery model for the NEON lead acid battery can not be established due to the fact that no information was available for the Voc and R. Therefore, the power control and battery modeling specific for the NEON must be developed to replace the corresponding models in the ADVISOR parallel model. Battery model should be constructed in a way in which there is no need for obtaining the Voc and R for determining the battery terminal output. A practical way of battery modeling will be developed from the test conducted on the battery. Also power control model will be developed from the test conducted on the APU for determining the power output

characteristics of the APU, also for determining the optimal power control strategy based on the throttle position. The analysis and model construction will be made in Chapter 3.

CHAPTER 3

NEON SIMULATION MODEL

In applying ADVISOR to simulate the performance of the University of Tennessee's hybrid electric vehicle NEON (UT-HEV NEON), there are several concerns regarding the specific model construction for the simulation of NEON. Among these, battery modeling and power control strategy are the major issues. In this chapter, battery modeling will be discussed and a practical model developed. The power control strategy will also be analyzed and a compatible model will be constructed. In addition, the parallel model is further expanded for simulation analysis.

1. Battery Modeling Discussion

Battery modeling in ADVISOR assumes that the open circuit voltage, *Voc*, and the internal resistance, *R*, are functions of the state of charge, SOC, only, which means that at a certain SOC of the battery, *Voc* and *R* are uniquely defined. In ADVISOR, both *Voc* and *R_discharge* & *R_charge* are assumed to be known parameters for simulation. It also assumes that the battery cell is a resistant source only, thus

$$V\_terminal = Voc - I*R \tag{3-1}$$

Apart from concerns over the assumptions made in ADVISOR, data on *Voc* and *R* as functions of SOC are difficult to obtain in practice. The reason is that *Voc* is defined in electrochemistry as the difference between potentials of the electrodes with no current flowing in the external circuit. The measurement of *Voc* requires that polarization-inducing currents be suppressed in the circuit for obtaining zero-current potentials between electrodes. This is achieved by employing instruments with high impedance for very low current consumption. The measurements should be made when the battery reaches its equilibrium state, which takes about 24 hours.

Without information on the *Voc* and the *R* as functions of the SOC in discrete or continuous form, the power output can not be determined as constructed in the ADVISOR battery model. In theory, the power output from the battery should be uniquely defined given the input power request, SOC and other conditions. To avoid the difficulties in obtaining the *Voc* and *R* for given SOC, it would be better to have *V_terminal* and *I* directly established as functions of the power request and the SOC.

1.1 Battery Capacity

Battery capacity is a parameter which is affected by many factors. Among these are:

- discharge rate
- heat evolution
- temperature
- aging
- discharging and charging pattern

Battery capacity can be defined by the time integration of the battery current (Ah) or the time integration of the battery power (Wh). The Ah capacity is less important than the Wh capacity from power considerations. Practically, it is easier to monitor current than power to determine the expected discharge duration from the discharge Ah capacity rather than the Wh capacity.

The battery capacity is sometimes higher if the discharge is intermittent than if it were continuous. From the capacity standpoint, an intermittent discharge is equivalent to a continuous discharge at a lowered current drain. This effect is caused by the "recovery" of cell electrodes during breaks in the intermittent discharge mode. However, it may happen that the discharge capacity is reduced when the discharge duration is prolonged (by smaller I_d or longer breaks). This is a result of self-discharge --- a complex of chemical processes on one or both electrodes of a cell which consume the reactants but generate no electric current. The self-discharge is measured by determining the absolute or relative loss of the electrode or cell

capacity resulting from the chemical processes or over a specified length of time. Self discharge is more significant for long duration discharge modes and increases with the cycling of the battery.

In Ah capacity calculations, the end-point voltage is normally chosen as the point when the terminal voltage drops rapidly. The Ah capacity is then obtained from the time elapsed and the average current draw during the test. However, in HEV and EV applications, the battery pack must provide a voltage above the minimum operating voltage requirement of the motor/controller, which may not be close to the battery end-point voltage as defined above. If the minimum operating voltage is higher than the end-point of the battery, then the available capacity should be determined by the minimum operating voltage, rather than by the end-point voltage. In this sense, we can say that the battery capacity, and thus the SOC, are arbitrarily defined to suit the specific purpose.

1.2 SOC Algorithm

The SOC is a parameter used to estimate the capacity of the battery. One of the biggest challenges in the development of advanced battery modeling is to determine and control the SOC of the battery pack while the HEV is in operation. Dynamic monitoring of the battery SOC is vital to the control and operation of the vehicle. The SOC is difficult to determine due to the complicated chemical reactions inside the battery. Also differences between the capacities of individual battery cells cause difficulties in representing the SOC. Complicated monitoring and control systems should be implemented for overall monitoring of the battery capacity, but concerns over the difference between battery cell capacity is beyond the scope of this study.

It would be desirable to have an algorithm which can be applied to different modes of battery operation to obtain a realistic representation of the SOC. The representation of the SOC should take into consideration the major factors which affect the capacity of the battery while still being practical. Some theoretical studies on SOC representation have been made in the past. Major algorithms developed include:

1.2.1 Mass recuperation model

In the JPL/Purdue model[15], recovery of the battery capacity from intermittent discharges is considered in the SOC determination by a "mass recuperation" concept. "Mass recuperation" reflects the fact that the capacity changes due to intermittent discharges and varies with the discharge rate. This model assumes that local reductions in electrolyte concentration limit the capacity at high discharge rates. It further assumes that there is an optimal capacity and that some of this capacity is recuperated during periods of little or no activity. This model accounts for capacity changes during intermittent discharging, but neglects self-discharge (which counter balance the capacity recovery). The SOC, under this algorithm, is determined with reference to the 5-hour discharge rate capacity, C_5, as

$$SOC(t+\delta t)=1-\frac{USEDCAP(t+\delta t)}{CAP(t+\delta t)} \tag{3-2}$$

where $USEDCAP = \int_0^t I dt$ and $CAP(t+\delta t)$ satisfy:

$$C_p + \tau \frac{dC_p}{dt} = \frac{K}{I_5^{N-1}} \tag{3-3}$$

The right hand side of the equation is the modified Peukert capacity at the C_5 discharge rate as established by Martin[15]. The left side of the equation takes into account the dynamic changes of the electrode and electrolyte ions. The formula states that the current I causes changes in ion concentration and the local ion concentration controls the battery voltage and the capacity. The parameter τ is the mass transfer time constant used to describe the battery capacity recuperation characteristics. It is assumed to be known for the specific battery type.

1.2.2 Fractional utilization model

The fractional utilization model [16] assumes that during each time increment of a driving schedule, a portion of the battery mass is depleted and a fraction of mass is regained during regenerative braking. This

mass concept is an equivalent representation of the SOC. The mass depletion during a given schedule is[16].

$$\Delta M = \sum_{i=1}^{t/\Delta t} \frac{sign(P_{D_i}) M \Delta t}{3600 \tau_i} \tag{3-4}$$

where

ι_i: time that battery pack can continuously discharge the constant specific power P_D before its terminal voltage drops below a previously agreed upon cutoff voltage level.

Δt: time increment

$sign(P_{Di})$: sign of the constant specific power (positive during mass recuperation, negative otherwise)

The SOC is determined from

$$SOC = 1 - \frac{\Delta M}{M} \tag{3-5}$$

The vehicle range can be predicted directly by the average mass consumption for each constant specific power running of the vehicle and the total mass available as per

$$\text{range} = \frac{M}{\Delta M} \tag{3-6}$$

The above two models bear some common features in representing SOC. They emphasize the mass recuperation concept. The defects of the above two models are:

- the mass concept is not an exact representation of the electrochemical and physicochemical process in battery, and the active mass is a parameter which is difficult to determine for the specific battery. Besides, the properties of the cell electrodes will be affected not only by the composition of the active mass but also by the production technology of the battery[12].

- other factors which dynamically affect the battery capacity are neglected, such as heating, discharging pattern, aging, and temperature.

- the total mass in the fractional utilization model, or the optimal capacity in the Purdue model, as a constant does not count the capacity losses due to repeated charging and discharging as well as capacity changes due to discharge rate.

In addition, for the fractional utilization model,

- the model applies to constant power discharge only, since the mass depletion, ΔM, is determined by the discharging time τ_i , a parameter measured with reference to constant power discharge.

For the Purdue model

- the mass transfer time constant τ for determining the mass recuperation is assumed to be supplied by the user, which makes the model difficult to apply in applications where this information is not known.

1.2.3 Other models

There are also other models presented in reference [15]. The basic features of those models are:

- models established for certain discharge patterns only, e.g. constant current withdraw or constant power discharges which render them not suitable for dynamic vehicle modeling;

- models not applicable to SOC representation due to the iterative calculation of current;

- models that indicate the SOC using the average time and instantaneous current I, which means that the algorithm for the SOC is not reliable in reflecting the dynamic changes of the SOC.

Since battery capacity is a parameter which is affected by many factors, the representation of the SOC is a complicated issue. It is difficult to develop a model which takes into account all the factors necessary while still being feasible for practical implementation and application. To avoid the obstacles in obtaining the perfect theoretical model, a practical solution is needed.

2. Practical Battery Model

2.1 Battery Test

If a method could be used that would lead to dynamic battery SOC monitoring, the battery capacity can be a real time parameter resulting from the instantaneous integration of the current curve. The need for a dynamic representation of the SOC and V_terminal as a function of the SOC and I without requiring the knowledge of Voc and R motivated the tests conducted on the battery pack used for the UT-HEV NEON. The purpose of the test is to associate the SOC changes with dynamic changes of battery terminal voltage and current, and generalize the information for dynamic representation of battery SOC and V_terminal in terms of SOC and I.

It should be pointed out that the model generated from the test data can be applied to the specific battery pack only, although the approach could be used for general purposes. Another limitation is that if some irreversible changes occur to the battery, their effects may not be counted in the model established. However, compared with the complexities involved in the accurate theoretical representation and the incidental or minor effects of some other factors, it is still a realistic way for battery modeling.

2.2 Battery Test Conditions

Tests were conducted on the battery pack used in the UT-HEV NEON. The test conditions are as follows:

- Battery

  The battery tested is a flooded lead-acid battery U1 DC9 provided by Exide Co. The Peukert curve based on the data supplied by the manufacturer as listed in Appendix 2 is shown in fig 3.1. The C_3 capacity is 22 Ah according to the manufacturer. The Peukert equation is shown in the figure. This curve is drawn assuming that the data in Appendix 2 is the capacity corresponding to the average battery discharge current.

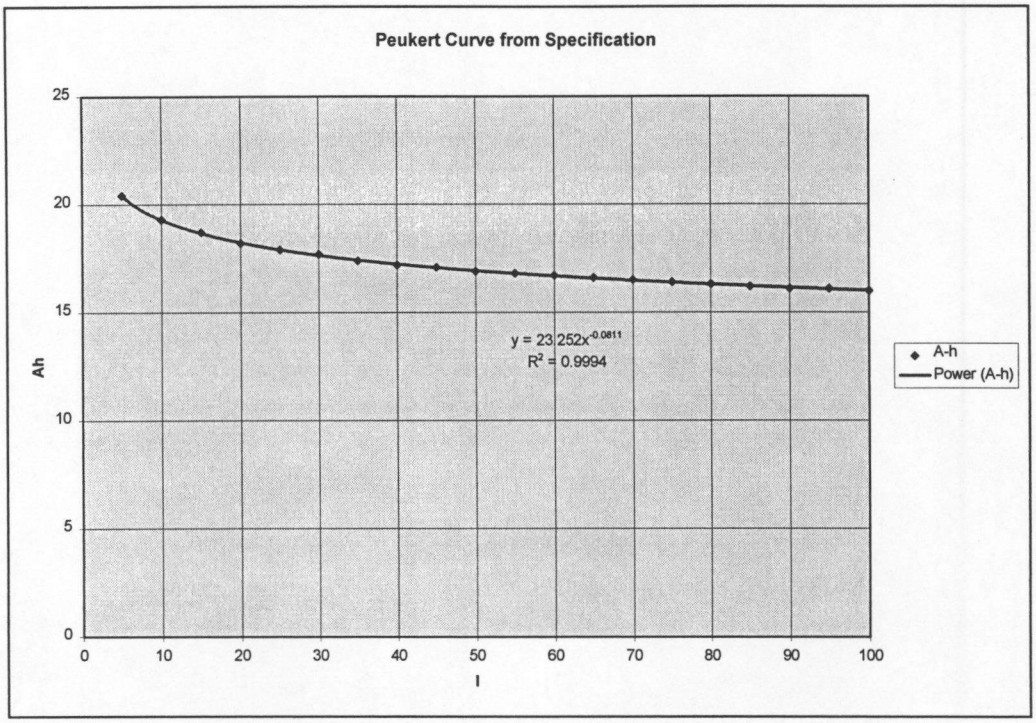


fig.3.1 Peukert Curve from the Exide Specification

- Data acquisition

Data acquisition was facilitated by means of a kilowatt-hour meter made by Cruising Equipment. The instrument can be used to obtain the battery current, I, terminal voltage, $V\_terminal$, and battery Ah and kWh capacities. The current is measured by a precise shunt resistor. The algorithm used by this instrument for the output Ah capacity and Wh capacity is by time integration of the current and the instantaneous power(I-V_terminal).

- Discharge pattern

Tests were conducted on the battery pack (16 batteries connected in series) by operating the vehicle on the chassis dynamometer to simulate a quasi-constant current withdrawal pattern as shown in fig.3.2. The pack terminal voltage drop is shown in fig.3.3. The voltage cutoff point is not controlled by the minimum required voltage for the operation of the motor/controller since the minimum voltage

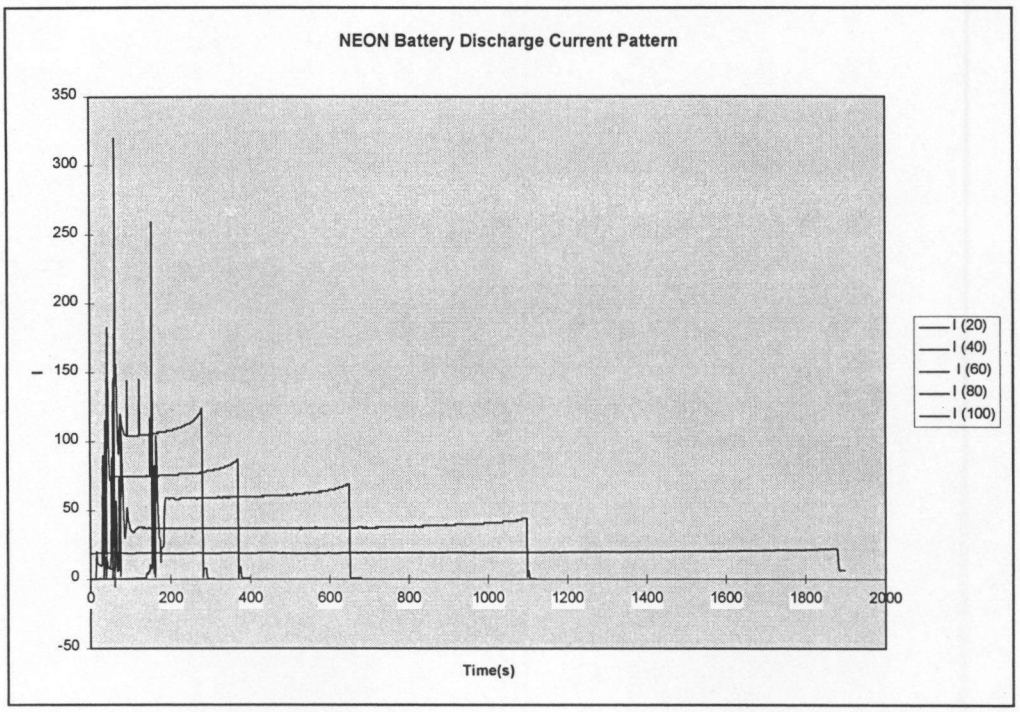


fig.3.2 NEON Battery Discharge Current Pattern

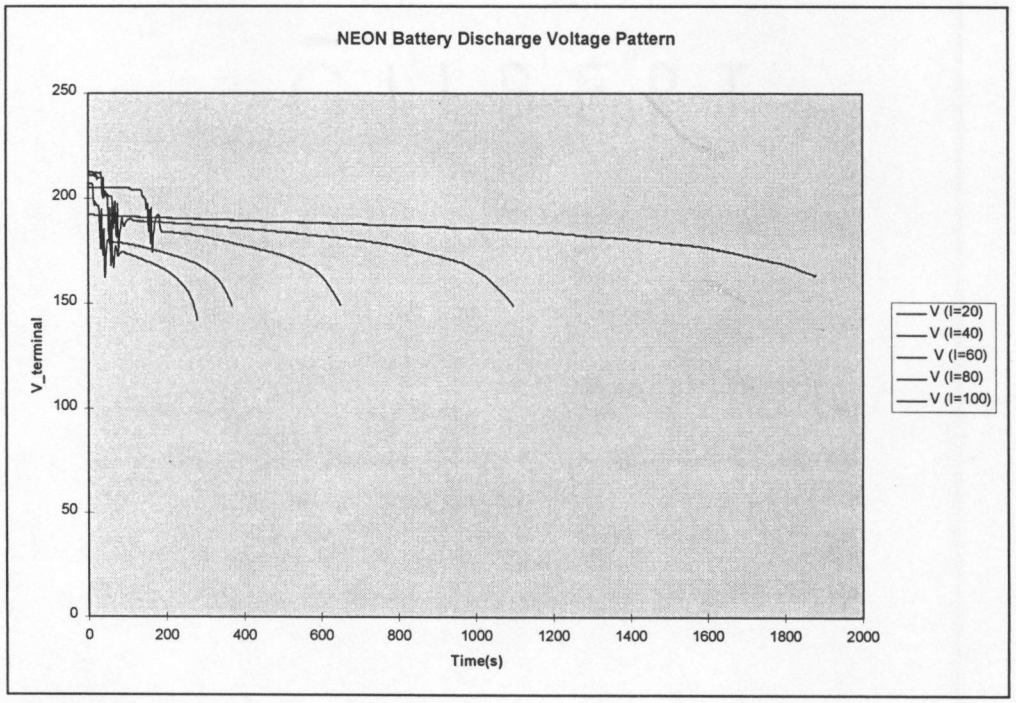


fig.3.3 NEON Battery Discharge Voltage Pattern

required by Unique Mobility CR20-300 motor controller is 60 V. The tests showed that the cutoff point for the battery should be 150V since the battery voltage starts dropping rapidly from that point down. The highest operating voltage of the battery is about 203 V, obtained from the 16 cells in the pack, with 12.6 V of nominal Voc for each cell. Therefore, the SOC is determined by setting SOC=0 when V_end=150 V, and SOC=1 when V_end=202V.

2.3 Test Result Analysis and Model Construction

2.3.1 Test verification of Peukert curve

A battery capacity curve was obtained from the data recorded. The Peukert curve is plotted from the maximum capacity and the average current as shown in fig.3.4. The test curve is extrapolated further to estimate the maximum capacity. Also included in this figure is the Manufacturer's Peukert curve for the nominal capacity as shown in fig.3.1.

It was noted that the tested battery capacity was less than the manufacturer's specification, and the Peukert curve derived from the test data followed a different trend than that from the specification as shown in fig.3.4. The data from the battery specification shows that the C_3 capacity of the battery occurred when the current I is between 5 to 10 Am. Since C_3 is normally referred to as the nominal capacity of the battery, the C_3 extrapolated from the test curve would not be a realistic representation of the battery capacity.

It is believed that the degradation of the battery capacity, hence the shifting of the Peukert curve was caused by deficient battery cells in the pack resulted from the prior use of the battery pack. Some of the cells were found out later to be in very serious condition. Due to limits imposed by the time schedule and the issues involved for replacing the defect batteries, the tests were not repeated. The data collected were used for deriving the simulation model in the following analysis. The deteriorated battery capacity will affect the model generalized from the test data, and thus affect the simulation prediction of the vehicle performance.

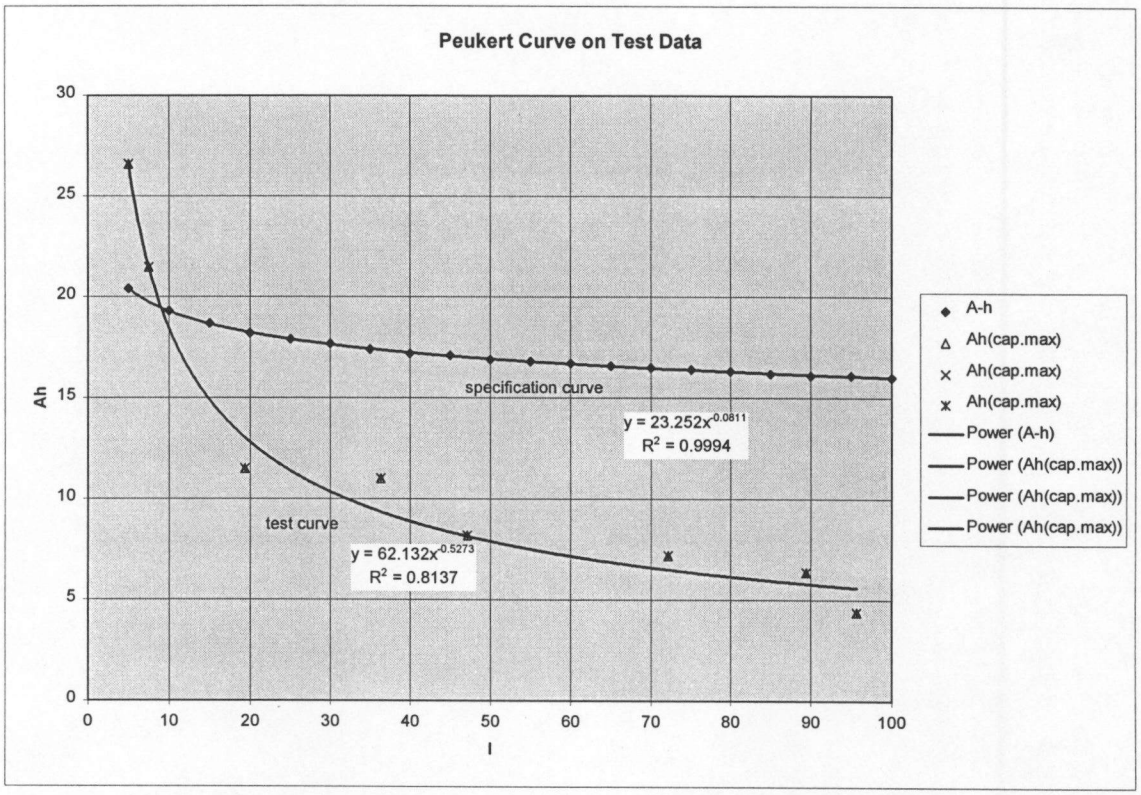


fig.3.4 Peukert Curve Comparison

2.3.2 Battery *V_terminal-I* curve under certain SOC

The SOC can be based on either Ah or kWh capacities. Calculations of the SOC for these test data show that for the tests conducted, the SOC curves resulting from the two approaches are very close to each other as can be seen from fig 3.5. For the analysis that follows, the SOC is based on the Ah capacity approach.

Using the SOC definition described above, the relationship between battery output *V_terminal* and *I* versus SOC can be derived. Fig.3.6 and fig.3.7 show the *V_terminal* and *I* under certain SOC respectively.

From fig.3.6 it is seen that the terminal voltage drop converges to the same point for several tests. This is because these tests are terminated at the same end-point voltage, V=150 V. The curves that do not converge to the above end point has a higher or lower cutoff point. The spikes in the current curves reflect the initial unstable period for speeding up during the tests.

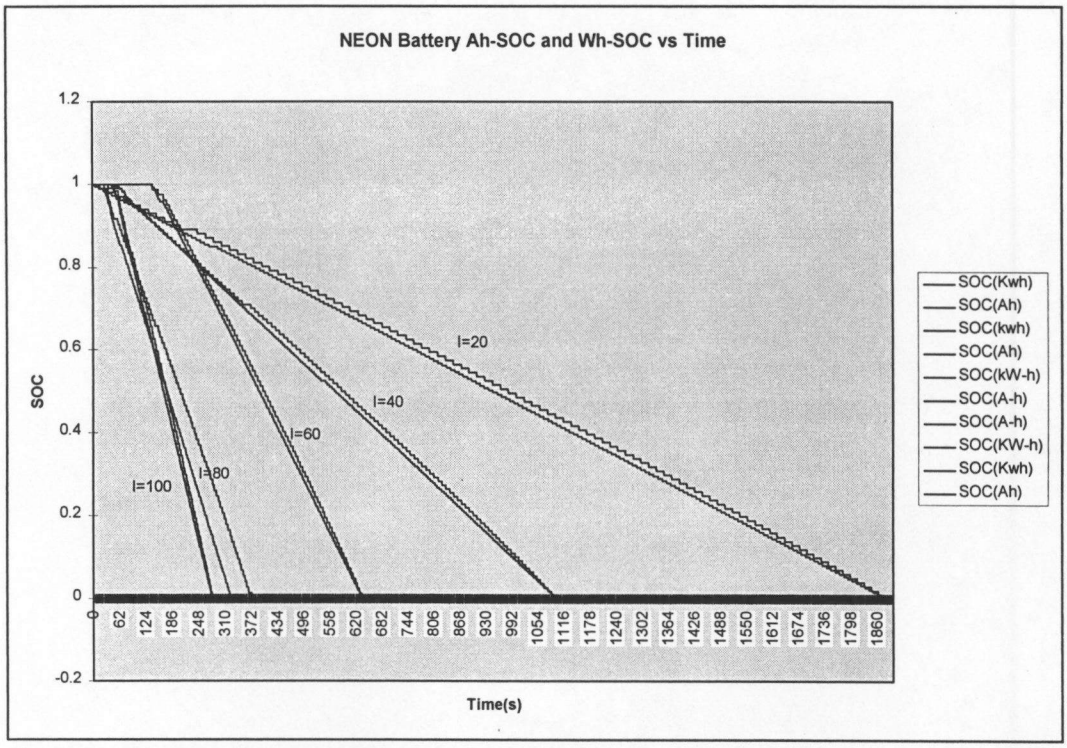


fig.3.5 NEON Battery Ah and Wh SOC Comparison

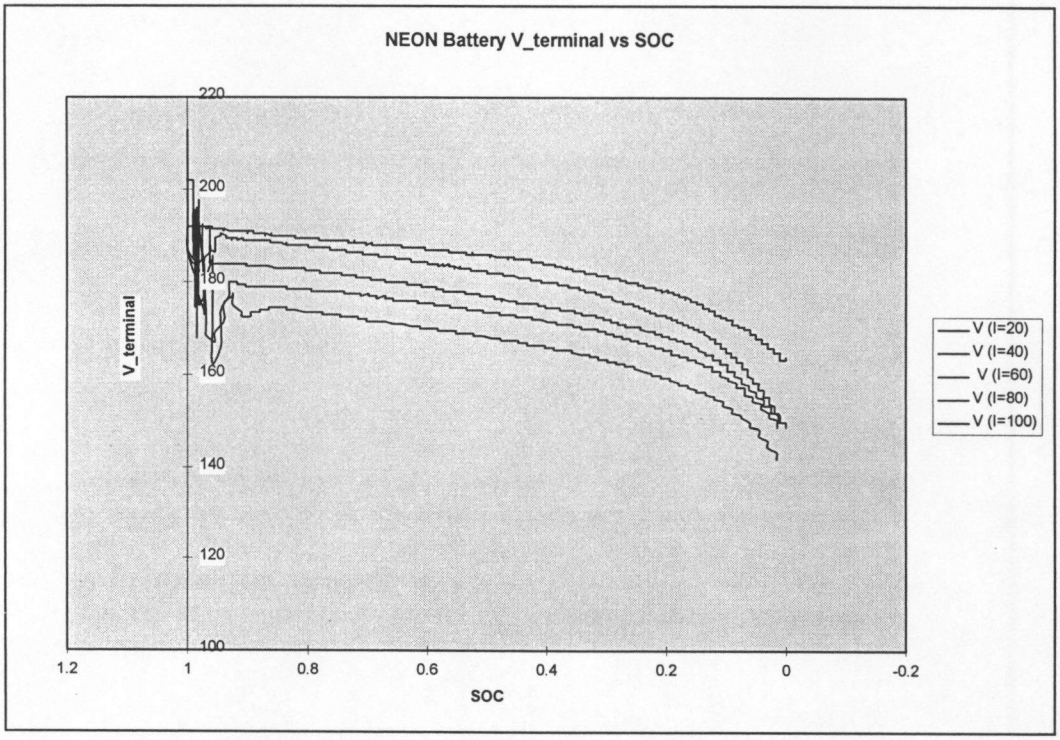


fig.3.6 NEON Battery *V_terminal* vs SOC

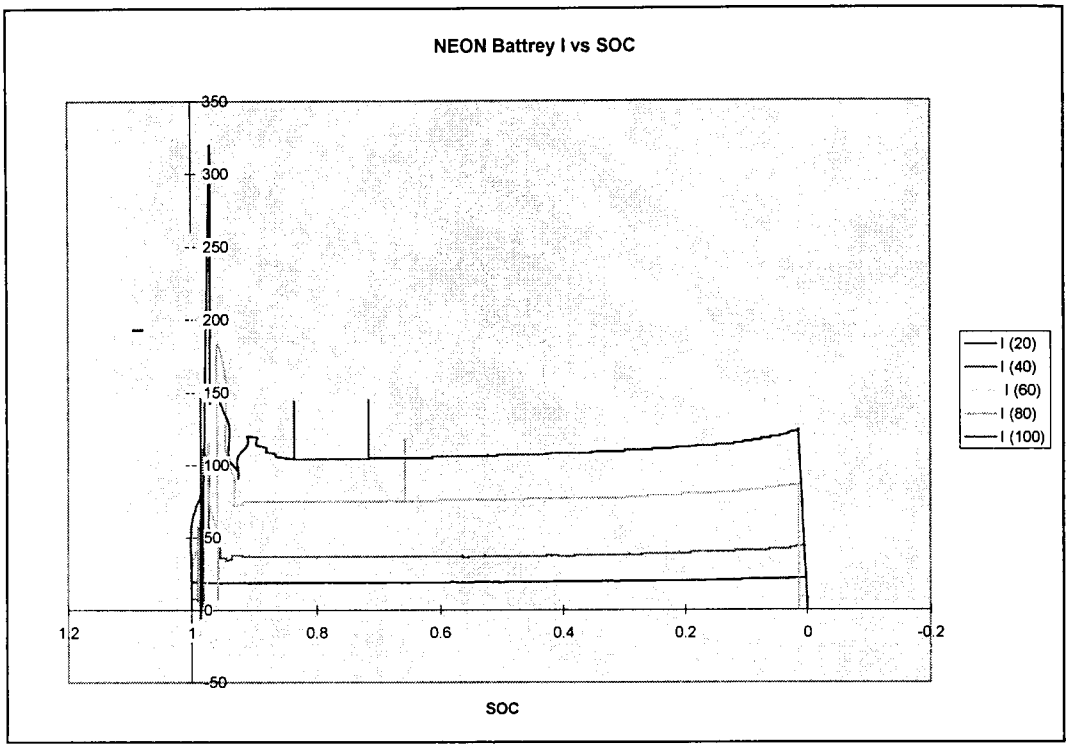


fig.3.7 NEON Battery I vs SOC

From the above two curves, curves of *V_terminal* versus *I* for various values of SOC can be developed as shown in fig.3.8. The SOC in fig.3.8 is represented from 0.05 to 0.95. This is because at SOC=0 and SOC=1 some abnormal output is observed and the corresponding data has to be abandoned. In these curves, spikes that appeared in the actual data recordings have been removed due to discrete data selection for deriving these curves. Therefore, the curves describe the situation of stable power delivery from the battery without unstable current changes as appeared in the test data.

Applying trendline curve fitting, we can obtain the equations for the curves of *V_terminal-I* corresponding to a given *SOC*. To generalize the equations for these curves, equations from the test data curve fitting in both first and second order polynomial as listed in Appendix 3, Table A.1 are analyzed.

The generalized equations are used to calculate several points corresponding to current *I* of 20,40, 60, 80 and 100 Am. The values obtained were then compared with the trendline formula for error checking. The

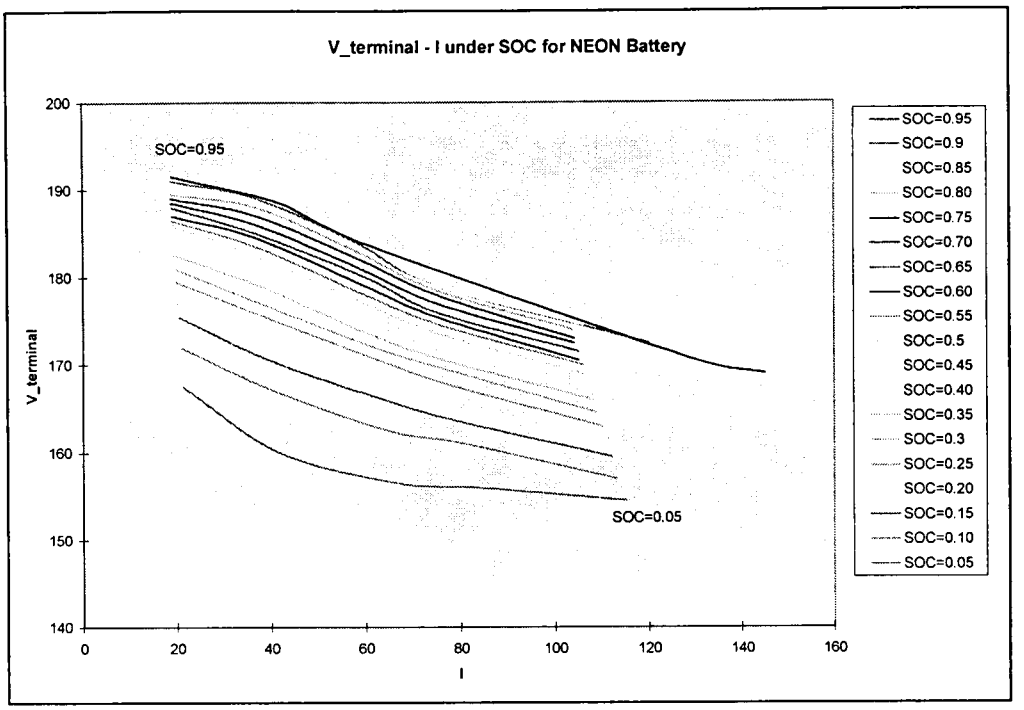


fig.3.8 V_terminal vs I under certain SOC for NEON Battery

results are listed in Appendix 3, Table A.2 and Table A.3 for 1st order and 2nd order curve fitting respectively. It can be seen that the relative errors between the generalized curve and the test curves are within 5%.

For convenience, the first order formulae are used for the simulation model development. A plot of the linearized curve is shown in fig.3.9.

With the equations generalized for *V_terminal* and *I*, the power output from the battery can be determined in conjunction with other constraints, such as controller current and voltage limits. This eliminates the need for dealing with *Voc*, *R_charging* and *R_discharging*.

The result obtained in terms of battery *V_terminal* versus *I* at given SOC is used for construction of the MATLAB/SIMULINK blockdiagram. The new blockdiagram is shown in fig.3.10, which replace the old battery blockdiagram in ADVISOR. The new block is built as per the following conditions:

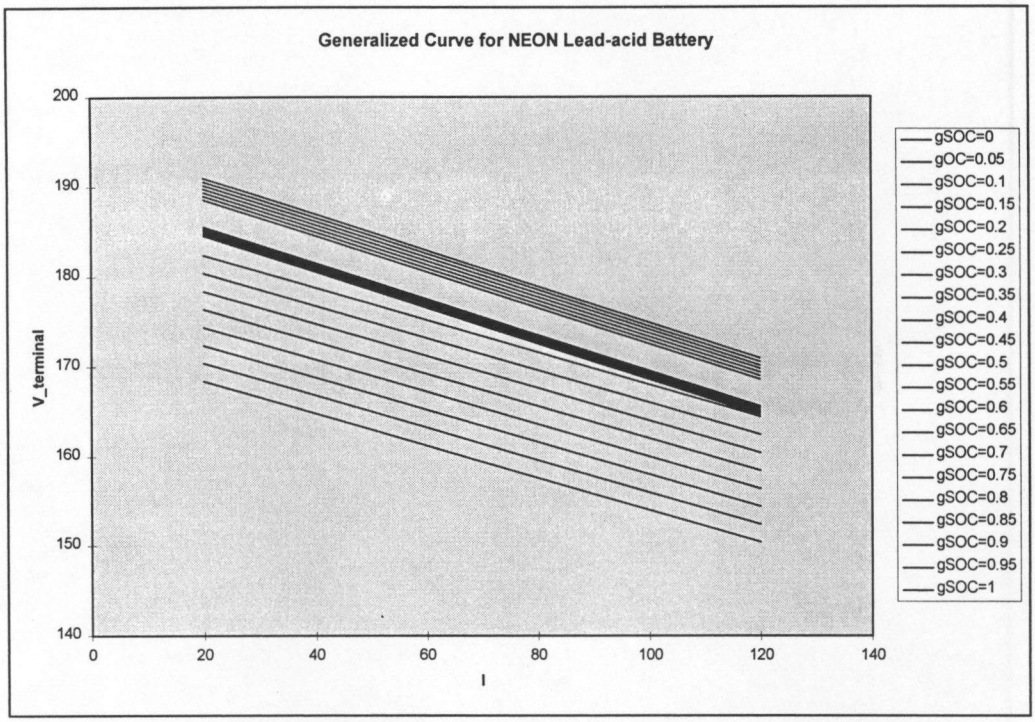


fig.3.9 Generalized Curve for NEON Battery

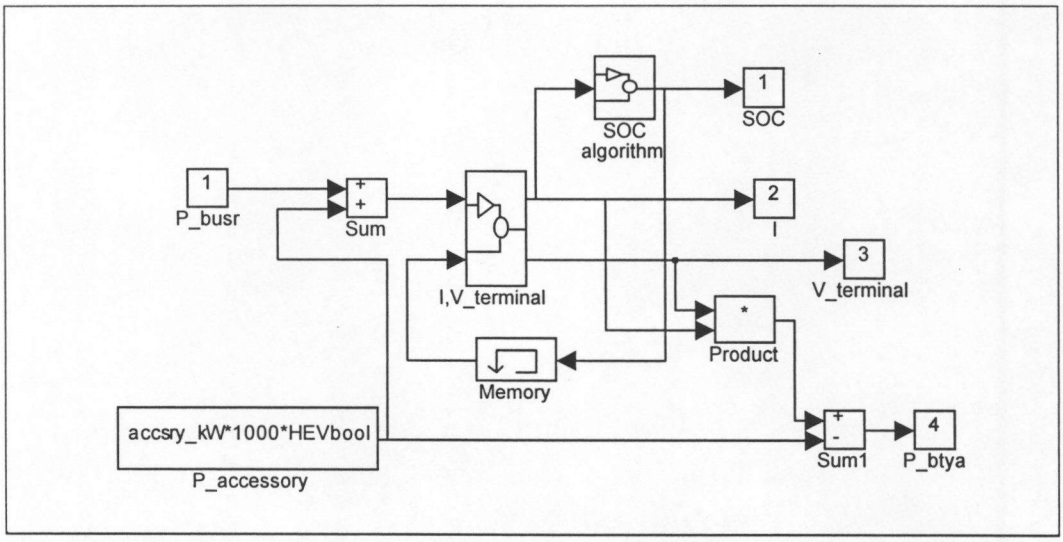


fig.3.10 NEON ESS Battery Blockdiagram

Given requested power *P_req* and SOC, according to the generalized formulae

$$V\_terminal=f(I, SOC) \tag{3-7}$$

From Appendix 3, Table A.1, the generalized expression for *V_terminal* and *I* at a given *SOC* can be expressed in the form:

$$V\_terminal=a*I+b+c*SOC \tag{3-8}$$

specifically

$$V\_terminal=-0.18*I+172+40*SOC \quad when\ SOC<0.4 \tag{3-9}$$

$$V\_terminal=-0.2*I+186.94+4*SOC \quad when\ SOC>=0.4 \tag{3-10}$$

The above formulae are different from those in Appendix 3, Table A.1 in that the derivation takes the sign of the discharge current to be positive. Since the battery current discharge is considered negative in ADVISOR simulation model, therefore the coefficient should be negative by this convention.

Since the power output should equal to the power request for the battery, then

$$P\_busr=I*V\_terminal \tag{3-11}$$

here *P_busr* is the requested power to the battery.

therefore,

$$P\_busr =I*(aI+b+c*SOC) \tag{3-12}$$

$$a*I^2+(b+c*SOC)*I-P\_busr =0 \tag{3-13}$$

solving the quadratic equation, we get

$$I = \frac{-(b + c * SOC) + \sqrt{(b + c * SOC)^2 + 4 * a * P\_busr}}{2 * a} \tag{3-14a}$$

The above solution demands the following conditions:

- $(b+c*SOC)^2+4*a*P\_busr>=0$
- when $P\_busr>0$, $I>0$; when $P\_busr<=0$, $I<=0$
- the current I can not exceed the limit of maximum controller current, *con_I_max*.

When the accessory load carried by the battery pack is considered, the current should be determined from

$$I = \frac{-(b + c * SOC) + \sqrt{(b + c * SOC)^2 + 4 * a * (P\_busr + P\_accesry)}}{2 * a} \qquad (3\text{-}14b)$$

With the value I determined, *V_terminal* can be found by equations (3-9) and (3-10). The constraint applied to the *V_terminal* calculation is that it must exceed the minimum operating voltage for the controller, *con_I_min*. This is checked by the switch block in the diagram to assure that the voltage output is proper for controller operation.

From the above voltage and current output, the available power from the battery, *P_btya,* can be computed as a feedback to the previous block to determine the actual vehicle speed.

2.4 Practical Model and ADVISOR Model Analysis

The *V_terminal-I* curve for a given SOC has demonstrated potential for simulation purposes. Since:

- It can be used for battery modeling for which data on *Voc* and *R* are not known;
- It simplifies the process for the construction of the simulation block;
- It can be used for different strategies for vehicle control

  This means that a different strategy can be adopted to determine the output parameter from input parameters since *V_terminal*, *I*, *SOC* and *P_req* are correlated with each other. Given any two of the parameters, another two would be uniquely defined.

- The practical model and the ADVISOR model are interchangeable.

This is because that the practical model can be established from the data available in ADVISOR. Also, the generalized curve formulae can be used to calculate the Voc and R. The interchangeability of the two models is illustrated as follows.

- Practical model to ADVISOR model

Since for any two points on the generalized curve, we have

$$V_1 = V_{oc} - I_1 * R \tag{3-15}$$

$$V_2 = V_{oc} - I_2 * R \tag{3-16}$$

then for a certain SOC, the R and Voc can be determined by

$$R = \frac{V_1 - V_2}{I_2 - I_1} \tag{3-17}$$

$$V_{oc} = I_1 * \frac{V_1 - V_2}{I_2 - I_1} + V_1 \tag{3-18}$$

For the Neon battery pack, from Appendix 3, Table A.2, we can obtain the R and the Voc for a given SOC from the generalized formulae and the test data formulae as listed in Table 3.1 and Table 3.2 respectively.

The R and Voc as shown in the above two tables are compared in fig 3.11 and fig.3.12, respectively. It can be noticed that the generalized results of R and Voc are very close to the test data. Therefore, it should be an acceptable approximation of the test data.

In this way, ADVISOR model parameters can be established. As ADVISOR requires that the input parameters R and Voc are interpreted with respect to the individual battery cell, the data from Table 3.1

Table 3.1 NEON Lead-acid Battery Voc and R from Generalized Formulae

SOC	*V_terminal(I=20)*	*V_terminal(I=100)*	*R(gen)*	*Voc(gen)*
0.00	168.40	154.00	0.18	172.00
0.05	170.40	156.00	0.18	174.00
0.10	172.40	158.00	0.18	176.00
0.15	174.40	160.00	0.18	178.00
0.20	176.40	162.00	0.18	180.00
0.25	178.40	164.00	0.18	182.00
0.30	180.40	166.00	0.18	184.00
0.35	182.40	168.00	0.18	186.00
0.40	184.54	168.54	0.20	188.54
0.45	184.74	168.74	0.20	188.74
0.50	184.94	168.94	0.20	188.94
0.55	185.14	169.14	0.20	189.14
0.60	185.34	169.34	0.20	189.34
0.65	185.54	169.54	0.20	189.54
0.70	188.54	172.54	0.20	192.54
0.75	188.94	172.94	0.20	192.94
0.80	189.34	173.34	0.20	193.34
0.85	189.74	173.74	0.20	193.74
0.90	190.14	174.14	0.20	194.14
0.95	190.54	174.54	0.20	194.54
1.00	190.94	174.94	0.20	194.94

Table 3.2 NEON Lead-acid Battery Voc and R from Test Formulae

SOC	*V_terminal(I=20)*	*V_terminal(I=100)*	*R(Test)*	*Voc(Test)*
0.00	164.80	154.52	0.13	167.37
0.05	164.80	154.52	0.13	167.37
0.10	170.95	158.19	0.16	174.14
0.15	174.49	160.64	0.17	177.95
0.20	176.98	162.68	0.18	180.55
0.25	179.02	164.21	0.19	182.72
0.30	180.41	165.61	0.19	184.11
0.35	182.07	166.80	0.19	185.89
0.40	183.40	167.78	0.20	187.31
0.45	184.70	168.52	0.20	188.74
0.50	185.55	169.50	0.20	189.56
0.55	186.28	170.58	0.20	190.20
0.60	187.12	171.16	0.20	191.11
0.65	187.89	172.00	0.20	191.86
0.70	188.60	172.92	0.20	192.52
0.75	189.43	173.69	0.20	193.36
0.80	190.09	174.57	0.19	193.97
0.85	190.44	175.25	0.19	194.24
0.90	191.13	175.76	0.19	194.97
0.95	191.69	176.79	0.19	195.41
1.00	191.69	176.79	0.19	195.41

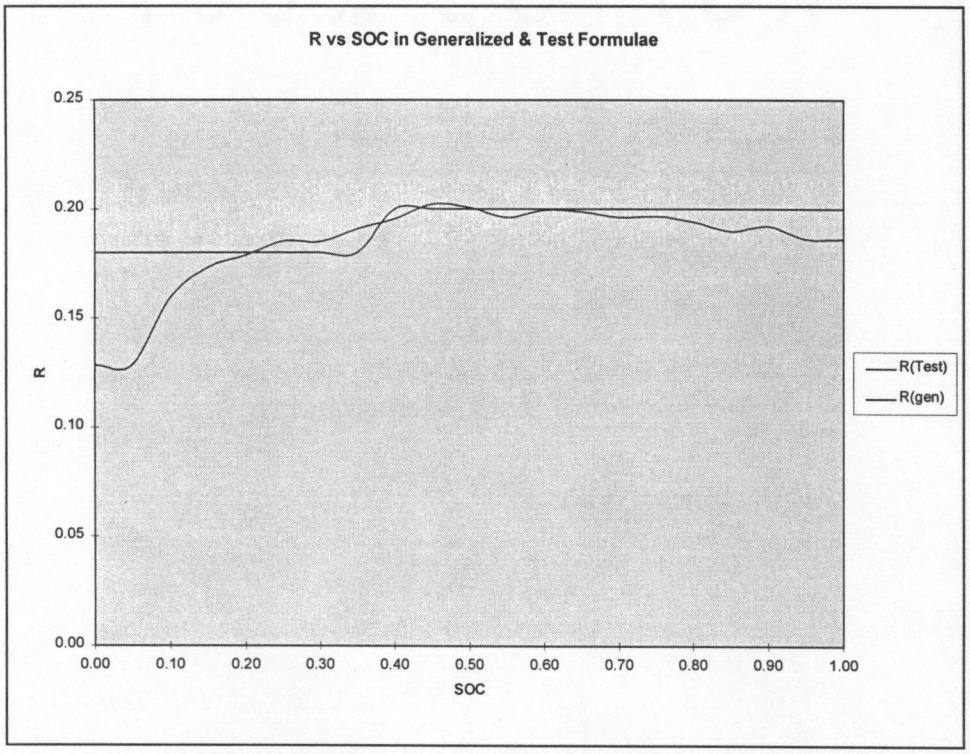


fig.3.11 Comparison of Battery R from Generalized & Tested Formulae

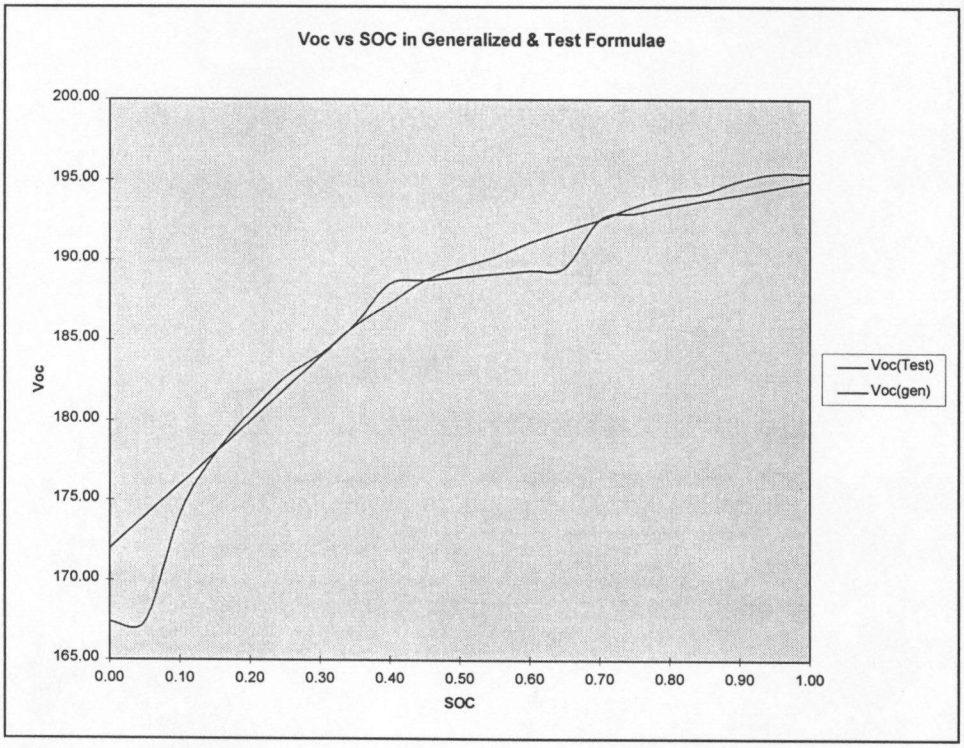


fig.3.12 Comparison of Battery Voc from Generalized & Tested Formulae

is converted as shown in Table 3.3. The file, NEONBT_E.M, constructed for simulation is listed in Appendix 4.

Note that the maximum Voc in Table 3.3 is Voc=12.18V, which is close to the nominal battery specification Voc=12.6V.

- ADVISOR model to practical model

  In the ADVISOR model, it is assumed that *Voc* and *R* at any given SOC are known. From this data, *V_terminal* and *I* curves for a given SOC can be derived, and further generalized for obtaining the parameters for the practical model.

  An example of the conversion is demonstrated through a battery file for the Horizon H12N85 battery included in ADVISOR. The curves generated from the file are shown in fig.3.13.

  It can be seen that the curves for the H12N85 battery are strictly linear. This reflects the assumption made by ADVISOR that that the *Voc* and *R* are functions of the SOC only.

  Using curve fitting, an equation for each curve is obtained as indicated in fig.3.13 Generalization of these equations give following formulae as:

  for 0<=SOC<0.4, V_terminal = 0.0027*I+11.904+(SOC-0.2)*1.8 (3-19a)

  or, V_terminal = 0.0027*I+1.8*SOC+11.544 (3-19b)

  for 0.4<=SOC<=1, V_terminal = 0.0017*I+12.636+(SOC-0.7)*1.4 (3-20a)

  or, V_terminal = 0.0017*I+1.4*SOC+11.656 (3-20b)

Table 3.3 NEON Battery Data for Simulation

SOC	0	0.1	0.2	0.3	0.4	0.5	0.6	0.7	0.8	0.9	1
R(gen.)	0.18	0.18	0.18	0.18	0.2	0.2	0.2	0.2	0.2	0.2	0.2
Voc(gen	10.75	11	11.25	11.5	11.78	11.81	11.83	12.03	12.08	12.13	12.18

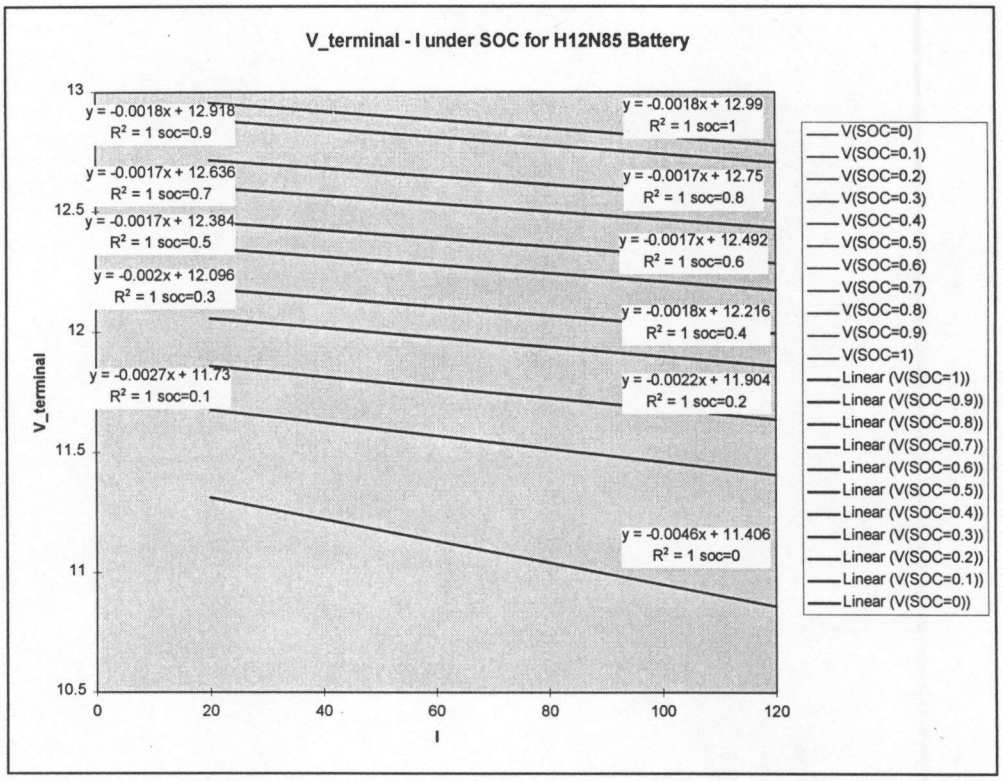


fig.3.13 *V_terminal - I* curve under SOC for H12N85 Battery

The generalized formulae and the trendline formulae are shown in Table 3.4. Data errors resulting from the generalized curve and the trendline curve are listed in Table 3.5.

Equations (3-19b) and (3-20b) should be modified by taking into account the sign convention in ADVISOR and the number of battery cells, i.e. 15, contained in the pack. Then,

for 0<=SOC<0.4, V_terminal =-0.0405*I+27*SOC+173.16 (3-21a)

for 0.4<=SOC<=1, V_terminal =- 0.0255*I+21*SOC+174.84 (3-21b)

The battery cell number is determined by the maximum battery pack voltage requiremnet of UT-HEV NEON and the cell terminal voltage output for the HORIZON battery. To achieve the same

Table 3.4 H12N85 Battery Trendline and Generalized Formulae

SOC	*Trendline Curve*	*Generalized Curve*
0	y=0.0046x+11.406	y=0.0027x+11.904+(soc-0.2)*1.8
0.1	y=0.0027x+11.730	y=0.0027x+11.904+(soc-0.2)*1.8
0.2	y=0.0022x+11.904	y=0.0027x+11.904+(soc-0.2)*1.8
0.3	y=0.0020x+12.096	y=0.0027x+11.904+(soc-0.2)*1.8
0.4	y=0.0018x+12.216	y=0.0017x+12.636+(soc-0.7)*1.4
0.5	y=0.0017x+12.384	y=0.0017x+12.636+(soc-0.7)*1.4
0.6	y=0.0017x+12.492	y=0.0017x+12.636+(soc-0.7)*1.4
0.7	y=0.0017x+12.636	y=0.0017x+12.636+(soc-0.7)*1.4
0.8	y=0.0017x+12.750	y=0.0017x+12.636+(soc-0.7)*1.4
0.9	y=0.0018x+12.918	y=0.0017x+12.636+(soc-0.7)*1.4
1	y=0.0018x+12.990	y=0.0017x+12.636+(soc-0.7)*1.4

Table 3.5 Error Checking for Generalized and Trendline V_terminal - I Curve for H12N85 Battery

	I=20			I=40			I=60			I=80			I=100		
SOC	*Gen.*	*Test*	*%E20*	*Gen.*	*Test*	*%E40*	*Gen.*	*Test*	*%E60*	*Gen.*	*Test*	*%E80*	*Gen.*	*Test*	*%E100*
0	11.5	11.6	-0.86%	11.6	11.7	-0.53%	11.68	11.7	-0.21%	11.8	11.76	0.12%	11.87	11.81	0.44%
0.1	11.78	11.8	0.05%	11.8	11.8	0.05%	11.89	11.9	0.05%	11.9	11.94	0.05%	12	11.99	0.05%
0.2	11.95	12	-0.08%	12	12	-0.17%	12.04	12.1	-0.25%	12.1	12.12	-0.33%	12.12	12.17	-0.41%
0.3	12.14	12.1	-0.02%	12.2	12.2	-0.13%	12.22	12.2	-0.24%	12.3	12.3	-0.36%	12.3	12.35	-0.47%
0.4	12.25	12.3	0.02%	12.3	12.3	0.03%	12.32	12.3	0.05%	12.4	12.35	0.06%	12.4	12.39	0.08%
0.5	12.42	12.4	0.23%	12.5	12.4	0.23%	12.49	12.5	0.22%	12.5	12.49	0.22%	12.55	12.53	0.22%
0.6	12.53	12.5	-0.03%	12.6	12.6	-0.03%	12.59	12.6	-0.03%	12.6	12.63	-0.03%	12.66	12.67	-0.03%
0.7	12.67	12.7	0.00%	12.7	12.7	0.00%	12.74	12.7	0.00%	12.8	12.77	0.00%	12.81	12.81	0.00%
0.8	12.78	12.8	-0.20%	12.8	12.8	-0.20%	12.85	12.9	-0.20%	12.9	12.91	-0.20%	12.92	12.95	-0.20%
0.9	12.95	13	0.03%	13	13	0.05%	13.03	13	0.06%	13.1	13.05	0.08%	13.1	13.09	0.09%
1	13.03	13.1	-0.49%	13.1	13.1	-0.47%	13.1	13.2	-0.46%	13.1	13.19	-0.44%	13.17	13.23	-0.42%

terminal voltage output as that from the 16 lead acid batteries, the HORIZON battery cell number should be 15.

Models as shown in fig.3.10 can be built up in a similar way for the HORIZON battery. The parameters from the generalized formulae are given as the following:

for 0<=SOC<0.4, a=- 0.0405 b=173.16 c=27 (3-22a)

for 0.4<=SOC<=1, a=- 0.0255 b=174.84 c=21 (3-22b)

3. The NEON Control Strategy

3.1 Power Control Strategy

The UT-HEV NEON is a parallel configuration with ESS-assist, which is different from the APU-assist parallel model in ADVISOR. The control of the power distribution is based on the throttle position (TP). Once the torque, or power delivered by the APU at the ESS assist threshold position of TP can not meet the vehicle requirements and the SOC is higher than SOClo, electric assist would be started.

The physical configuration of the NEON APU and the motor is shown in fig.3.14. The torque delivered from both the APU and the motor are combined through a one-way clutch. It is a sprag type used in conjunction with the stock Neon clutch. It assures that the APU provides positive torque only for driving the vehicle and regeneration. The electric motor can not drive the APU and the APU can not provide braking torque because of the one-way clutch. To insure the optimal operating speeds for both power sources, a motor to APU gear ratio (mot_to_ICE_gr) of 1.3 :1 is selected using Gates sprockets and a 36 mm wide Polychain (this is also referred to as pulley ratio between APU and motor).

The Torque-speed maps of the APU and the motor adopted for the UT-HEV NEON are derived from the data contained in ADVISOR as can be seen from fig.3.15. The function of the torque coupler is to couple the power from these two power sources as per the control startegy. The power distribution in each driving mode is analyzed below.

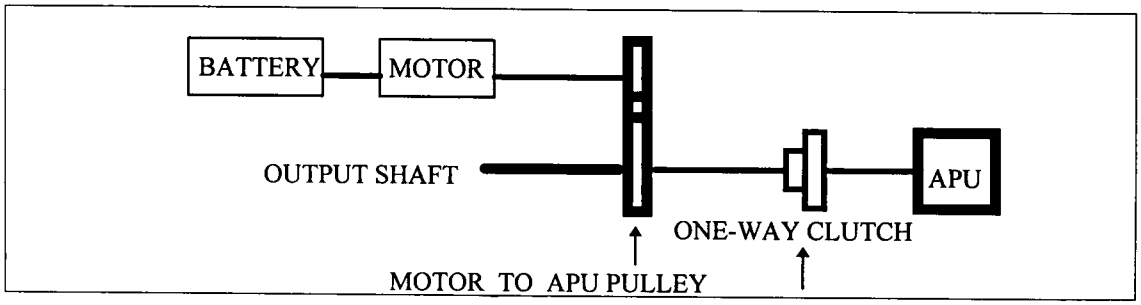


fig.3.14 NEON Torque Coupler Configuration

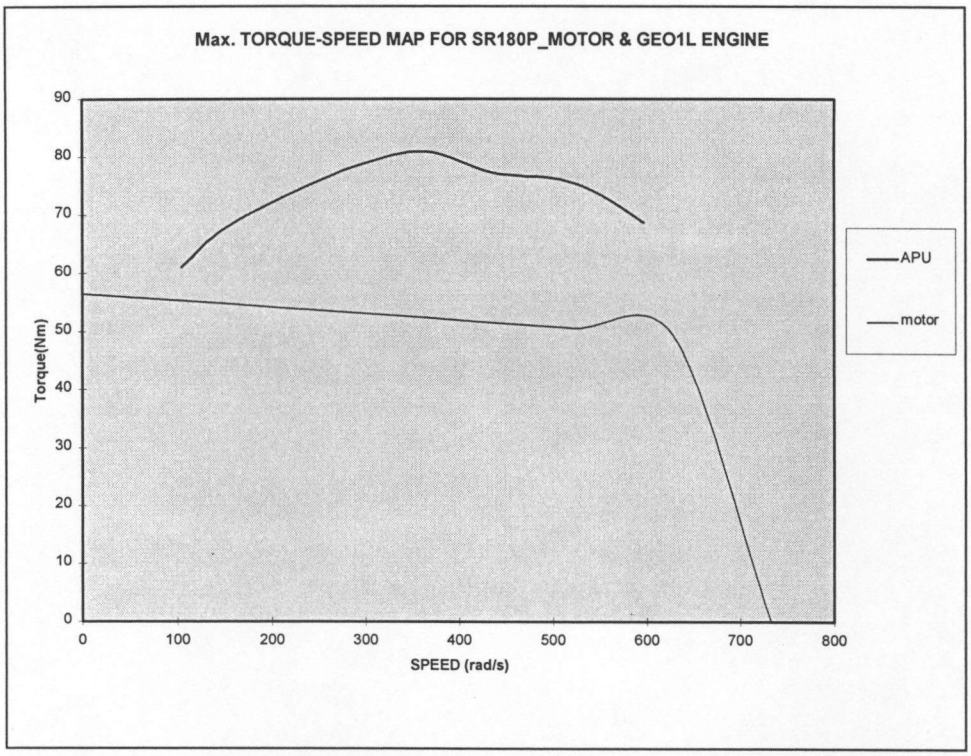


fig.3.15 Torque- Speed map of APU and MOTOR of UT-HEV NEON

3.1.1 HEV mode power control

The APU torque is determined by the throttle position which also determines the torque output from the motor in the HEV mode. If the threshold TP is reached and the torque delivered by the APU can not meet the requested torque, then the motor torque would be started and would be proportional to the throttle position in excess of the threshold value. The torque provided by the motor is governed by the following equation:

$$T_{\_mot} = T_{\_mot\_\max} * \frac{TP - TP_{\_threshold}}{1 - TP_{\_threshold}} \tag{3-23}$$

$$\omega_{\_mot} = \omega_{\_APU} * \text{mot\_to\_ICE\_gr} \tag{3-24}$$

Equation (3-23) indicates that the electric assist would start at the threshold position of TP, and would reach its maximum when the throttle reaches its full position. Equation (3-23) applies only to the situation

when TP is greater than TP_threshold. The threshold position should be determined in light of the characteristics of the available torque output from the APU vs TP as analyzed later in this chapter from the test data.

The total torque provided by both the APU and the motor should be equal to the requested torque, i.e.

when $T\_{req} > T\_{APU\_threshold}$ AND SOC>SOClo

$$T\_avail = T\_{APU\_avail} + T\_{mot}/mot\_to\_ICE\_gr \quad (3\text{-}25)$$

where T_{mot} is defined by equation (3-23), and T_{APU_avail}, the available APU torque output, is determined by the throttle position and APU speed in accordance with the formulae established from the APU test as analyzed later.

3.1.2 Conventional mode power control

The conventional mode, which means that the vehicle is driven by the APU only with no ESS_assist or regeneration, occurs in two cases, i.e.

when $T\_{req} <= T\_{APU\_threshold}$ AND SOC=SOChi (i.e. no regeneration needed), then

$$T\_{mot} = 0 \quad (3\text{-}26)$$

$$T\_{APU\_avail} = T\_{APU\_threshold} \quad \text{when} \quad T\_{req} = T\_{APU\_threshold} \quad (3\text{-}27)$$

$$T\_{APU\_avail} = T\_{req} \quad \text{when} \quad T\_{req} < T\_{APU\_threshold} \quad (3\text{-}28)$$

where T_{req} is the requested torque from the transmission.

- when $T\_{req} > T\_{APU\_threshold}$ AND SOC<=SOClo (i.e. no ESS assist available)

$$T\_{req} = T\_{APU\_threshold} \quad (3\text{-}29)$$

$$T\_{mot} = 0 \quad (3\text{-}30)$$

The conventional mode should occur only instantaneously in the FUDS and the HIWAY cycles.

3.1.3 Regeneration

The NEON battery SOC control is an SOC sustaining strategy which means that battery charging may occur at either P_req>0 or P_req<0. The SOC sustaining strategy attempts to keep the battery SOC at SOC_hi. The battery charging and discharging limits are set as SOClo=0.2 and SOChi=0.8. The regeneration is started when the SOC is below SOChi and when there is extra power available from the APU. The regeneration is disabled when the SOC level reaches SOChi. The constraints applied to the upper limit of the regeneration level, i.e. the maximum power available for recharging the battery is the threshold power corresponding to the threshold position of the throttle, at which APU should provide the maximum torque for both powering the vehicle and regeneration.

Once in regeneration, the motor is working as a generator driven by the APU. The motor speed is governed by equation (3-24). The torque of APU and the torque of the motor are related by the fixed motor to APU gear ratio, mot_to_ICE_gr, i.e.

when $T_{\_req} < T_{\_APU\_threshold}$ AND SOC<SOChi

$$T_{\_mot} = -(T_{\_APU\_threshold} - T_{\_req})/mot\_to\_ICE\_gr \quad (3\text{-}31)$$

3.1.4 Regenerative braking

Battery charging can be possible in another case, i.e. regenerative braking which occurs when the power requested is negative P_req<0 (corresponding to vehicle deceleration or traveling down grades). The braking energy is retrieved for charging the battery.

In this case, the throttle is closed and the torque output of the APU is

$$T_{\_APU\_avai} = 0 \quad (3\text{-}32)$$

The speed of the APU is either idling or zero, depending on the control scheme. The motor speed would be associated with the transmission speed as per equation (3-24).

The motor torque would be determined by the regeneration level set up by the vehicle control strategy. The range of the regenerative braking torque would be from 0 to the maximum torque of the motor under the given motor speed. The regenerative braking is activated when the SOC is below 1. For the model constructed for NEON, regeneration for SOC retaining is limited by SOChi=0.8, and regenerative braking for recharging the battery is controlled by SOC=1 for the maximum recovery of the braking energy.

3.2 Power Control Module

To gain insight into controlling both the APU and the ESS power by TP, tests were conducted on the GEO engine of the NEON. The purpose of the tests was to obtain the relationship between the torque deliverable from APU and the throttle position at various APU speeds. The test data was gathered for APU speeds between 1,540 rpm and 3,000 rpm (which represents the normal speed range of APU operation). The results are plotted in fig.3.16.

From the figure, we can see that in the speed range of 1,500 to 2,500, there is overlapping between the curves of $T_{\_APU\_avail}/T_{\_APU\_max}$ vs TP. The three curves can be generalized by the thicker curve as indicated in fig.3.16. We assume that it represents the APU speed range from above APU idle speed to 2,750 rpm. For speeds over 2,750 rpm, we assume that the curve under 3,000 rpm would be the generalized one.

Performing curve fitting, we see that the closest linear representation of each generalized curve would be a combination of two linear curves as shown in fig.3.17. The corresponding trendline formulae are found as indicated in the figure. The expression of these curves are as follows:

for APU_idlespd$<\omega_{_APU}$ <2,750 rpm AND TP<=0.11

$$T_{\_APU\_avail}/T_{\_APU\_max} = 8.8636*TP - 1E\_16 \quad (3\text{-}33)$$

for APU_idlespd$<\omega_{_APU}$ <2,750 rpm AND TP>0.11

$$T_{\_APU\_avail}/T_{\_APU\_max} = 0.0574*TP + 0.9598 \quad (3\text{-}34)$$

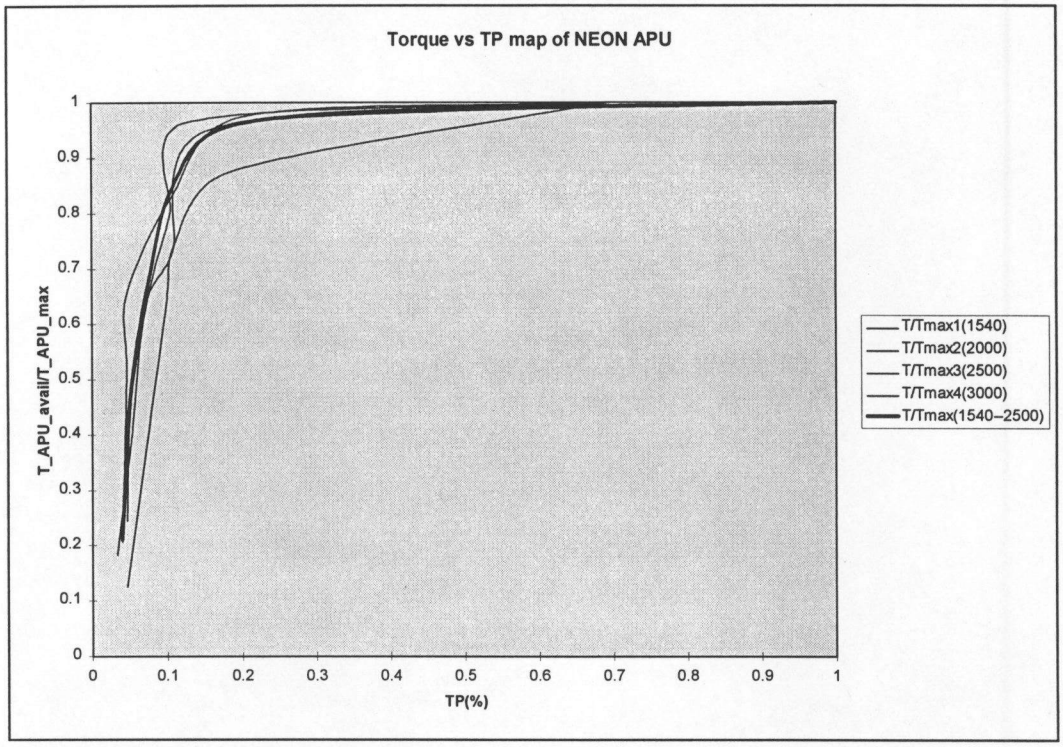


fig.3.16 NEON GEO 1L Engine $T_{\_APU\_avail}/T_{\_APU\_max}$ vs TP Map

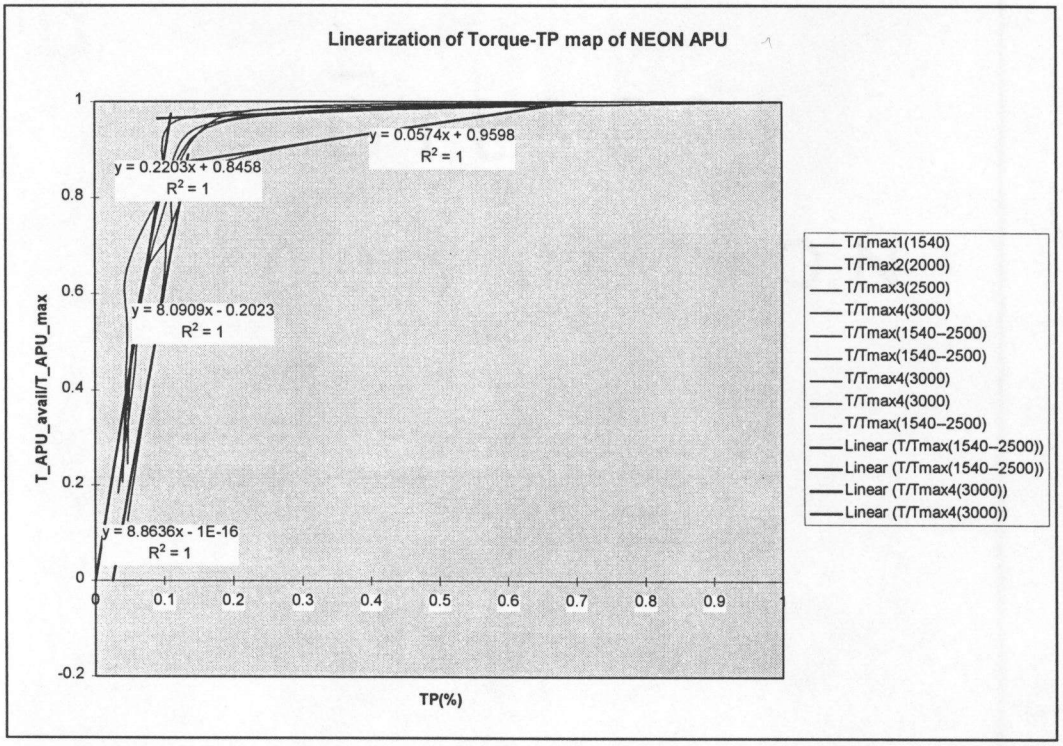


fig. 3.17 Linearization of $T_{\_APU\_avail}/T_{\_APU\_max}$ vs TP Map for NEON Geo 1L Engine

for $2{,}750<\omega_{\_APU}<5{,}000$ rpm AND $TP<=0.135$

$$T_{\_APU\_avail}/T_{\_APU\_max} = 8.0909*TP-0.2023 \quad (3\text{-}35)$$

for $2{,}750<\omega_{\_APU}<5{,}000$ rpm AND $TP>0.135$

$$T_{\_APU\_avail}/T_{\_APU\_max} = 0.2203*TP+0.8458 \quad (3\text{-}36)$$

The idle speed of the APU used for the UT-HEV NEON is APU_idlespd=62.8 rad/s (see Appendix 6).

From the map, we see that the torque output is not affected by the throttle position when the throttle position(TP) is greater than 0.7, i.e. TP>0.7. This implies that the throttle used for the NEON is larger than what is needed. The threshold position of the TP is set as TP_threshold=0.5 based on these curves for simulation, since in the range of TP>0.5, there is no significant change of torque output vs maximum torque. In other words, the output torque is close to the maximum torque from the APU, so the ESS should be started to provide extra power.

From the empirical formulae as well as the power control scheme for ESS-assist, regeneration and regenerative braking as described above, the power control model for the NEON can be developed. The blockdiagram corresponding to the Torque Coupler Module in ADVISOR parallel mode. The subsystem for P_req>0 and P_req<=0 are built as described below.

3.2.1 Blockdiagram for P_req>0

The new module for P_req>0 is shown in fig.3.18.

The function of this block is to calculate the torque and speed output available from the APU and to determine the torque request to the motor for ESS power. The threshold torque is also obtained as an input to determine the APU and motor output. Also included is the APU inertia power calculation. The block TP-TORQUE is shown in fig.3.19. The available APU torque, $T_{\_APU\_avail}$, is calculated from the TP in accordance with equations (3-33), (3-34), (3-35) and (3-36) in the block T-APU_a. From the TP, $T_{\_APU\_avail}$, SOC and APU speed, the torque output from the motor can be determined for different driving

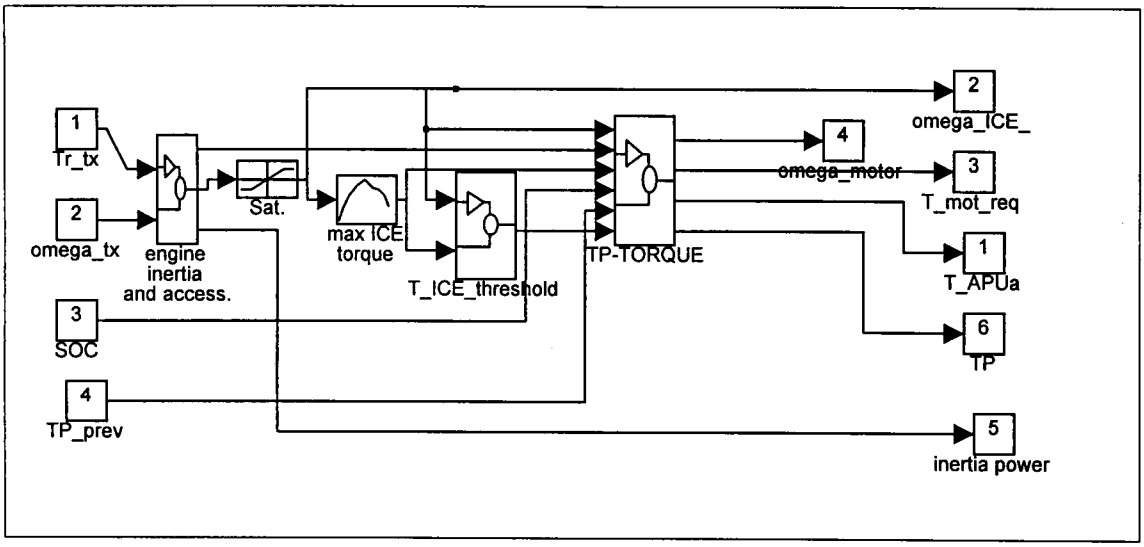


fig.3.18 Torque Coupler Module for P_req>0

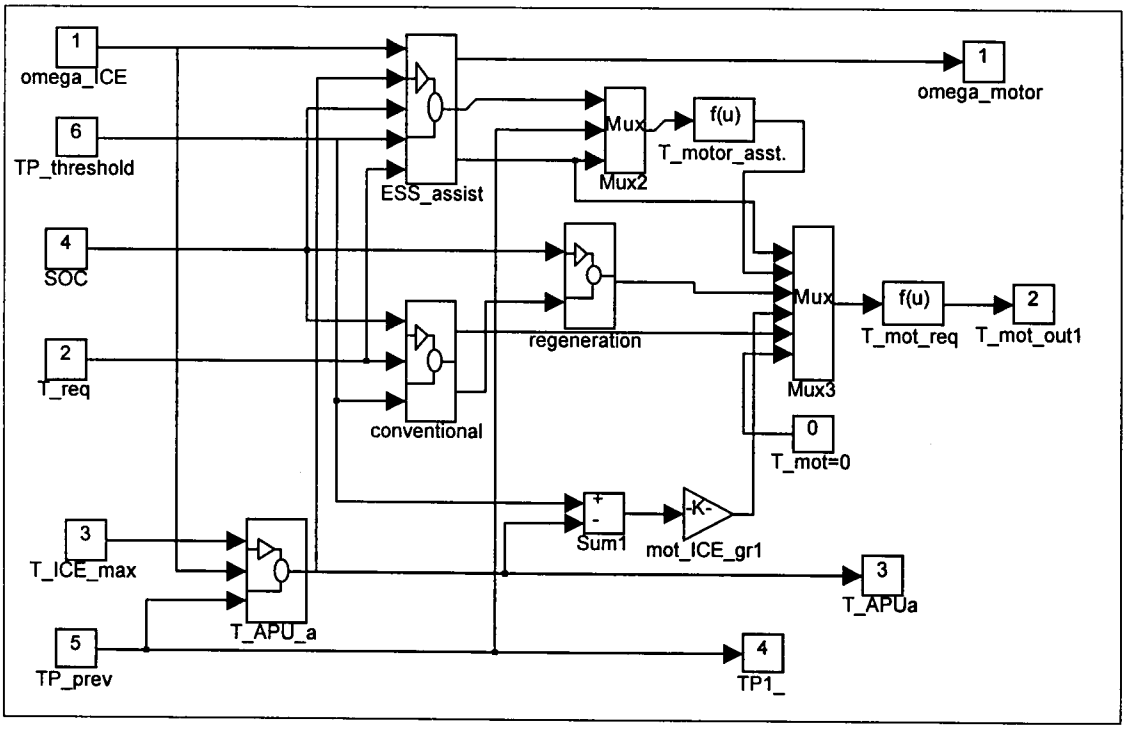


fig.3.19 TP & Torque block for P_req>0

modes. The ESS-assist, Conventional and Regeneration blocks are Boolean operations for determining the conditions for power output from the ESS. The regeneration is controlled by the flag variable *regeneration* in the block to indicate whether the battery power control is in SOC sustaining (*regeneration* =1) or SOC depleting (*regeneration*=0) mode. The regeneration is disabled once the battery SOC reaches SOChi. Regeneration would not be activated if the battery is at SOChi or if the threshold power is fully demanded by the road load, even the SOC is below SOChi.

Fig.3.20 shows the subsystem TP-reset. The TP is adjusted from the comparison between the power requested and the power available. At each iteration, the throttle position would be reset by increment, decrement or remain at the previous position based on whether the power exceeds or is insufficient to meet the demand.

3.2.2 Power Blockdiagram P_req<=0

This case involves the regenerative braking scheme. The block is built as in fig.3.21.

The APU is idling or off depending on the scheme adopted. The motor torque is determined by the regeneration level set up as a variable, *regen_level*, for controlling the regenerative braking torque between zero to the maximum motor torque at the given speed.

The Torque Coupler subsystem is then implemented as shown in fig.3.22, with the additional output of throttle position compared with the ADVISOR model.

4. Other Revisions to ADVISOR

For the purpose of the evaluation of UT-HEV NEON, other revisions have also been made to ADVISOR. As a result, the direct output from the GUI menu is expanded to include:

- vehicle acceleration and range
- battery output V_terminal, I, and energy

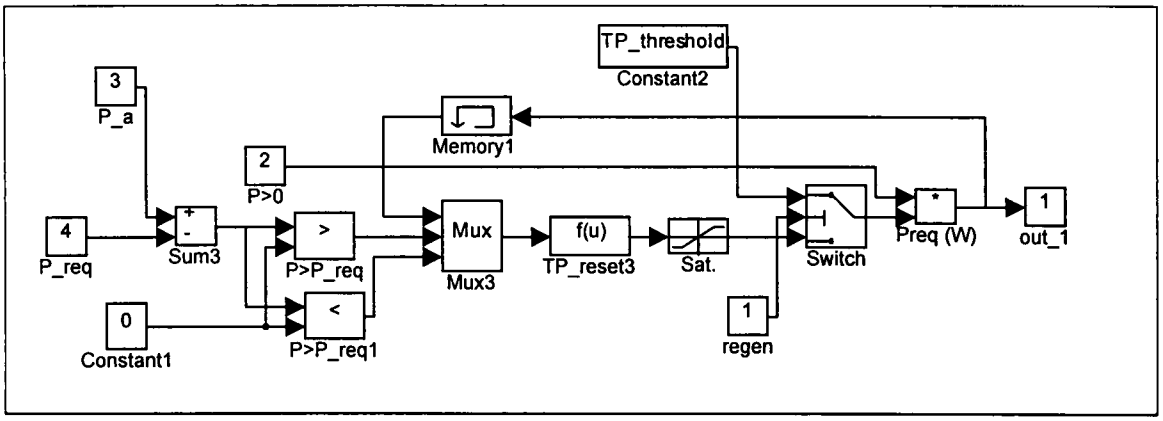


fig.3.20 TP_reset subsystem

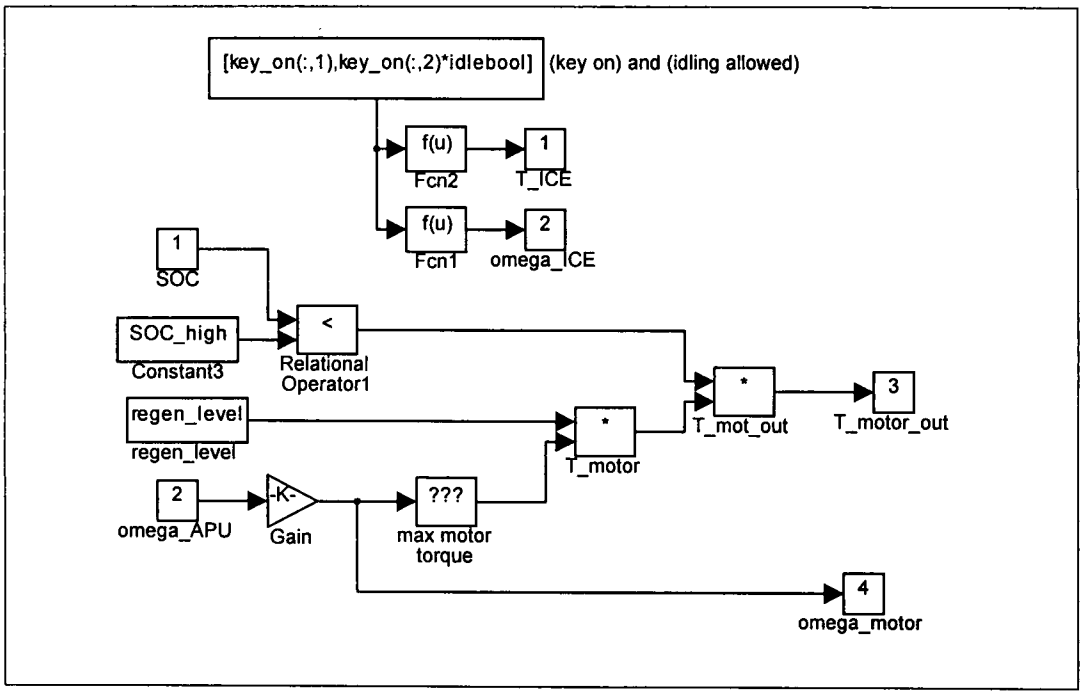


fig.3.21 Torque Coupler Module P_req<=0

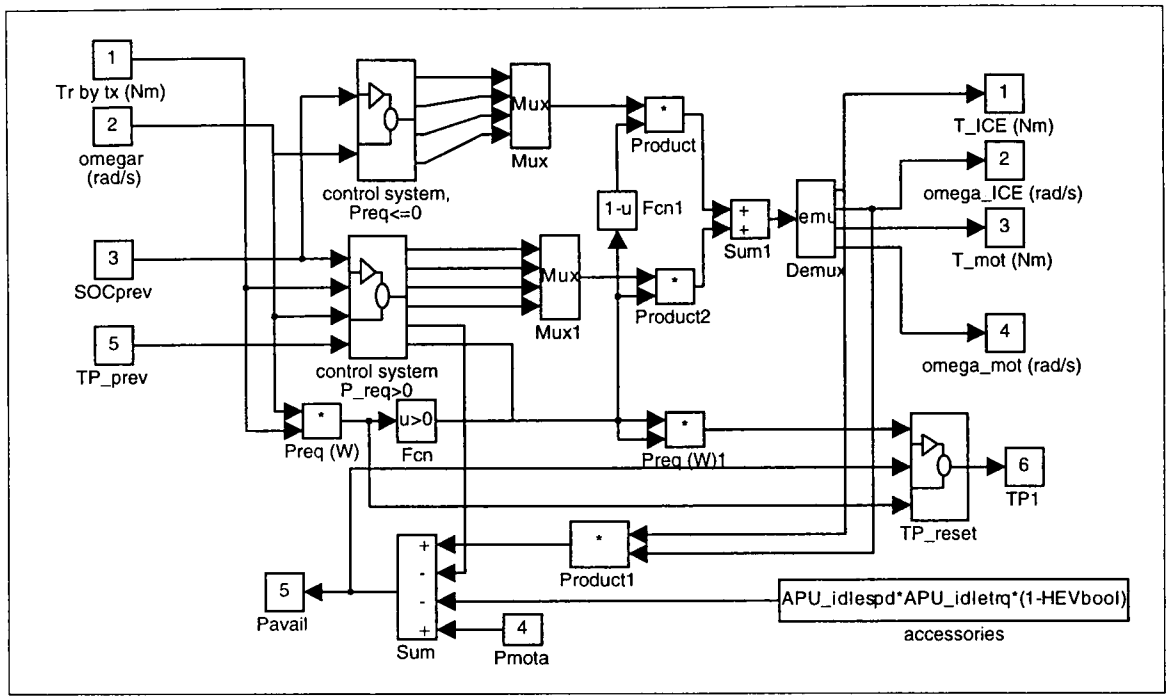


fig.3.22 Torque Coupler Module for NEON Simulation

- throttle position output, and/or gear ratio
- EV and conventional mode simulation options

It should be pointed out many more variables can be analyzed by generating the output files as needed. In fact, virtually all the variables defined for the model construction can be plotted for analysis.

From this parallel model for NEON simulation, the throttle position, gear ratio and the SOC can be directly plotted or their data be gathered for real time indication of the simulation which can be used as parameters for the vehicle driver module.

The GUI interface with above revisions as shown in fig.3.23 is implemented by the file listed in Appendix 7. The parallel model for the UT-HEV NEON is shown in fig.3.24.

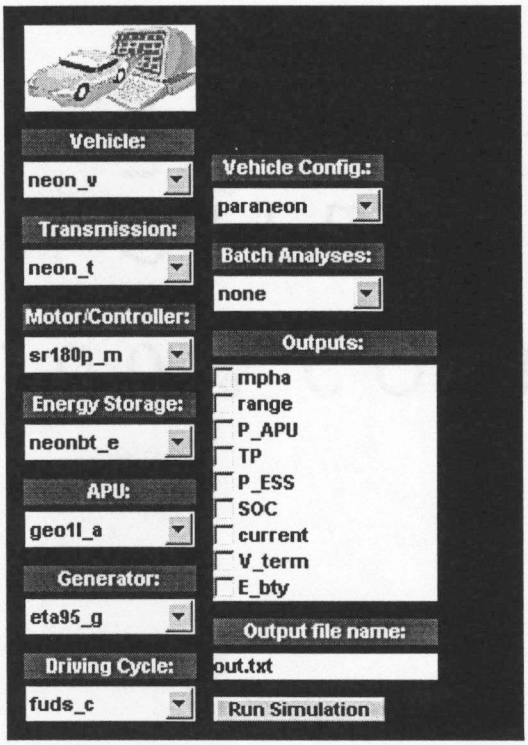


fig.3.23 Revised GUI for NEON Parallel model simulation

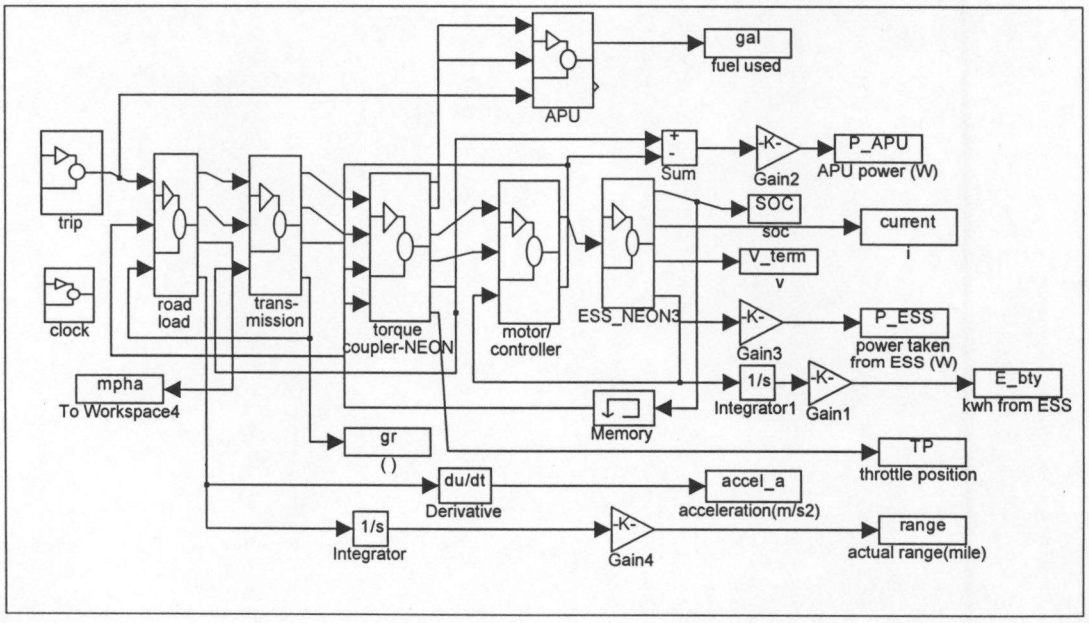


fig.3.24 Parallel Model for UT-HEV NEON

CHAPTER 4

NEON SIMULATION

1. Introduction

In this chapter, the practical battery model developed in this thesis is validated through comparisons with the ADVISOR battery model. Vehicle simulations are made to evaluate the performance of the UT-HEV NEON for both the urban driving cycle (FUDS) and the highway driving cycle (HIWAY). An analysis is made of the simulation results, conclusions are generated from the analysis and some recommendations are made based on the simulation analysis.

2. Validation of the Battery Model

The practical battery model was developed in the previous chapter for the practical battery simulation modeling. Both the ADVISOR model and the Practical model assume that the battery charging pattern and the battery discharging pattern are the same, i.e. the voltage and the current curves for the battery under charging and discharging are the same curve, although the current is in opposite directions for charging and discharging.

To validate the accuracy of the Practical model, simulations have been made with the original ADVISOR "PARALLEL" model to compare the output from the ADVISOR battery model with that from the Practical model for NEON battery. Since the two different models are built with the same input variables (SOC and power request to ESS) and output variables (V_terminal and I), the output differences between the two battery models would validify the accuracy of the model.

2.1 Validation Simulation Analysis

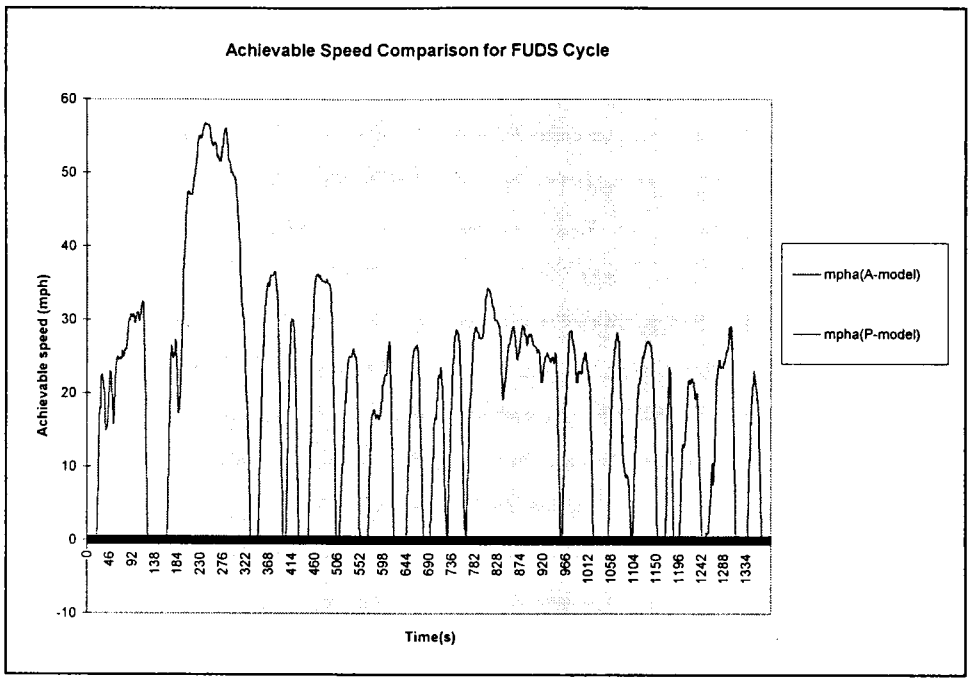
The simulation was run using the FUDS and HIWAY driving cycles, with the following vehicle component files loaded:

- NEONBT_E.M--- NEON battery model; as listed in Appendix 4;
- SR180P_M.M--- SR180P motor used for the NEON. The efficiency map is shown in Appendix 1;
- GEO1L_A.M--- GEO11L APU used for the NEON; as listed in Appendix 6;
- NEON_V.M---NEON vehicle file, as listed in Appendix 9;
- NEON_T.M---NEON transmission file, as listed in Appendix 10;

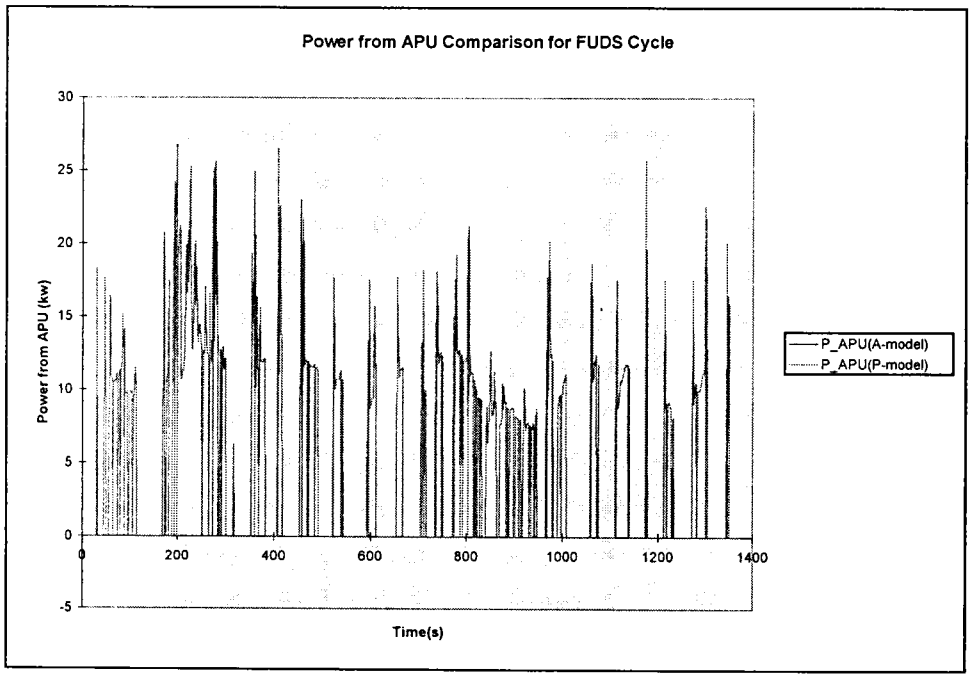
The direct output from the NEON parallel configuration is constructed in such a way that it would plot directly:

- achievable speed, mpha (miles/hour)
- power from APU for driving the vehicle
- power from ESS
- SOC
- battery current, I
- battery terminal voltage, V_terminal
- battery energy

The above outputs for both the FUDS and HIGHWAY schedules from both models are compared and plotted in fig.4.1 and fig.4.2. An analysis is made below.

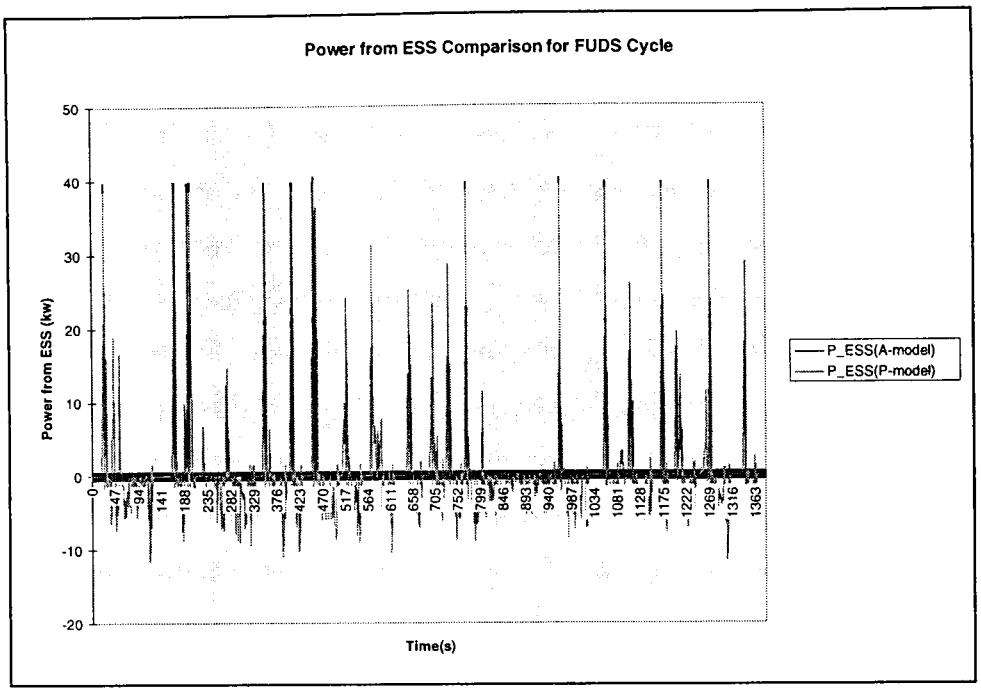


a. Achievable speed(mph)

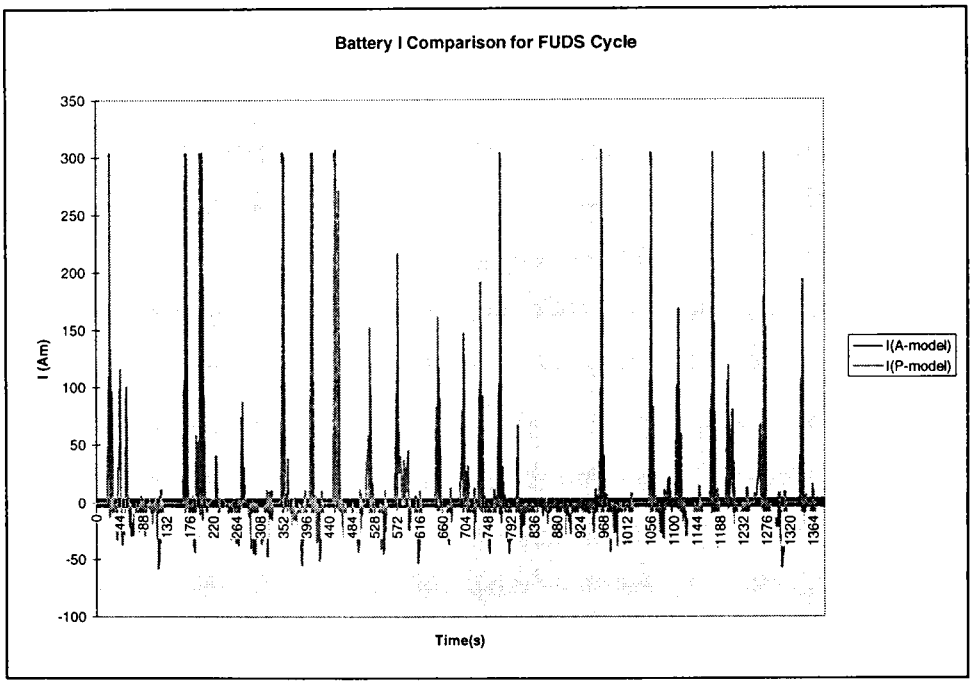


b. Power from APU

fig.4.1 Battery Model Validation Simulation in FUDS Cycle

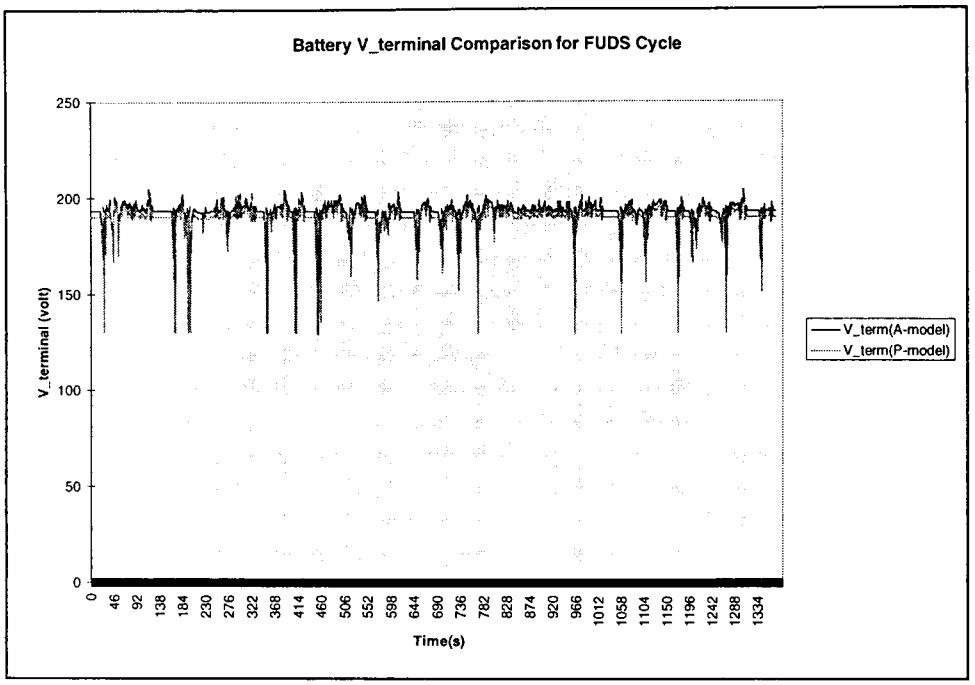


c. Power from ESS

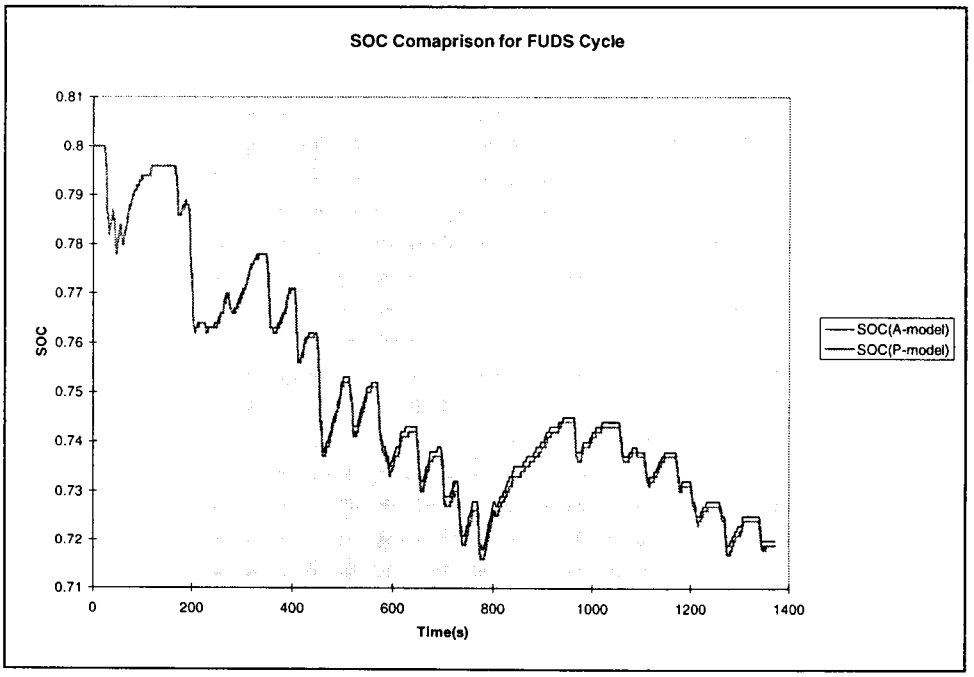


d. Battery current

fig.4.1 (Continued)

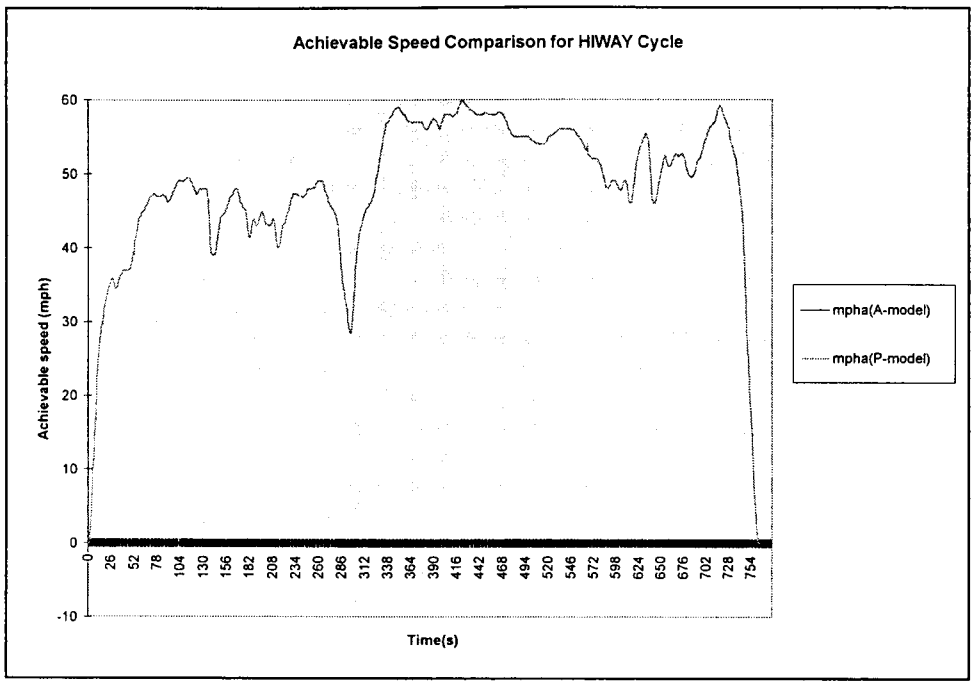


e. Battery terminal voltage

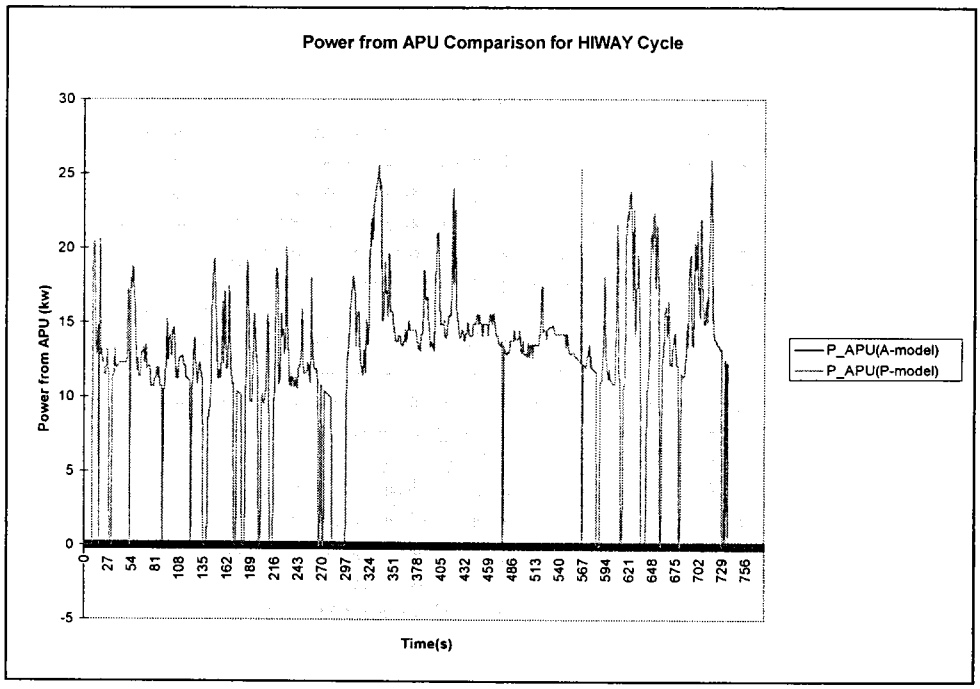


f. SOC

fig.4.1 (Continued)

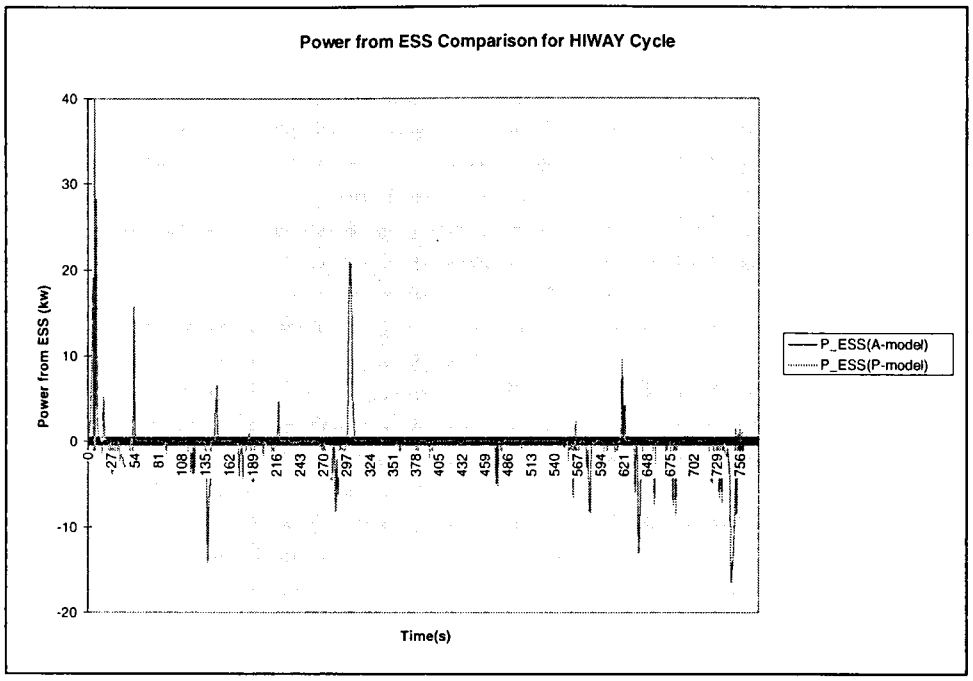


a. Achievable speed(mph)

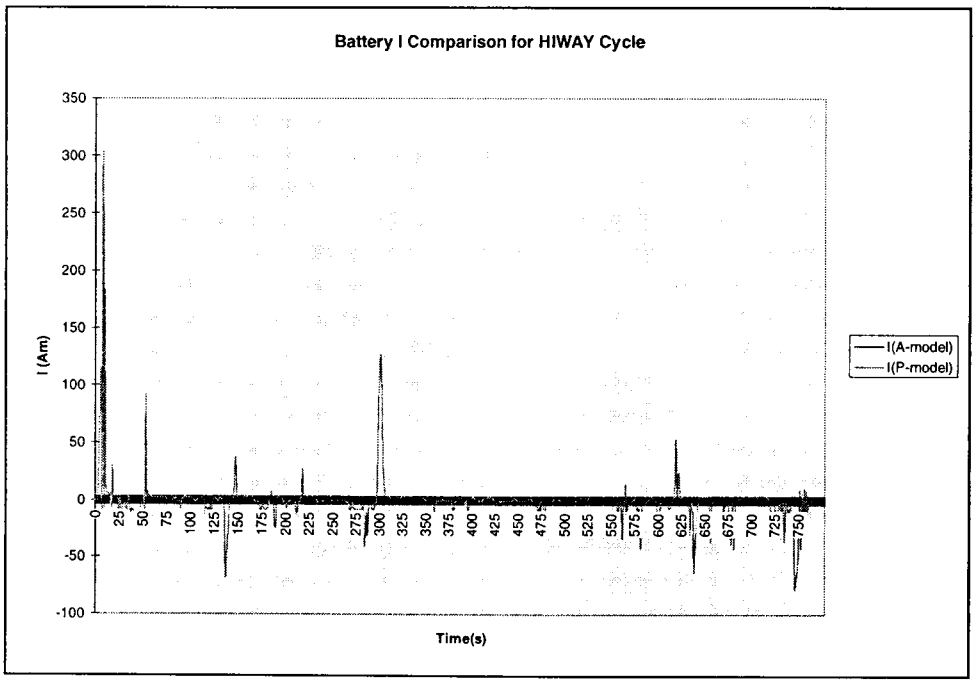


b. Power from APU

fig.4.2 Battery Model Validation Simulation in HIWAY Cycle

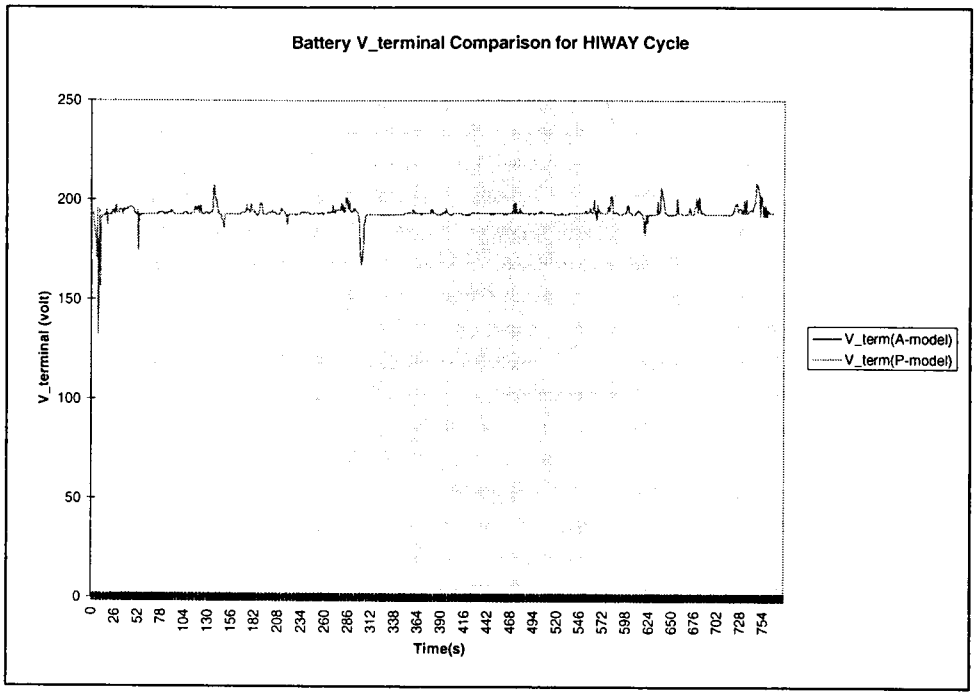


c. Power from ESS

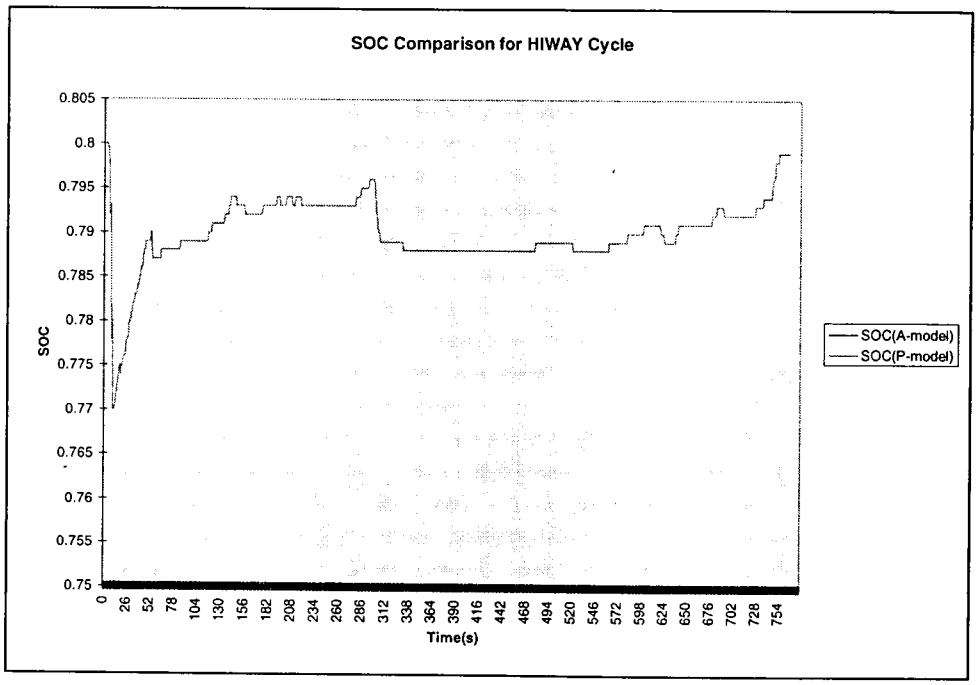


d. Battery current

fig.4.2 (Continued)



c. Battery terminal voltage



f. SOC

fig.4.2 (Continued)

2.1.1 Achievable speed and range

The achievable speed under FUDS and HIWAY cycles are plotted in fig.4.1a and fig.4.2a, it can be noticed that both battery models resulted in the vehicle meeting the specified speed-time target traces.

2.1.2 Power output and battery parameters

Fig.4.1b and fig.4.2b show the power output from the APU for driving the vehicle in FUDS and HIWAY cycle respectively. Again, they are the same for both models.

The power output from the ESS during FUDS cycle is plotted in fig4.1c. It can be seen that there is only slight disagreement between the output from the A-model and the P-model. Difference can be observed from the terminal voltage output and the battery current output for FUDS cycle in fig. 4.1d and fig.4.1e. The difference is also reflected by the SOC comparison as shown in fig.4.1f.

However, in HIWAY cycle, from fig.4.2c we can see that the power taken from ESS are identical for both model outputs. The same is true with the current and the terminal voltage output curves from the two models as shown in fig.4.2d and fig.4.2e. Therefore the SOC values for the two models are the same as shown in fig.4.2f.

The output differences as observed from the FUDS cycle for V-terminal, I, P-ESS and SOC between the P-model and the A-model are caused by the approximations in generating the Voc and R for the ADVISOR battery model from the V_terminal and I curve as used for the Practical model. However, the difference is small, maximum difference in V_treminal is about 2 V which leads to the SOC differs by 0.01. Therefore, it can be negligible for our analysis. We can say that the two models are basically in good agreement in generating the output from the given input. The P-model is validated for use in the battery simulation.

3. NEON Simulation

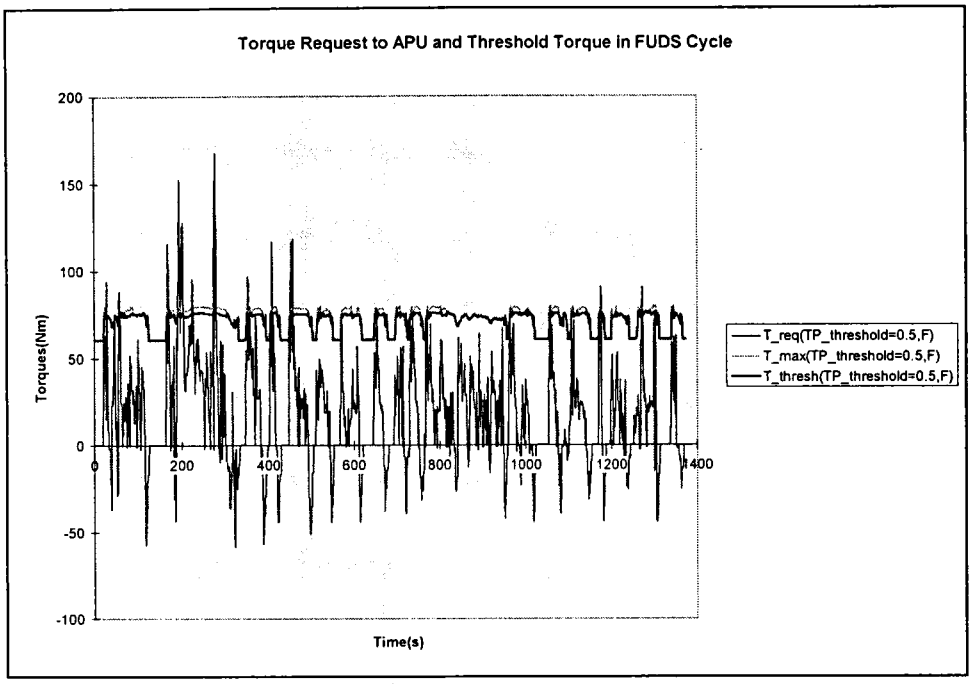
3.1 NEON Model Parameter

For a given vehicle configuration and control scheme, the vehicle performance is determined by the power provided for driving the vehicle. As far as the power control concerned, one characteristic of the NEON is that it incorporates regeneration and regenerative braking into the control scheme. The regeneration, regenerative braking and ESS assist are all controlled by the position of the throttle. Regeneration can occur when the APU can provide extra power to charge the battery other than driving the vehicle. The threshold power of the APU for both driving the vehicle and regeneration is set at the power output corresponding to the throttle position at 50% of the full operating range of the throttle, as described in chapter 3. For the given configuration of the NEON, the total torque requests to the APU and the ESS, and the threshold torques for regeneration during both the FUDS and HIWAY cycles are plotted in fig.4.3. Also plotted in the figure is the maximum torques of the APU at the given speed, which are linearly associated with threshold torque based on the analysis in chapter 3 (see fig.3.17 and fig.3.18) It is clear that for most of the cycle, the positive torque requests are below the threshold torque, therefore regeneration could occur. The occurrences of ESS assist can also be identified as they take place in the regions where the torque requests are greater than the threshold torque. When the torque request is negative, regenerative braking would be effective.

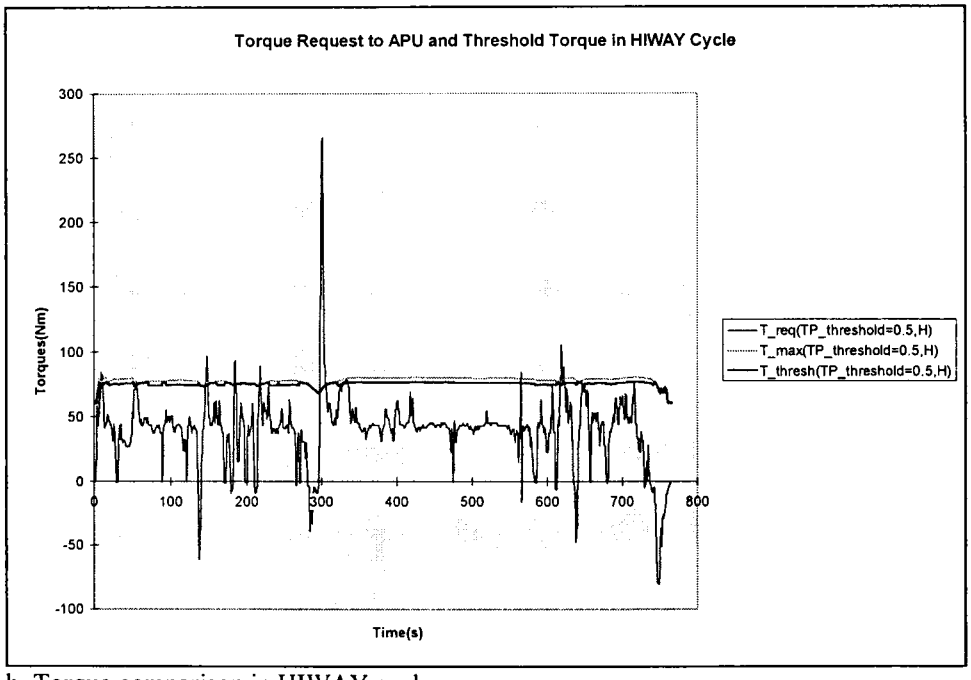
3.2 Basic model for simulation

The purpose of the simulation is to estimate the effects of different control parameters on the performance of the vehicle in terms of speed, acceleration, power consumption from the APU for driving the vehicle, power from the ESS, battery terminal voltage and current, as well as the SOC. Some other parameters representing the vehicle performance are also analyzed.

It should be noted that the power from the APU is plotted for the power used for driving the vehicle. The total power from the APU may differ from this power when regeneration occur. In that case the total power would be the threshold power of the APU while the power for driving the vehicle would be determined by the requested power from the wheel load. For the purpose of our analysis, the power for driving the vehicle



a. Torque comparison in FUDS cycle



b. Torque comparison in HIWAY cycle

fig.4.3 Comparison of Torque Request to APU & ESS vs APU Threshold torque

is of most concern since it determines the vehicle speed and acceleration. The total power output from the APU is relevant to the calculation of the fuel consumption and the emissions which are not the focus of study of this thesis.

The configuration of the vehicle as a basis for the parametric analysis of the vehicle performance would be of the model representing NEON components and control scheme. The vehicle components would be the same as listed in section 2.1 of this chapter. The major parameters affecting the power control is set up as shown below by default, which is the basis of parametric analysis.

regeneration=1;

regen_level=1;

APU_trq_scale=1;

SOCinit=0.8, SOC=0.2~0.8 for regeneration, SOC=0.2~1 for regenerative braking;

TP_threshold=0.5;

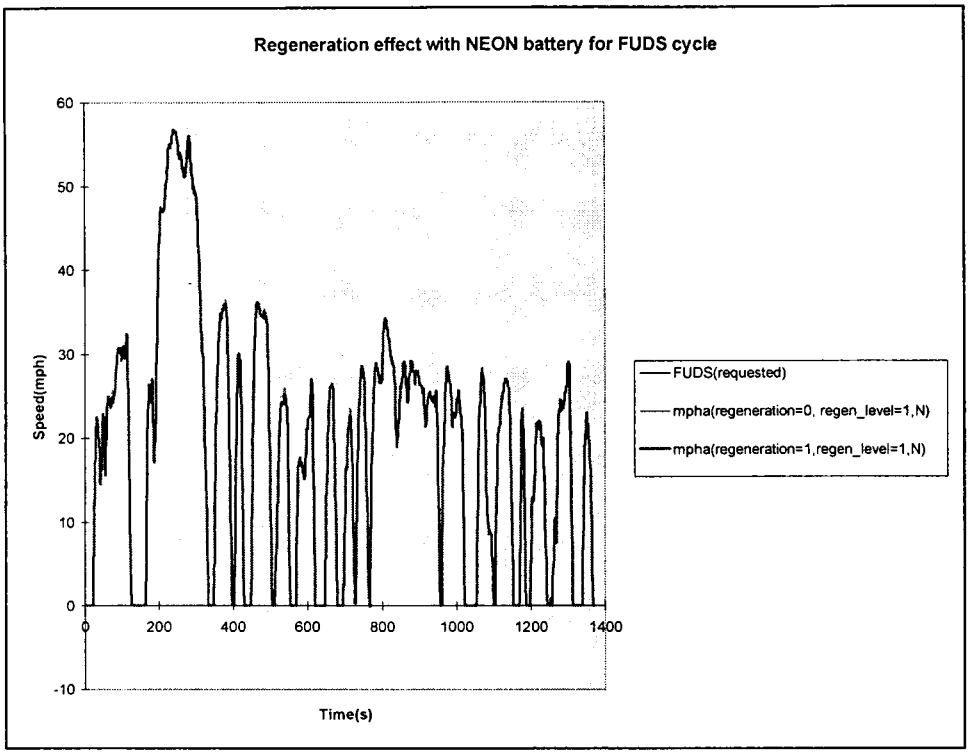
3.3. Parametric Analysis

Major parameters analyzed below concerning the vehicle power control including the APU power capacity, regeneration, regenerative braking effect, threshold position for ESS assist and regeneration, SOC of the battery, battery capacity and transmission. Other parameters such as torque output from the APU will also be analyzed when necessary.

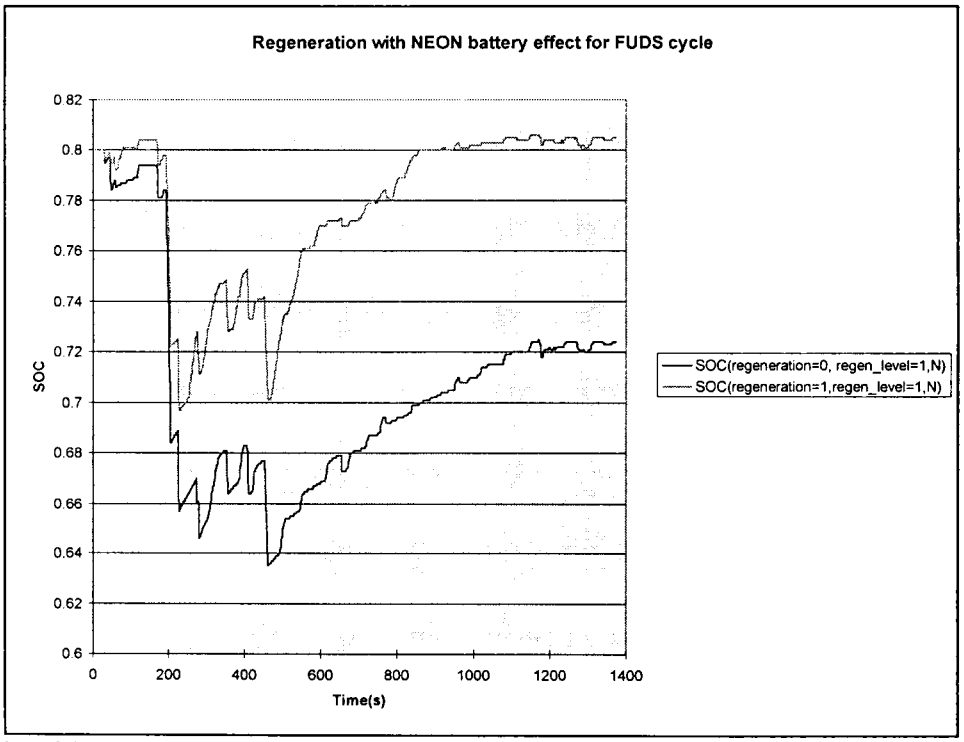
3.3.1 Regeneration

Regeneration is incorporated into the control strategy of the NEON and is represented by the parameter, regeneration, in the simulation model. Regeneration is controlled by setting the value of regeneration at 0 or 1, which enables or disables regeneration. Under the NEON configuration, SOC is controlled to be within 0.2 to 0.8 for regeneration, and from 0.2 to 1 for regenerative braking energy recovery. Plots of the output parameters with and without regeneration are shown in fig.4.4 for the FUDS cycle and in fig.4.5 for the HIWAY cycle. From the plots, it can be observed that

- Regeneration has no effect on the ability of the vehicle to follow the cycle, the requested speed is achieved when regeneration is enabled or disabled;

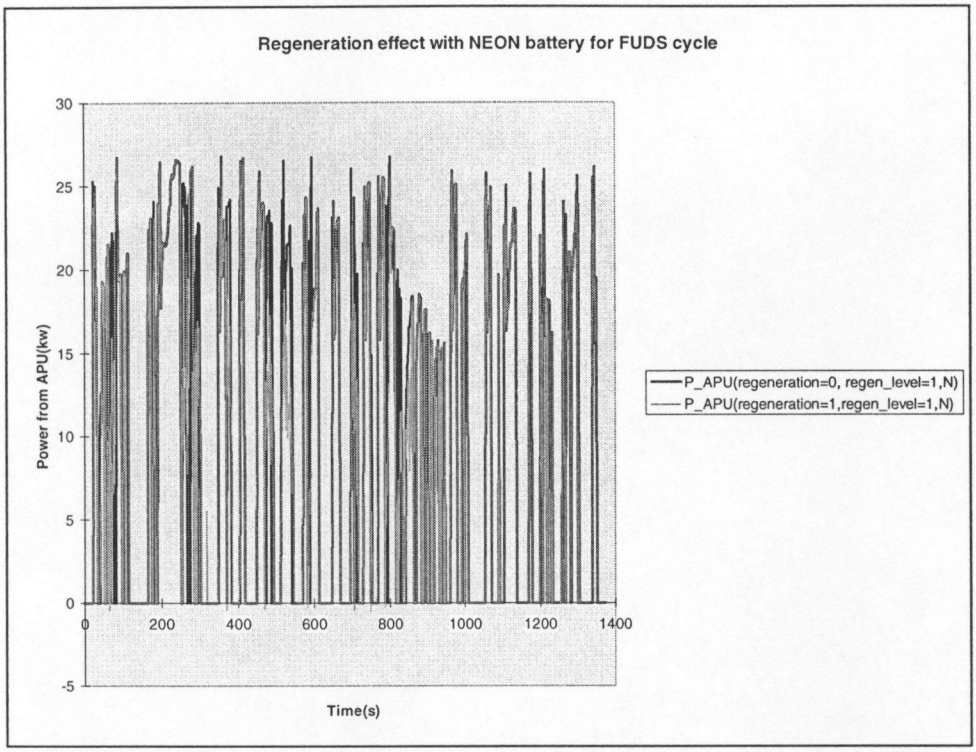


a. Achievable speed

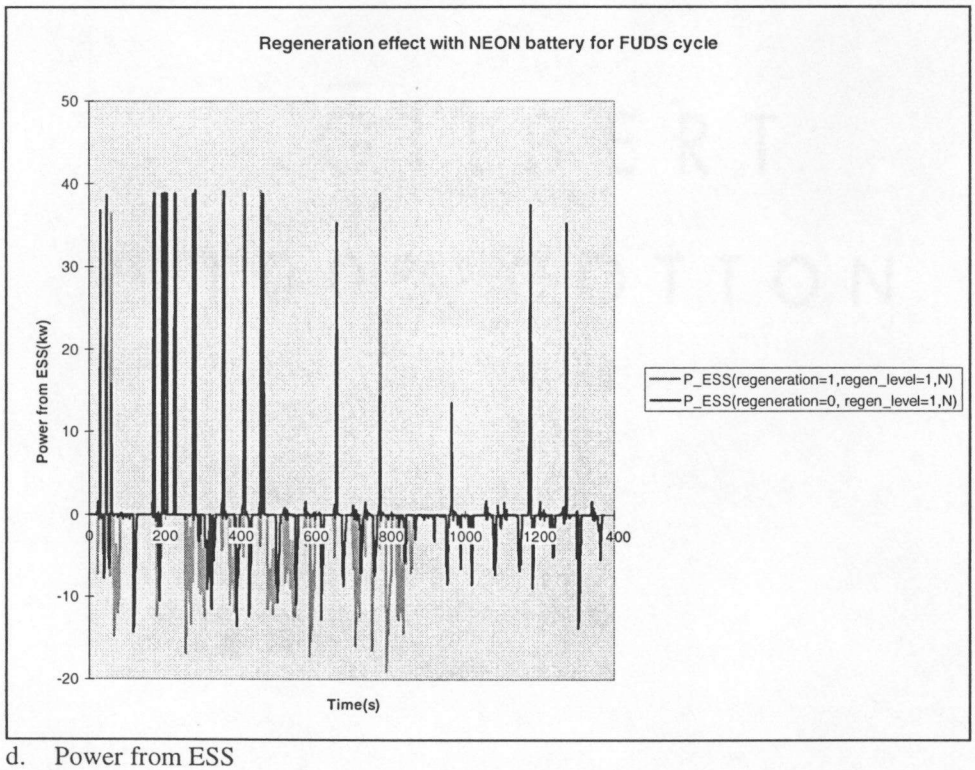


b. SOC

fig.4.4 Regeneration Effect with NEON Battery for FUDS Cycle

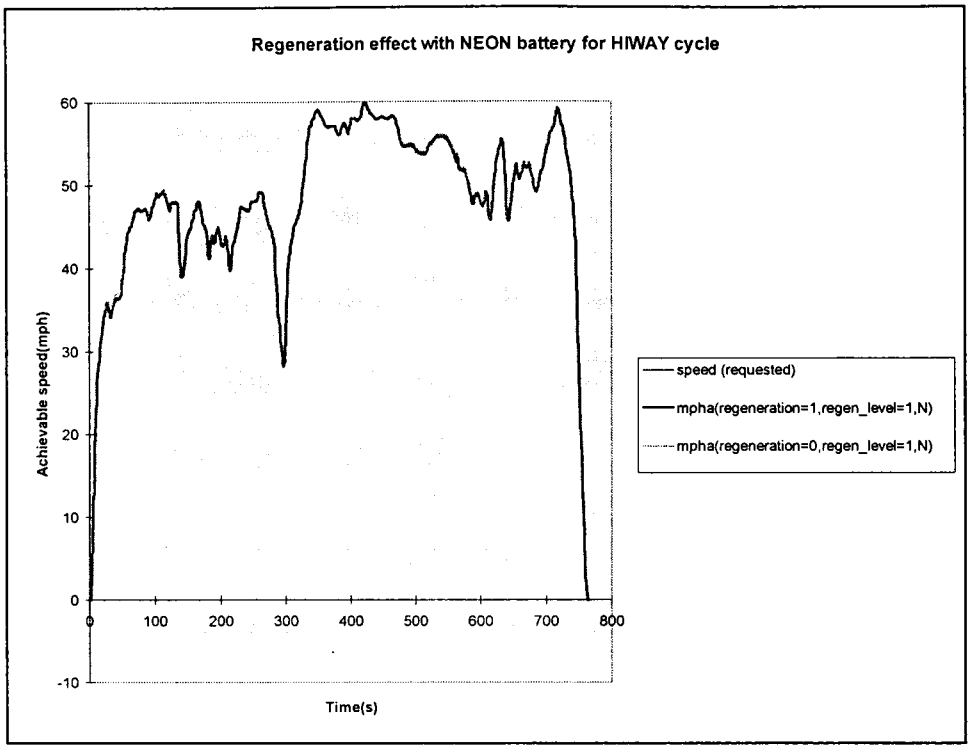


c. Power from APU

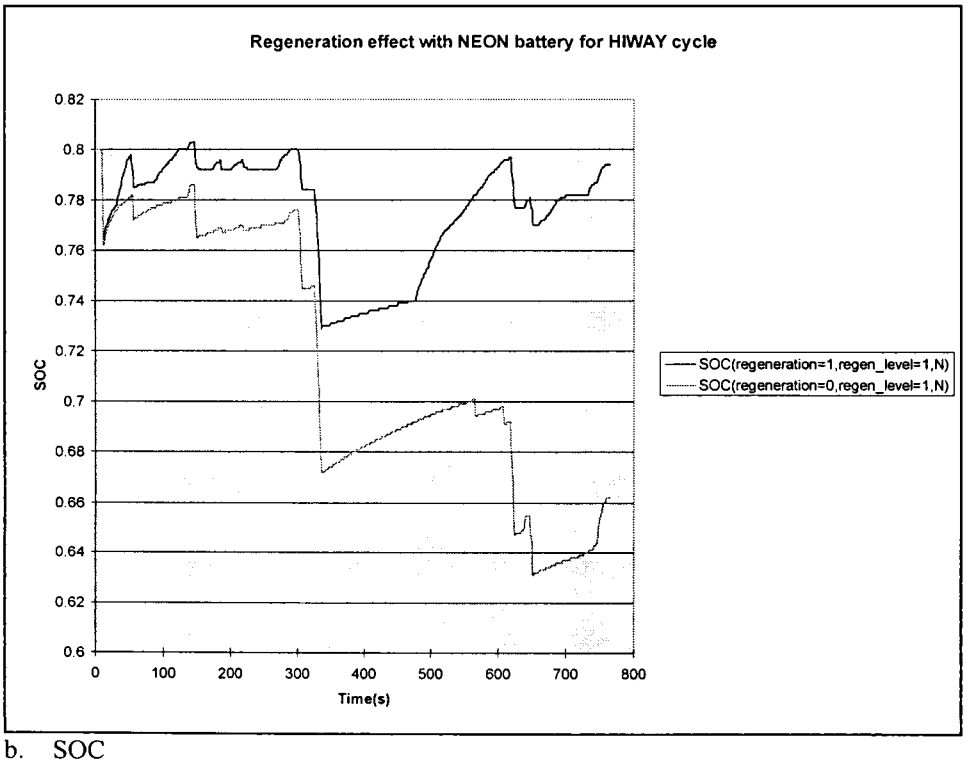


d. Power from ESS

fig.4.4 (Continued)

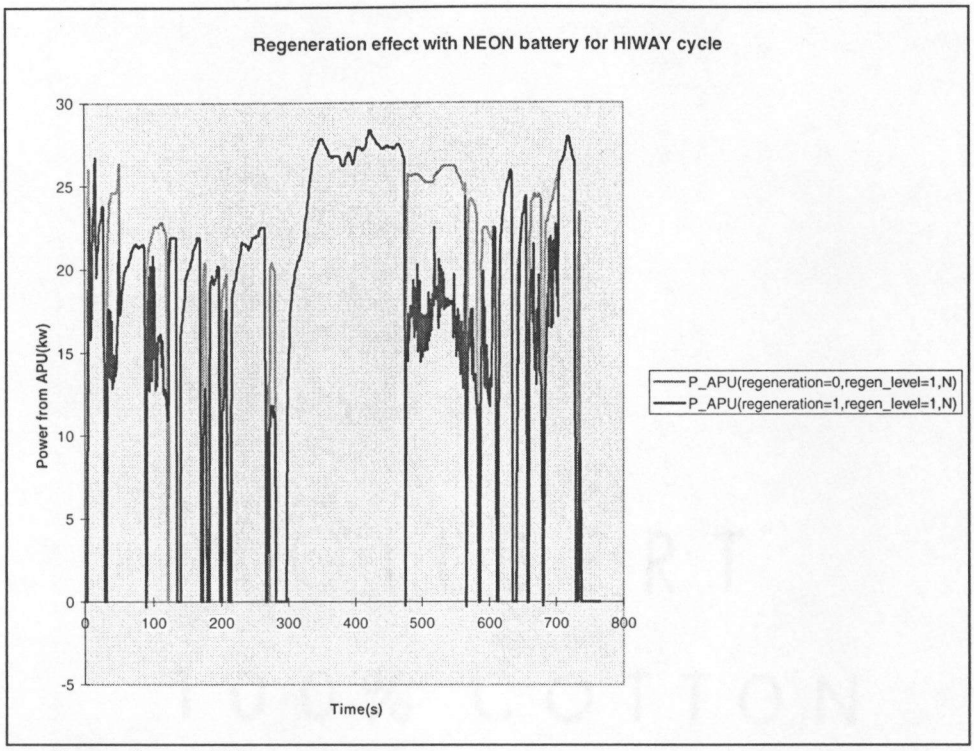


a. Achievable speed

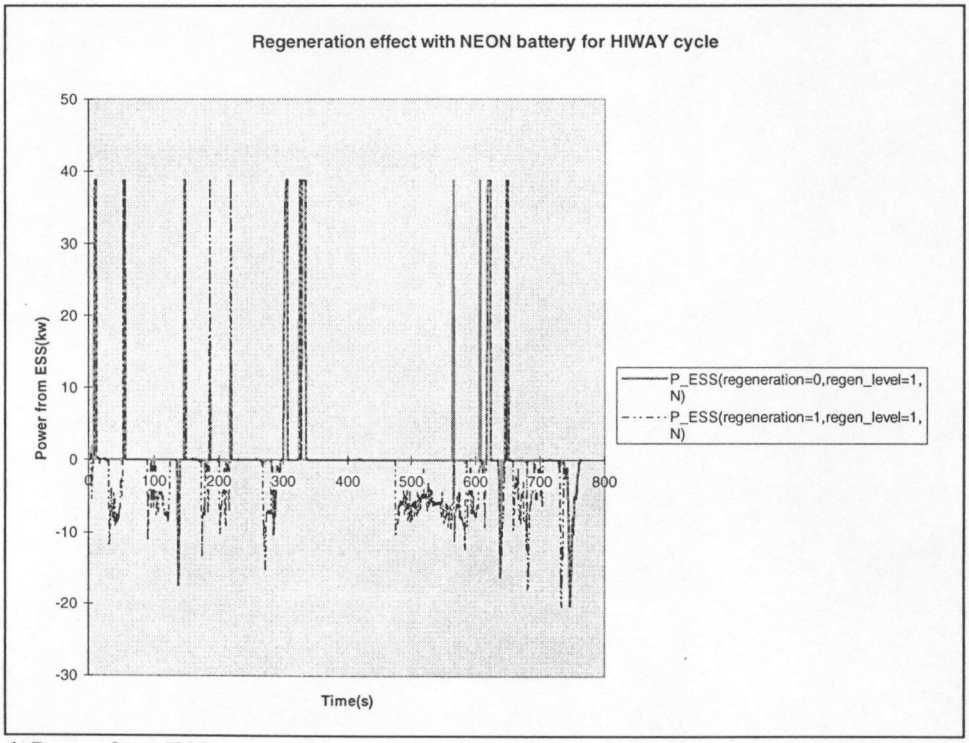


b. SOC

fig.4.5 Regeneration Effect with NEON Battery for HIWAY Cycle



c. Power from APU



d. Power from ESS

fig.4.5 (Continued)

This is because that for the given APU and the initial SOC condition, there is enough power from the APU and the ESS for driving the vehicle.

- Regeneration affects the APU power output;

  Regeneration affects the power required from APU because when regeneration occurs, the APU power for driving the vehicle is the requested power from the wheel load, and the total power delivered from the APU is the threshold power. Therefore, the APU power curves and the throttle position curves are different depending on whether or not regeneration is used.

- Regeneration affects the ESS power;

  Since the battery SOC during the whole cycle is different with regeneration, the battery terminal voltage and current curves are different. As a result, the power from the battery may be different. From the current and the ESS power curves, we can see that there is a significant difference between the negative portion of the current and the ESS power when regeneration is enabled as compared to when it is disabled.

- SOC recovery

  With regeneration and regenerative braking, the SOC is regained in the FUDS cycle as shown in fig.4.4(b) and not fully recovered in the HIWAY cycle as indicated in fig.4.5(b). From the SOC curve, it can also be seen that more ESS assist is provided in the FUDS cycle since SOC goes lower in fig.4.4(b) than that in fig.4.5(b). Without regeneration the SOC can not be fully recovered for either cycle.

- Regeneration effect with different battery

  As to the regeneration effect on the SOC, the battery capacity or battery type should be considered since the purpose of regeneration is to maintain the battery SOC during the driving cycle. The battery SOC changes are affected not only by the power withdrawal or power input to the battery but also by the total capacity of the battery itself. As indicated in the analysis of the previous chapter, the SOC is a relative measure of the battery's remaining capacity. For different batteries, the SOC change may be different for the same driving cycle.

Simulations are made with the H12N85 HORIZON battery for comparison as shown in fig.4.6 and fig.4.7 for FUDS cycle and HIWAY cycle respectively. By comparison of fig. 4.4(b) with fig. 4.6(b), and fig. 4.5(b) with fig. 4.7(b), it can be seen that the SOC varies slightly for the H12N85 battery in both cycles, and the final SOC value regained from regenerative braking and with or without regeneration is higher than with the NEON battery. This is because the H12N85 has a higher capacity (maximum 85 Ah) than the NEON battery (maximum 25 Ah). For the same amount of power output, the SOC changes would be smaller for the HORIZON battery.

3.3.2 Effect of regenerative braking energy recovery level

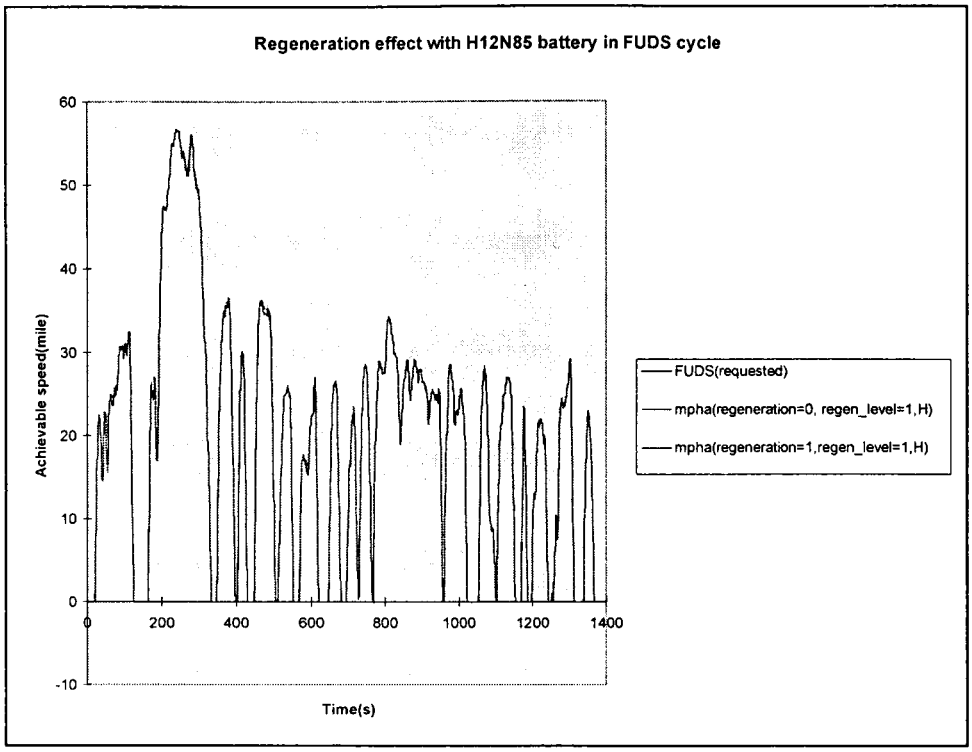
Simulations can be run using different assumptions about the level of the regenerative braking energy recovery. That is, it can be assumed that the negative torque range of the motor could be identical to the positive torque range, or the magnitude of the negative torque could be only a fraction of the positive torque. The level of the regenerative braking is dictated by the control parameter, regen_level, which can be set from 0 to 1 continuously for scaling down the torque. Plots of the output parameters from the simulations are shown in fig.4.8 and fig.4.9 for both cycles with regen_level set at 0, 0.5 and 1. For the maximum regenerative braking energy recovery, the SOChi is set at 1 instead of 0.8 as in the regeneration analysis. This is to make maximum use of the regenerative braking energy.

The occurrence of regenerative braking can be seen in fig4.3(a) and fig.4.3(b) whenever the torque request is negative. It can be noticed that in the FUDS cycle, regenerative braking take place more frequently than in the HIWAY cycle. From fig.4.8 and fig.4.9, it can be noticed that:

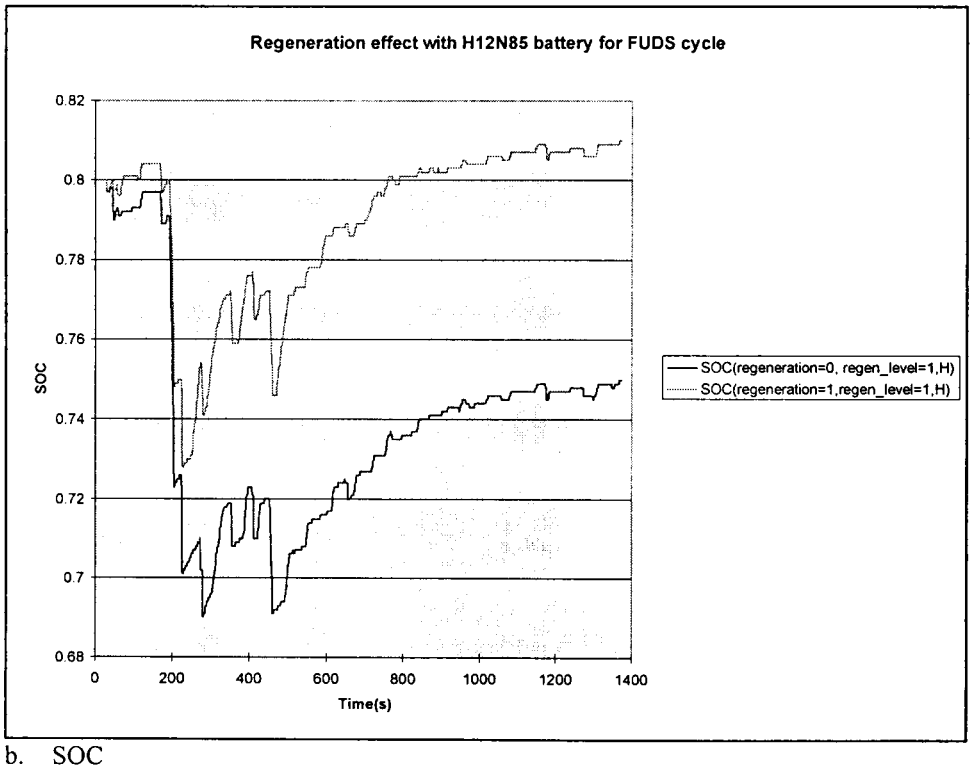
- the *regen_level* has negligible effect on the achievable speed, and therefore the actual range;

  The speed profile is achieved because at the given APU power capacity and the battery SOC condition, i.e. SOC_init=0.8, sufficient power can be delivered from both the APU and the ESS for both cycles no matter how high the regenerative braking level is, or whether it is totally canceled.

  when regenerative braking is in effect, curves of power from ESS, power from APU and hence, the throttle position are affected. The occurrence of the regenerative braking means that the throttle

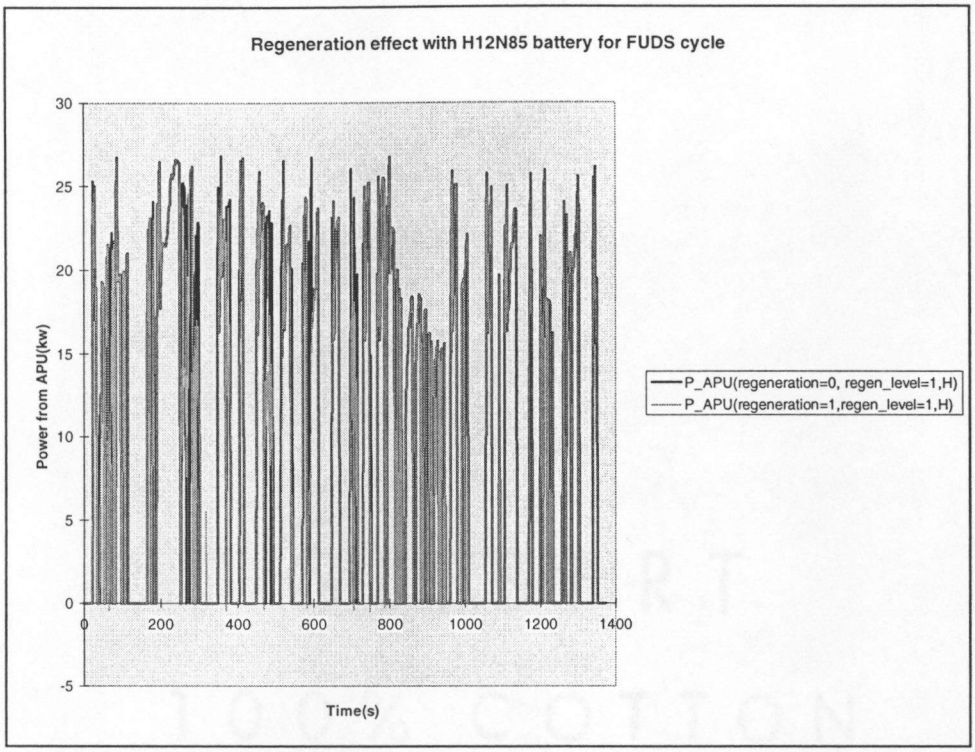


a. Achievable speed

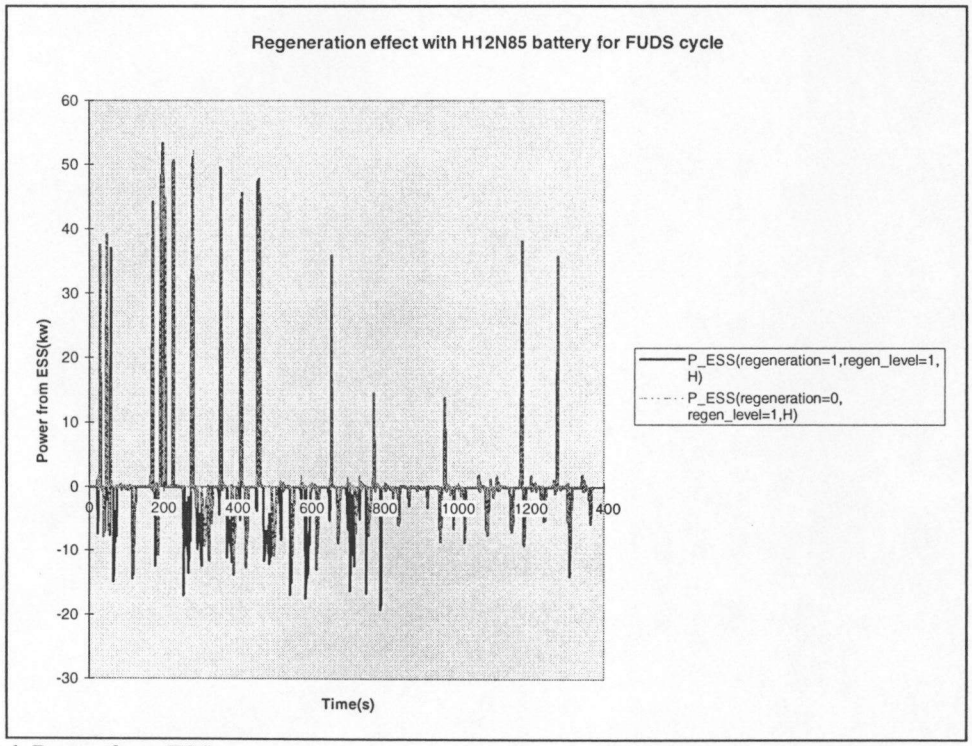


b. SOC

fig.4.6 Regeneration Effect with H12N85 Battery for FUDS Cycle

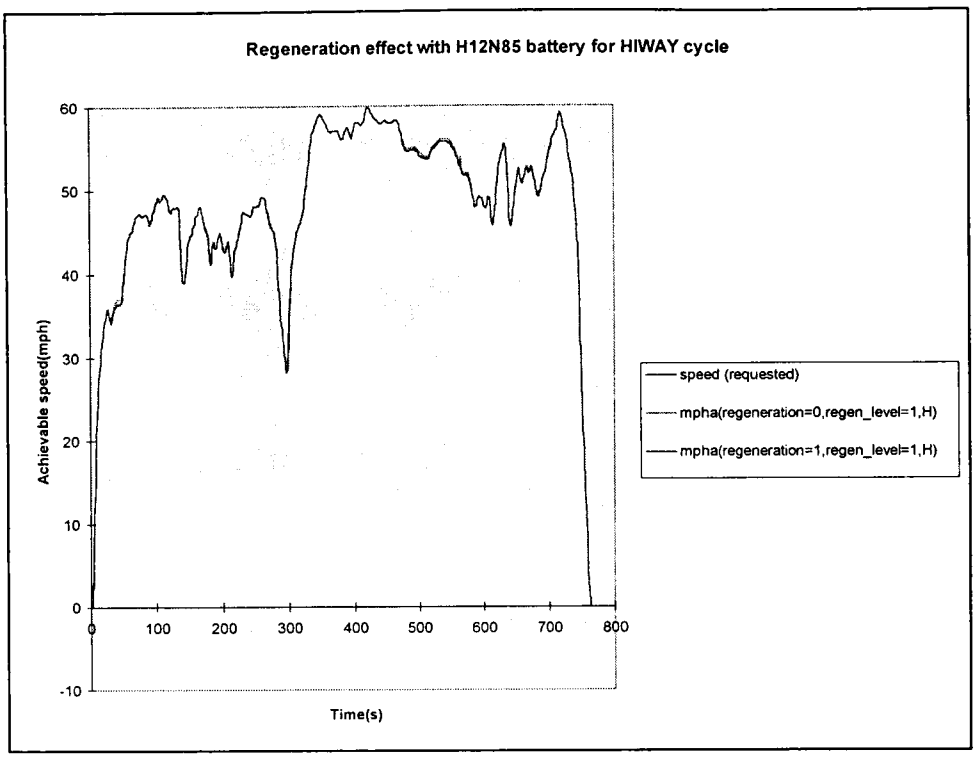


c. Power from APU

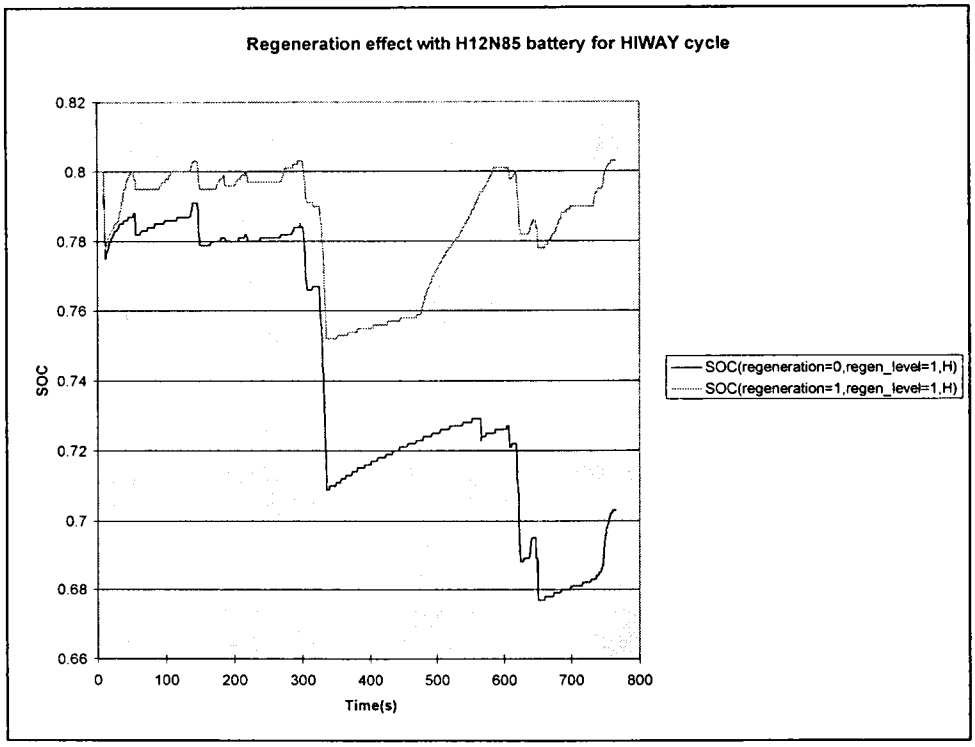


d. Power from ESS

fig.4.6 (Continued)

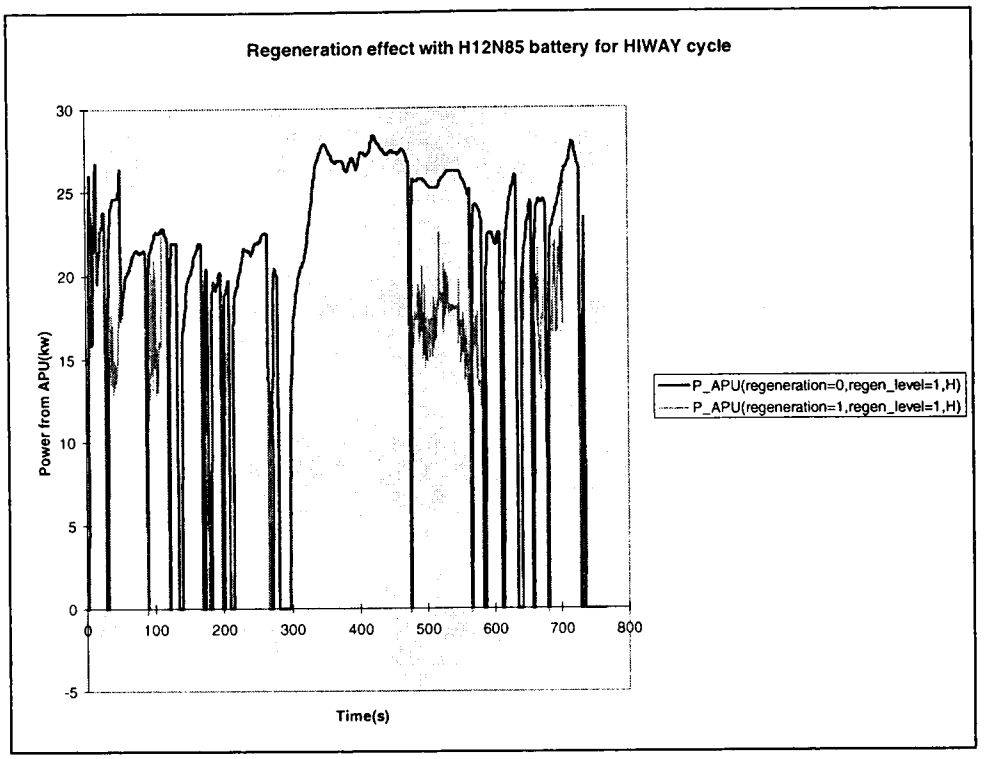


a. Achievable speed

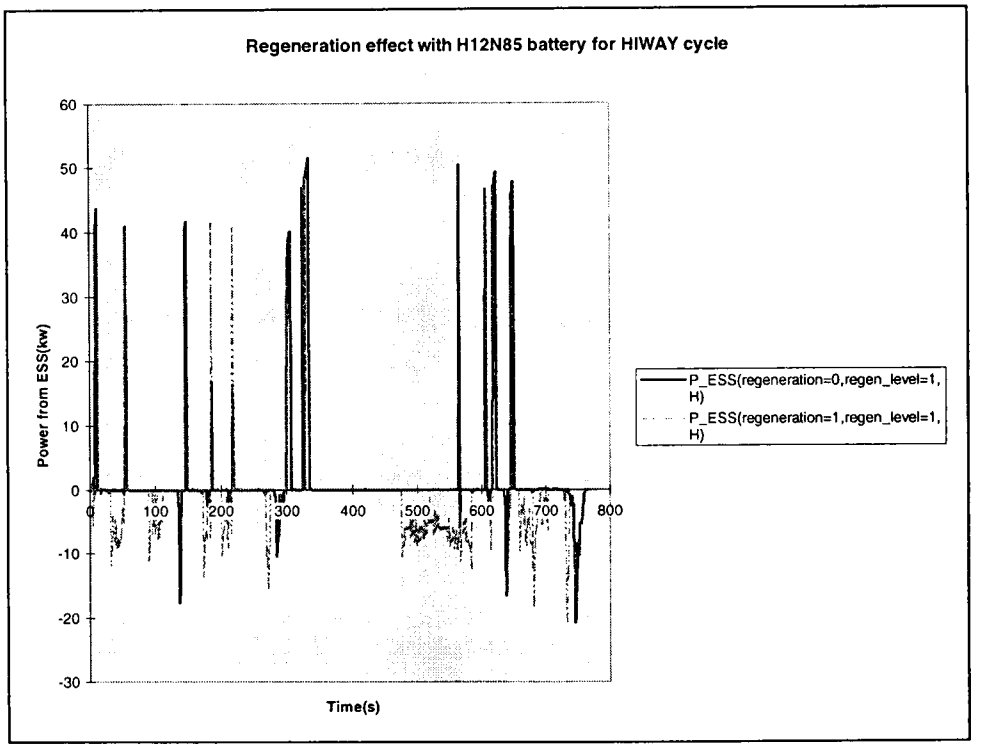


b. SOC

fig.4.7 Regeneration Effect with H12N85 Battery for HIWAY Cycle

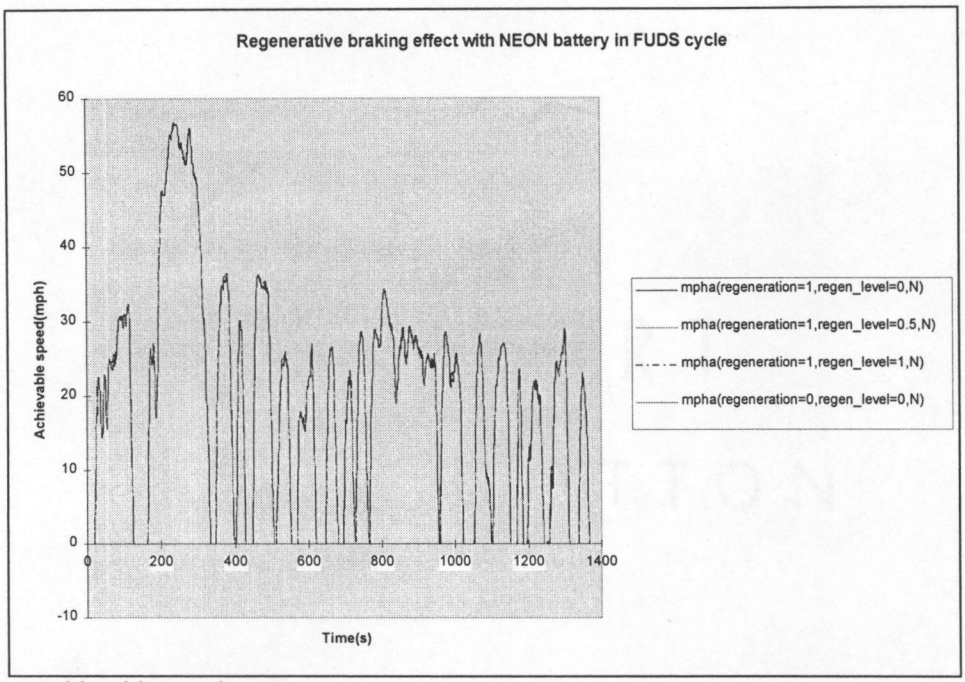


c. Power from APU

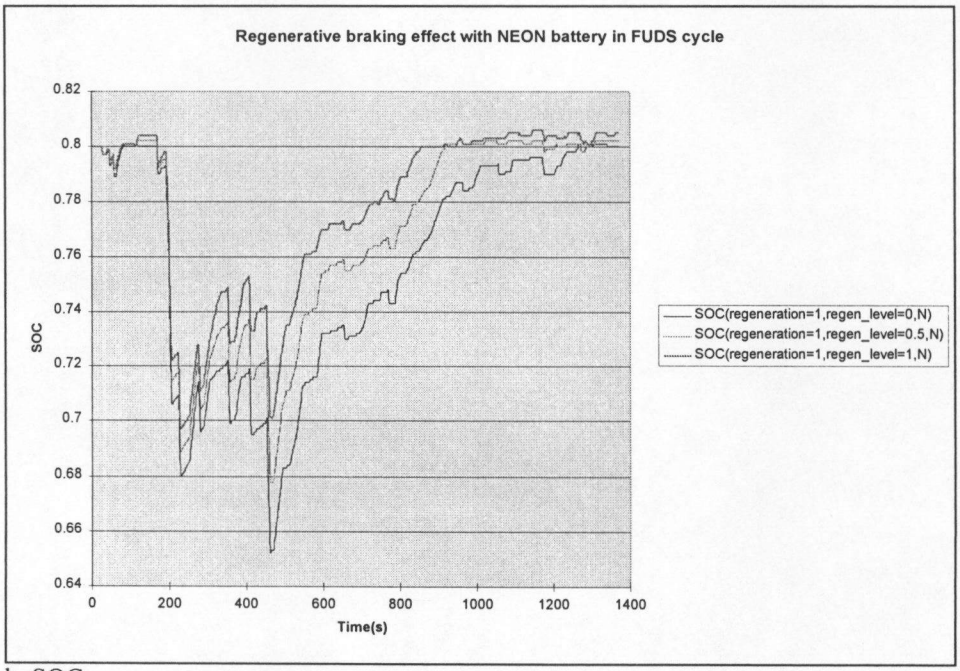


d. Power from ESS

fig.4.7 (Continued)

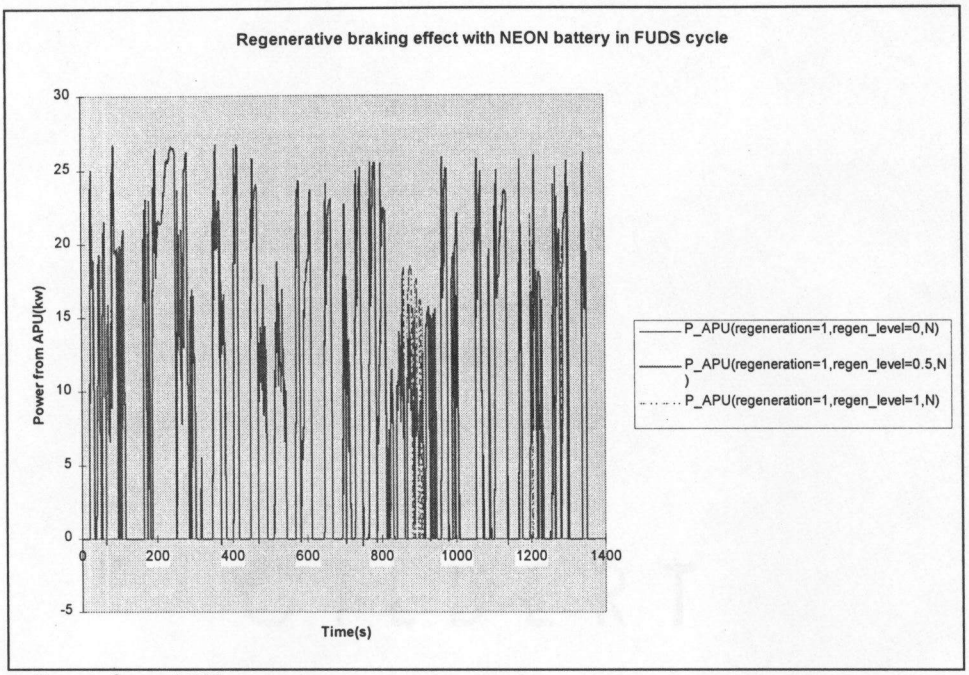


a. Achievable speed

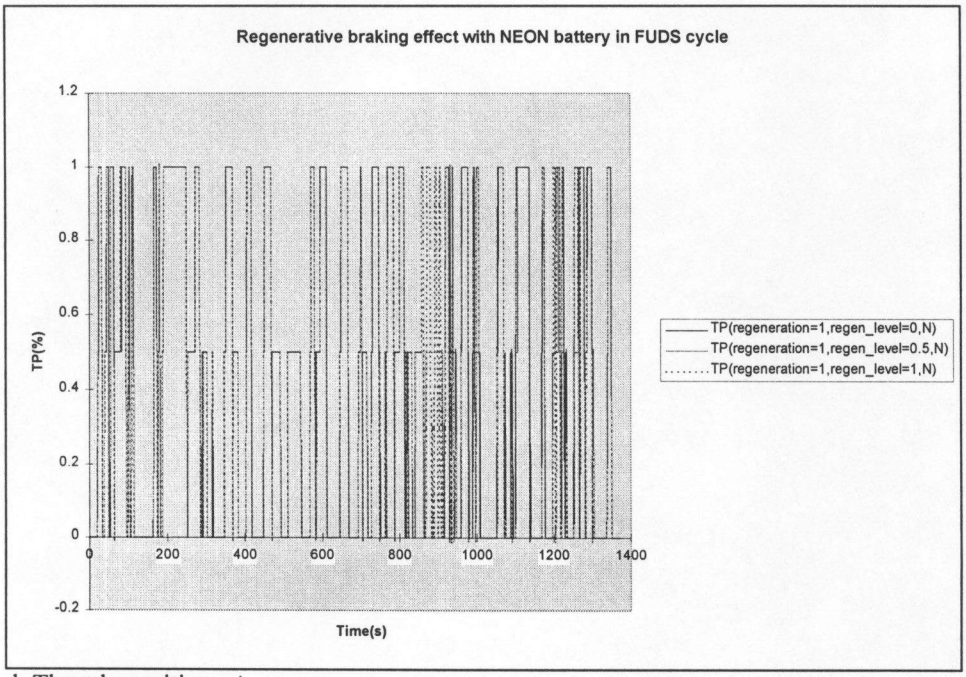


b. SOC

fig.4.8 Regenerative Braking Effect with NEON Battery for FUDS Cycle

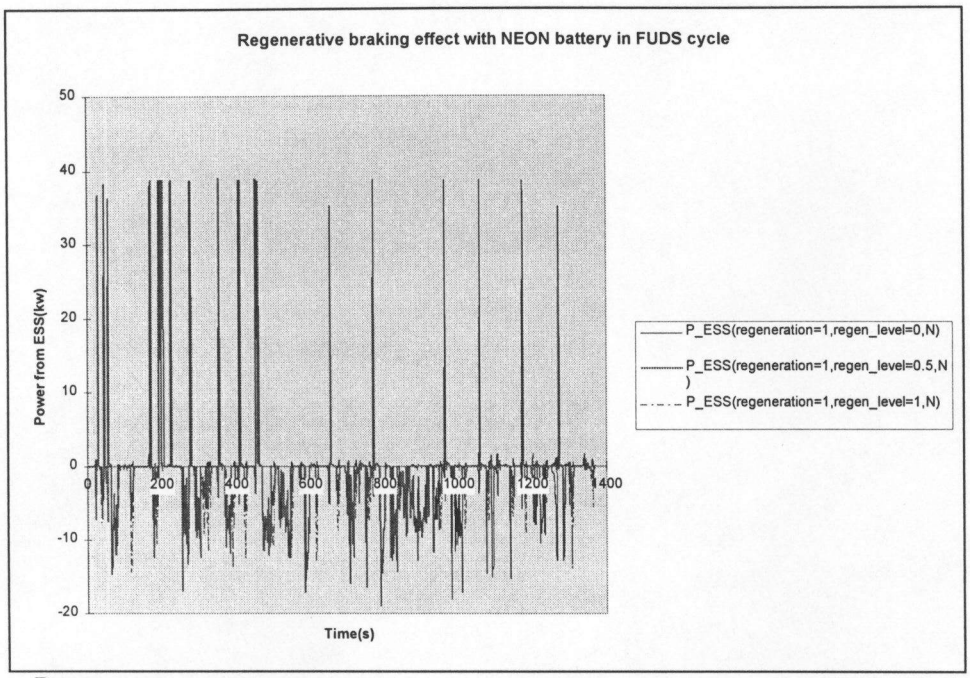


c. Power from APU

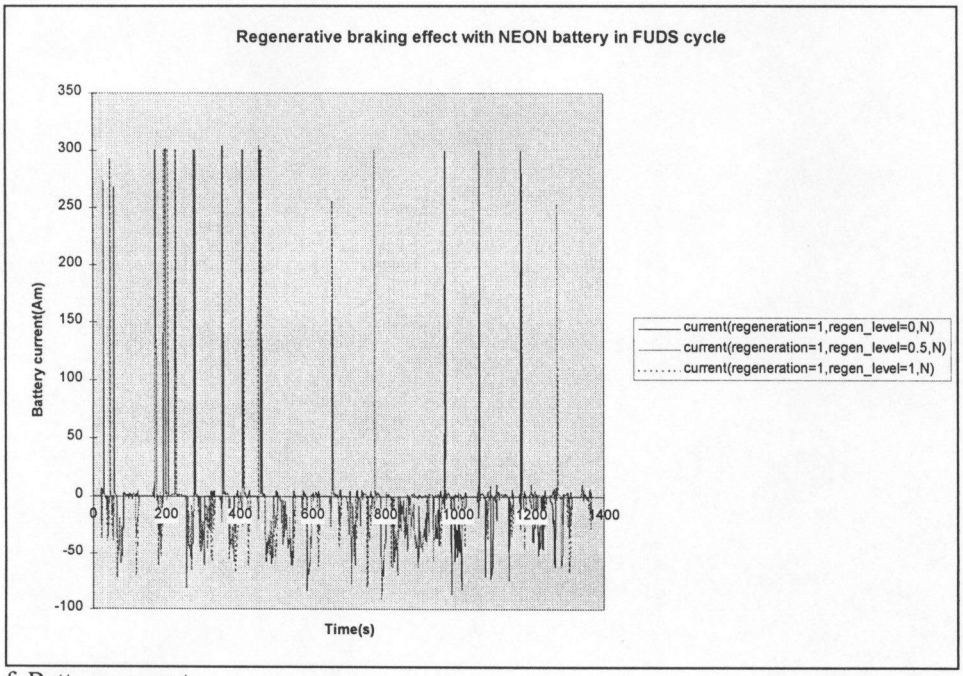


d. Throttle position

fig.4.8 (Continued)

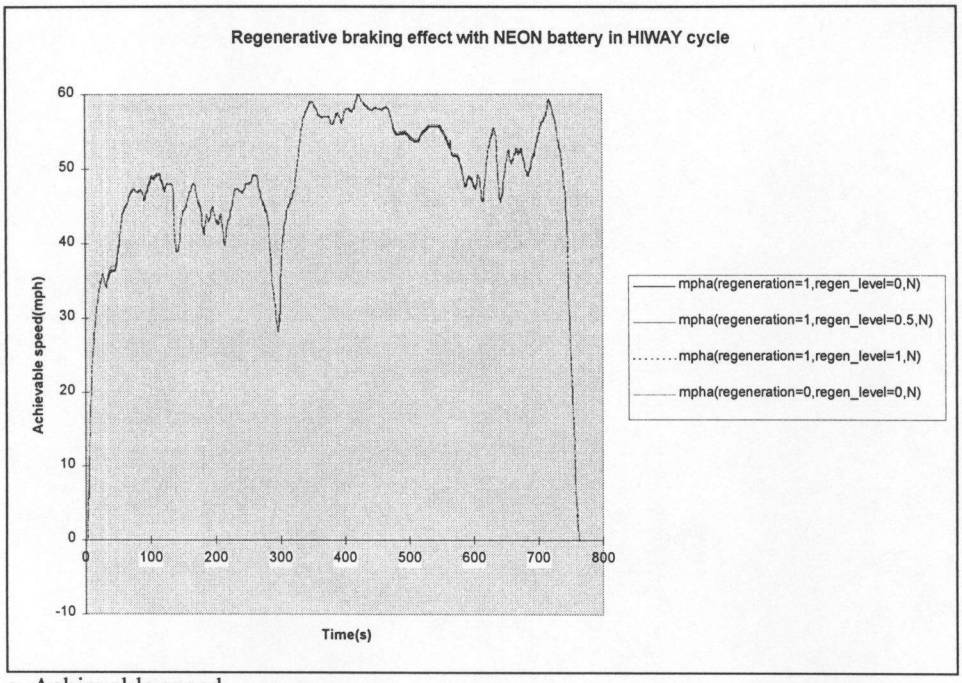


e. Battery power

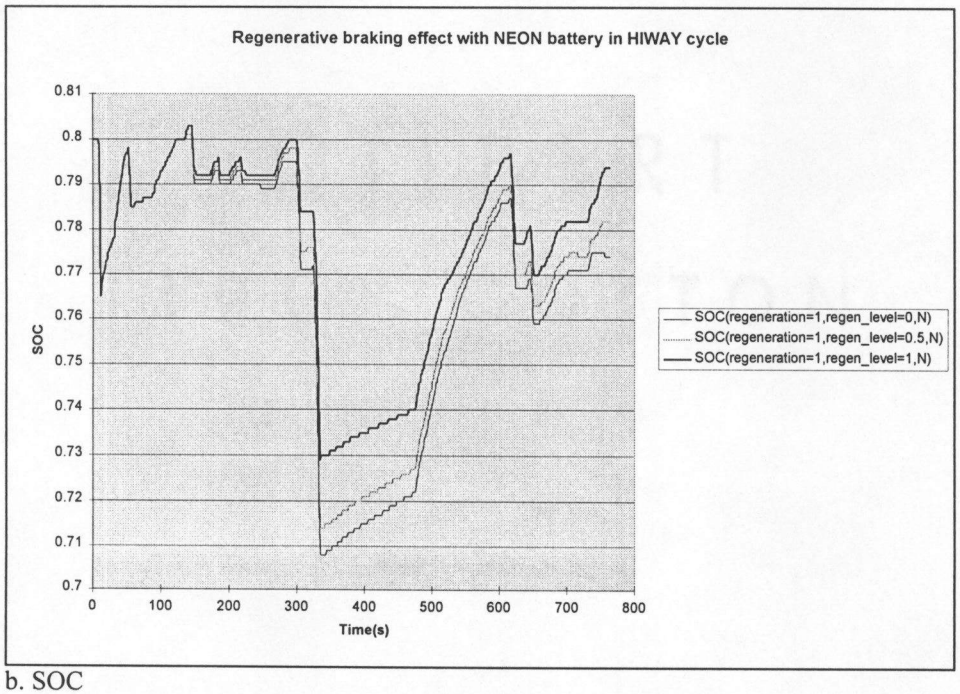


f. Battery current

fig.4.8 (Continued)

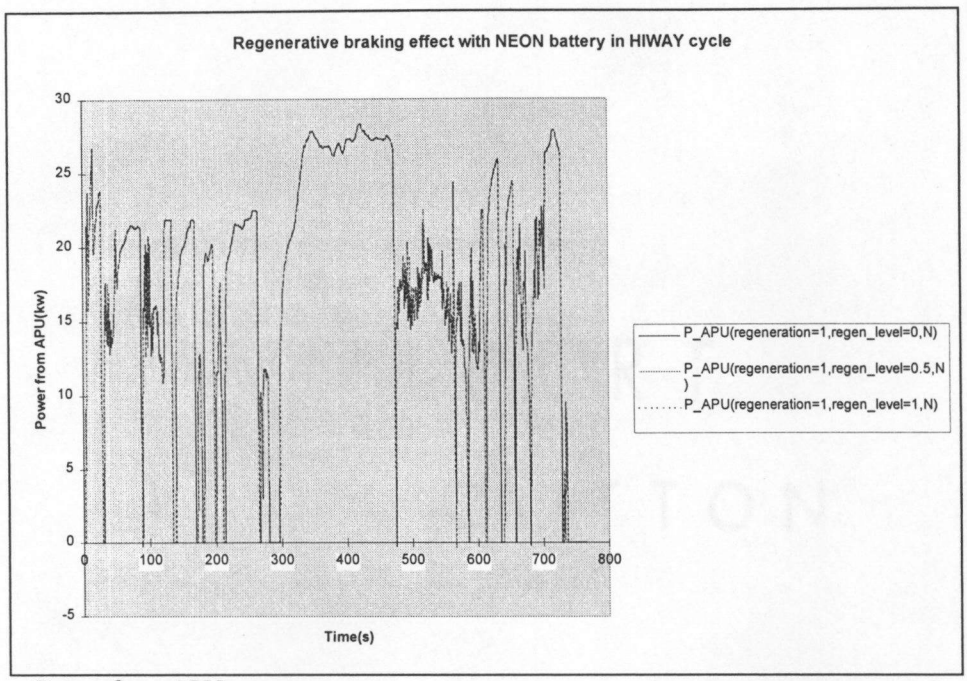


a. Achievable speed

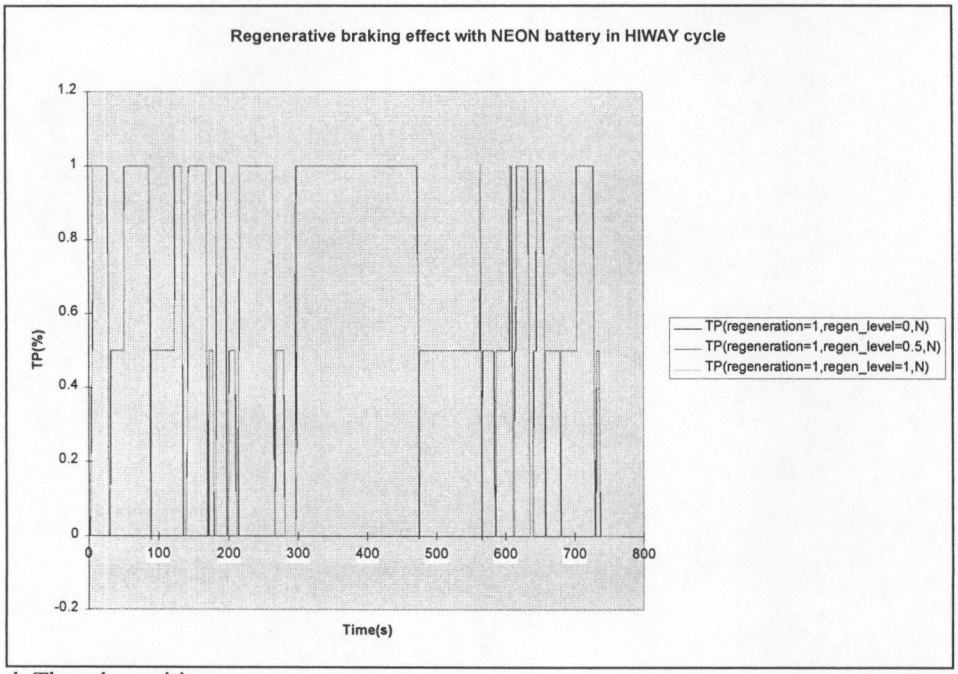


b. SOC

fig.4.9 Regenerative Braking Effect with NEON Battery for HIWAY Cycle

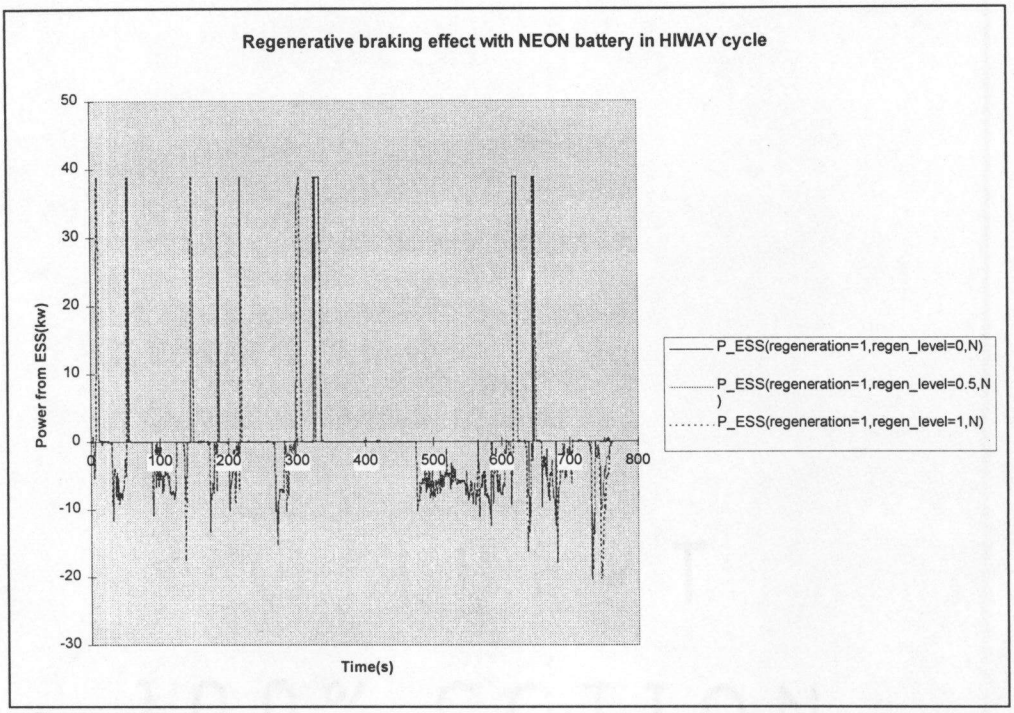


c. Power from APU

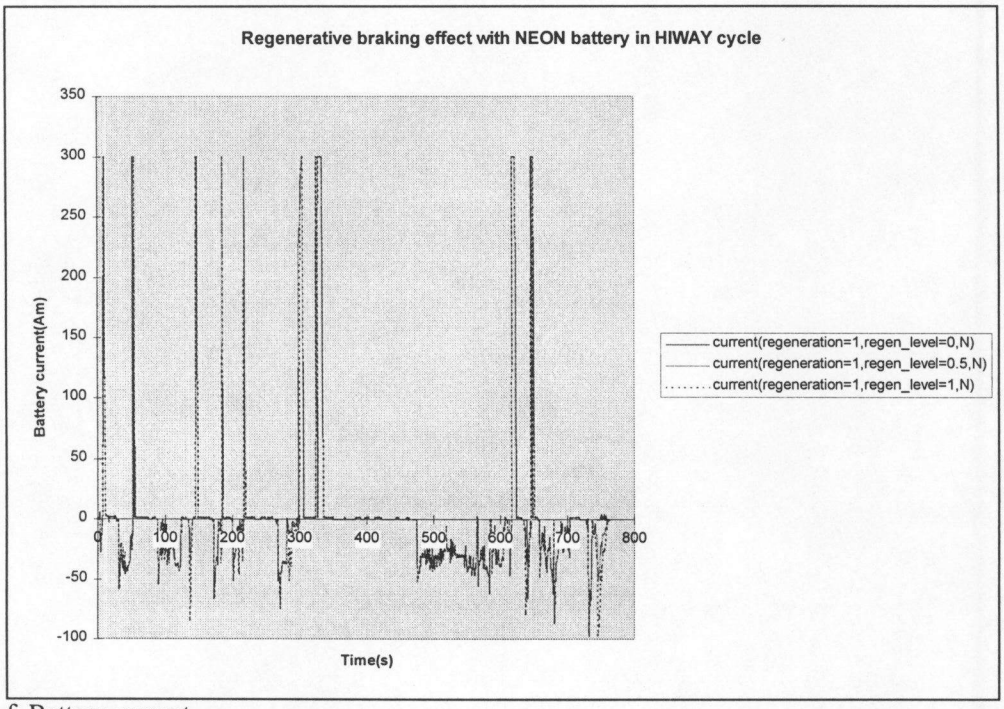


d. Throttle position

fig.4.9 (Continued)



e. Battery power



f. Battery current

fig.4.9 (Continued)

position, TP=0. As regen_level increases, more power is recovered to charge the battery. For most of the HIWAY cycle, the above curves are identical regardless of the regen_level except at several spots where regenerative braking energy is recovered at a different level. The *regen_level* would affect the SOC since energy recovered by the battery would be different for different regen_level, the SOC increases with increases of the regen_level. With the NEON battery in the FUDS cycle, when the regen_level is set at 0.5, the SOC value can be regained. However, the SOC is only partially recovered in the HIWAY cycle even when the regeneration and regen_level are both set at 1.

- Simulations are made with the H12N85 battery (fig.4.10 and fig.4.11) for the FUDS and HIWAY cycles, the SOC drops less and the final SOC regained is higher than in the case with NEON battery.

3.3.3 Comparison for regeneration and regenerative braking effect on SOC and power output

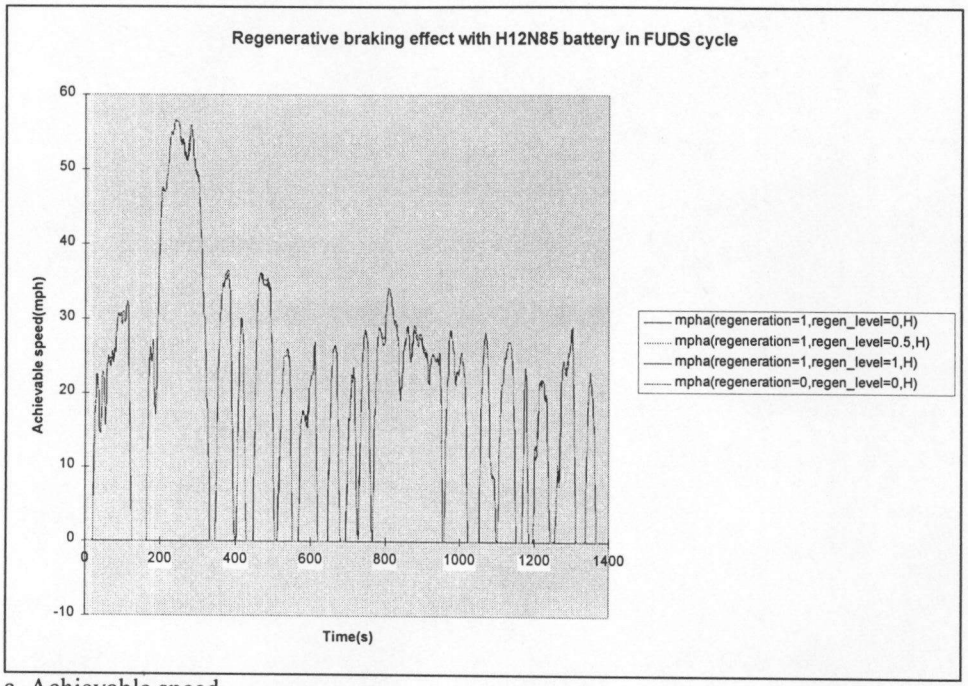
3.3.3.1 SOC recovery

To compare the relative contributions of regeneration and regenerative braking to the SOC recovery, SOC changes are compared from the above simulation by parametric control of the regeneration and regenerative braking effect. Fig.4.12 shows the SOC recovery under different schemes for both the NEON battery and the H12N85 HORIZON battery in both FUDS and HIWAY cycles. In all the cases, it can be observed that for the given vehicle configuration, regeneration contributes more than regenerative braking to the SOC recovery.

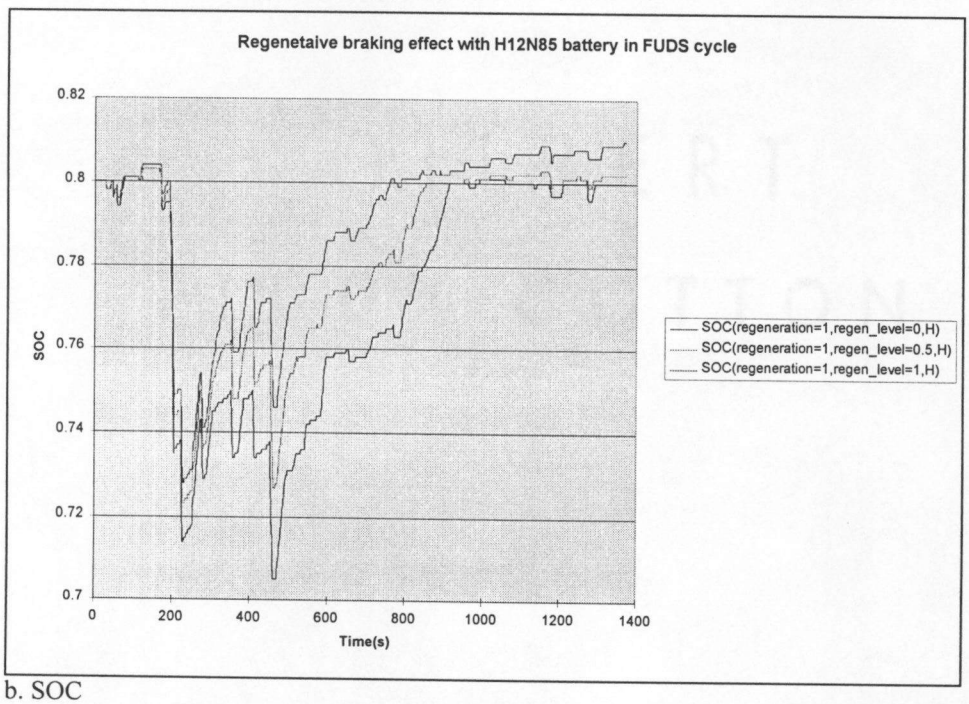
If the SOC value regained by means of regeneration or regenerative braking during the cycle, the vehicle range can be said unlimited. If the SOC can not be recovered, the vehicle range would be limited by reaching SOClo=0.2.

3.3.3.2 Power output

The power output from the APU and from the ESS with respect to the speed profile of the vehicle as affected by different set-up of regeneration and regenerative braking control parameter are combined and plotted in fig.4.13 and fig.4.14 for the NEON battery, and in fig.4.15 and fig.4.16 for the H12N85 HORIZON battery in the FUDS and the HIWAY cycle respectively. From these plots, power of ESS

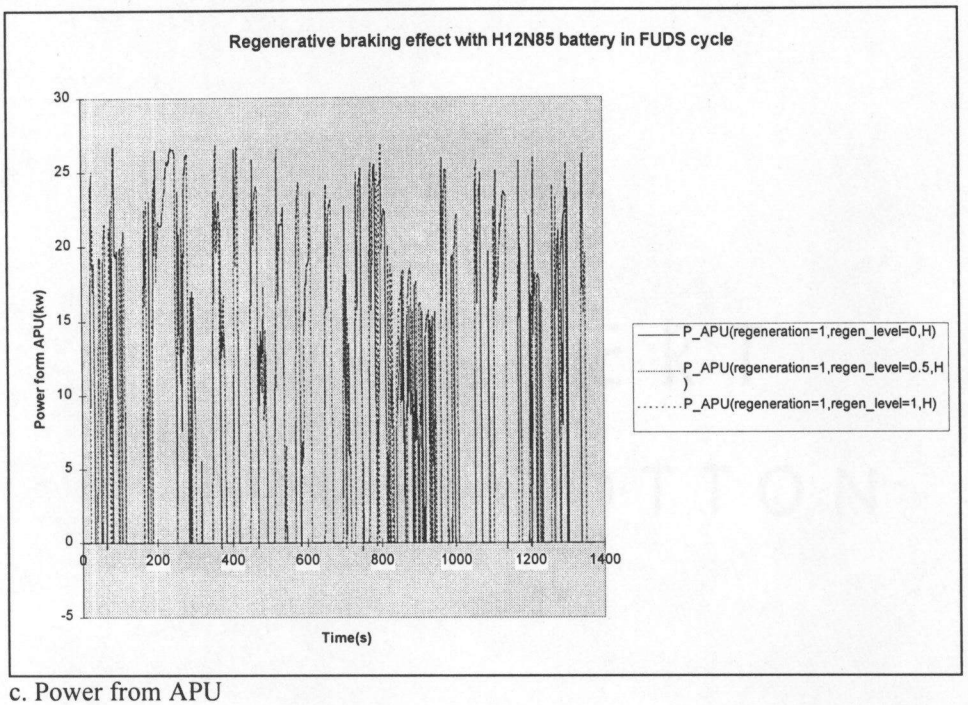


a. Achievable speed

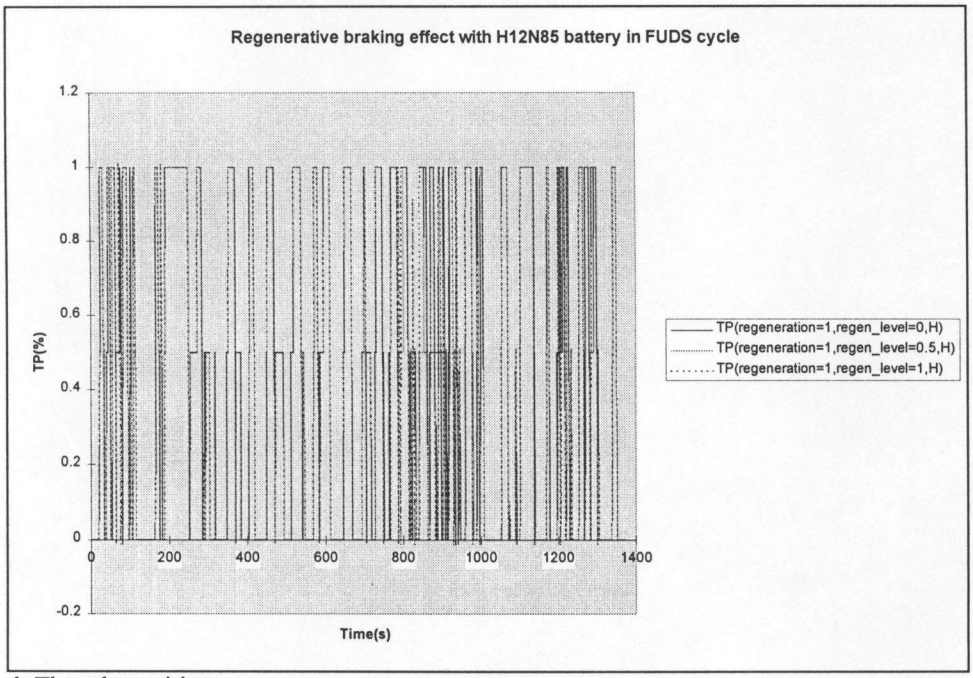


b. SOC

fig.4.10 Regenerative Braking Effect with H12N85 Battery for FUDS Cycle

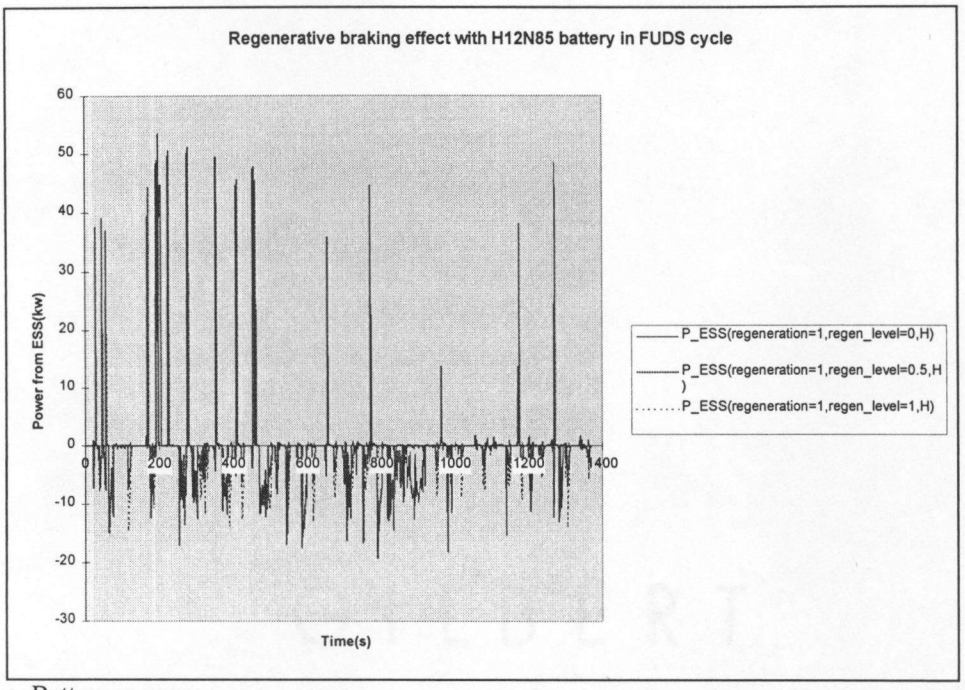


c. Power from APU

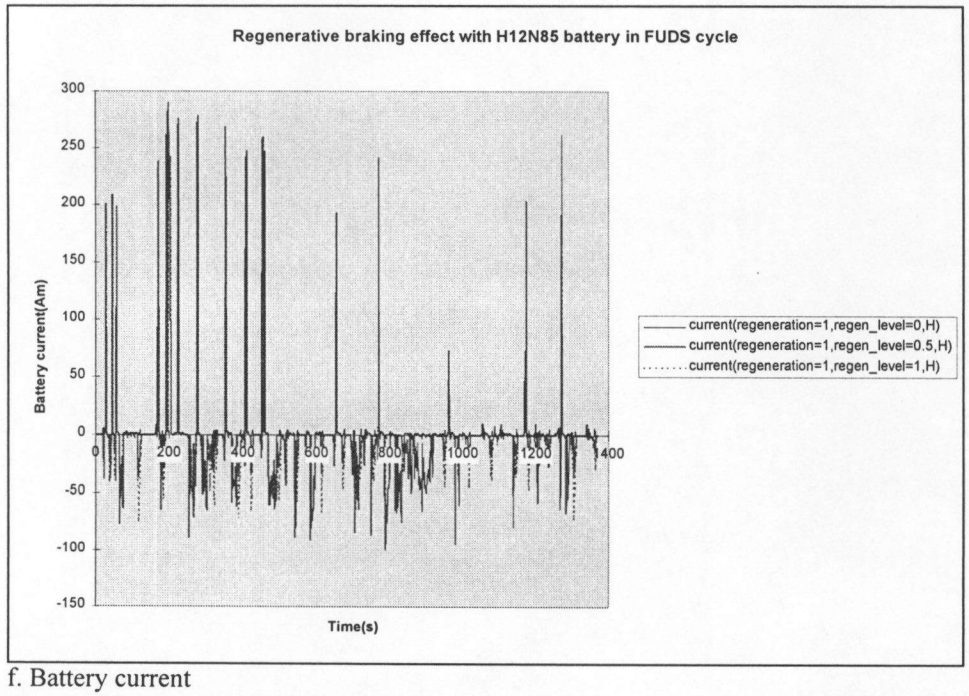


d. Throttle position

fig.4.10 (Continued)

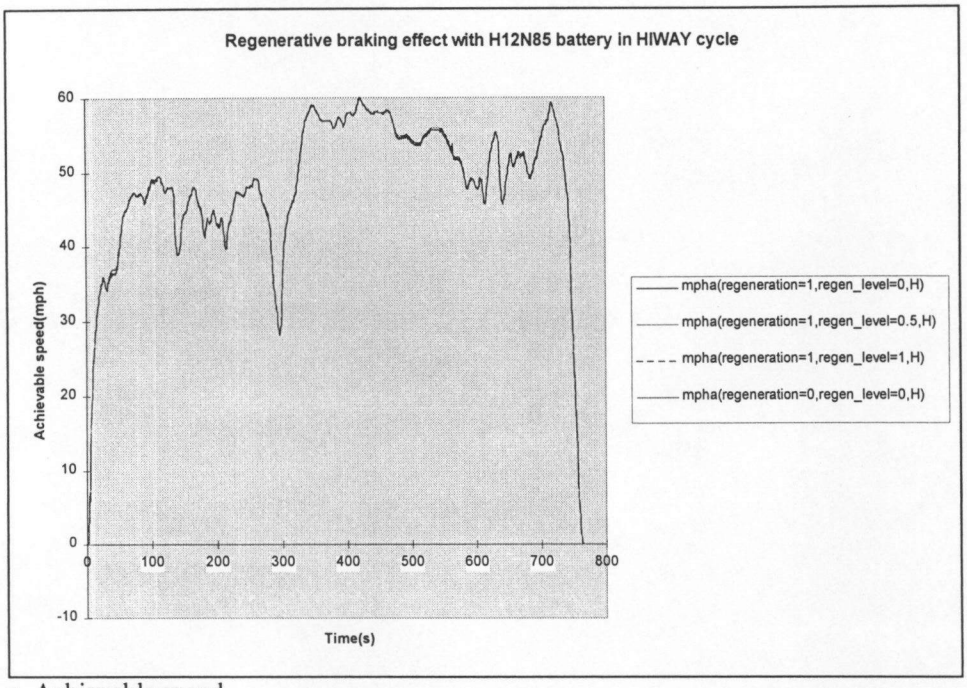


e. Battery power

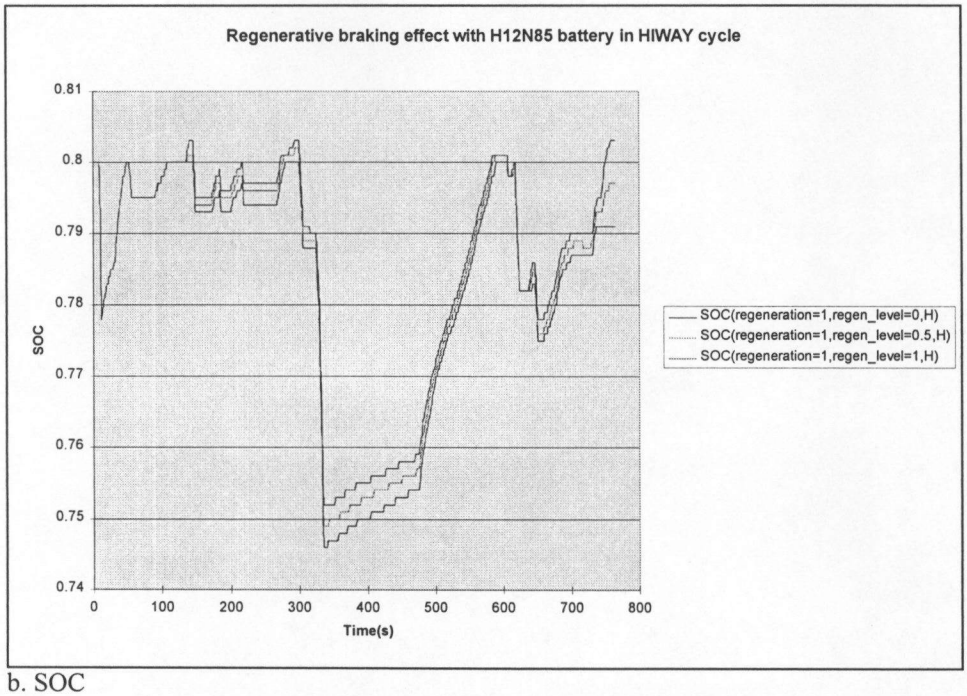


f. Battery current

fig.4.10 (Continued)

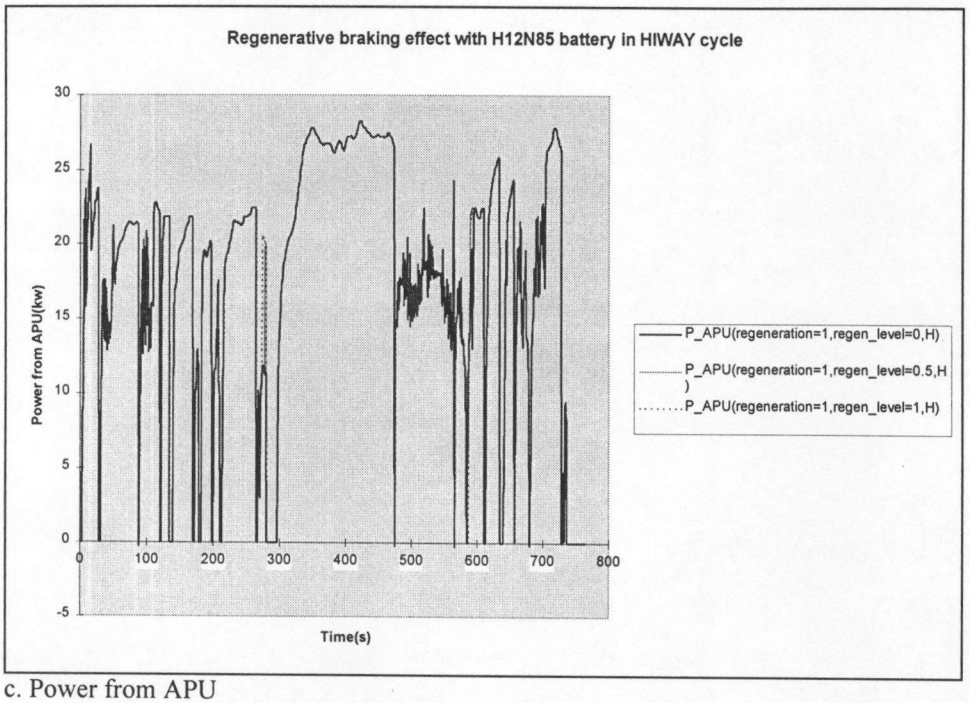


a. Achievable speed

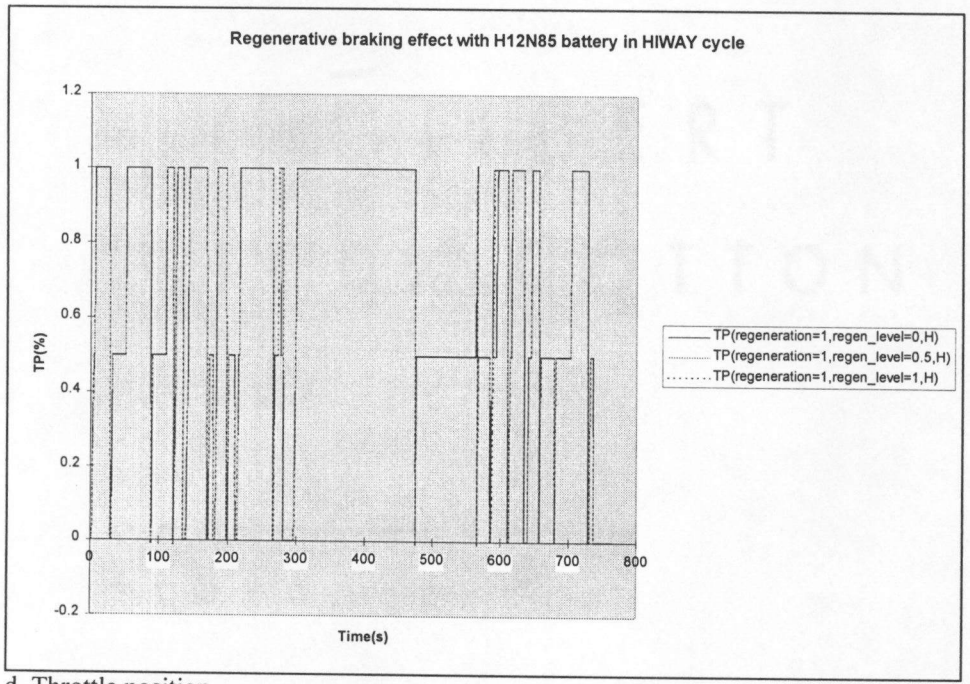


b. SOC

fig.4.11 Regenerative Braking Effect with H12N85 Battery for HIWAY Cycle

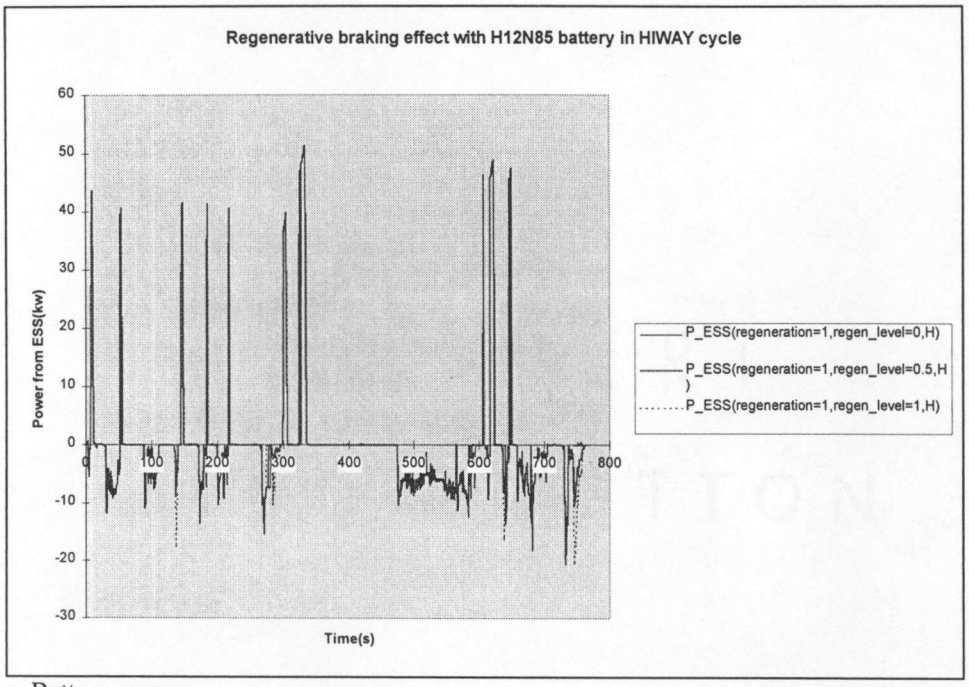


c. Power from APU

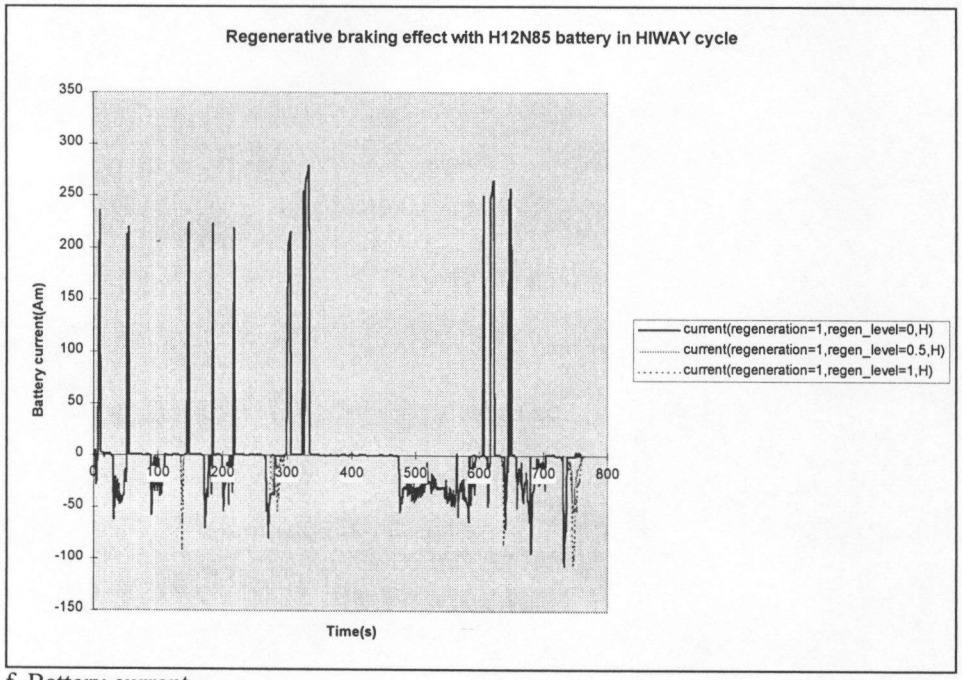


d. Throttle position

fig.4.11 (Continued)

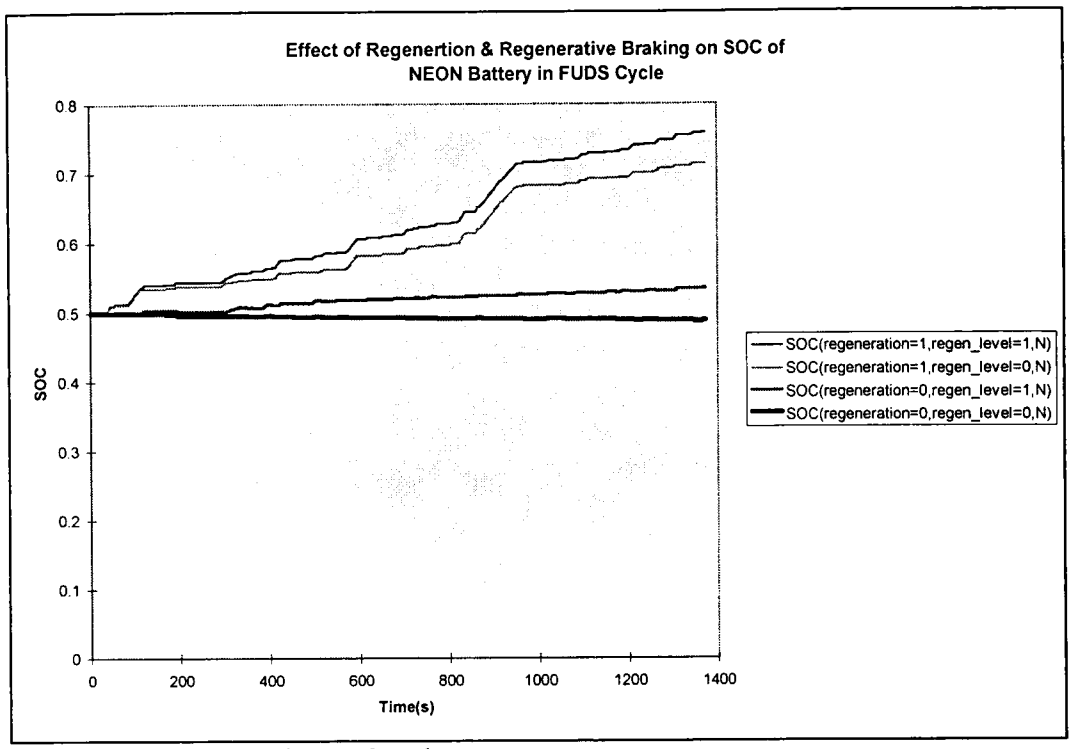


e. Battery power

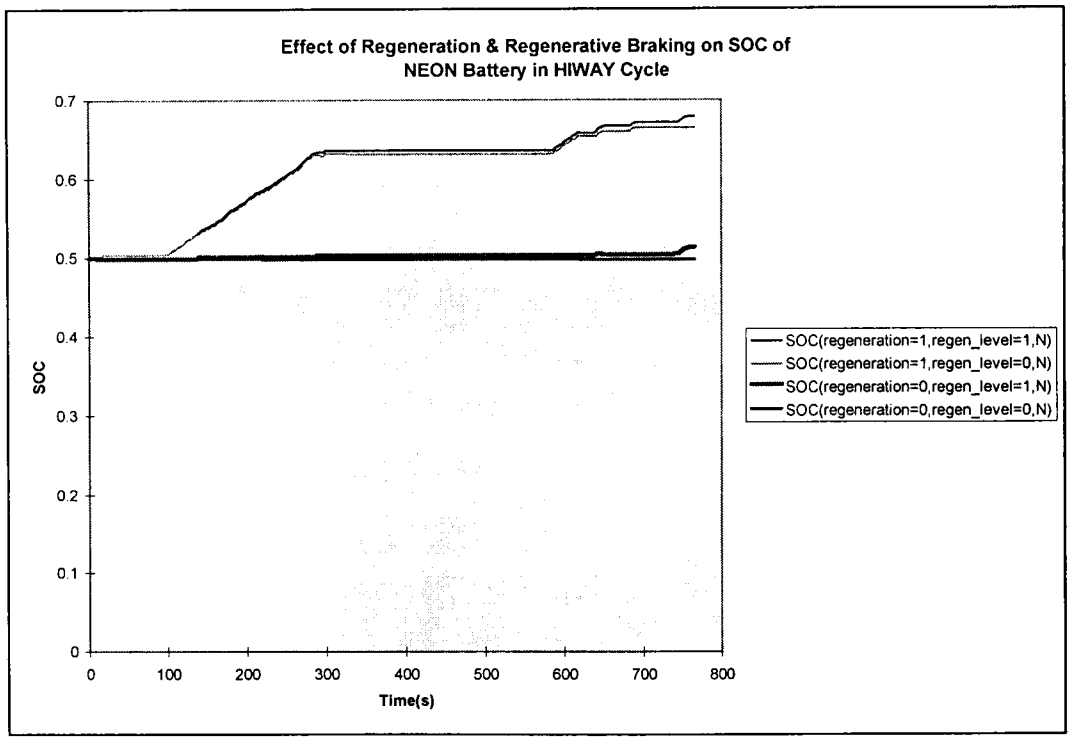


f. Battery current

fig.4.11 (Continued)

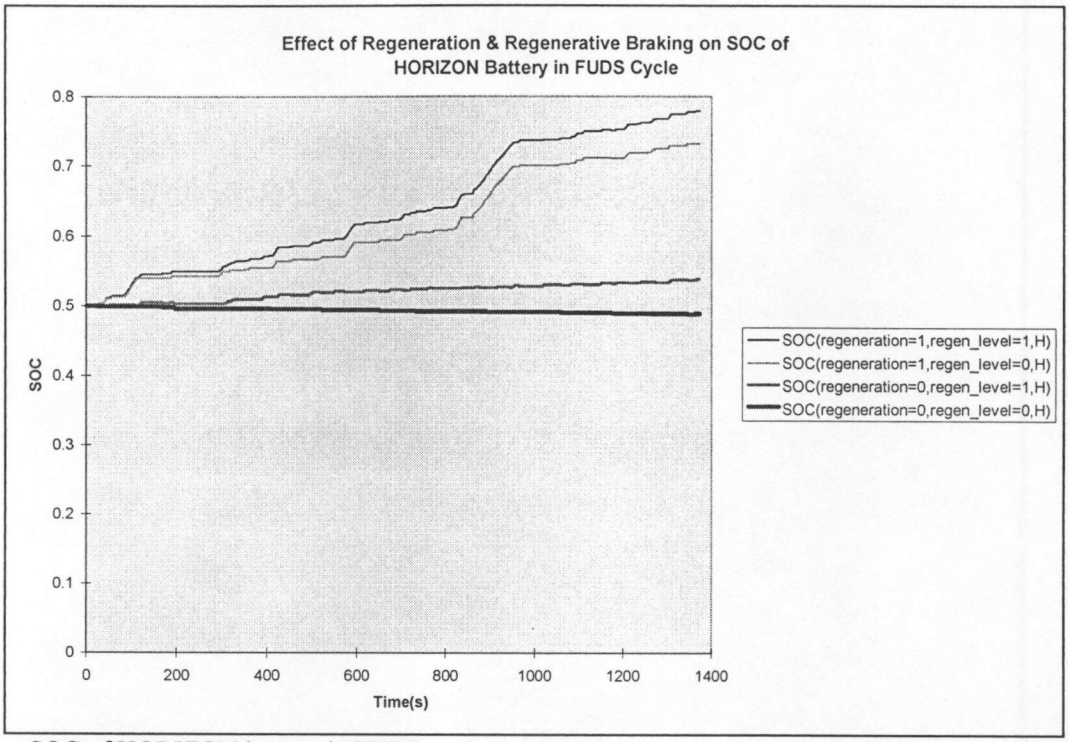


a. SOC of NEON battery in FUDS cycle

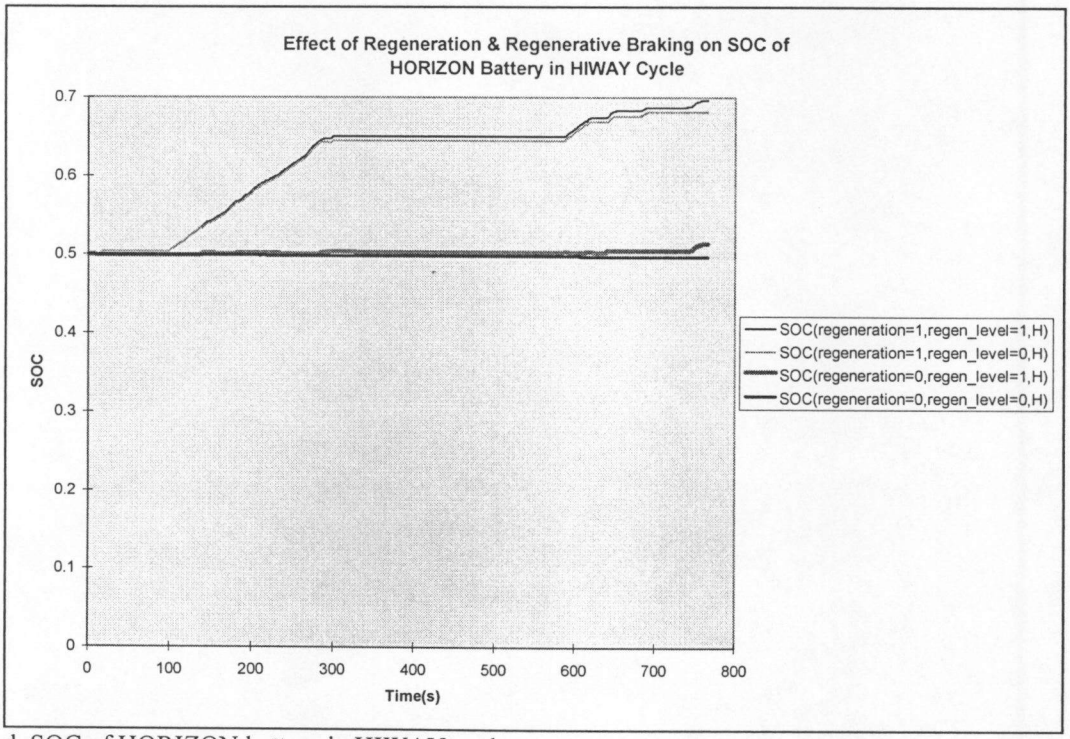


b. SOC of NEON battery in HIWAY cycle

fig.4.12 SOC Recovery in Different Control Scheme

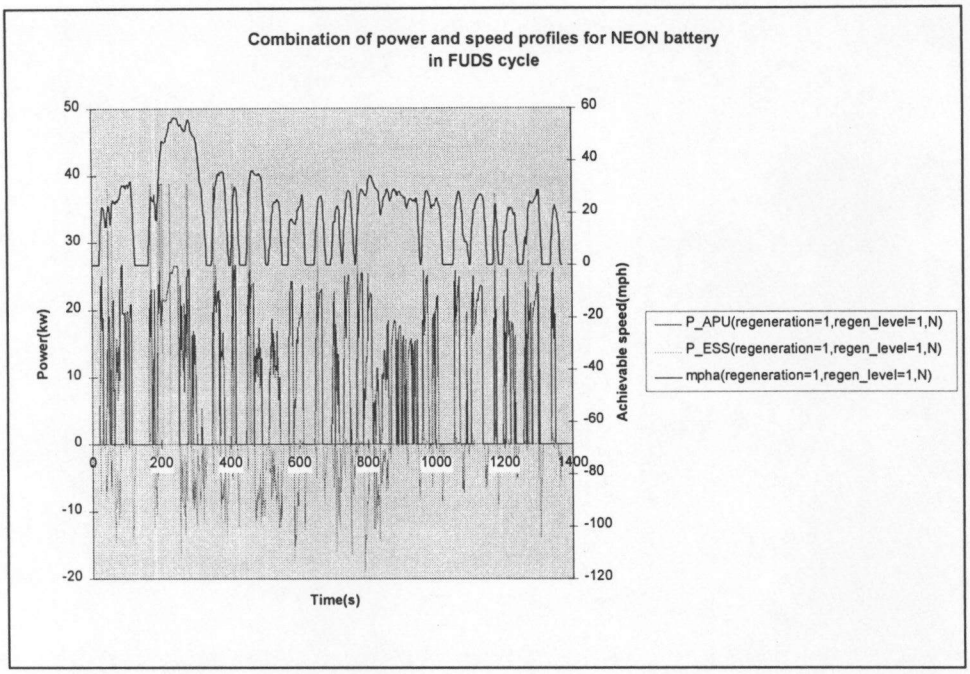


c. SOC of HORIZON battery in FUDS cycle

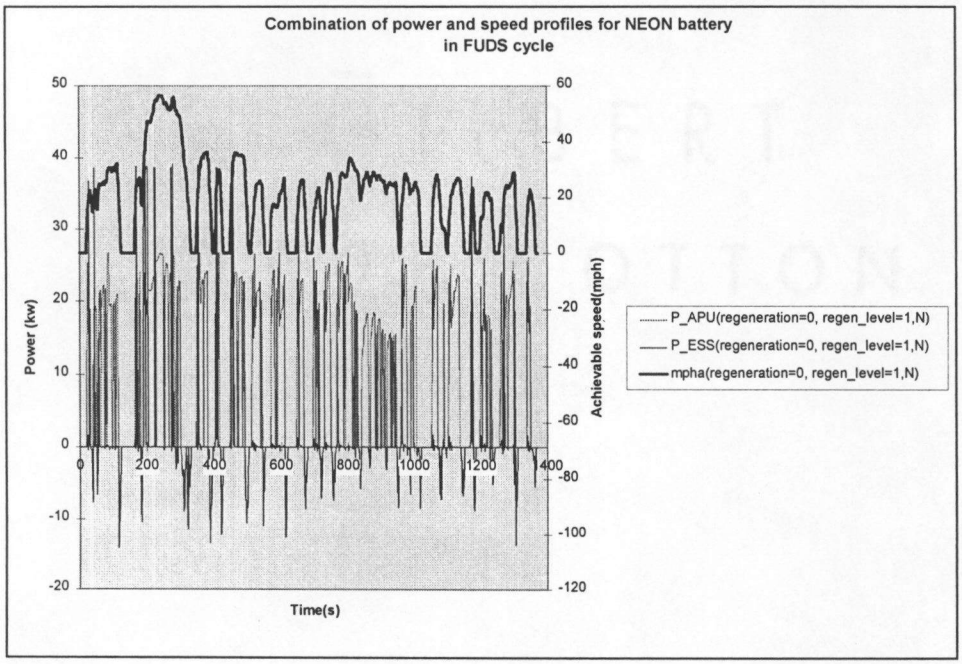


d. SOC of HORIZON battery in HIWAY cycle

fig.4.12 (Continued)

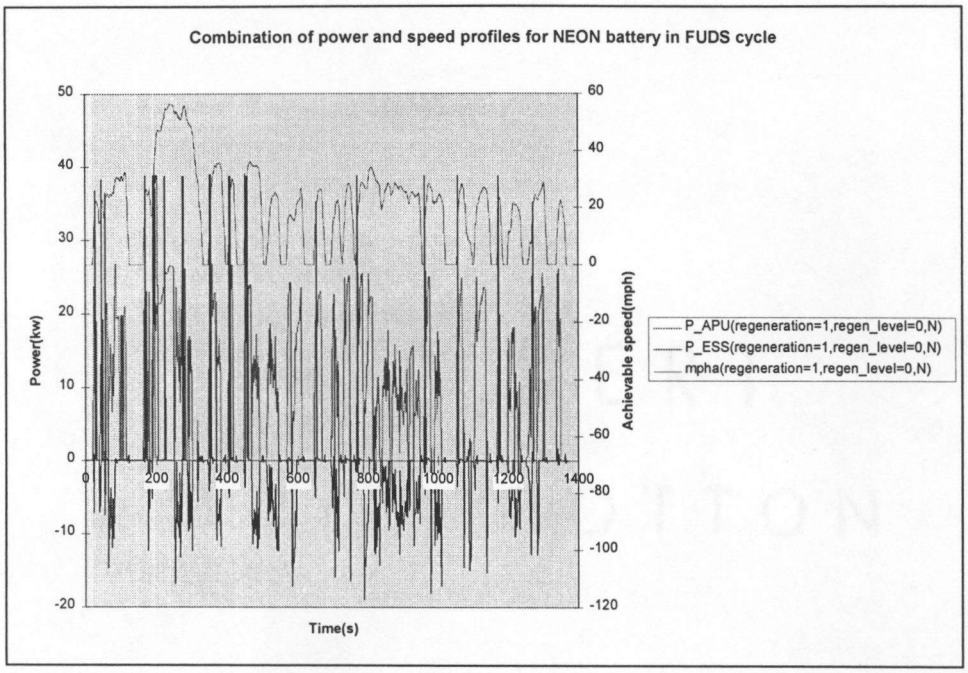


a. regeneration=1, regen_level=1

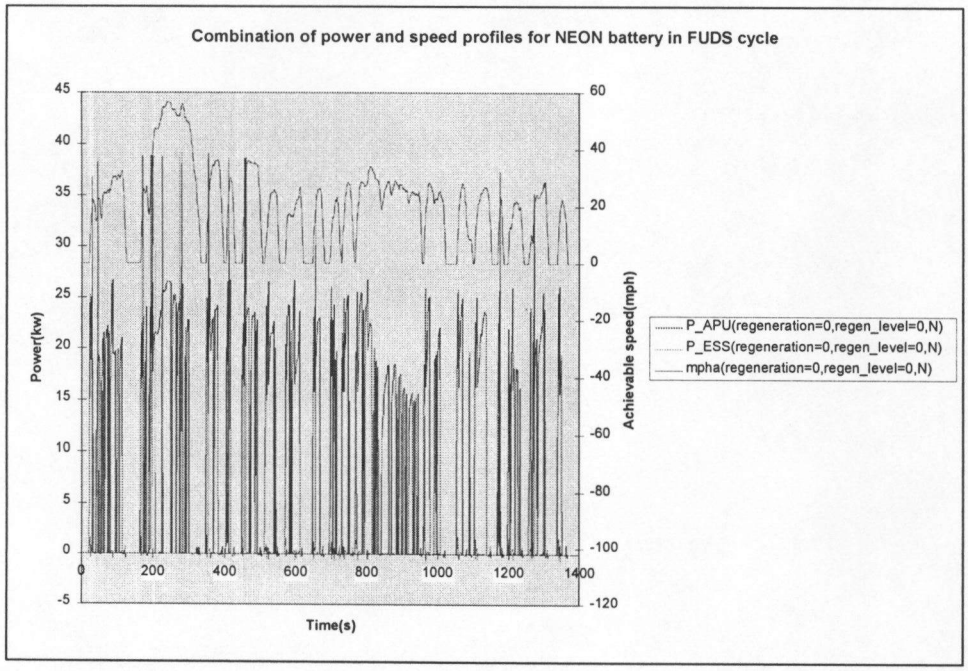


b. regeneration=0, regen_level=1

fig.4.13 Combination of Power and Speed Curves for NEON Battery in FUDS Cycle

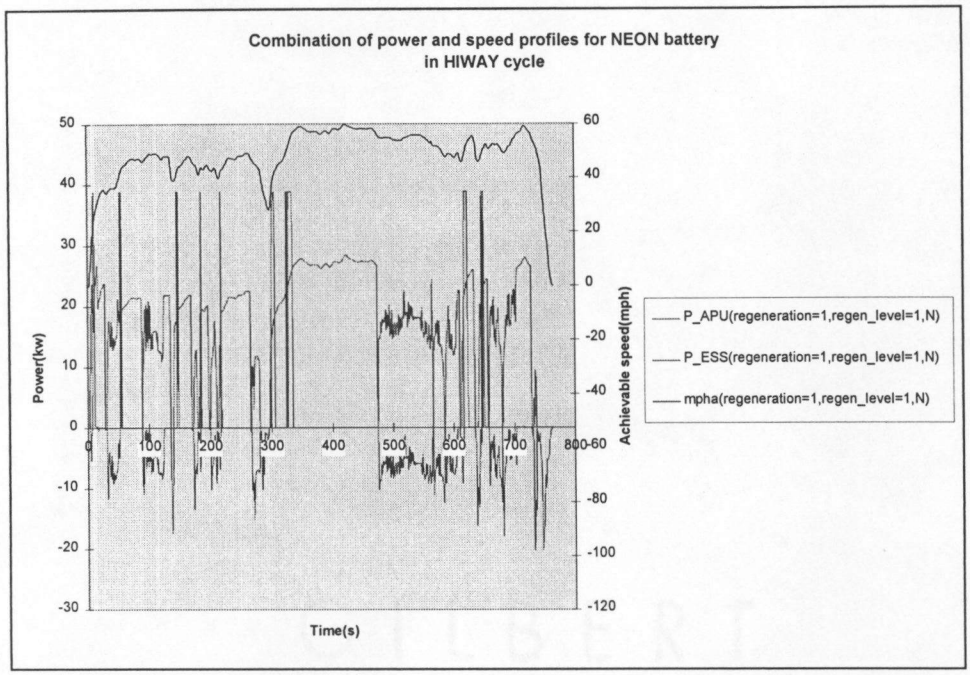


c. regeneration=1, regen_level=0

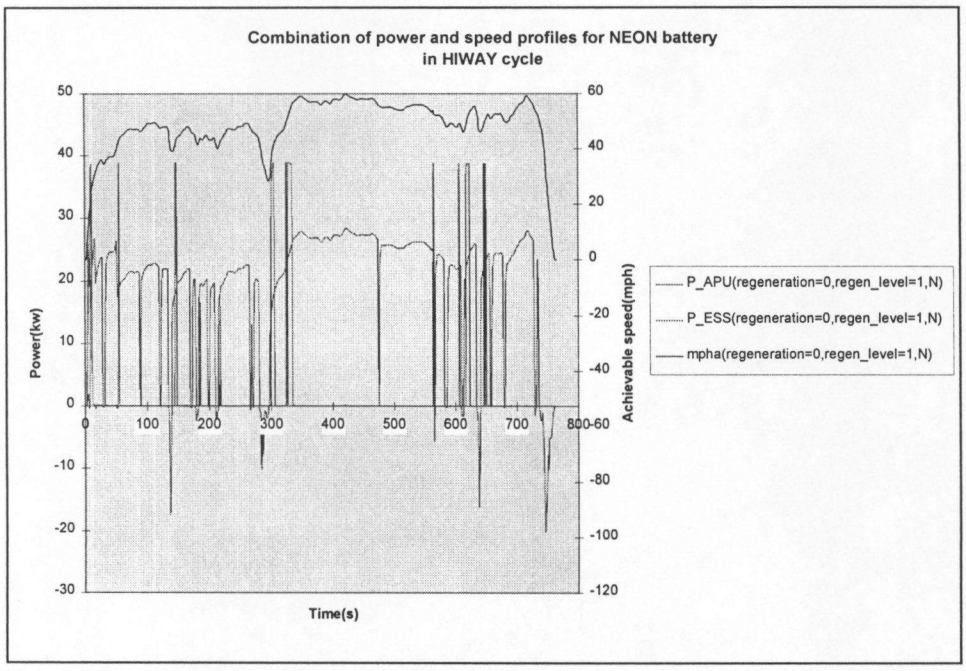


d. regeneration=0, regen_level=0

fig.4.13 (Continued)

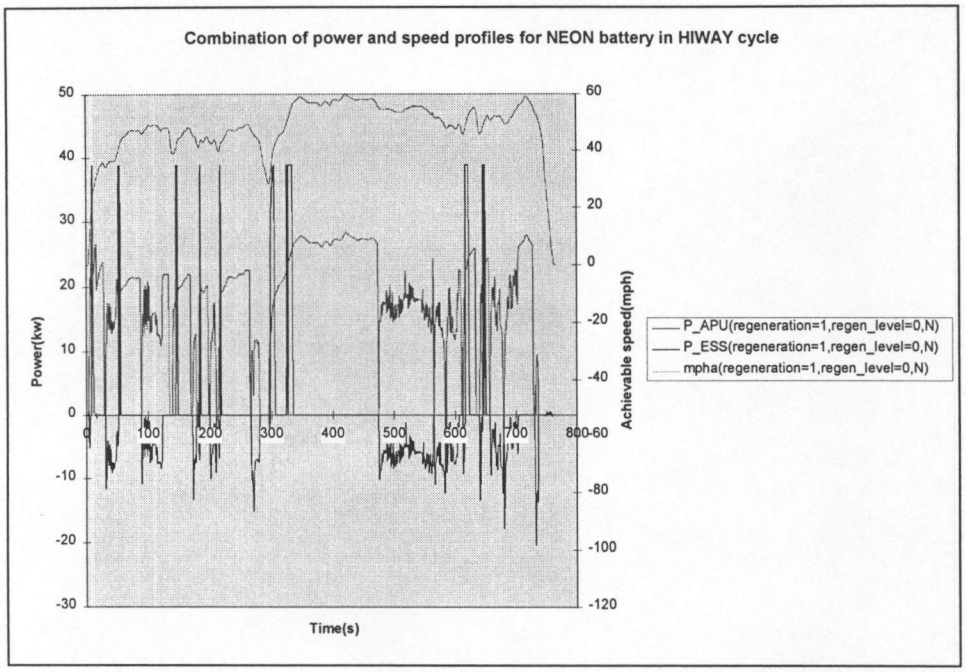


a. regeneration=1, regen_level=1

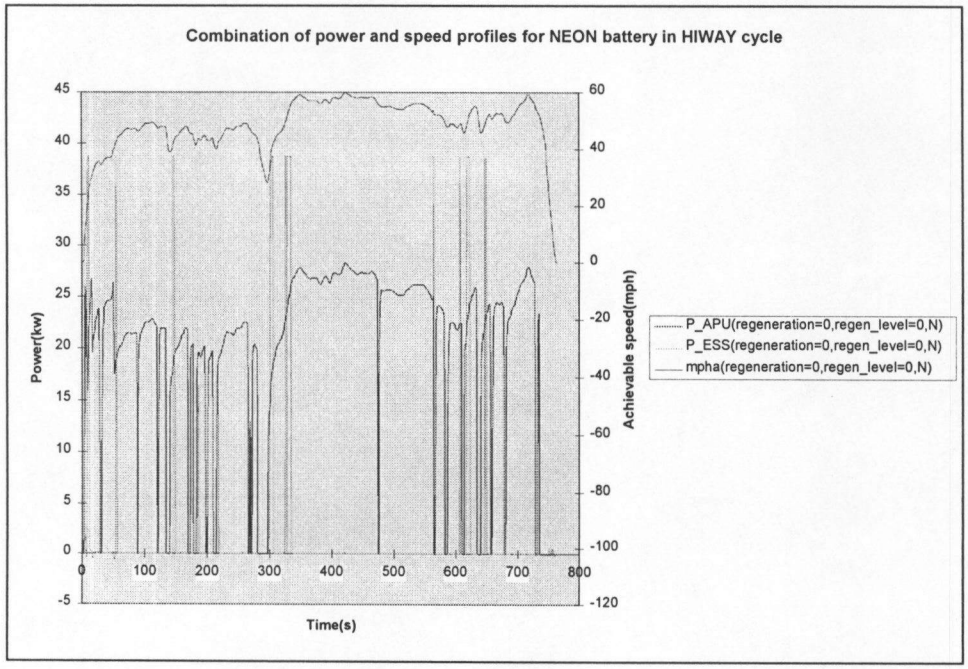


b. regeneration=0, regen_level=1

fig.4.14 Combination of Power and Speed Curves for NEON Battery in HIWAY Cycle

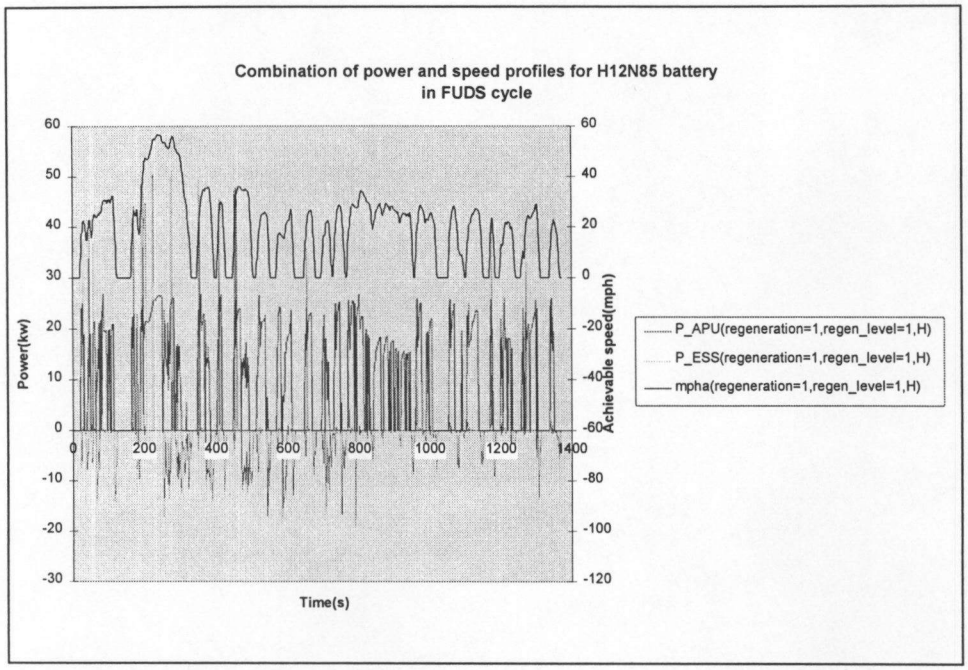


c. regeneration=1, regen_level=0

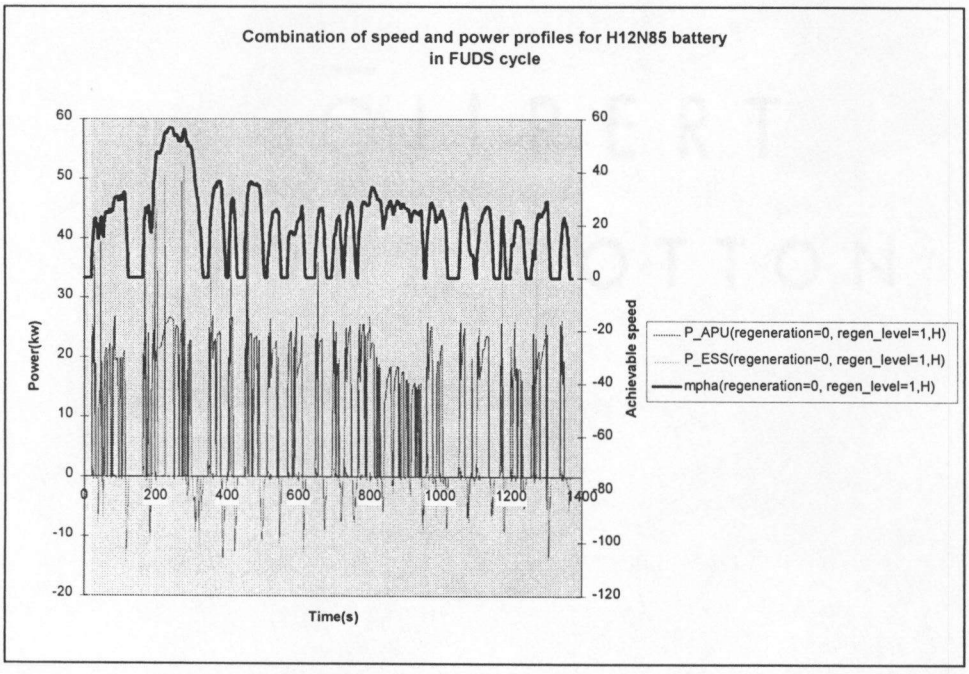


d. regeneration=0, regen_level=0

fig.4.14 (Continued)

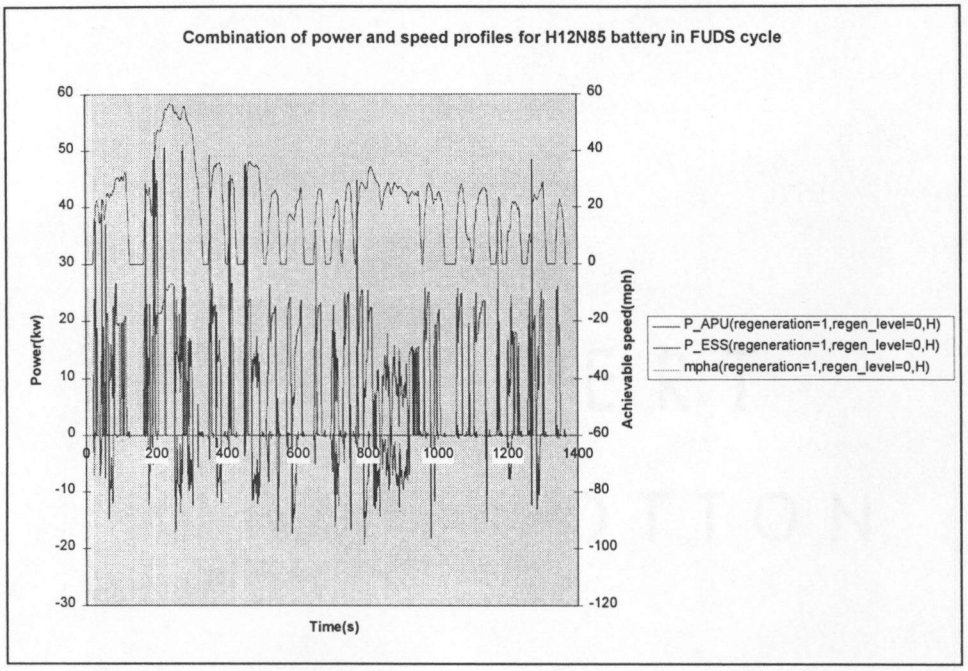


a. regeneration=1, regen_level=1

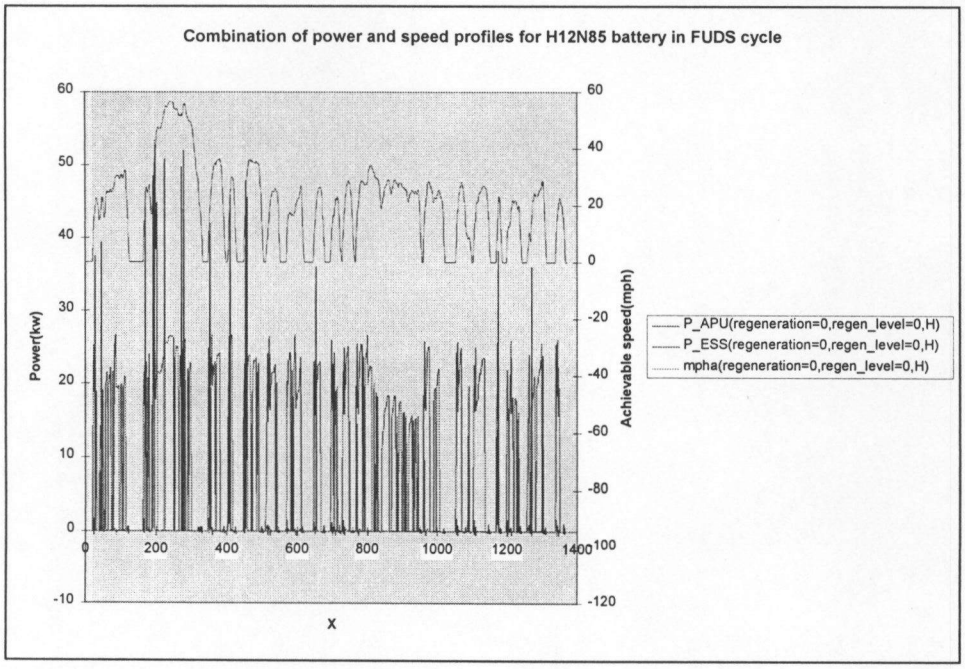


b. regeneration=0, regen_level=1

fig.4.15 Combination of Power and Speed Curves for H12N85 Battery in FUDS Cycle

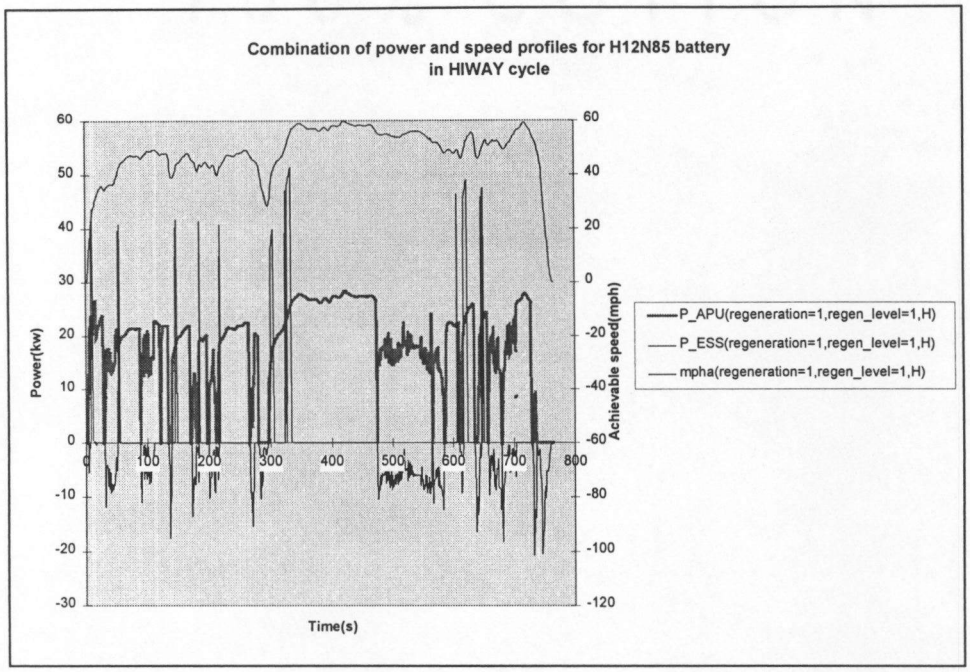


c. regeneration=1, regen_level=0

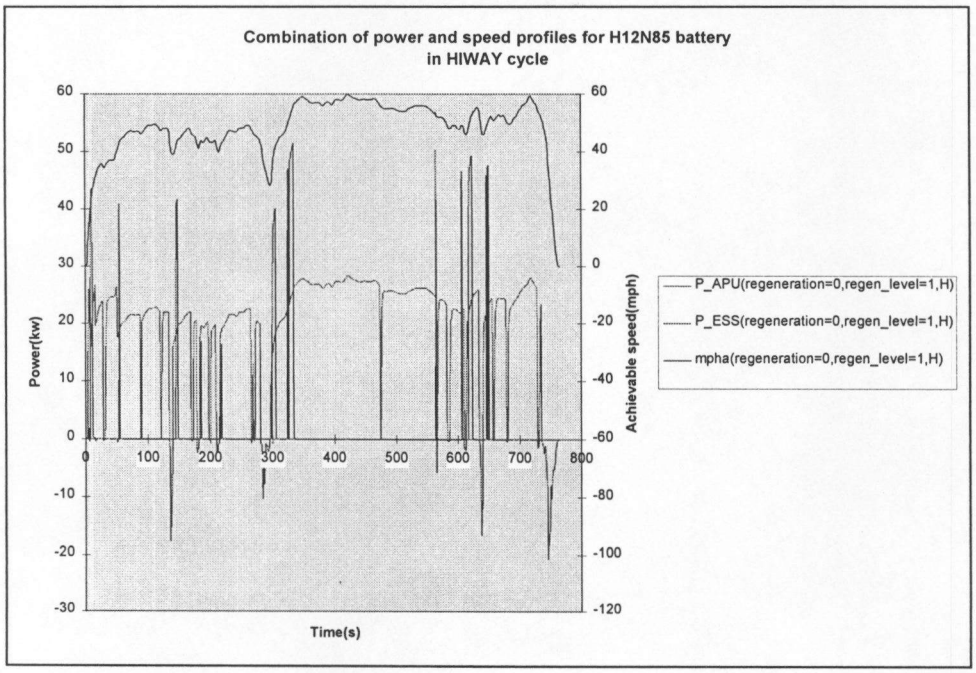


d. regeneration=0, regen_level=0

fig.4.15 (Continued)

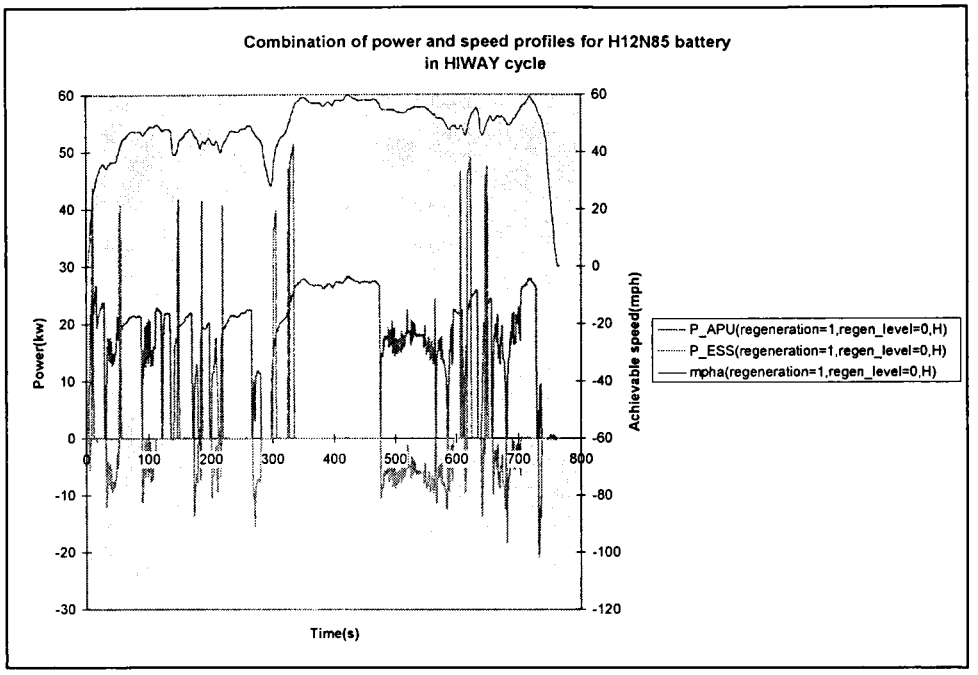


a. regeneration=1, regen_level=1

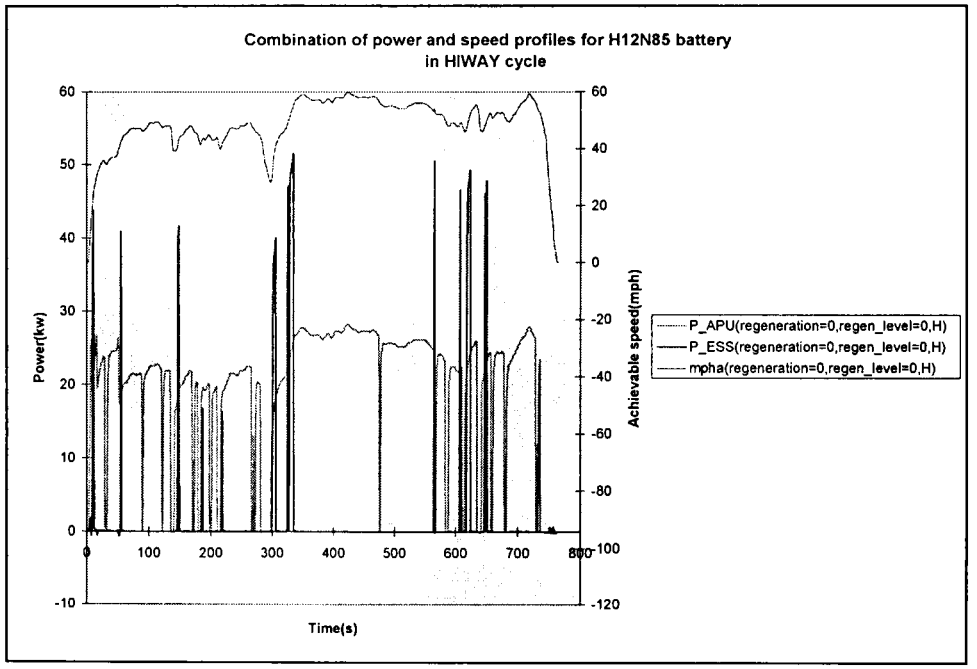


b. regeneration=0, regen_level=1

fig.4.16 Combination of Power and Speed Curves for H12N85 Battery in HIWAY Cycle



c. regeneration=1, regen_level=0



d. regeneration=0, regen_level=0

fig.4.16 (Continued)

assist, regeneration and regenerative braking can be identified directly or through comparison. Besides, the relative magnitude of the power curves as affected by the control parameters can be viewed clearly.

It can be noticed that regeneration and regen_level have very limited effect on the speed profile. Even when regeneration and regenerative braking are both suppressed, the vehicle would still be able to achieve the speed requested. This suggest that the APU used has a fairly high capacity for the driving pattern.

3.3.4 Initial SOC value

The initial SOC value is controlled by the parameter SOC_init. From the previous simulation we have seen that the APU provides most of the power for driving the vehicle in the NEON configuration. The ESS assist power is relatively small. Therefore, as long as the SOC can be maintained to enable the battery to deliver certain power when assist is requested, the SOC_init value should have little effect on the speed. The power curves would vary, however, since for different SOC the power delivered from the ESS is different.

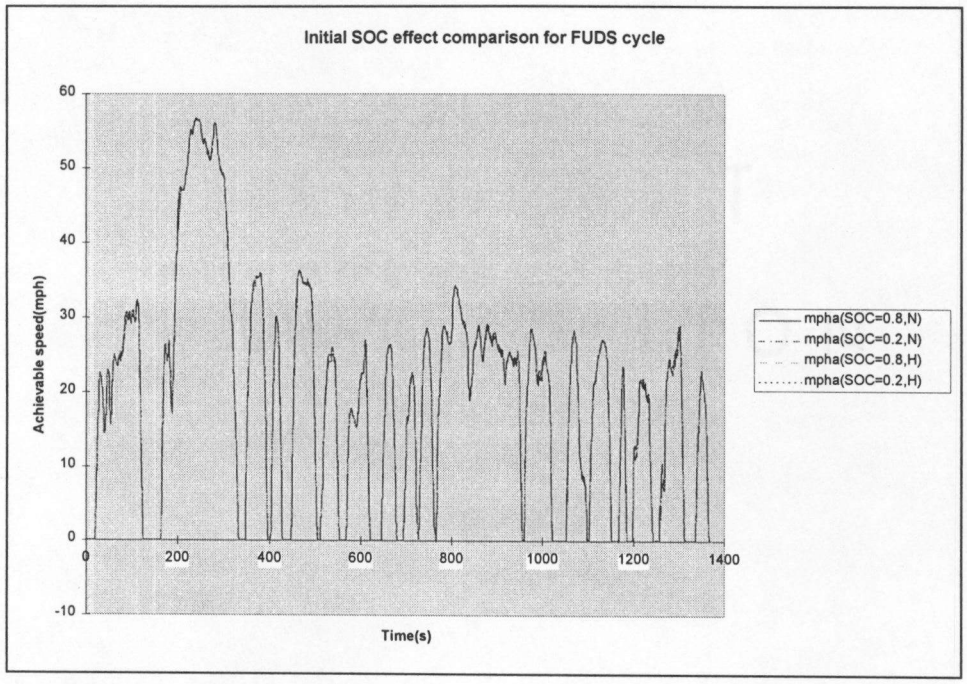
The above analysis is supported by the simulation results as plotted in fig.4.17 and fig.4.18. We can see that even when the initial SOC is at SOClo, speed requested is still achievable due to the high APU power output. The SOC value increases during the driving cycle due to regeneration and regenerative braking.

The simulations from both the NEON battery and the H12N85 HORIZON battery are presented as well. The legend of the curves with 'N' denotes simulation results with the NEON battery, and 'H' for the H12N85 HORIZON battery.

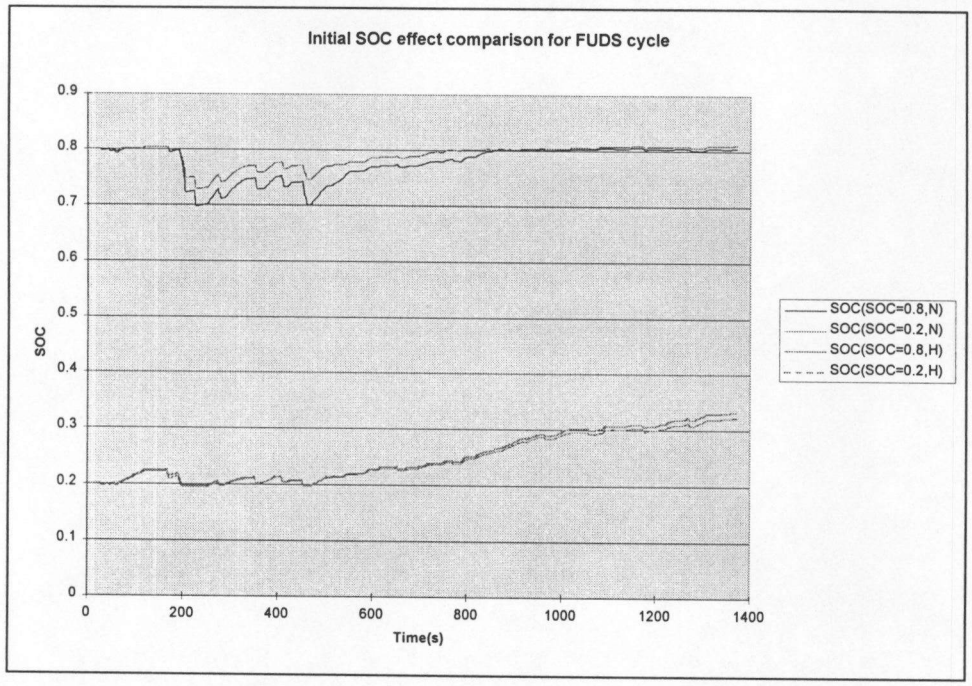
3.3.5 Threshold position effect

The threshold position of the throttle is based on fig.3.18. In all the prior simulations, the TP_threshold was set at 0.5. The threshold position affects the threshold power for regeneration and ESS assist. The effect of this variable is simulated by setting the TP_threshold at 0, 0.2, 0.5 and 0.7 with the NEON battery when regeneration and regenerative braking are fully activated. Plots of the results are shown in fig.4.19 for the FUDS cycle and in fig.4.20 for the HIWAY cycle. The results show that:

- for the given APU, the speed profile is achievable at different threshold position;

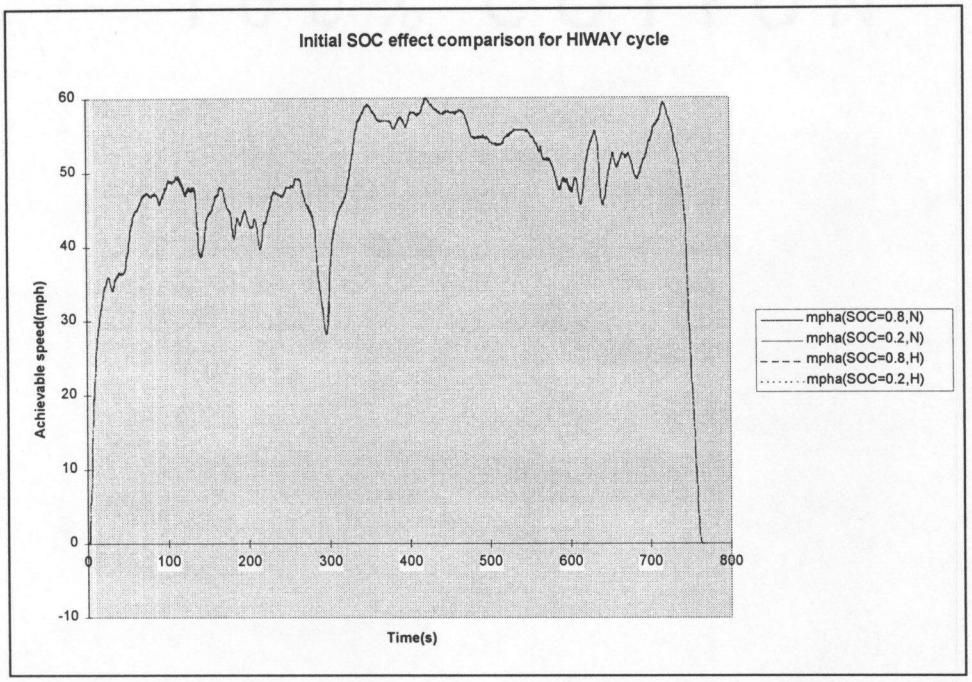


a. Achievable speed

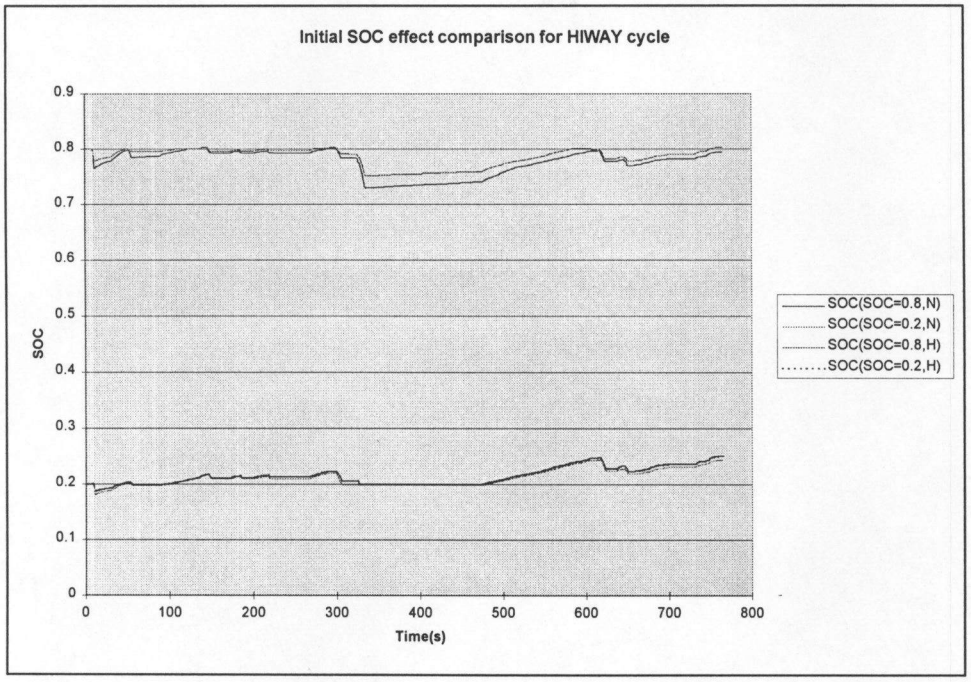


b. SOC

fig.4.17 SOCinit Effect Comparison for FUDS Cycle

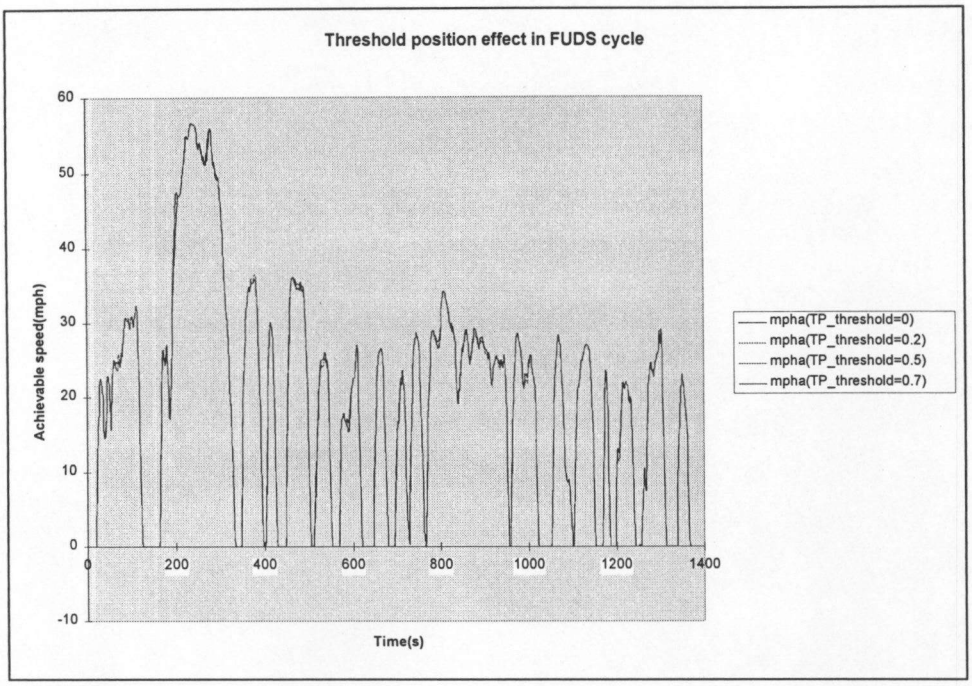


a. Achievable speed

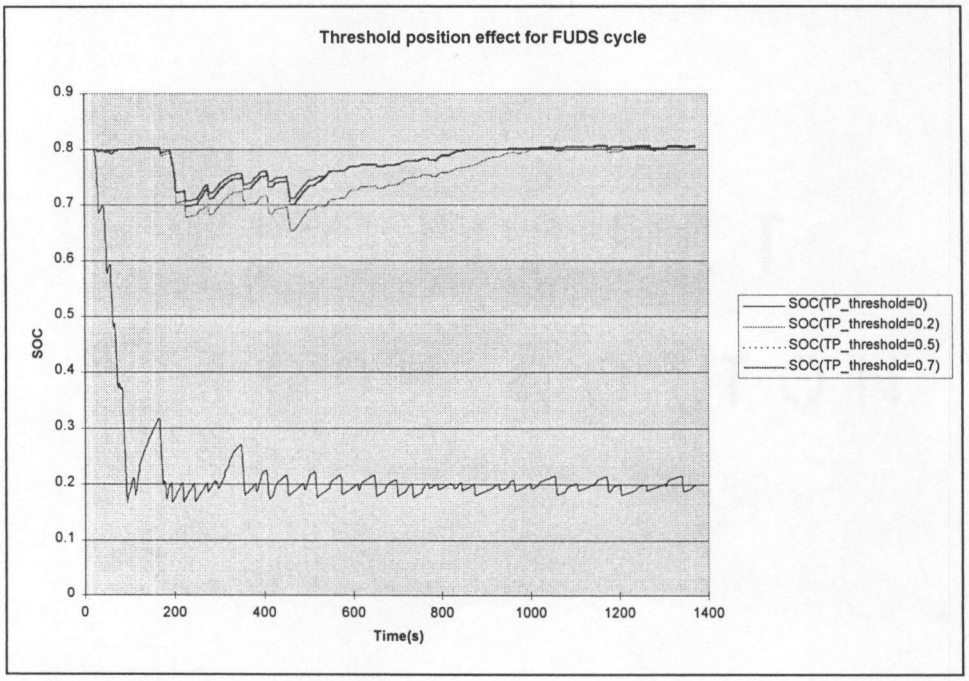


b. SOC

fig.4.18 SOCinit Effect Comparison for HIWAY Cycle

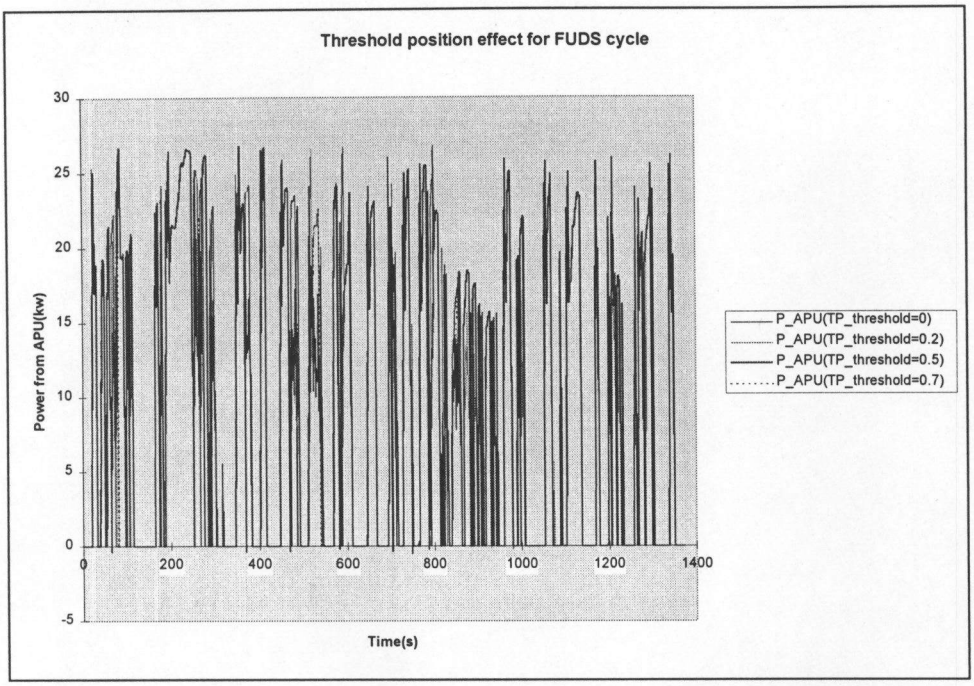


a. Achievable speed

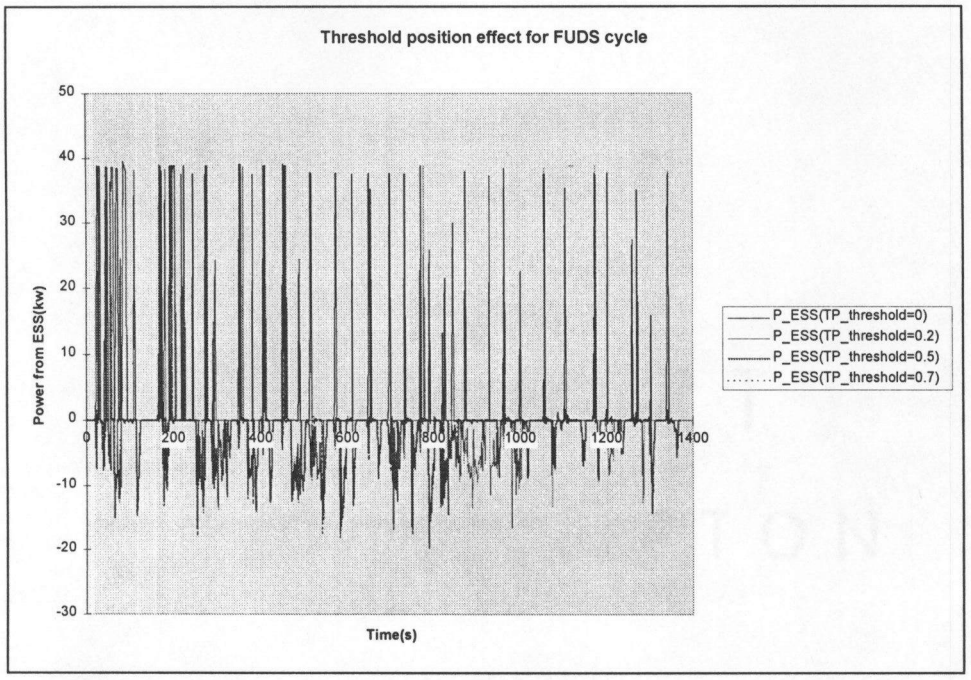


b. SOC

fig.4.19 Threshold Position Effect of the Throttle for FUDS Cycle

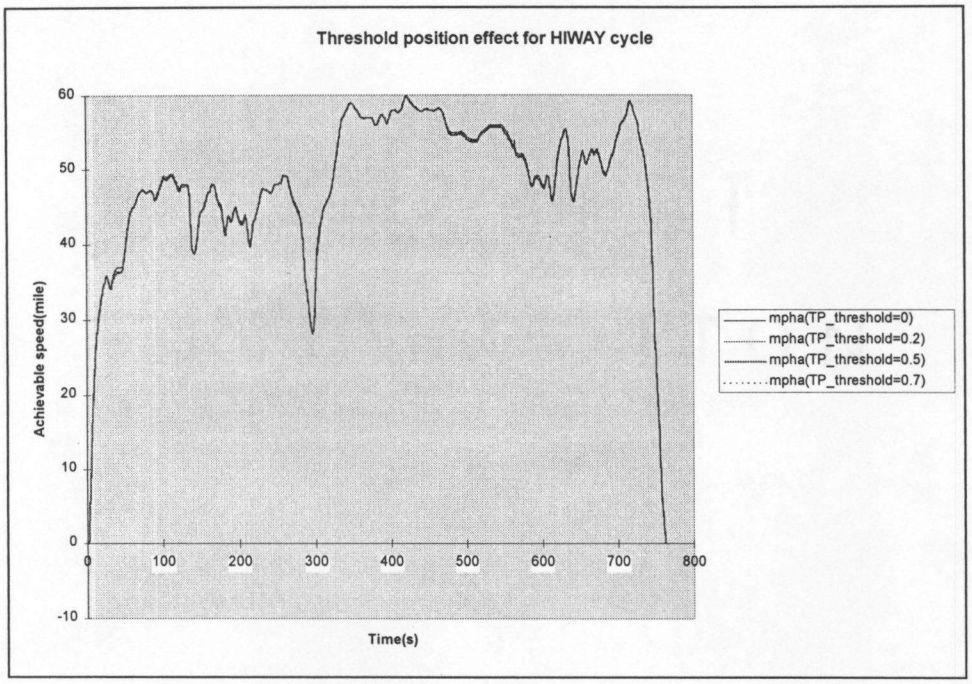


c. Power from APU

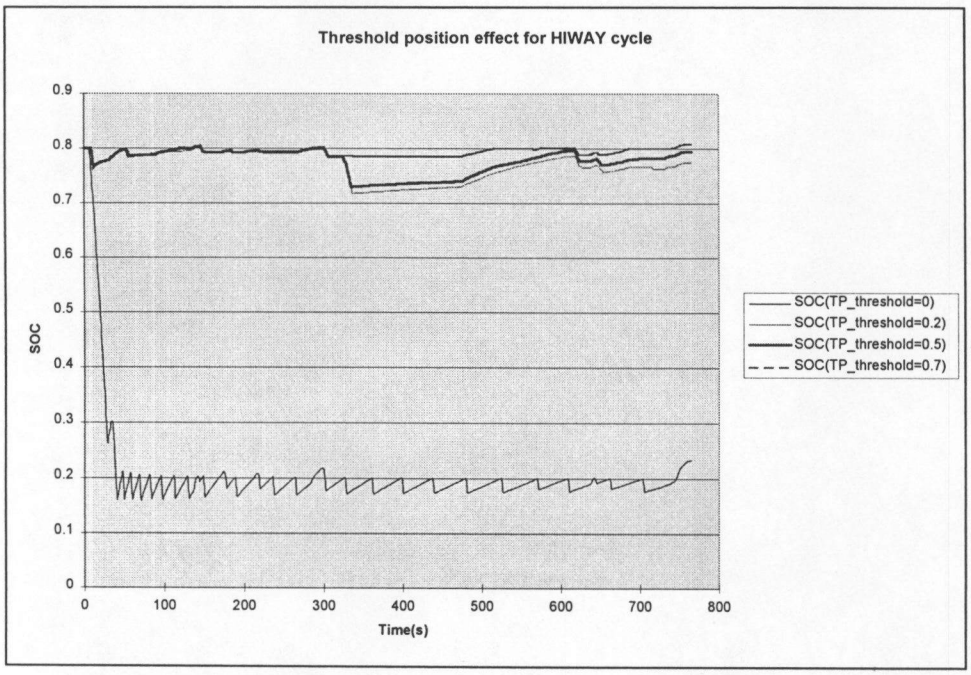


d. Power from ESS

fig.4.19 (Continued)

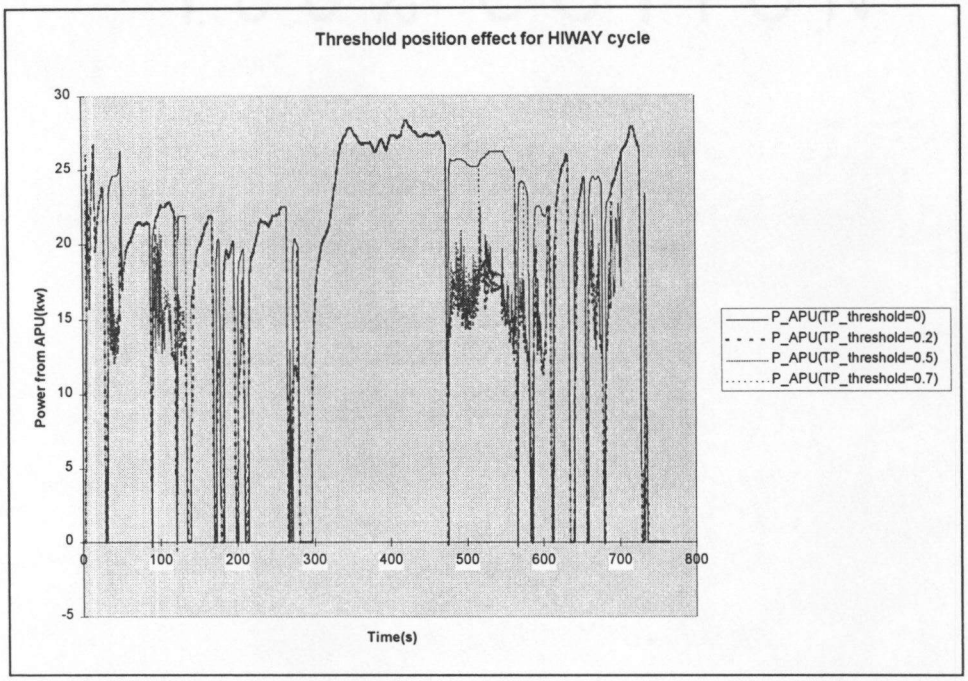


a. Achievable speed

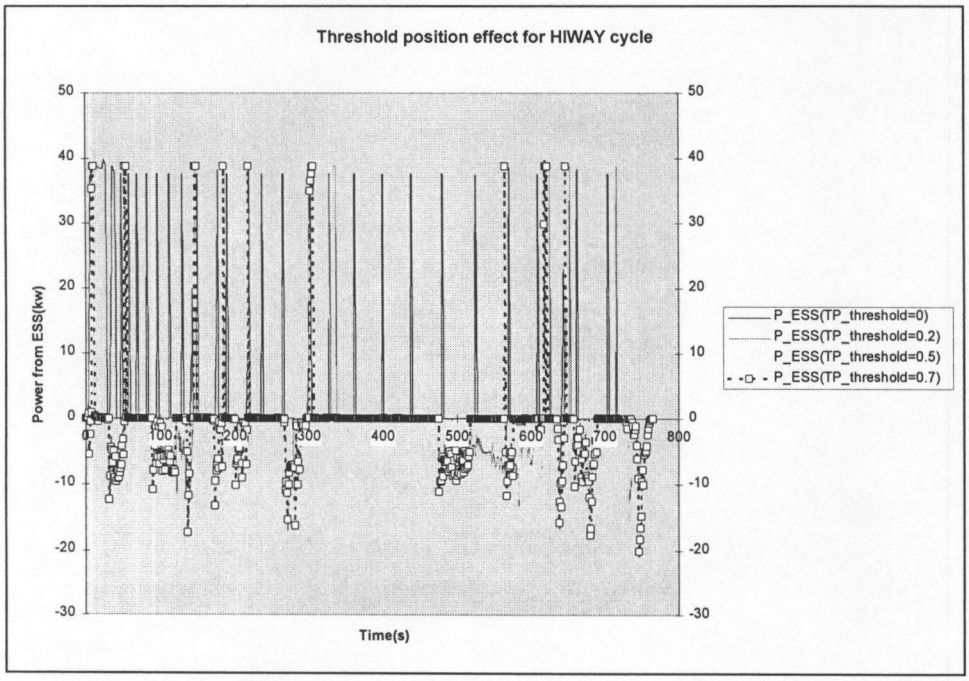


b. SOC

fig.4.20 Threshold Position Effect of the Throttle for HIWAY Cycle



c. Power from APU



d. Power from ESS

fig.4.20 (Continued)

- at TP_threshold=0, i.e. the threshold position of the throttle is set at zero, regeneration is completely eliminated. Therefore, the SOC of ESS drops quickly and can not be regained during the cycle when only regenerative braking is effective;
- when the ESS assist comes at an early TP position (e.g. TP_threshold =0.2), the SOC drops lower since more power is taken from ESS. However, the SOC recovers in the FUDS cycle, but is not fully recovered in HIWAY cycle.

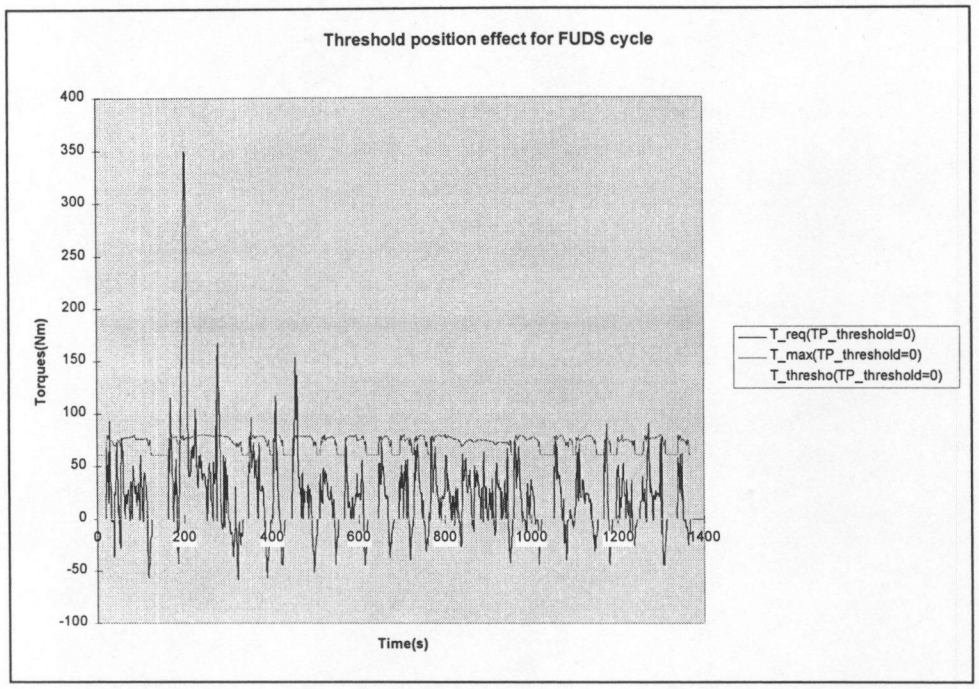
  This is caused by the changes of torque request vs torque threshold at different TP_threshold. Fig.4.21 for the FUDS cycle and fig.4.22 for the HIWAY cycle show the threshold torque and requested torque changes due to the change of TP_threshold. The regeneration capability decrease as the threshold value decreases.

  It can be seen that from above curves that in FUDS cycle more regeneration occur, so the SOC is fully recovered even when the threshold value is 0.2. The final SOC values close to SOChi at different TP_threshold position is a result of regeneration suppression after SOC reaches SOChi. However, in the HIWAY cycle the regeneration can not make the SOC regained to the initial SOChi when the threshold value is at 0.2.
- At TP_thrshold =0.7, the SOC remains close to the initial SOC during the whole cycle. This is partly because ESS assist is invoked less during the whole cycle and the increased threshold torque means more regeneration power is available for recharging the battery.

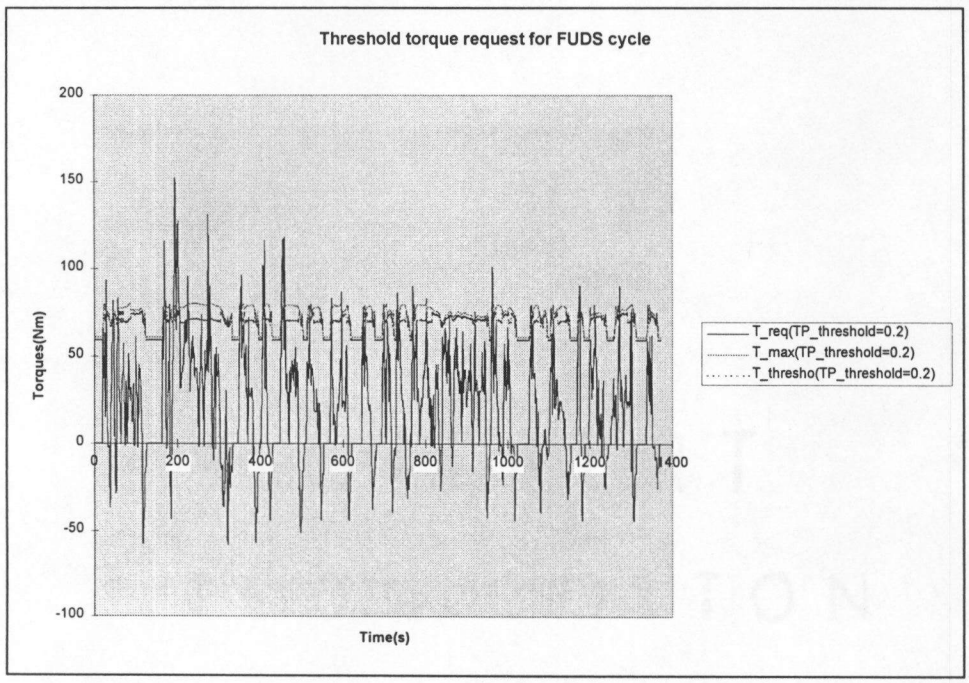
Therefore, for effective control of the vehicle, the optimal threshold position of the throttle could be around 0.5 to prevent depleting the battery SOC and to maintain a reasonable amount of ESS assist. The threshold position should not be over 0.7 for activating the ESS assist for driving the vehicle, and it should not be below 0.2 for SOC sustaining by regeneration.

3.3.6 APU power capacity analysis

From previous analysis we see that the APU contributes the majority of the power for driving the vehicle. With the current APU, the vehicle is running mostly in the conventional mode, driven by the APU only.

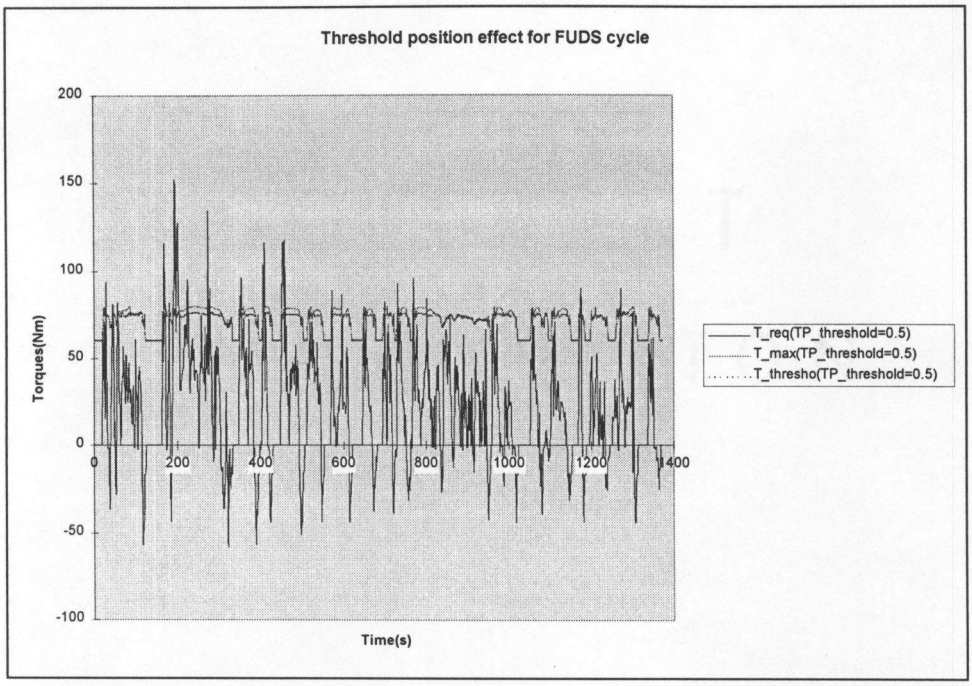


a. TP_thrshold =0

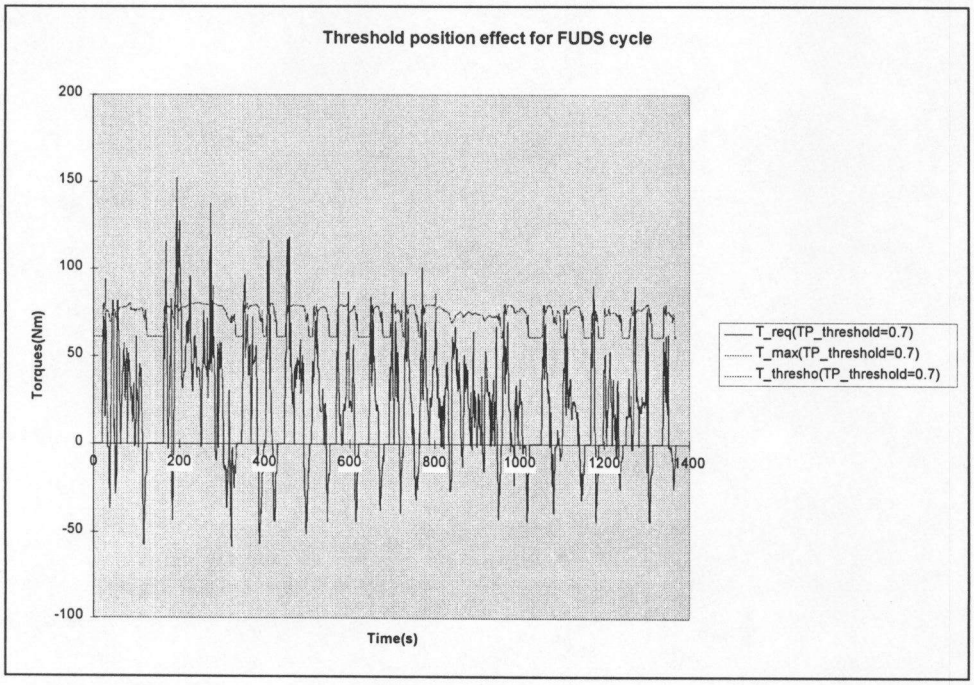


b. TP_threshold =0.2

fig. 4.21 Threshold Position Effect on the Torque of APU in FUDS Cycle

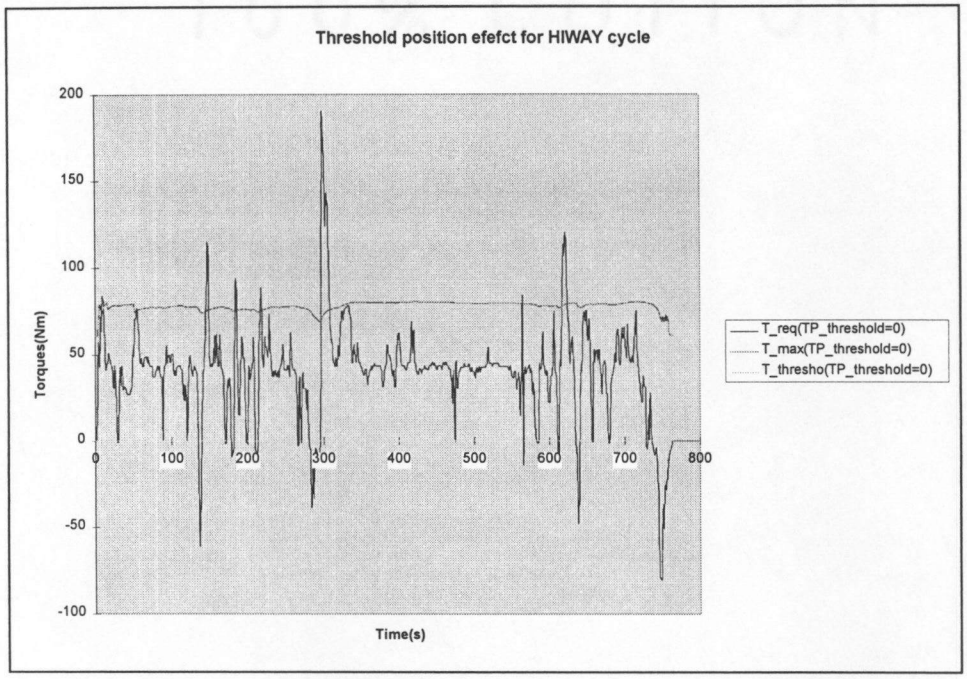


a. TP_thrshold =0.5

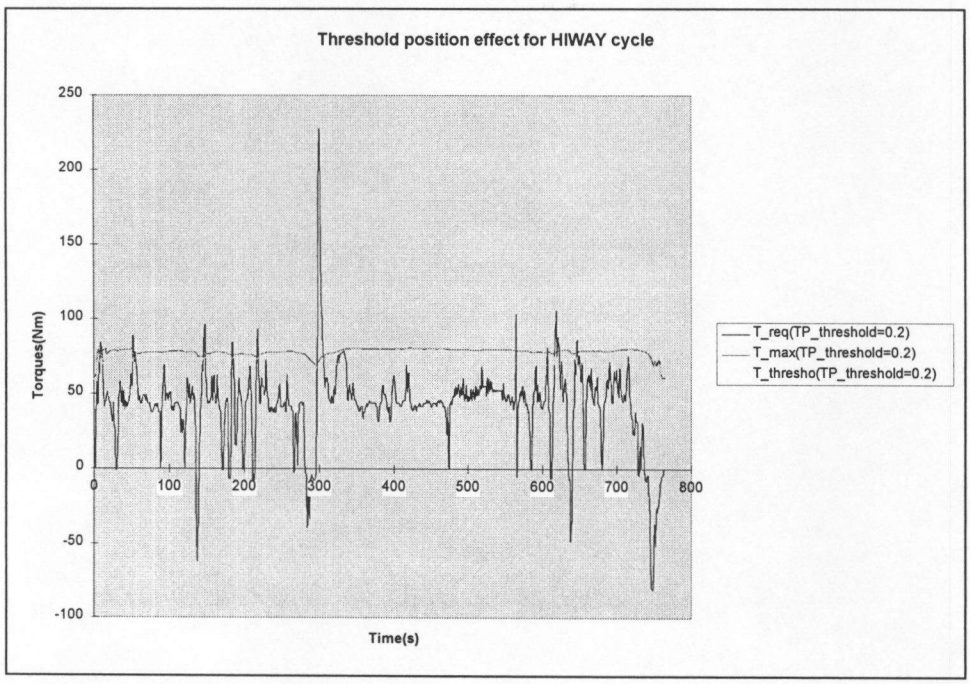


b. TP_threshold =0.7

fig. 4.21 (Continued)

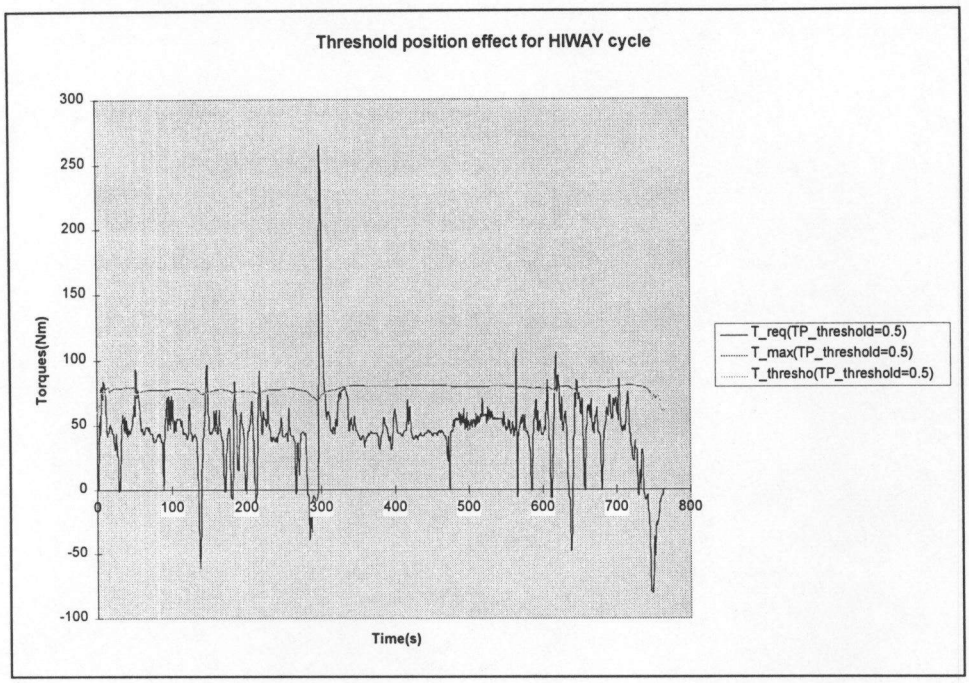


a. TP_thrshold =0

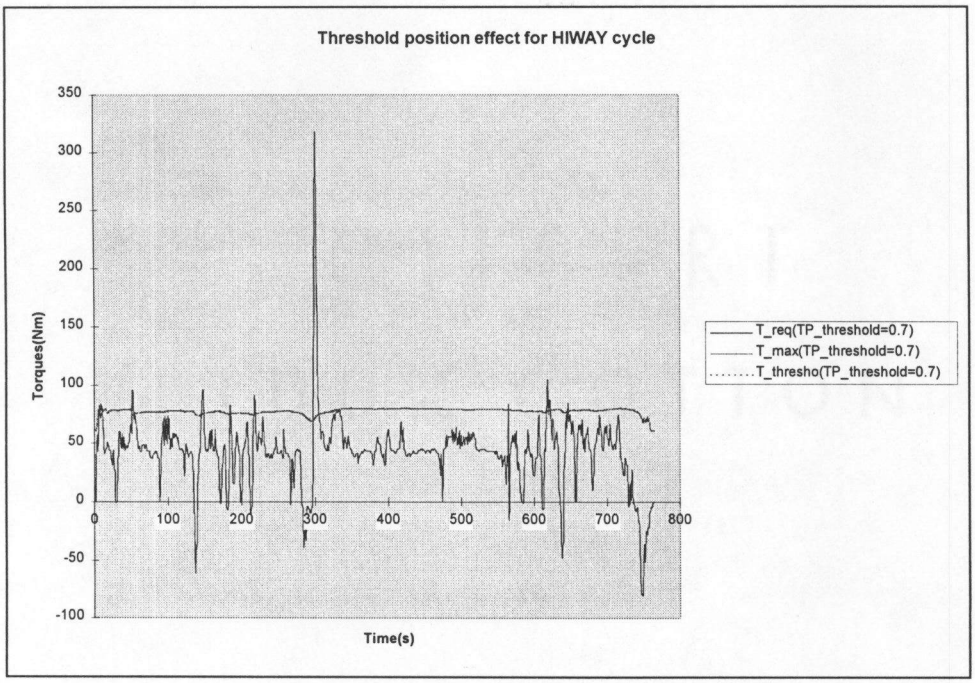


b. TP_threshold =0.2

fig.4.22 Threshold Position Effect on the Torque of APU in HIWAY Cycle



a. TP_thrshold =0.5



b. TP_threshold =0.7

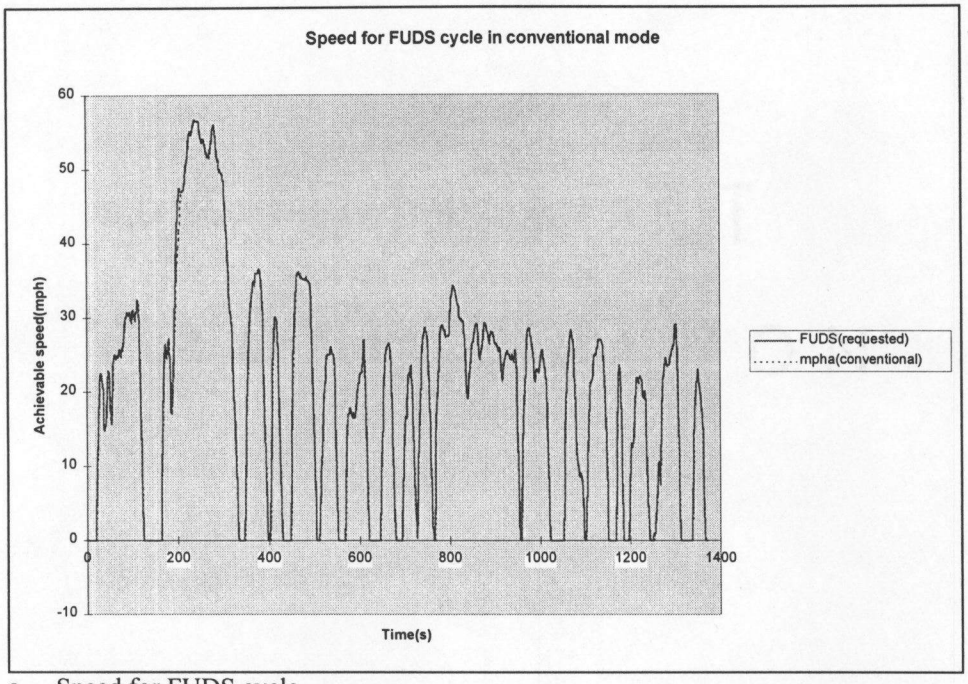
fig.4.22 (Continued)

This may not be the ideal design of the NEON HEV, since the whole idea behind the ESS-assist HEV is to minimize the power capacity of APU for driving the vehicle.

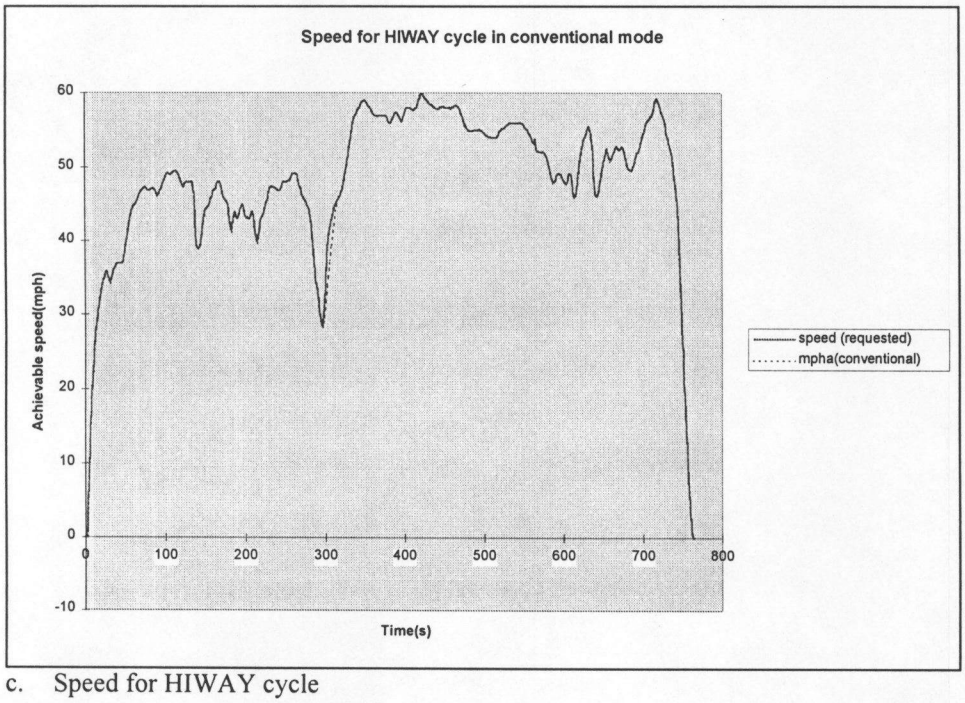
To examine the APU power capacity relative to the requested power for both FUDS and HIWAY cycles, plots have been made from the simulation with the power from the ESS diminished. The achievable speed is compared with the requested speed in the plots as shown in fig.4.23. It can be seen that without ESS assist, the vehicle can achieve most of the speed request by using the APU only.

To see the effect of the APU power capacity on the vehicle performance, a simulation was made by scaling down the GEO1L engine maximum torque output. When all the other components are set as before for the NEON, except using the H12N85 HORIZON battery, simulation results are plotted in fig.4.24 for FUDS cycle and in fig.4.25 for HIWAY cycle with the APU_trq_scale set at 0.5, 0.8 and 1 respectively. It can be noted from the comparison of the plotted curves that:

- the power from the APU increases and the power from the ESS decreases as the factor increases. The achievable speed approaches more close to the requested speed when the APU power increases;
- while the APU provides most of the power for driving the vehicle, the ESS power increases as the scale factor decreases;
- when the factor is 0.5, the SOC drops quickly and can not be recovered during the cycle. This is because that as the maximum torque from the APU is reduced, the threshold torque of the APU is reduced accordingly. Fig 4.26 show the requested torque and threshold torque at APU_trq_factor=0.8 and 0.5 respectively. The same information for APU_trq_factor=1 is shown in fig.4.3. We see that for both the FUDS and the HIWAY cycles, when the factor is 0.5, the requested torque and the threshold torque are getting close, regeneration capabilities are significantly impaired compared to the case of APU_trq_factor=0.8. As a result, the SOC can not be recovered.
- for the case when the factor is 0.8, there is more ESS assist compared to the case using the original APU. However, notice that the SOC can not be fully regained during each cycle. This may be a compromise between reducing the APU capacity for HEV operation and attaining sustained SOC from regeneration.

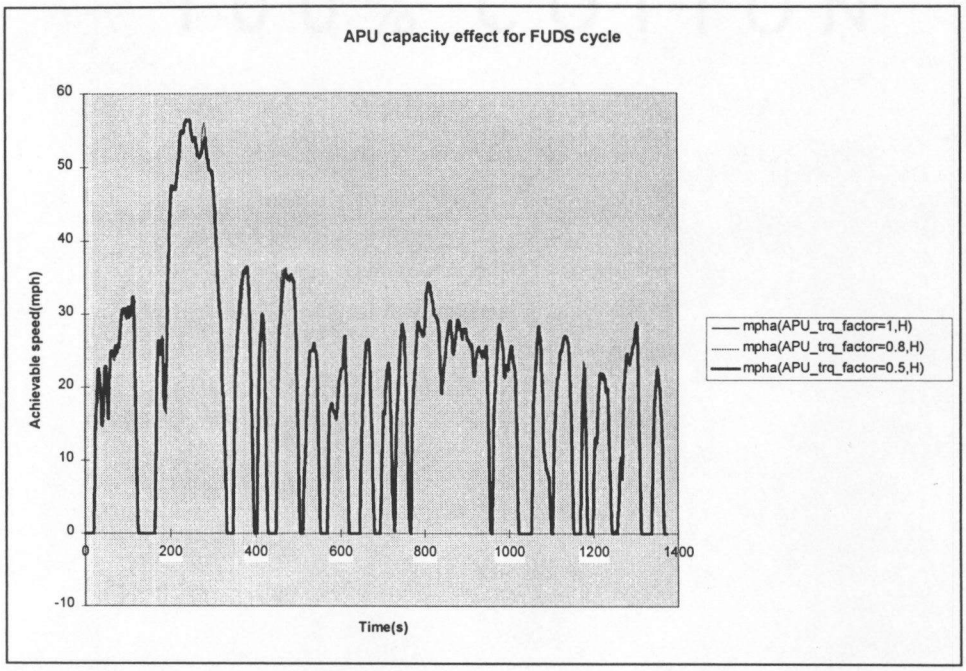


a. Speed for FUDS cycle

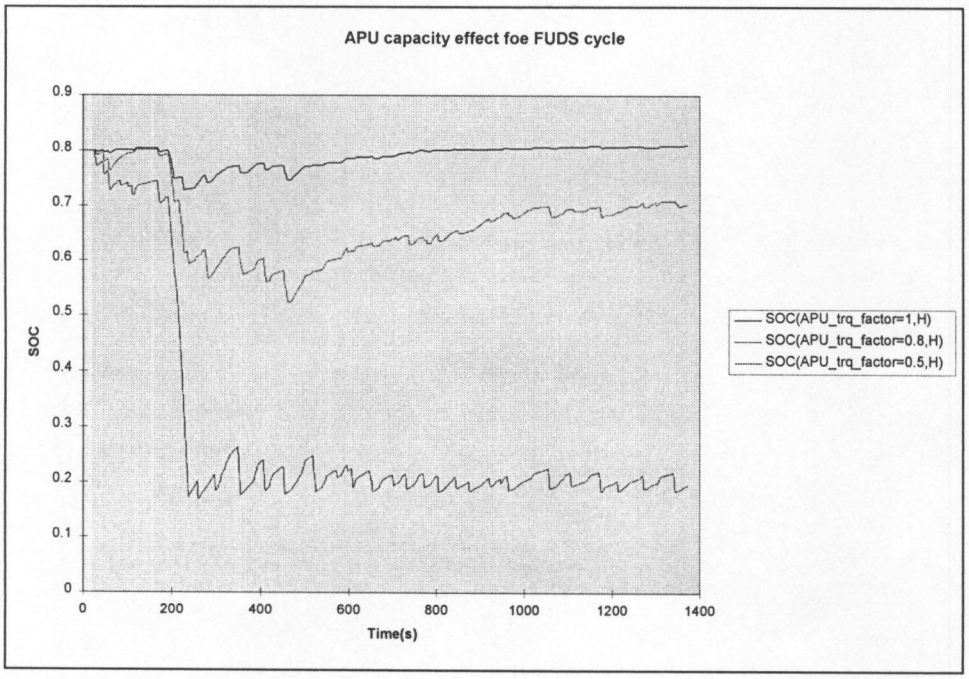


c. Speed for HIWAY cycle

fig.4.23 Comparison of Requested and Achievable Speed and Range in Conventional Mode Driving

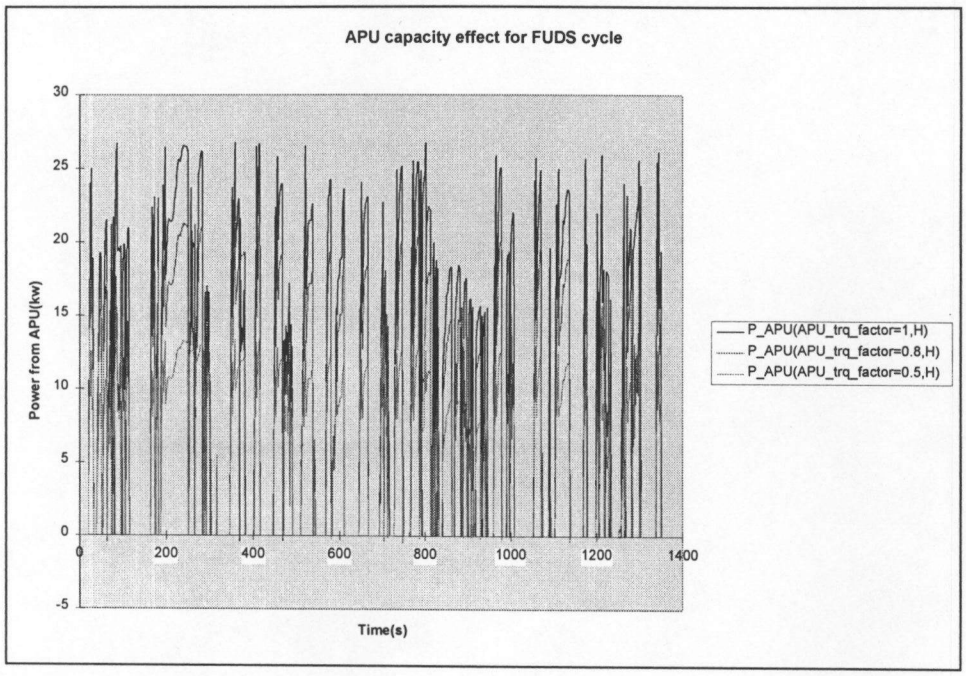


a. Achievable speed

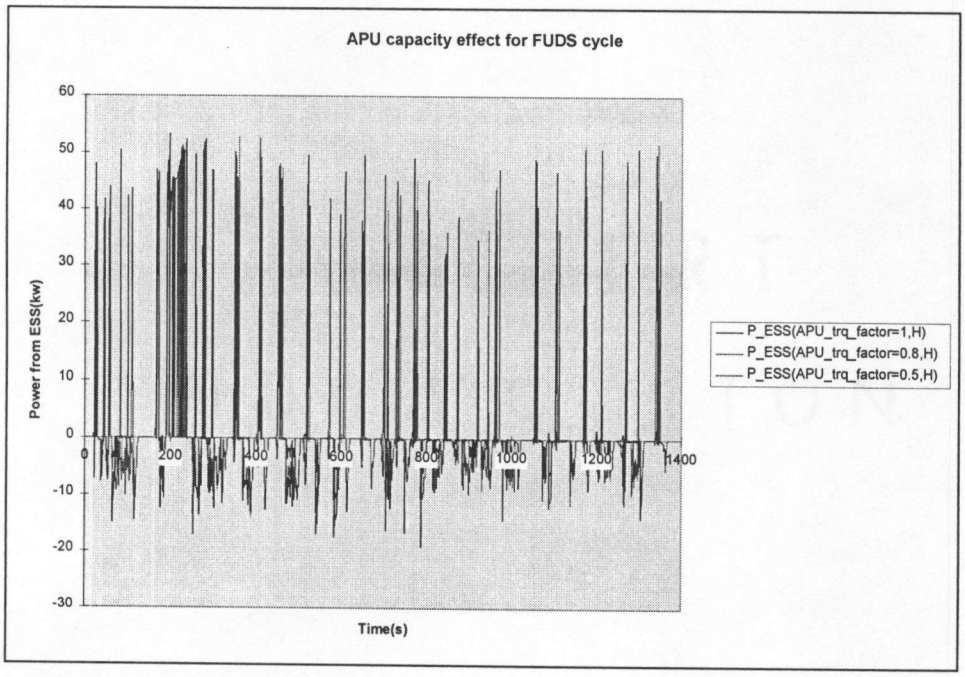


b. SOC

fig. 4. 24 APU Power Effect on the Vehicle Performance in FUDS Cycle, with H12N85 HORIZON Battery

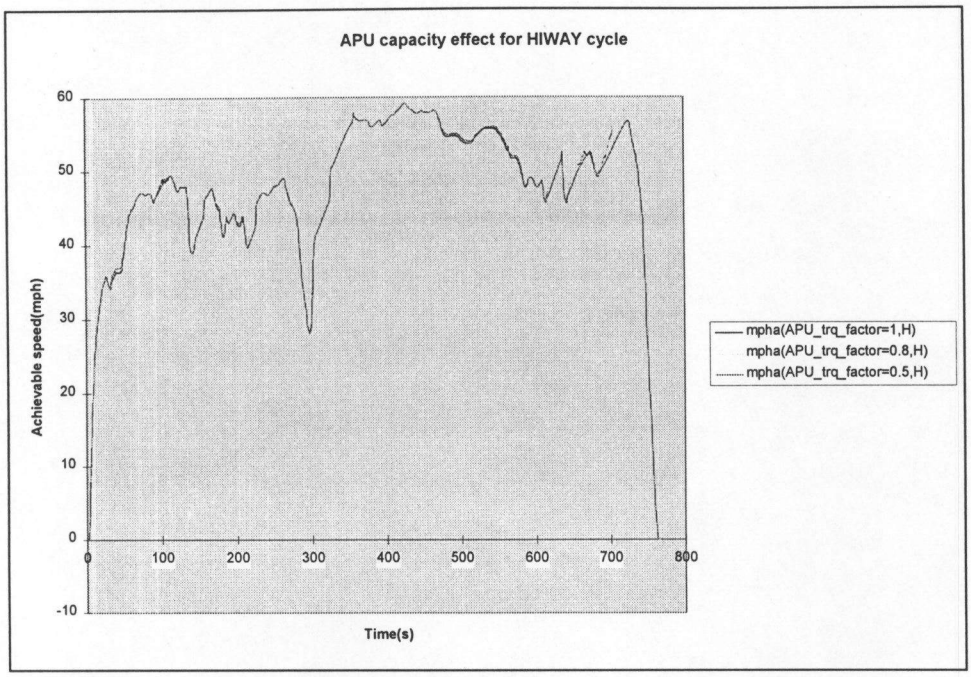


c. Power from APU

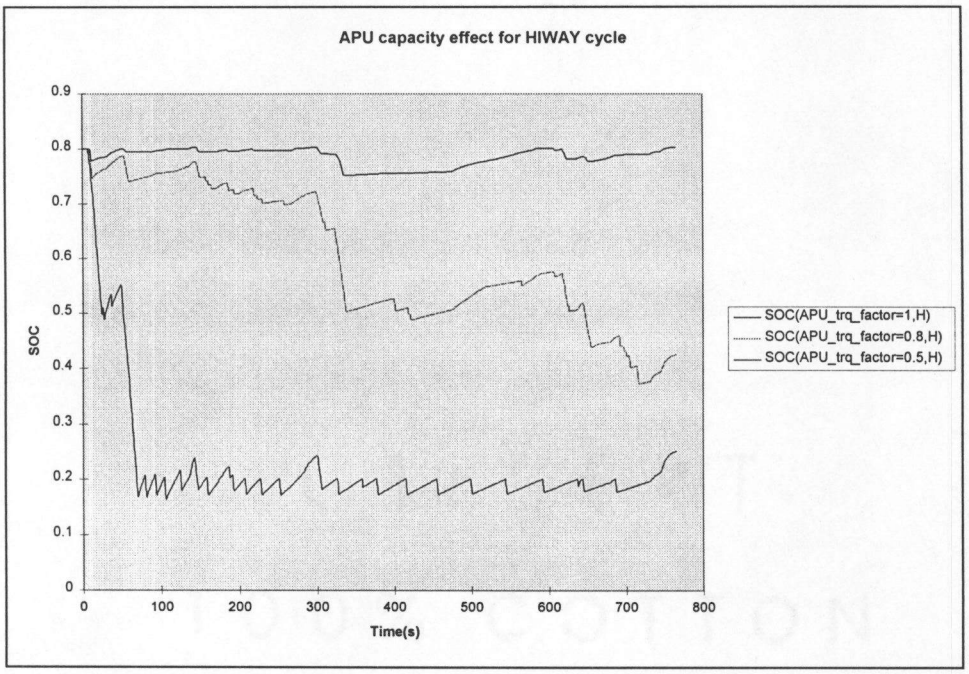


d. Power from ESS

fig. 4. 24 (Continued)

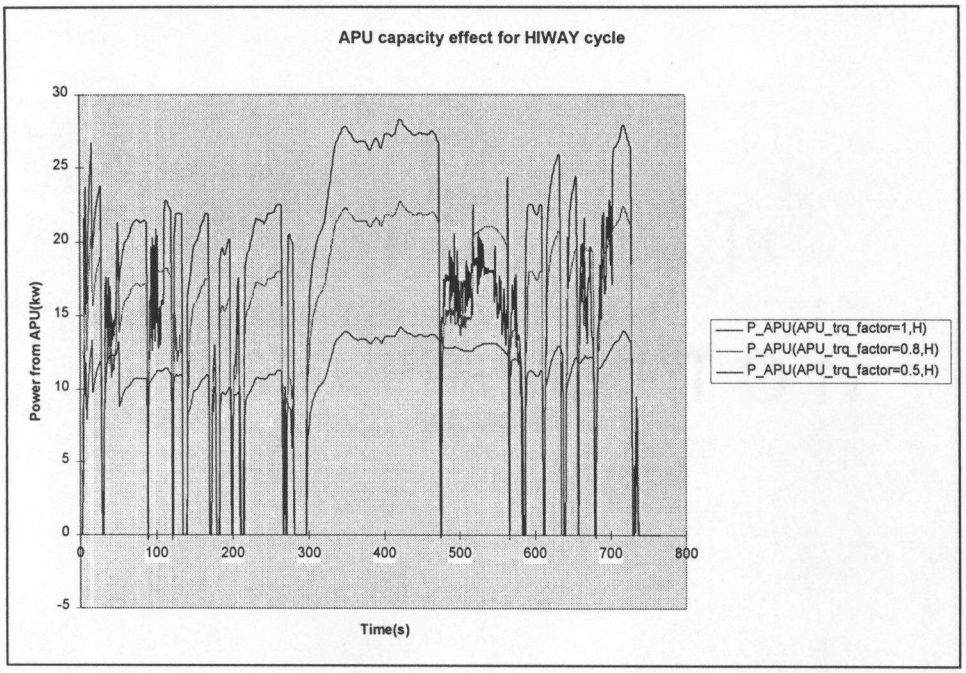


a. Achievable speed

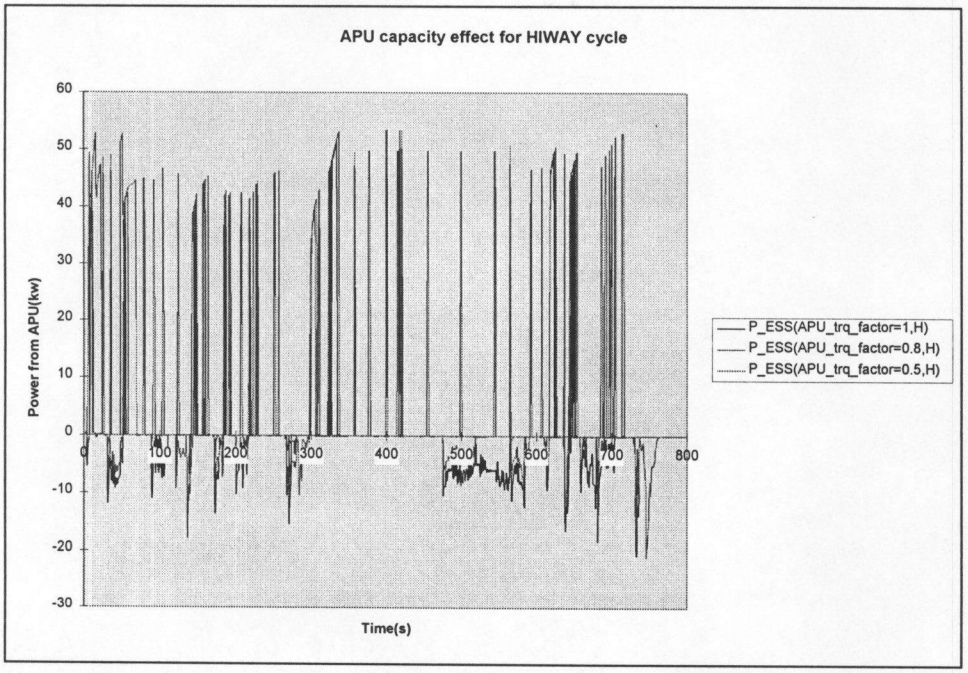


b. SOC

fig.4.25 APU Power Effect on the Vehicle Performance in HIWAY Cycle, with H12N85 HORIZON Battery

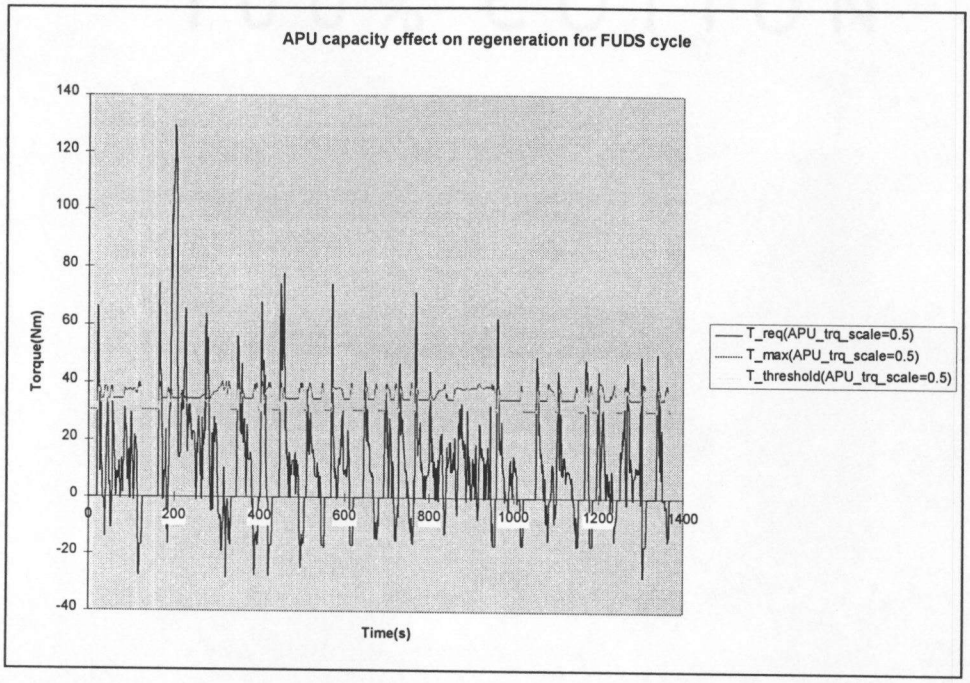


c. Power from APU

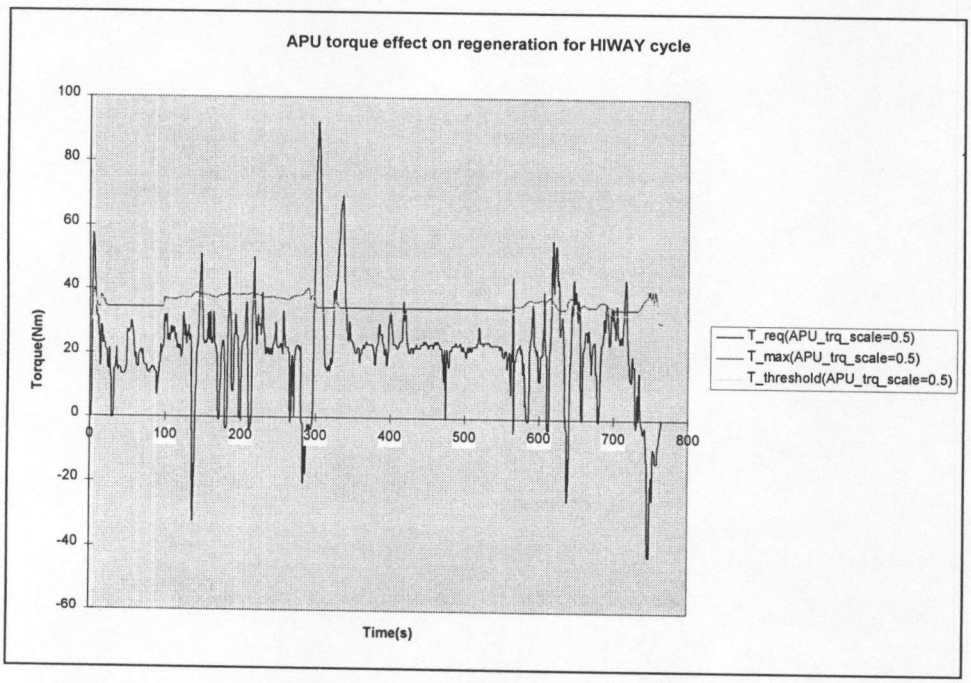


d. Power from ESS

fig.4.25 (Continued)

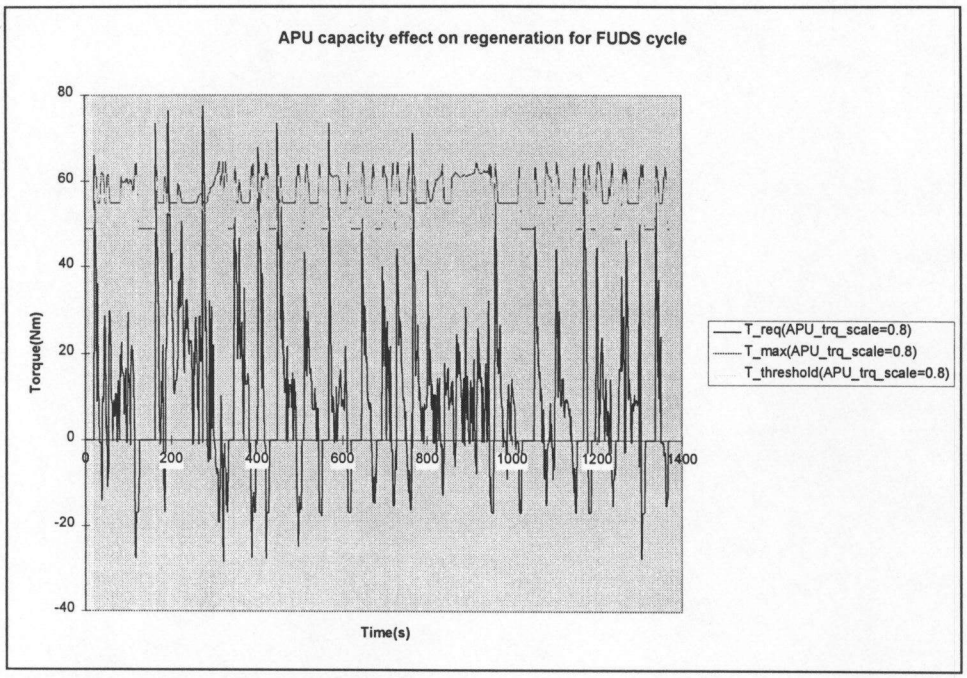


a. APU_trq_scale=0.5 for FUDS cycle

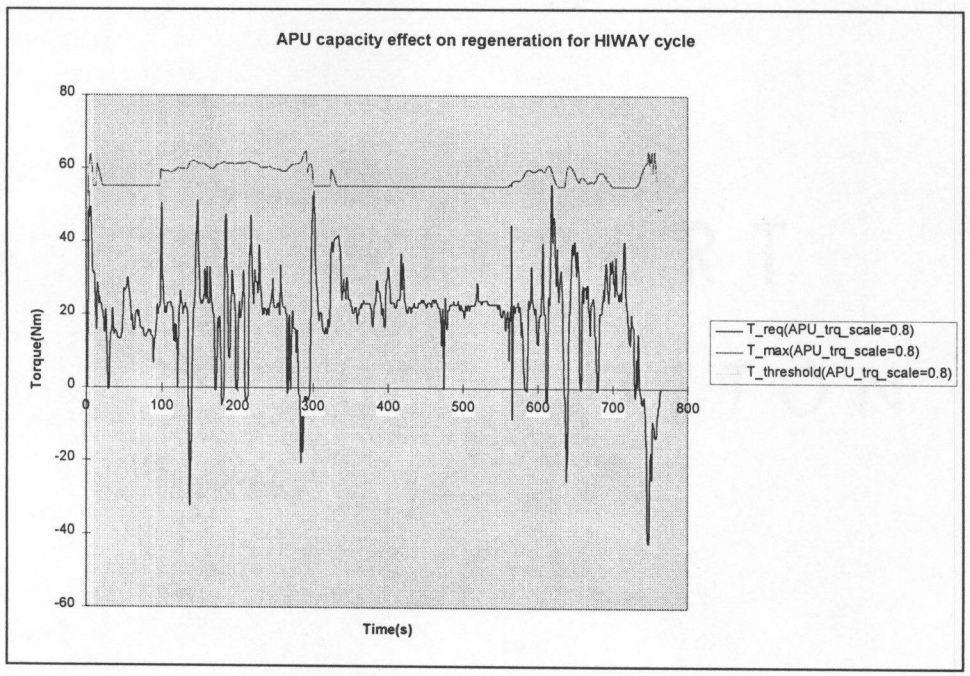


b. APU_trq_scale=0.5 for HIWAY cycle

fig.4.26 Torque Request and Threshold Torque of APU with Different APU_trq_factors



a. APU_trq_scale=0.8 for FUDS cycle



b. APU_trq_scale=0.8 for HIWAY cycle

fig.4.26 (Continued)

- when the battery capacity is reduced, the final SOC would be even lower than with the NEON battery shown in fig.4.27 and fig.4.28.

Based on the simulation results, we can conclude that for the purpose of reducing APU capacity while maintaining fairly good vehicle performance and sustainable SOC of the battery, a higher capacity battery is much preferable to the one with lower capacity. Besides, we know that when reducing the capacity of the APU, it can not be lower than the half of the present APU capacity if the vehicle is to operate as a charge sustaining hybrid vehicle.

3.3.7 Transmission effect

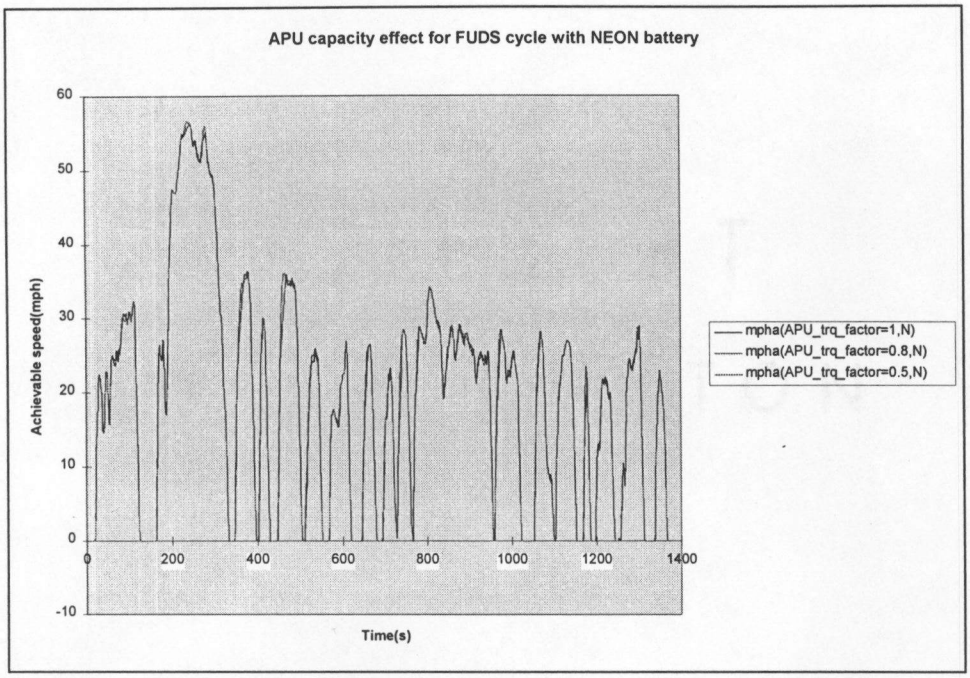
Simulation of transmission effect is made with two different transmission files. The NEON transmission was used for the previous analysis. Another transmission has been incorporated into ADVISOR. The major difference of NEON transmission and ADVISOR transmission, M5SPD, is the gear ratio as listed in Table 4.1. The speed torque map and the efficiency map of the two transmissions are identical.

The simulation results with the NEON battery and two different transmissions are plotted in fig.4.29 and fig.4.30 for the FUDS cycle and for the HIWAY cycle respectively. It can be noticed that:

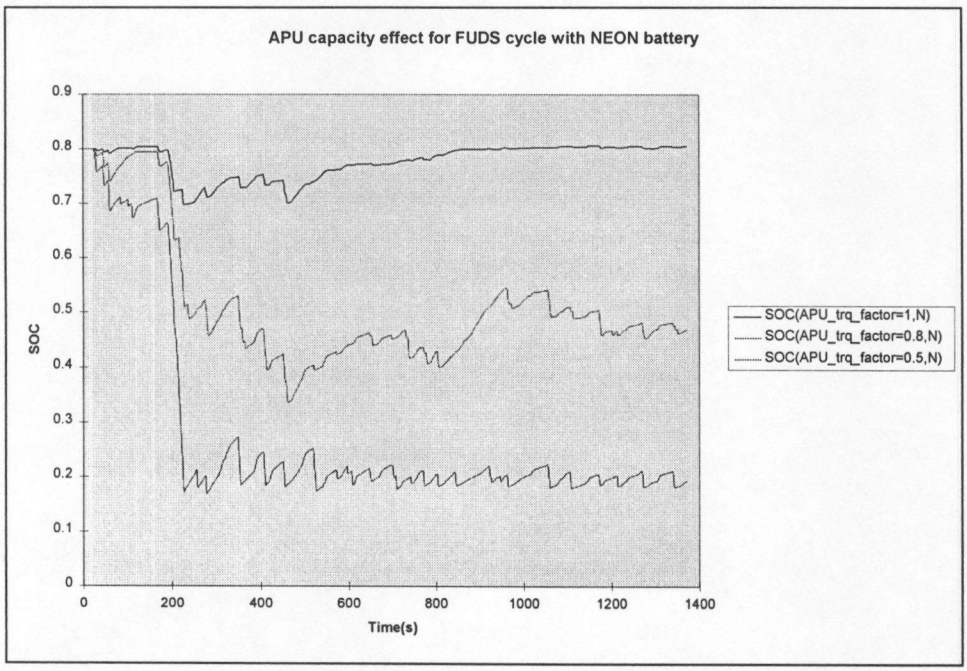
- the transmission has no effect on the speed and range profiles;
- in the FUDS cycle, both transmissions enable SOC to be fully recovered;
- in the HIWAY cycle, the NEON transmission enables the SOC to be recovered while the M5SPD transmission can not enable SOC to be recovered;

Table 4.1 Transmission Comparison

	gr_num #1	gr_num#2	gr_num#3	gr_num#4	gr_num#5
NEON_T	17.7	10.65	6.8	5.15	3.6
M5SPD_T	12.36	6.67	4.67	3.52	2.65

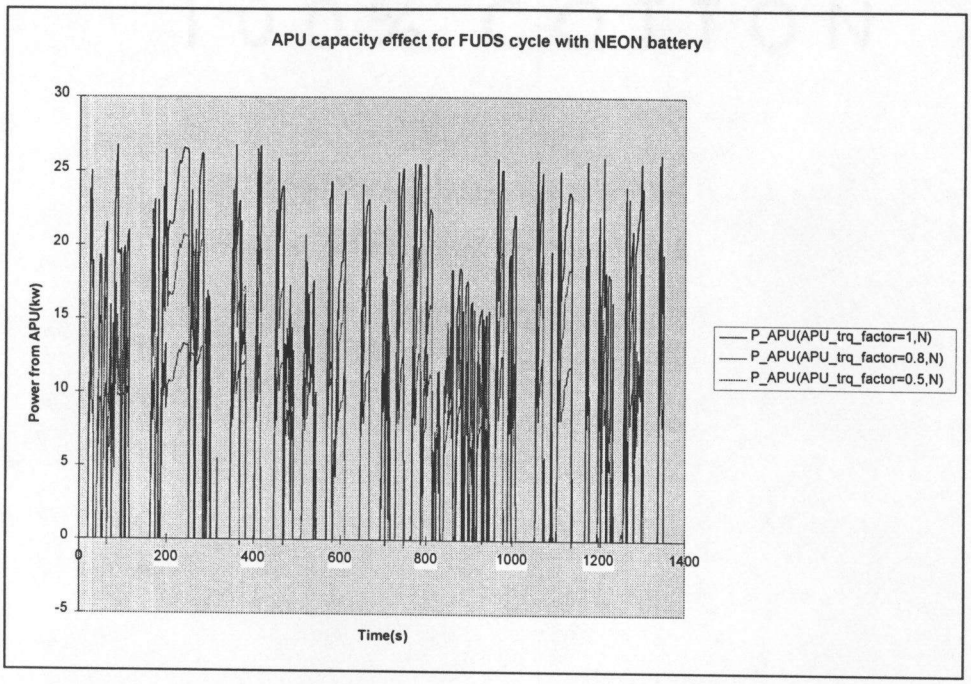


a. Achievable speed

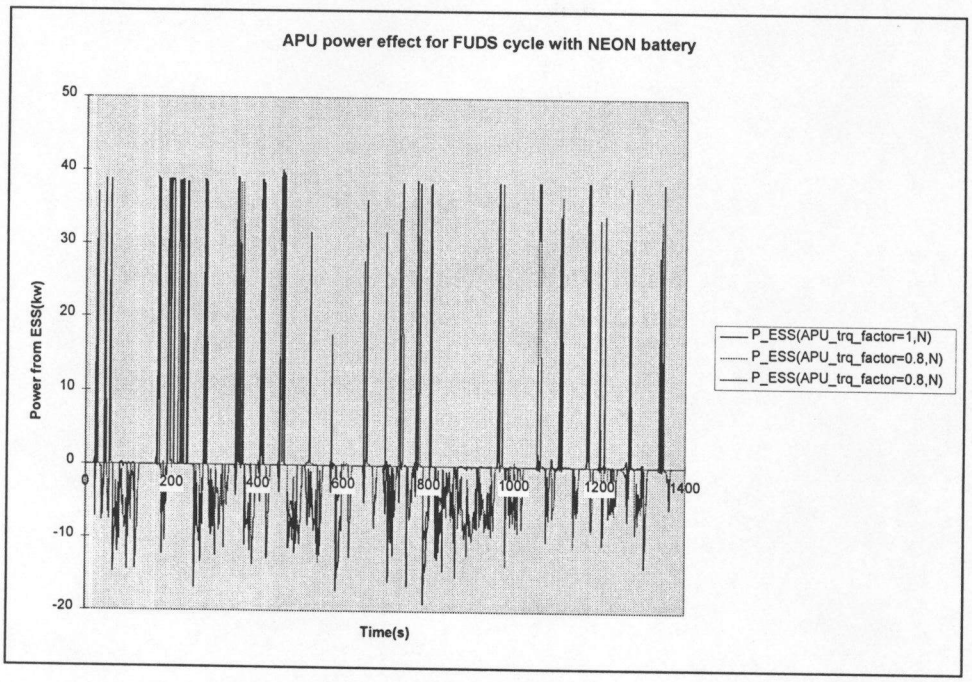


b. SOC

fig. 4.27 APU Power Effect on the Vehicle Performance in FUDS Cycle, with NEON Battery

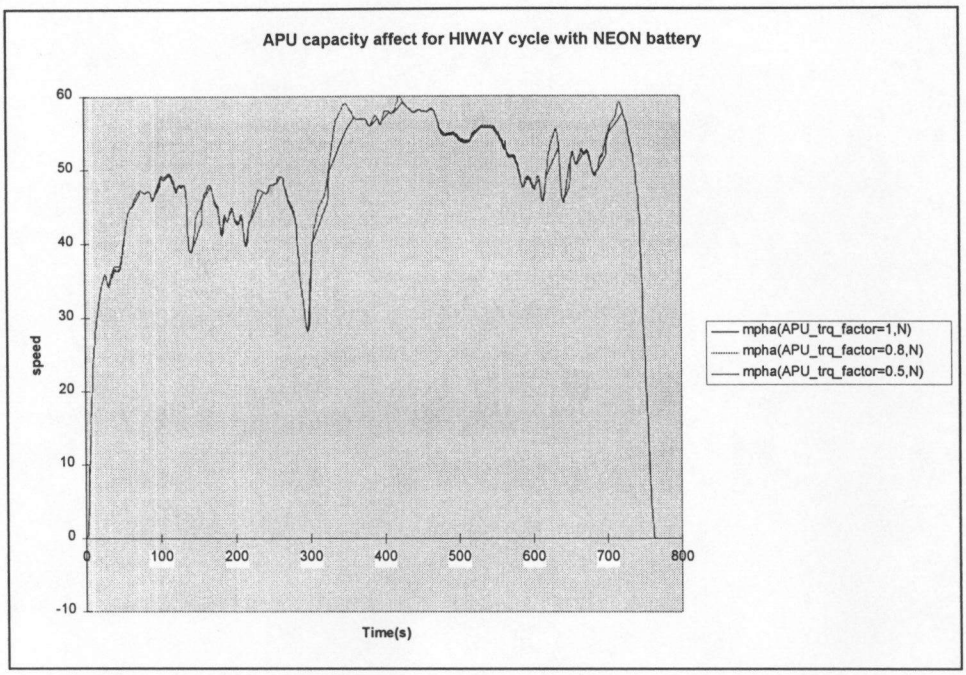


c. Power from APU

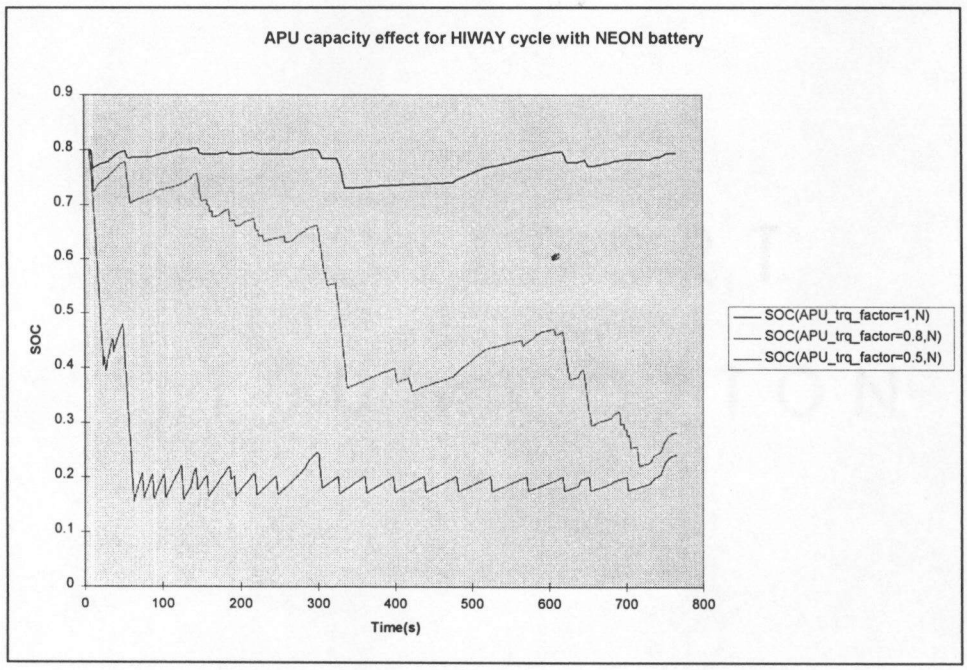


d. Power from ESS

fig. 4.27 (Continued)

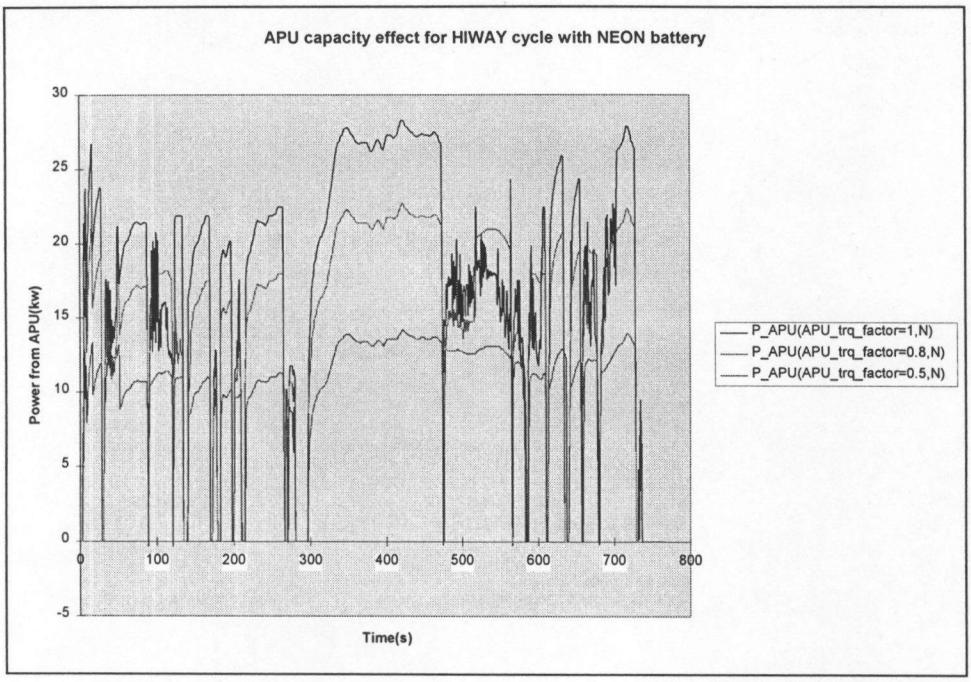


a. Achievable speed

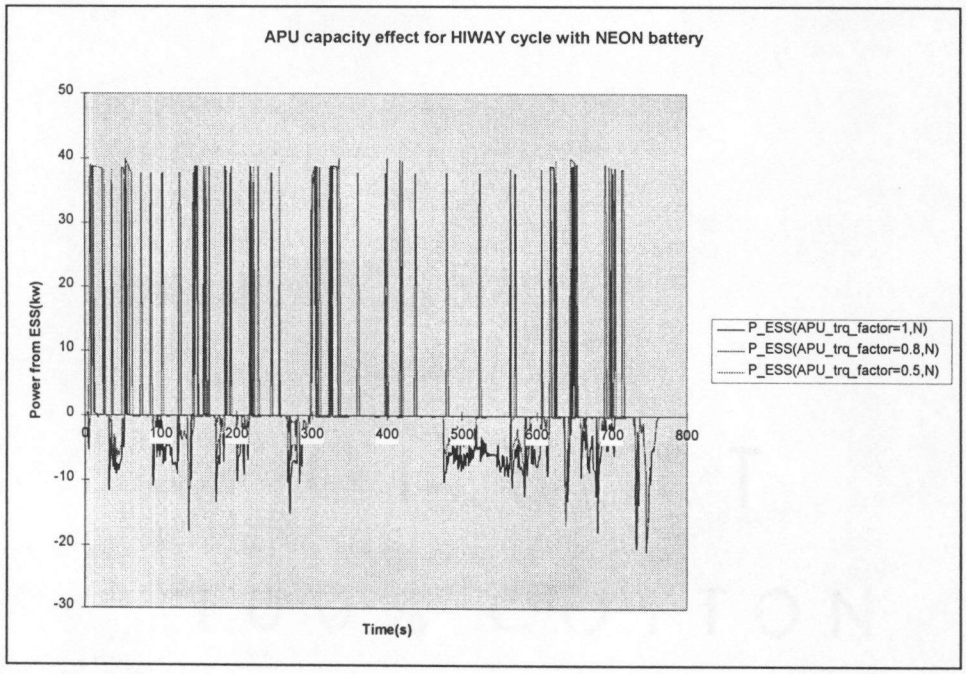


b. SOC

fig.4.28 APU Power Effect on the Vehicle Performance in HIWAY Cycle, with NEON Battery

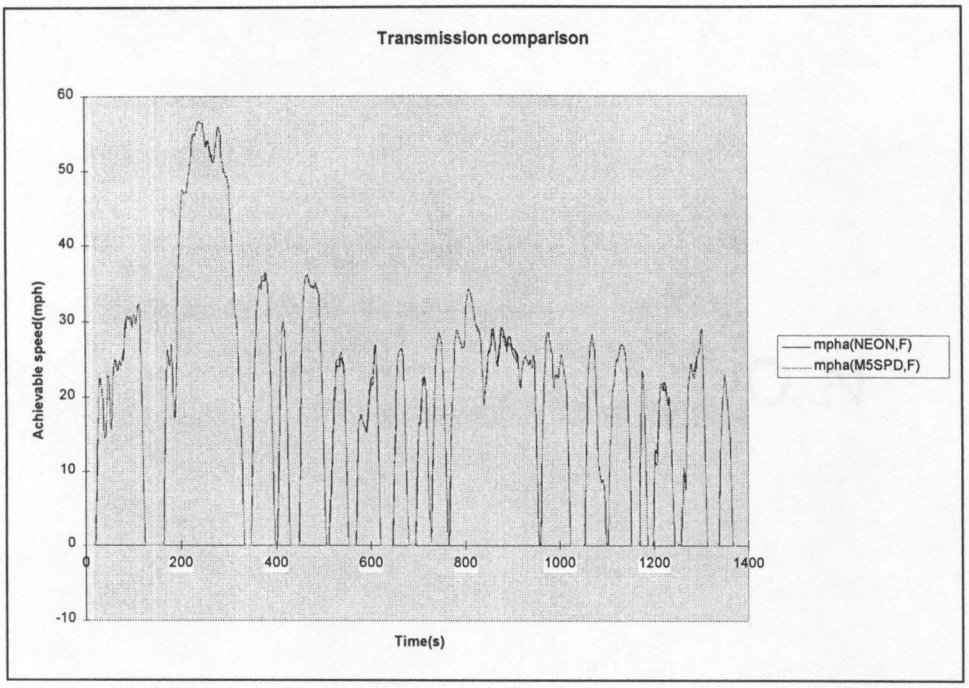


c. Power from APU

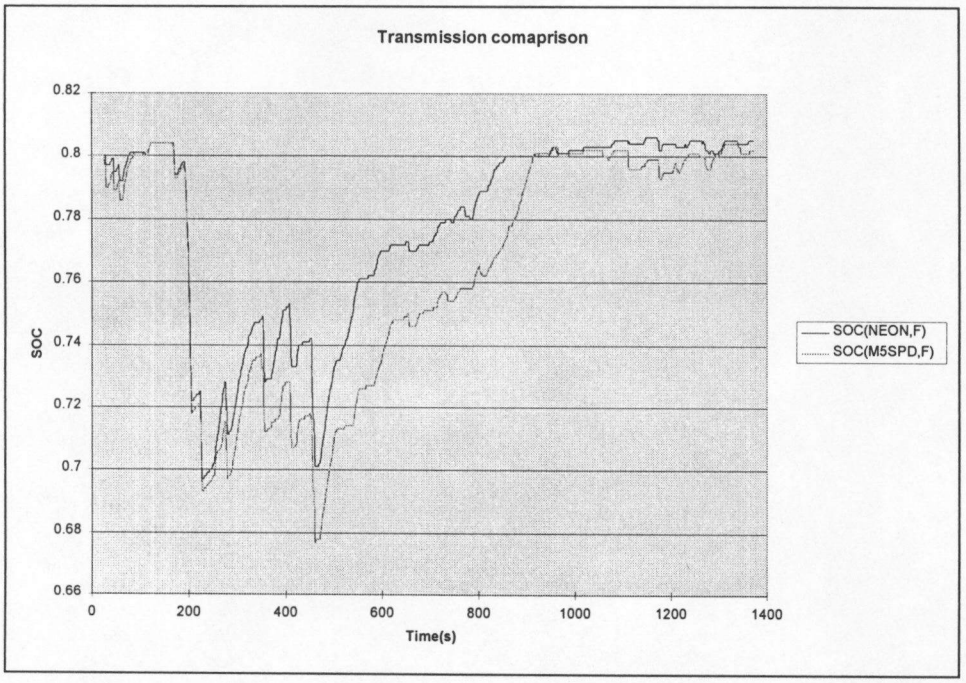


d. Power from ESS

fig.4.28 (Continued)

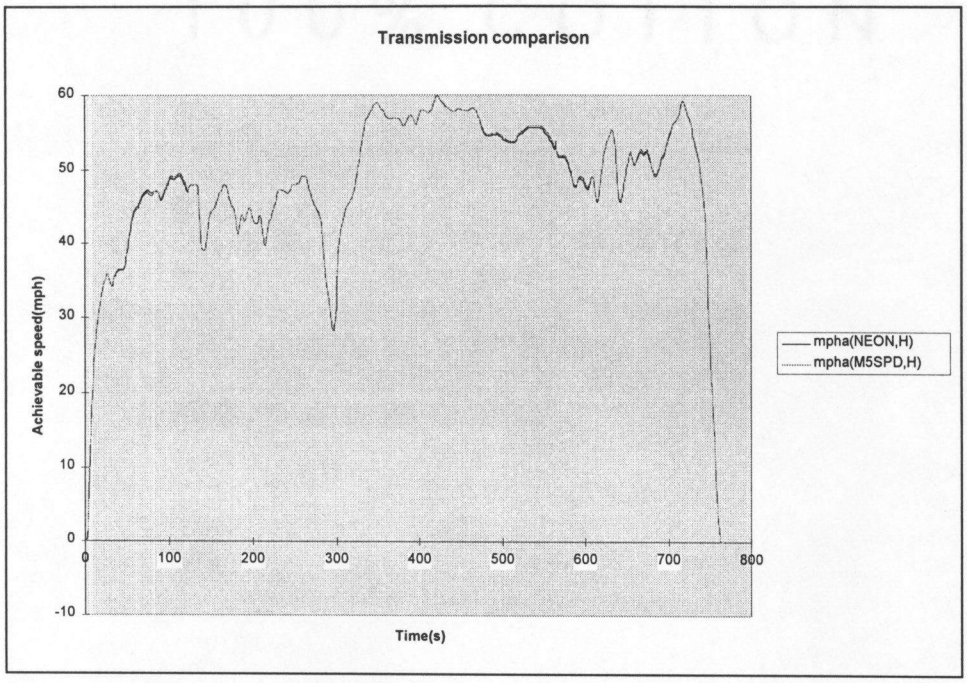


a. Achievable speed

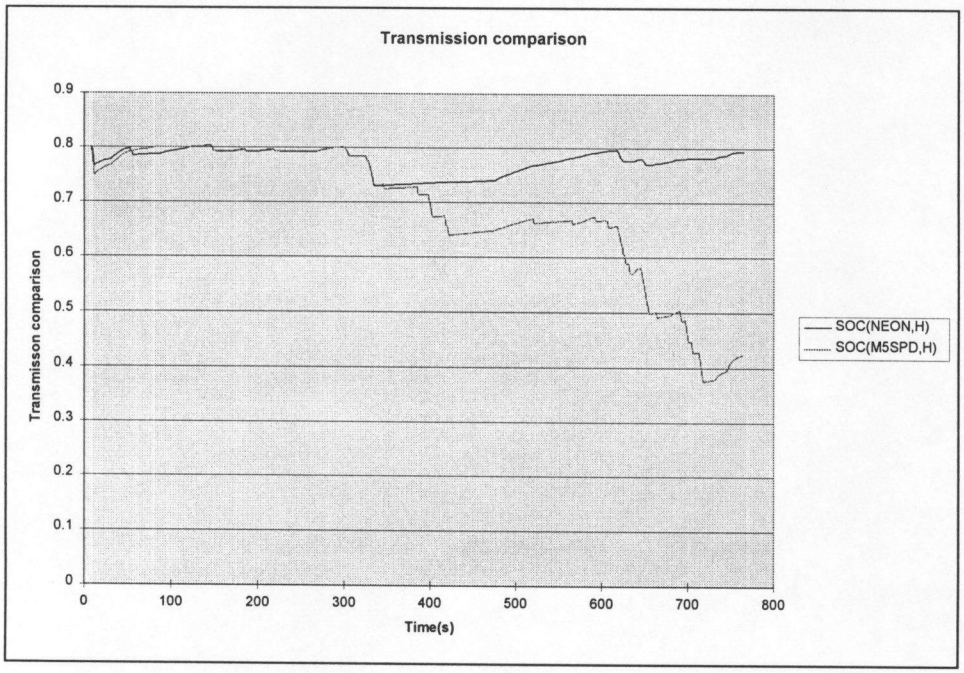


b. SOC

fig.4.29 Transmission Comparison for FUDS Cycle



a. Achievable speed



b. SOC

fig.4.30 Transmission Comparison for HIWAY Cycle

This is caused by the change of the APU speed and torque profile. In the FUDS cycle, the transmission change leads to change of APU speed and torque request from transmission to Torque Coupler Module. The differences as a result of the changes in requested torque vs threshold torque for the two different transmissions are not significant. Therefore, the regeneration and regenerative braking energy for recharging the battery are very close. However, in the HIWAY cycle, the speed and torque changes the APU results in much deviation in the regeneration capability, which causes different final SOC values.

From this simulation we can conclude that for the current NEON transmission speed-torque profile, the NEON gear ratio range is preferable for both the HIWAY and the FUDS driving patterns in terms of power distribution and the regeneration capability.

3.4 EV Range

The EV range was predicted by the simulation model with the NEON battery and the HORIZON battery. The EV performance with the NEON battery is plotted in fig.4.31 for the FUDS cycle, in fig.4.32 for the HIWAY cycle, and with the H12N85 HORIZON battery in fig.4.33 for the FUDS cycle, and in fig.4.34 for the HIWAY cycle. The simulation assumes that regen_level=1, SOC initial value is at 0.8, and SOC limits are SOC=0.2~0.8. It can be seen that

- there is a significant difference between the requested speed and the available speed, the speed achievable diminishes as battery SOC goes low;
- with the NEON battery, the SOC drops more quickly than the HORIZON battery SOC in each cycle. As a result, the H12N85 HORIZON battery gives rise to more range than the NEON battery. For both batteries, the power provided can last for 10 FUDS cycles and 15 HIWAY cycles. The final range achieved are listed in Table 4.2.

Table 4.2 EV Range Simulation Results

Battery type	Range(mile)	
	FUDS	*HIWAY*
NEON battery	8.59	14.99
H12N85 HORIZON battery	18.05	32.11
standard 1 cycle range	7.45	10.25

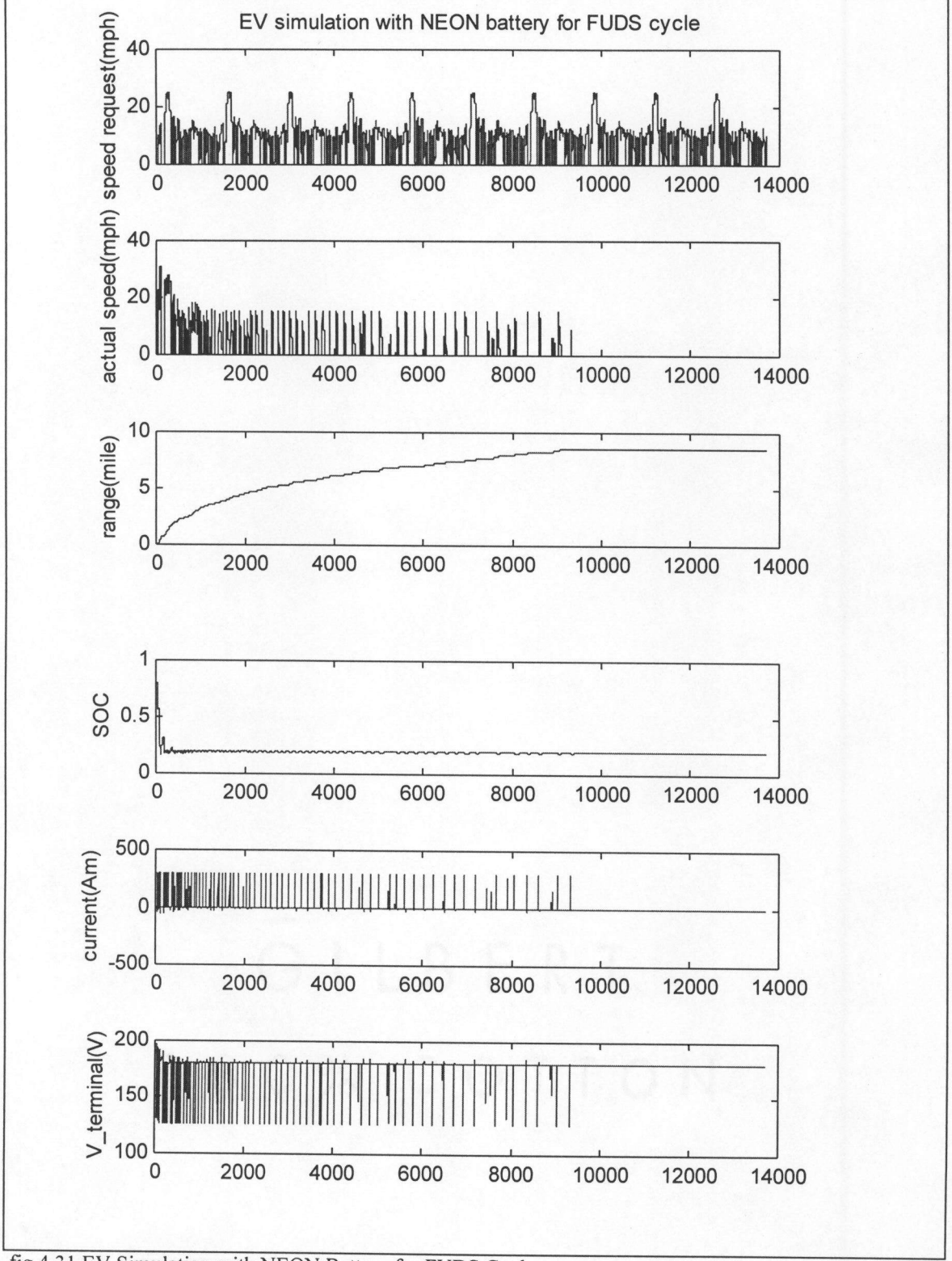


fig.4.31 EV Simulation with NEON Battery for FUDS Cycle

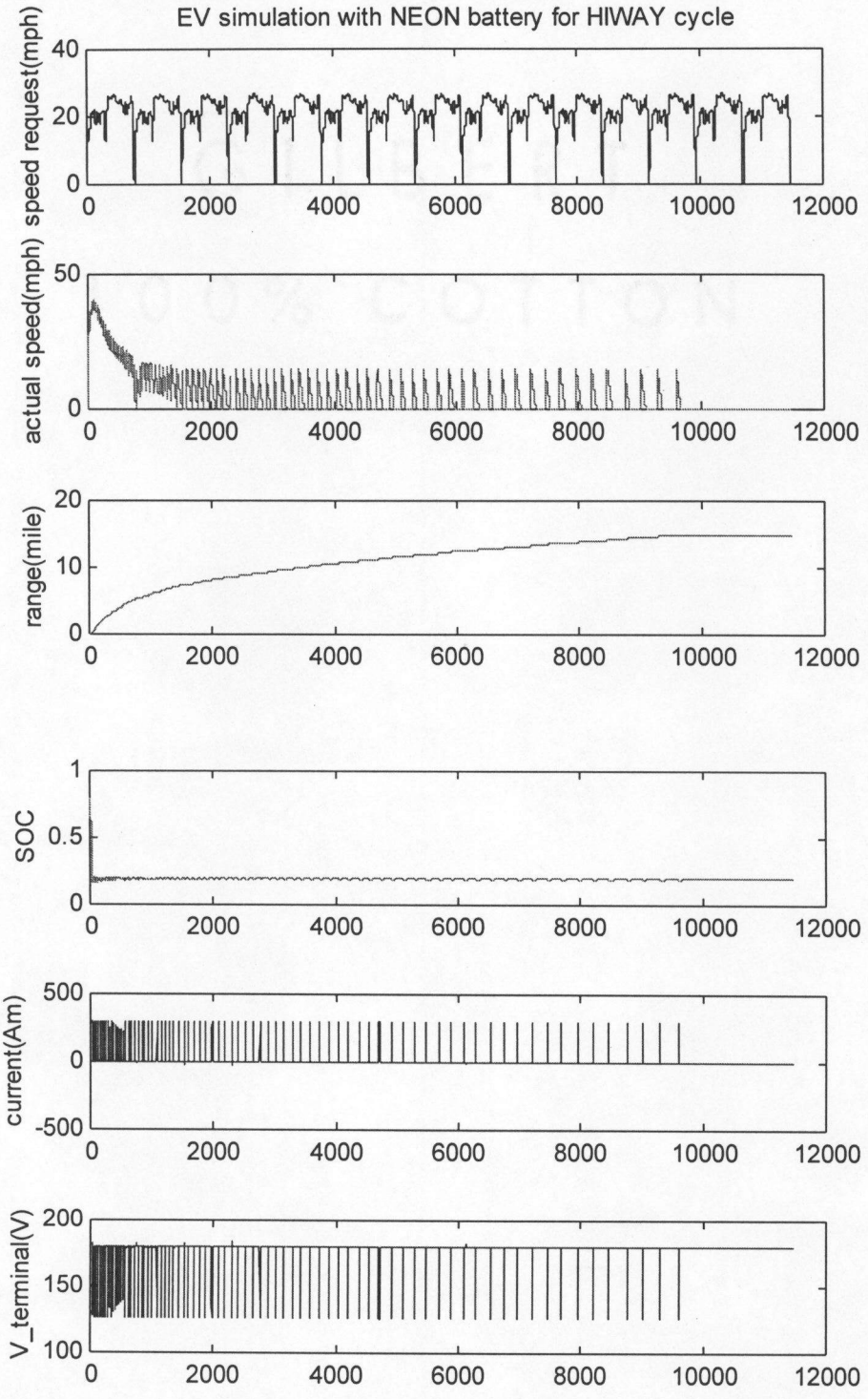


fig.4.32 EV Simulation with NEON Battery for HIWAY Cycle

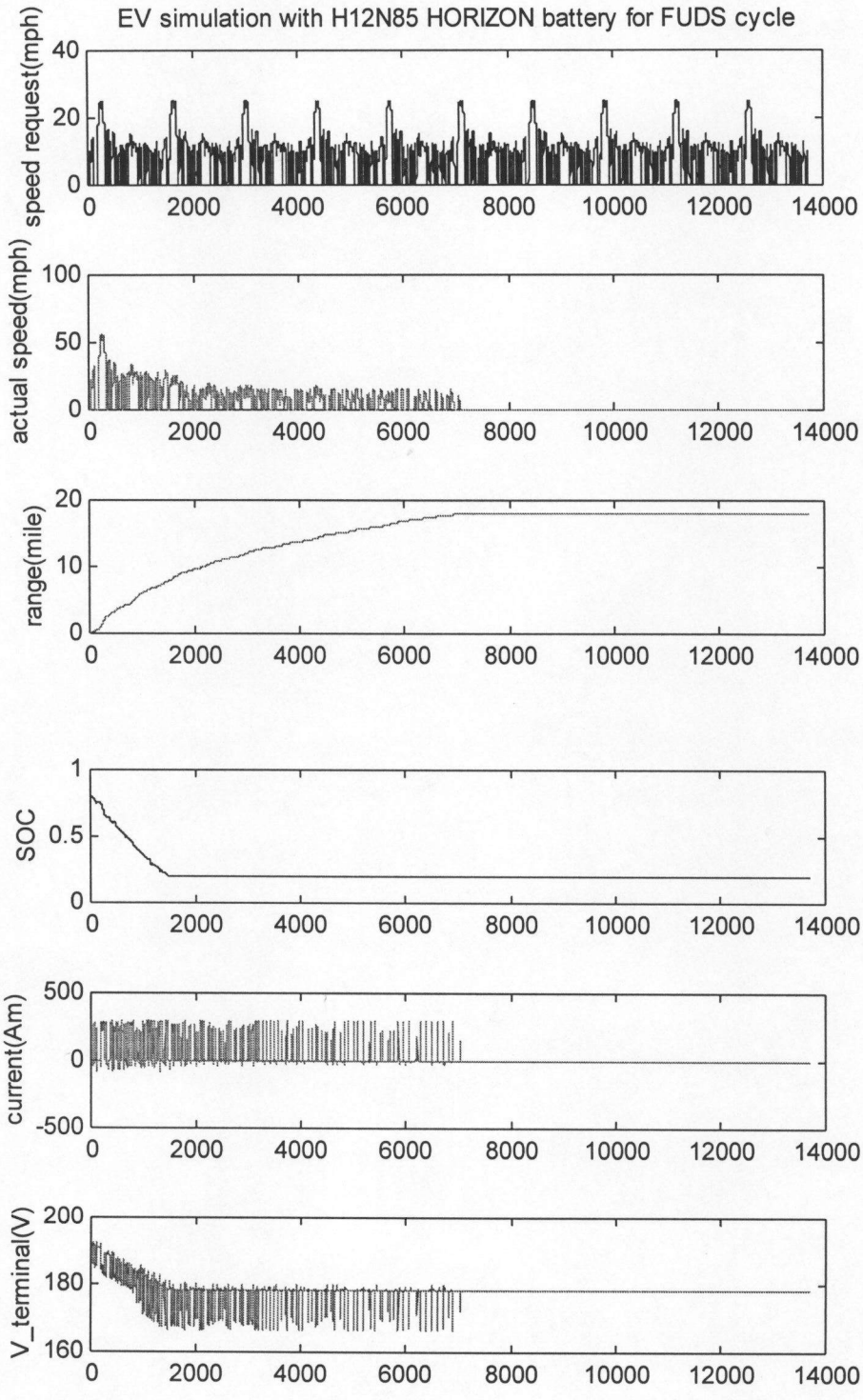


fig.4.33 EV Simulation with H12N85 HORIZON Battery for FUDS Cycle

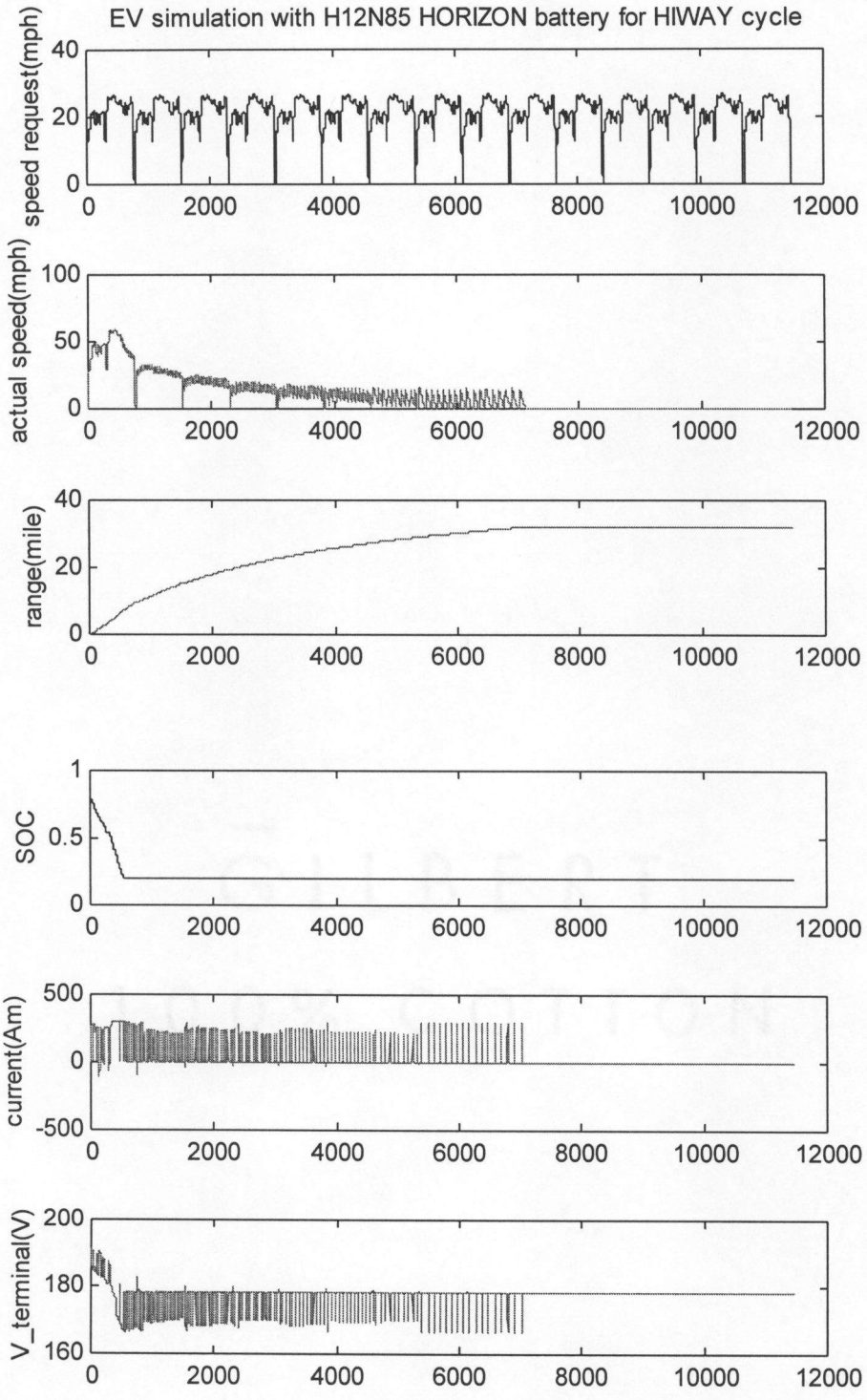


fig.4.34 EV Simulation with H12N85 HORIZON Battery for HIWAY Cycle

3.5 Maximum Acceleration Effort

The maximum acceleration effort simulates the maximum speed achievable within 20 seconds when the vehicle starting from standstill. The major factors analyzed for evaluating the effect on the maximum acceleration are the APU power, transmission and ESS capacity. Simulations were made with different combinations of the APU power capacity (APU_trq_scale=1, APU_trq_scale=0.8), ESS (NEON battery and HORIZON battery), and transmission (NEON transmission and M5spd transmission) for both the HEV and the EV mode driving conditions. The results of the final speed of the vehicle from these simulation are summarized in Table 4.3. Fig.4.35 are plots from the simulation for the HEV mode driving condition with APU_trq_scale=1. Fig.4.36 are results from the EV mode simulation, with APU_trq_factor=1.

For the HEV mode acceleration, it can be noted that:

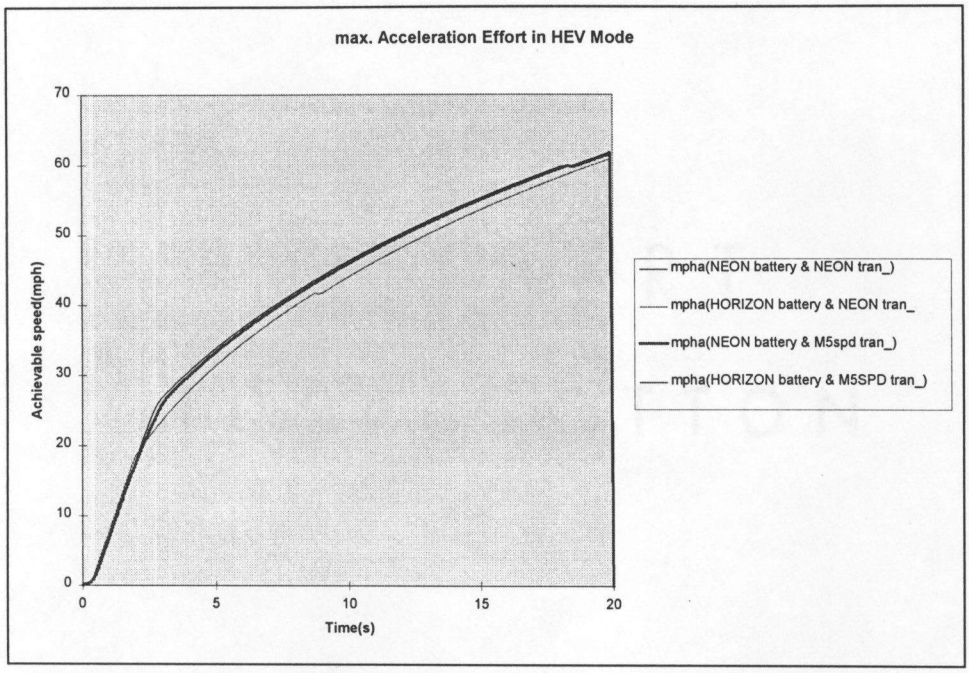
- with different batteries and two different transmissions, there is no significant difference between the achievable speed;
- the transmission plays a more important role than the battery in obtaining higher acceleration. M5SPD transmission yields higher achievable speeds. But with APU power, the difference is not significant since the APU power compensated the power difference of motor due to transmission;
- the difference in the battery Ah capacity has no noticeable effect on the acceleration since their power output are close to each other, although the SOC of the HORIZON battery changes less than the NEON battery;

For EV mode acceleration,

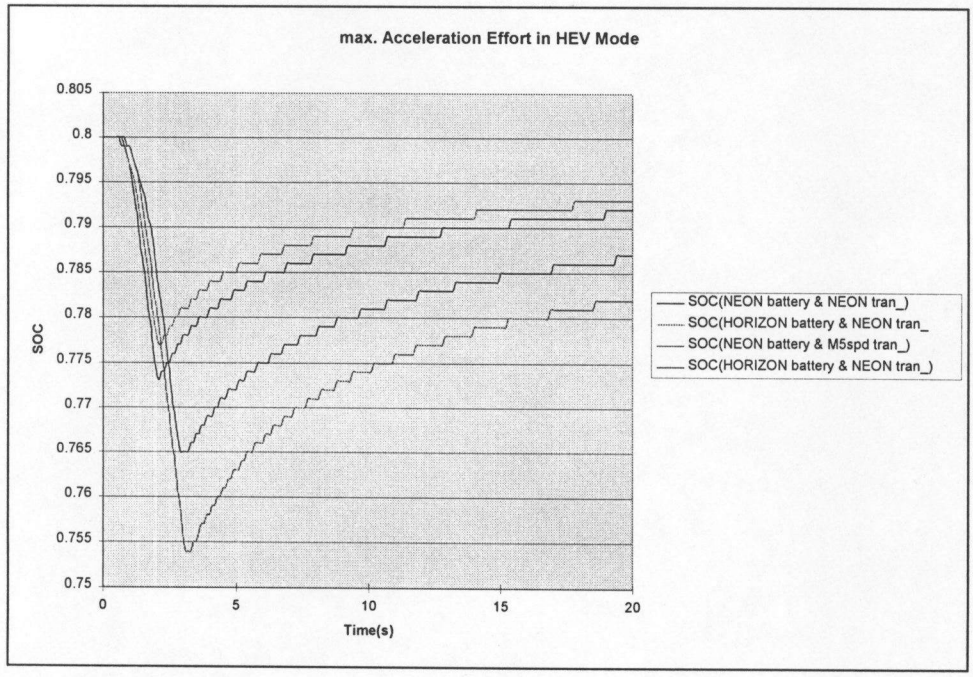
- there is significant contrast in the final speed achievable with different transmission. M5SPD transmission is a better choice for high EV acceleration. Battery capacity effect is negligible.

Table 4.3 Max. Acceleration Effort Simulation

	HEV MODE(APU_trq_scale=1)		HEV MODE(APU_trq_scale=0.8)		EV MODE	
	NEON Battery	*HORIZON Battery*	*NEON Battery*	*HORIZON Battery*	*NEON Battery*	*HORIZON Battery*
NEON Transmission	69.47	70.20	54.98	54.99	19.41	19.41
M5SPD Transmission	72.87	74.34	56.34	56.64	27.75	27.76

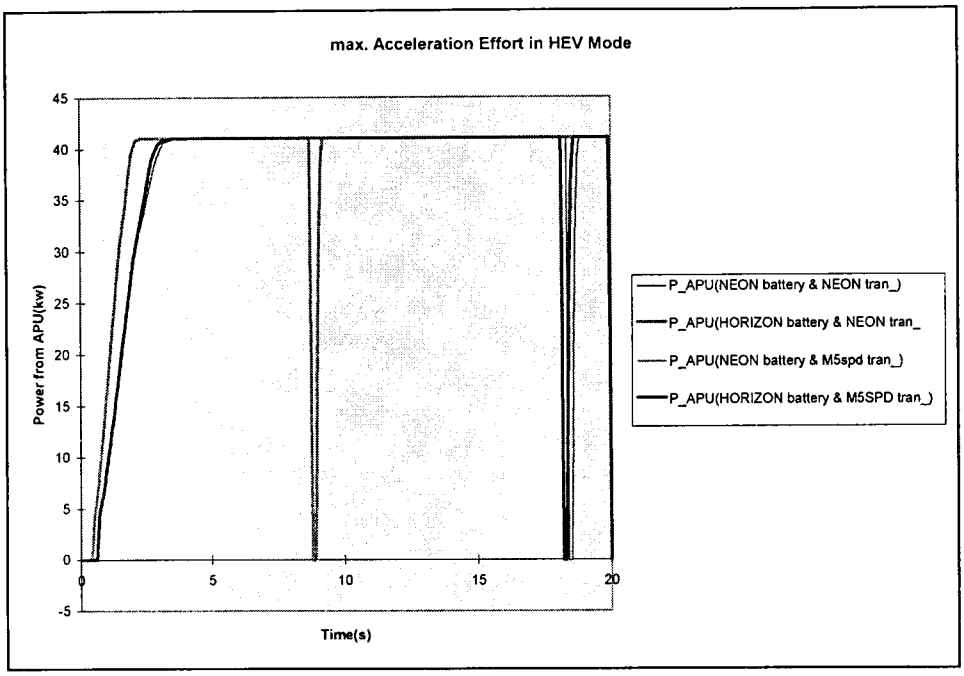


a. Achievable speed

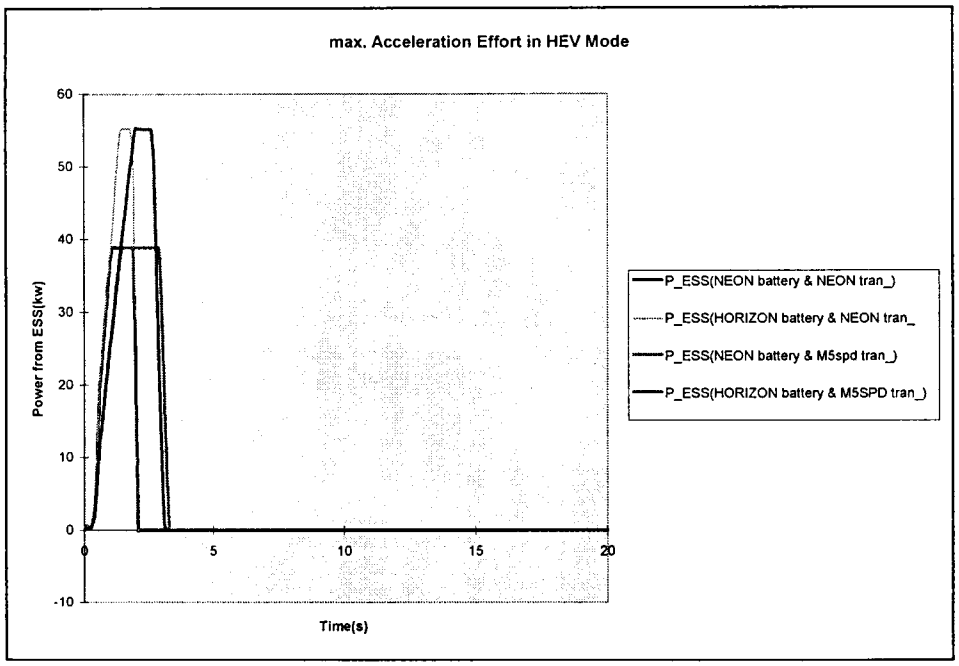


b. SOC

fig.4.35 Maximum Acceleration Effort Simulation in HEV Mode

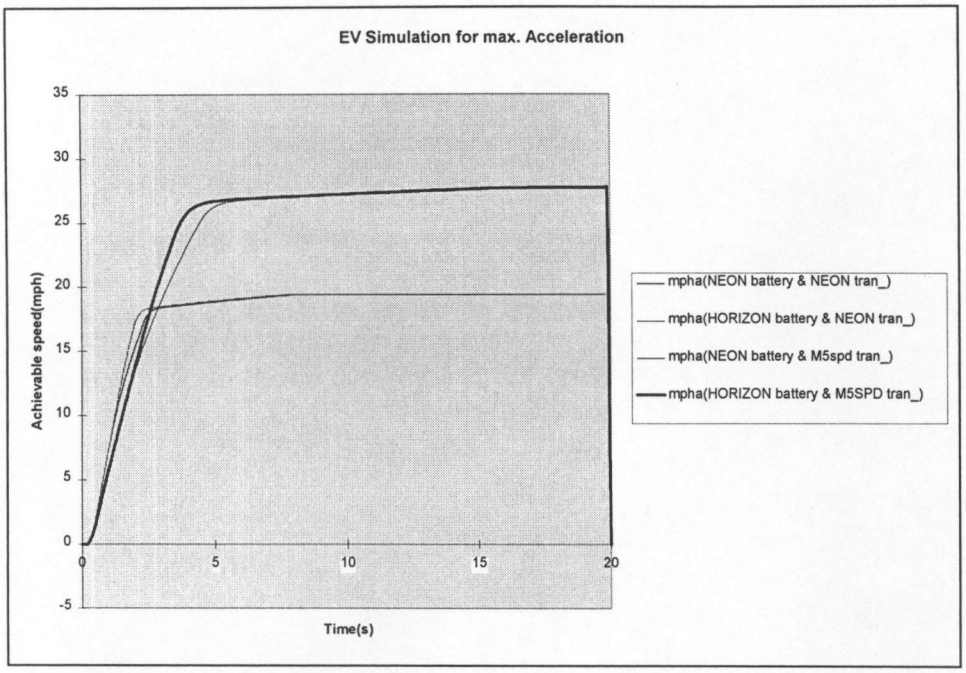


c. power from APU

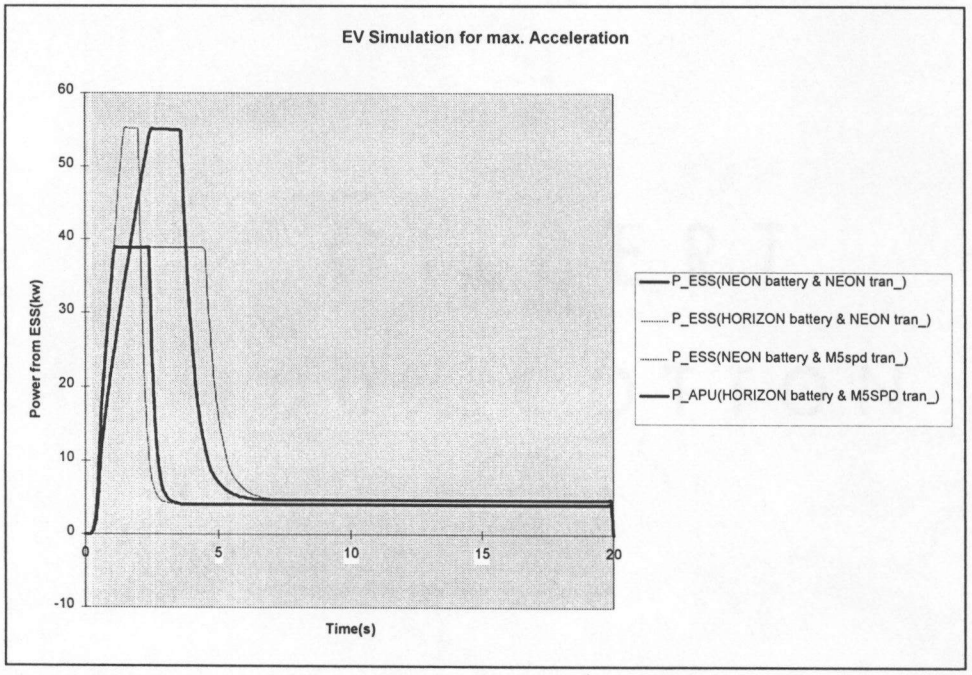


b. Power from ESS

fig.4.35 (Continued)



a. Achievable speed



b. Power from ESS

fig.4.36 Maximum Acceleration Effort Simulation in EV Mode

The similar power capacity from the two different batteries are resulted from the particular selection of the two battery pack, which is made with the same terminal voltage requirements as determined by the NEON specification. The battery capacity has no significant effect on the power output from the battery since at different SOC battery terminal voltage and the current are not significantly different.

The transmission effect is due to the fact that different gear ratio from the different transmission results in different speed of the motor, hence the power output from the motor. In the HEV mode, the APU power compensated for the differences in the power from the motor. Therefore, the transmission effect is more pronounced in the EV mode.

The simulation results suggest that for thsi particular transmission power profile, the M5SPD gear ratio range results in higher acceleration, although its effect on the HIWAY driving condition is not preferable. Since the transmission effect on the vehicle performance is more complicated. The selection of the transmission should be based on its overall effect on the performance of the vehicle and the particular application of the vehicle design.

The acceleration of the vehicle should improve with a higher power capacity battery. However, as dictated by the vehicle design, the NEON has its specific power requirement to the battery which needs to be compatible with the motor/controller operating specification. Therefore, simulation is not made to evaluate this unfeasible choice.

CHAPTER 5

CONCLUSION

A model for HEV simulation has been developed with the NEON power control strategy and battery modeling. From this model the UT HEV NEON performance has been analyzed by parametric analysis of the vehicle components and power control parameters. The simulation results predict the vehicle performance and provide insight into the improvement of the vehicle design with different design options.

1. NEON Simulation Model Characteristics

The NEON simulation model constructed in this thesis differs from the reference model ADVISOR in its power control scheme and battery modeling. The simulation of a power control scheme based on the throttle position has been implemented in this model. Meanwhile, the model has been constructed to be applicable for EV and conventional vehicle simulations. This simulation model not only represents the unique features of the specific configuration and power control scheme of the UT-HEV NEON, but also it includes features which are considered fundamental for a HEV, such as regeneration and regenerative braking. Therefore, it has the potential for wider application in HEV and EV performance analysis.

The battery modeling developed in this thesis provides a practical way of battery modeling with simplified model construction and accurate output results. It is based on the generalized expression from the test data for the terminal voltage of the battery as a function of the SOC and the battery current I. It eliminates the need for obtaining Voc and R of the battery, which are generally not available for battery products and not directly measurable on the HEV. This battery model is also interchangeable with the ADVISOR battery model for simulation, which makes it applicable with different model developments and applications. A wide spectrum of parameters can be analyzed with this model, which allows for the evaluation of the vehicle performance to be made to a large extent and with different focuses.

2. Evaluation and Recommendations from the Simulation Results

Simulations of the UT-HEV NEON have been made with different vehicle power control parameters and component designs. Major output parameters are analyzed for evaluation of the vehicle performance. Recommendations are derived from these simulation analysis. Major conclusions drawn from the simulation are described below.

2.1 APU Power Capacity

The APU adopted for NEON, GEO1L, has a high power capacity which results in high capability for regeneration but limited ESS assist in both the FUDS and the HIWAY driving schedules. This contradicts the objective of the HEV design since one reason for HEV operation is to use of the ESS power to reduce the APU capacity requirements.

To modify the APU capacity, a capacity around 80% of the current capacity is recommended to maintain the SOC by regeneration and to allow for a certain degree of ESS assist. Further reduction of APU capacity will compromise the regeneration capability for sustaining the SOC. The APU capacity can not be reduced to 50% of the current capacity since this will significantly impair the regeneration. As a result, the SOC of the battery will be completely depleted during the driving cycle.

2.2 Regeneration and Regenerative Braking Effect

The regeneration capability is affected by many factors including the APU power capacity, the threshold position of the throttle and the transmission. A high capacity APU has higher capability for regeneration. For the NEON configuration, regeneration plays a major role in battery SOC sustaining in both FUDS and HIWAY cycle. Regenerative braking contribution to SOC recovery are relatively limited compared with regeneration.

2.3 Throttle Position Control

The most important parameter for throttle position control is the threshold position for ESS assist and for regeneration control. In the case of NEON, the threshold position can be set around 0.5 to allow for reasonable regeneration and ESS assist. A higher threshold position means less ESS assist and high regeneration, a lower threshold position means more ESS assist and less regeneration. The threshold position should not be set as low as 0.2. This is because that at this threshold value regeneration would

almost be suppressed completely and ESS assist starts earlier, which results in quick SOC depletion and inability to recover the SOC.

Another suggestion is that for the purpose of APU power control, the throttle used for this vehicle can be reduced to about 70% of the current throttle opening since at this position the APU power has reached its maximum output.

2.4 Battery

A higher capacity battery would be desirable for reducing the APU power capacity while maintaining good performance of the vehicle. A higher capacity battery also means a higher and more stable SOC in the driving cycle. Therefore it promises more EV range and can provide more ESS assist power when needed.

The battery initial SOC value would not seriously affect the achievable speed when the APU capacity is high. The SOC can be increased during the cycle from regeneration and regenerative braking so as to provide ESS assist later. For the current APU of the NEON, the vehicle can be started for the FUDS cycle and the HIWAY cycle when the SOC is at SOClo.

As far as acceleration of the vehicle concerned, battery capacity has basically no effect on the maximum acceleration achievable in both HEV mode and in EV mode.

2.5 Transmission

The transmission has an effect on the power distribution from the APU and the ESS by changing the APU and the motor speeds. From simulations with two transmissions having identical speed-torque map and different gear ratios, i.e. NEON transmission and M5SPD transmission, it is recommended that the NEON gear ratio is preferred for SOC recovery through regeneration. However, the M5SPD transmission gear ratio leads to a higher acceleration in EV mode for this particular transmission power profile and gear shift scheme.

2.6 Maximum Acceleration Effort

The maximum acceleration of NEON is mainly affected by the power capacity of the APU and ESS, different transmission have some effect on the power output. A higher APU power capacity results in

higher acceleration in HEV mode. For the given two transmission options, the M5SPD gear ratio tends to give rise to higher speed achievable. The transmission effect is more distinct in EV mode.

The effect of the battery capacity on the maximum acceleration is negligible when the power available from the different batteries are very close to each other.

2.7 EV Range

A battery with higher capacity would leads to a longer range and gradual SOC changes..

3. Future Work

It is recommended that vehicle tests on dynamometer and vehicle road tests should be conducted for validation of the simulation results. The component modification made to the vehicle may need more detailed simulation results as per the specific emphasis in the vehicle performance improvement.

4. Summary

In conclusion, the evaluation of the vehicle performance based on the simulation serves to guide the modifications of the vehicle. Since the vehicle performance is the result of a combination of the different factors, the optimal design and performance of the vehicle should be achieved on the basis of comprehensive study of the different factors. The simulation model provides access to the analysis necessary for this purpose.

REFERENCES

REFERENCES

1. International Energy Agency, "*Electric Vehicles: Technology, performance and potential*", Paris, OECD/IEA 1993.
2. Hae-woo Park, Chang-Seok Han, Chul-Soo Kim, Bong-Ho Lee, and Young-Woo Kim, *"Ni/MH Battery Charger with a Compensator for Electric Vehicles"*, SAE 960447.
3. Talor Moore, *"Near-Term Battery"*, EPRI JOURNAL April/May 1994.
4. Talor Moore, *"The Push for Advanced Battery"*, EPRI JOURNAL April/May 1991.
5. Dennis Simanaitis, *"Electric Vehicles"*, ROAD & TRACK, May 1992.
6. Fritz Kalhammer, *"R&D Status Report, Energy Management and Utilization Division"*, EPRI JOURNAL January/February 1987.
7. Cathering Anderson and Erin Pettit *"The effect of APU characteristics on the design of Hybrid Control Strategies for Hybrid Electric Vehicle"*, SAE 950493.
8. W.W.MARR, W.J. WALSH and SYMONS *"Modeling battery performance in electric vehicle applications"*, Energy Conservation Management, Vol.33, No.9 1992.
9. A.R. Landgrebe and J.Milliken, *"Exploratory Technology Research in Support of the U.S. department of Energy Electric and Hybrid Vehicle Program"*, Annual Automotive Technology Development Customers' Coordination Meeting, Oct.28~Nov.1,1996.
10. Kenneth, L. Heitner, *"Electric Vehicle Energy Storage Requirements,"* Annual Automotive Technology Development Customers' Coordination Meeting, Oct.28~Nov.1,1996.
11. C.J. Faramandi, *" Electrochemical Capacitor Technology for Automotive Applications"*, Annual Automotive Technology Development Customers' Coordination Meeting, Oct.28~Nov.1,1996.
12. V.S. Bagotzky and A.M. Skundin, *"Chemical Power Sources"*, Academic Press 1980.

    A. Kalberlah, *"Hybrid Drive System for Cars"*, Automotive Engineering, July 1991, volume 99, number 7.
13. A. Kalberlah, *"Electric Hybrid Drive System for Passenger Cars and Taxis"*, Volkswagen AG, Wolfburg, Germany.
14. T.R.Crompton, *"Battery Reference Book"*, second edition, Butterworth Heinemann.
15. H. Lee Martin and R. Eugene Goodson, *"New Concept in Battery Performance Simulation and Monitoring"*, EV EXPO 80, Cervantes Convention Center, St. Louis, Missouri, May 20-22, 1980.
16. P. Chapman and M. Aston, *"A Generic Battery Model for Electric and Hybrid Electric Vehicle Simulation Performance Prediction"*, Electric and Hybrid Electric Vehicles: procedings of the International Association for Vehicle Design, Special Publication SP2, 1982.
17. Phoenix Electric Auto Association, *" GM's EV-1 is generating excitement"*, Electric Vehicle Webdirectory: http://www.doe.ev.com.
18. Hybrid Electric Vehicle Web directory, http:// www.doe.hev.gov.
19. Electrosource, Inc., "*Horizon Battery Specification*", 1997.

20. USABC, *"Bridging the R&D and Commercialization Gap"*, USABC Winter 1996.

21. 1996 HEV Neon Design Team, *"University of Tennessee Second Generation Neon Hybrid Electric Vehicle"*.

22. California Air Resource Board(CARB) *"Staff Report: 1994 Low Emission Vehicle and Zero Emission Vehicle Program Review"*, Mobile Source Division, 1994.

23. California Air Resource Board(CARB) *"Technical Support Document Zero-Emission Vehicle Update"*, Mobile Source Division, 1994.

24. R.P.G. Health and C.Y. Mo "A modular approach to Powertrain Modeling for the Prediction of Vehicle Performance, Economy and Emission", SAE 960427.

25. Idaho National Engineering Laboratory *"Dynamometer Testing of the Ford Ecostar Electric Vehicle #41"*, DOE/ID -10518 September 1995.

26. A.F. Burke, *"Hybrid/Electric Vehicle Design Options and Evaluations"*, SAE 920447.

27. Raymond A. Sutula, *"The Department of Energy's High-power Energy Storage Programs"*, Annual Automotive Technology Development Customers' Coordination Meeting, Oct.28~Nov.1,1996.

28. Harold Haskins, *"Energy Storage Requirements for Hybrid Systems"*, Annual Automotive Technology Development Customers' Coordination Meeting, Oct.28~Nov.1,1996.

29. Tien Duong, *"Procedures for Testing of Electric Vehicle Batteries under USABC"*, Annual Automotive Technology Development Customers' Coordination Meeting, Oct.28~Nov.1,1996.

30. Lawrence J. Oswald and Gerald D. Skellenger, *"General Motors Hybrid Propulsion Systems Development Program"*, Annual Automotive Technology Development Customers' Coordination Meeting, Oct.28~Nov.1,1996.

31. Gary L. Hunt and Timothy C. Murphy, *"Measuring Peak Power On Electric Vehicle Battery"*, Annual Automotive Technology Development Customers' Coordination Meeting, Oct.28~Nov.1,1996.

32. B.K. Powell and T.E. Pilutti, *"A Range Extender Hybrid Electric Vehicle Dynamic Model"*, Procedings of the 33rd Conference on Decision and Control, December 1994.

33. *"The GM Ovenic Nickle Metal Hydride Electric Vehicle Battery"*, Annual Automotive Technology Development Customers' Coordination Meeting, Oct.28~Nov.1,1996.

34. W.W. Marr and W.J Walsh, *"Life Cycle Cost Evaluations of Electric/Hybrid Vehicles"*, Energy Conservation Management, Vol.33 No.9 1992.

35. Keith B. Wipke, Nicole Hill and Robert P. Larson, *"Analysis of Data from Electric and Hybrid Electric Vehicle Student Competations"*, http:// www.doe.hev.gov.

36. Cole, G.H., *"Simplev: A Simple Electric Vehicle Simulation Program Version 2.0"*, DOE/ID-10293-2, April 1993.

37. W.W. Marr, "User's Guide to EAGLES Version 1.1: An Electric-and Gasoline-Vehicle Fuel-Efficiency Software Package", ANL/ESD-27, January,1995.

38. Gregory W. Davis and Frank C. Madeka, *"The effect of Regenerative Braking on the Performance and Range of the AMPhibian II Hybrid Electric Vehicle"*, SAE 950957.

39. Matthew Cuddy, *"A Comparison of Modeled and Measured Energy Use in Hybrid Electric Vehicle"*, SAE 950459.
40. C.H. Kim, S.B.Koh and E. NamGoong, *"Comparison Between On-Road and Simulated Performance of the KEV Electric Vehicle"*, SAE 951069.

41. Cruising Equipment Co., *"Installation Manual: KiloWatt-Hour +Meter"*, Seattle, WA, February 1993.

42. Cruising Equipment Co., *"Installation Manual: KiloWatt-Hour +2 Meter"*, Seattle, WA, February 1995.

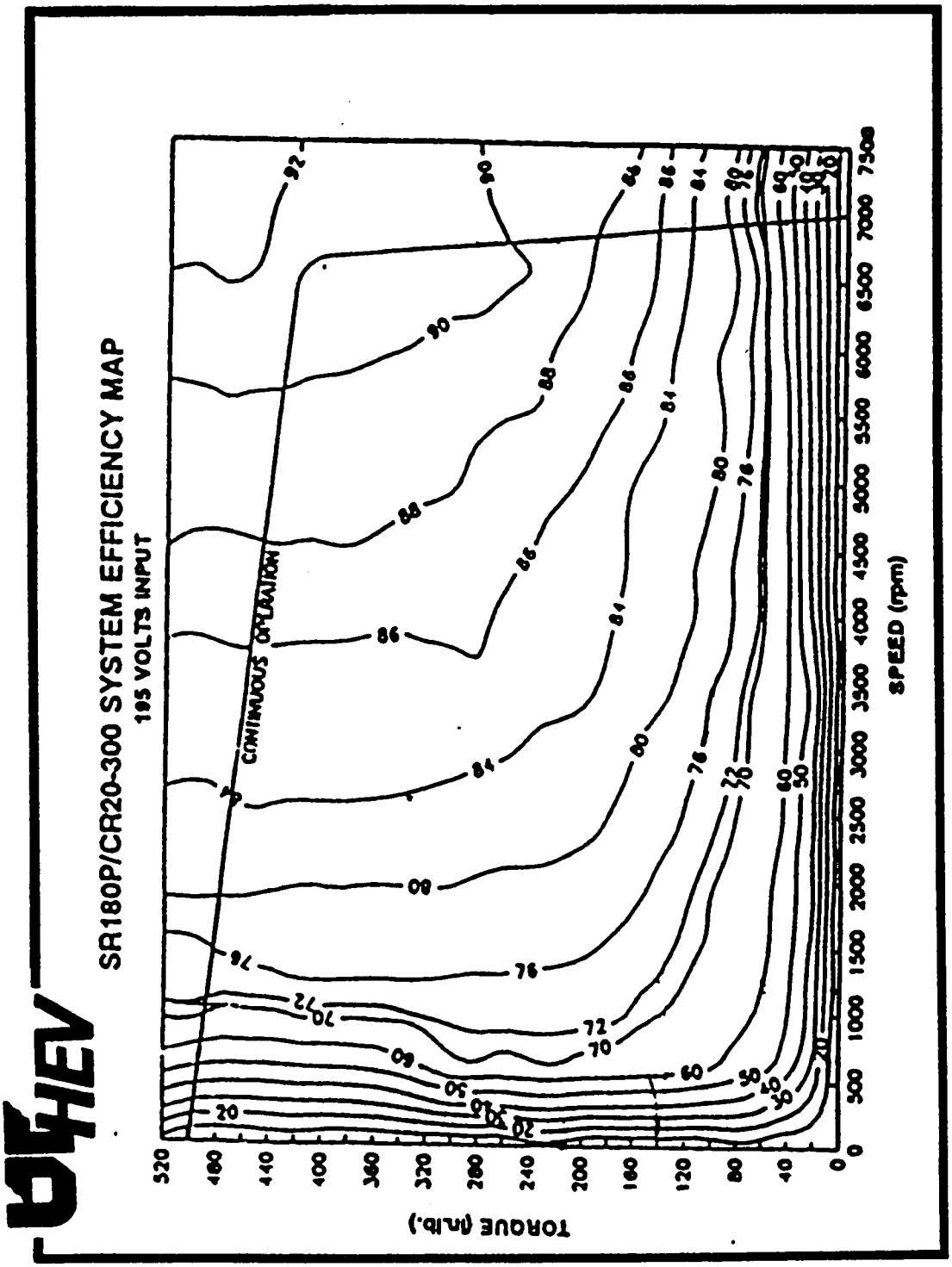
APPENDICES

CONTENTS OF APPENDICES

Appendix 1 Motor speed and torque map and specifications from manufacturer 174
Appendix 2 Battery specifications from manufacturer 175
Appendix 3 Test data on the NEON lead acid battery 176
Appendix 4 MATLAB file: NEONBT_E.M 179
Appendix 5 MATLAB file: H12N85_E.M 180
Appendix 6 MATLAB file: GEO1L_A.M 181
Appendix 7 MATLAB file: GUINEON.M 184
Appendix 8 MATLAB file: NEONBAT.M 187
Appendix 9 MATLAB file: NEON_V.M 191
Appendix 10 MATLAB file: NEON_T.M 192
Appendix 11 MATLAB file: NEONSET.M 194

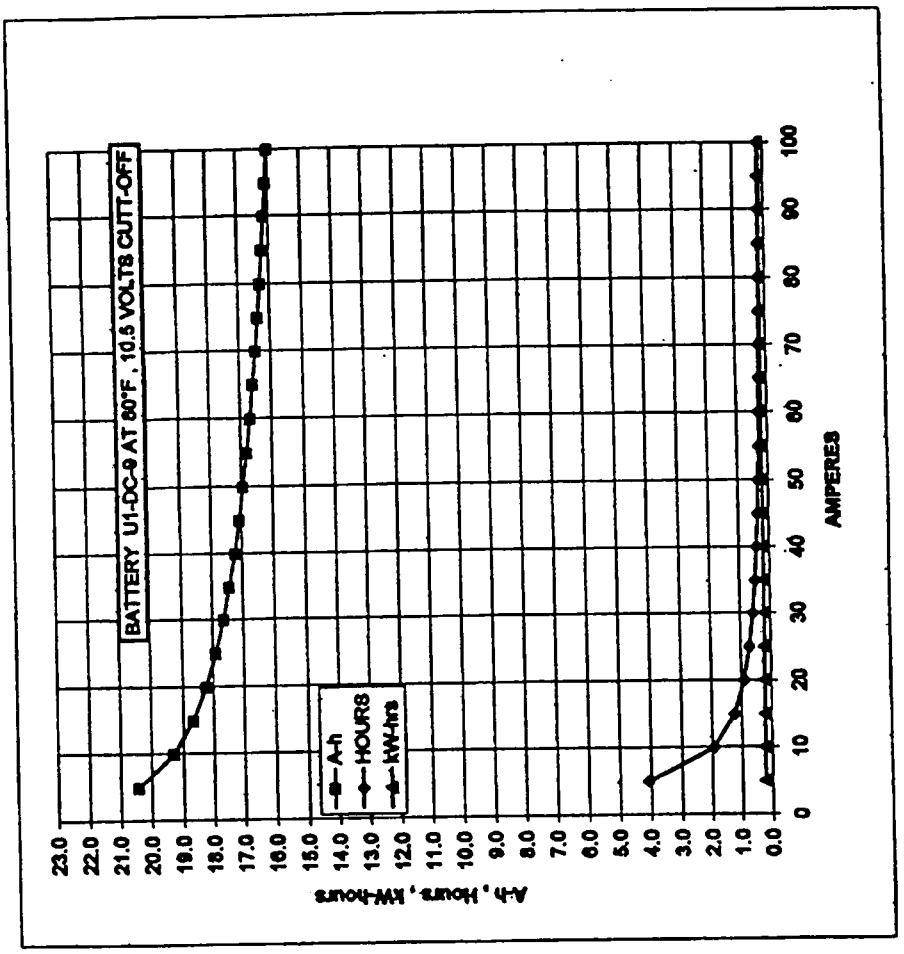
Appendix 1

MOTOR SPEED AND TORQUE MAP AND SPECIFICATIONS FROM MANUFACTURER



Appendix 2

BATTERY SPECIFICATIONS FROM MANUFACTURER



FFFPEUKERT.U1

EXIDE CORPORATION

DATE01/7/93

AMPS	HOURS	A-h	kW-hrs
5	4.1	20.4	0.22060
10	1.9	19.3	0.21606
15	1.2	18.7	0.21102
20	0.9	18.2	0.20618
25	0.7	17.9	0.20240
30	0.6	17.7	0.19949
35	0.5	17.4	0.19701
40	0.4	17.2	0.19486
45	0.4	17.1	0.19303
50	0.3	16.9	0.19139
55	0.3	16.8	0.18992
60	0.3	16.7	0.18858
65	0.3	16.6	0.18736
70	0.2	16.5	0.18624
75	0.2	16.4	0.1852
80	0.2	16.3	0.18423
85	0.2	16.2	0.18333
90	0.2	16.1	0.18248
95	0.2	16.1	0.18168
100	0.2	16.0	0.18093

Note:
Kilowatt-hr per battery is based on an average voltage of 11.3 volts / battery

Appendix 3

Test Data on the NEON Lead acid Battery

Table A.1 Generalized and Test Curve Formulae in First Order and Second Order

SOC	*1st order generalized curve*	*1st order test curve*	*2nd order generalized curve*	*2nd order test curve*
0	Y=0.18*X+172+40*soc	Y0=0.1285*X+167.37		
0.05	Y=0.18*X+172+40*soc	Y0=0.1285*X+167.37	y=0.0009x^2+0.29x+(soc-0.1)*4+181	y=0.002x^2+0.4027x+174.55
0.1	Y=0.18*X+172+40*soc	Y0=0.1595*X+174.14	y=0.0009x^2+0.29x+(soc-0.1)*4+181	y=0.0009x^2+0.2853x+177.39
0.15	Y=0.18*X+172+40*soc	Y0=0.1731*X+177.95	y=0.0009x^2+0.29x+(soc-0.1)*4+181	y=0.0009x^2+0.293x+181.01
0.2	Y=0.18*X+172+40*soc	Y0=0.1787*X+180.55	y=0.0009x^2+0.29x+(soc-0.1)*4+181	y=0.0008x^2+0.285x+183.22
0.25	Y=0.18*X+172+40*soc	Y0=0.1851*X+182.72	y=0.0006x^2+0.26x+184.55+(soc-0.25)*30	y=0.0006x^2+0.259x+184.55
0.3	Y=0.18*X+172+40*soc	Y0=0.185*X+184.11	y=0.0006x^2+0.26x+184.55+(soc-0.25)*30	y=0.0005x^2+0.2552x+185.84
0.35	Y=0.18*X+172+40*soc	Y0=0.1909*X+185.89	y=0.0006x^2+0.26x+184.55+(soc-0.25)*30	y=0.0006x^2+0.2697x+187.82
0.4	Y=0.2*X+186.94+4*soc	Y0=0.1953*X+187.31	y=0.0006x^2+0.26x+184.55+(soc-0.25)*30	y=0.0006x^2+0.2705x+189.13
0.45	Y=0.2*X+186.94+4*soc	Y0=0.2022*X+188.74	y=0.0006x^2+0.26x+184.55+(soc-0.25)*30	y=0.0003x^2+0.2441x+189.75
0.5	Y=0.2*X+186.94+4*soc	Y0=0.2006*X+189.56	y=0.0006x^2+0.26x+184.55+(soc-0.25)*30	y=0.0006x^2+0.273x+191.29
0.55	Y=0.2*X+186.94+4*soc	Y0=0.1962*X+190.2	y=0.0006x^2+0.26x+184.55+(soc-0.25)*30	y=0.0004x^2+0.2506x+191.49
0.6	Y=0.2*X+186.94+4*soc	Y0=0.1995*X+191.11	y=0.0001x^2+0.22x+191.58+(soc-0.6)*4	y=0.0001x^2+0.216x+191.51
0.65	Y=0.2*X+186.94+4*soc	Y0=0.1986*X+191.86	y=0.0001x^2+0.22x+191.58+(soc-0.6)*4	y=0.0003x^2+0.2335x+192.68
0.7	Y=0.2*X+186.94+8*soc	Y0=0.196*X+192.52	y=0.0001x^2+0.22x+191.58+(soc-0.6)*4	y=0.0001x^2+0.2109x+192.87
0.75	Y=0.2*X+186.94+8*soc	Y0=0.1967*X+193.36	y=-0.0002x^2+0.175x+192+(soc-0.75)*10	y=-0.0002x^2+0.1743x+192.83
0.8	Y=0.2*X+186.94+8*soc	Y0=0.194*X+193.97	y=-0.0002x^2+0.175x+192+(soc-0.75)*10	y=-0.0002x^2+0.1738x+193.49
0.85	Y=0.2*X+186.94+8*soc	Y0=0.1899*X+194.24	y=0.0001x^2+0.2x+194.4+(soc-0.85)*30	y=0.00005x^2+0.1968x+194.4
0.9	Y=0.2*X+186.94+8*soc	Y0=0.1921*X+194.97	y=0.0001x^2+0.2x+194.4+(soc-0.85)*30	y=0.0003x^2+0.2327x+196.03
0.95	Y=0.2*X+186.94+8*soc	Y0=0.1862*X+195.41	y=0.0001x^2+0.2x+194.4+(soc-0.85)*30	y=0.00005x^2+0.1955x+195.67
1	Y=0.2*X+186.94+8*soc	Y0=0.1862*X+195.41		

Table A. 2 First Order Formulae Error Checking for NEON Battery V_terminal - I Curve for the Given SOC

	I=20			*I=40*			*I=60*			*I=80*			*I=100*		
SOC	*Gen.*	*Test*	*%E20*	*Gen.*	*Test*	*%E40*	*Gen.*	*Test*	*%E60*	*Gen.*	*Test*	*%E80*	*Gen.*	*Test*	*%E100*
0	168.40	164.80	2.18%	164.80	162.23	1.58%	161.20	159.66	0.96%	157.60	157.09	0.32%	154.00	154.52	-0.34%
0.05	170.40	164.80	3.40%	166.80	162.23	2.82%	163.20	159.66	2.22%	159.60	157.09	1.60%	156.00	154.52	0.96%
0.1	172.40	170.95	0.85%	168.80	167.76	0.62%	165.20	164.57	0.38%	161.60	161.38	0.14%	158.00	158.19	-0.12%
0.15	174.40	174.49	-0.05%	170.80	171.03	-0.13%	167.20	167.56	-0.22%	163.60	164.10	-0.31%	160.00	160.64	-0.40%
0.2	176.40	176.98	-0.33%	172.80	173.40	-0.35%	169.20	169.83	-0.37%	165.60	166.25	-0.39%	162.00	162.68	-0.42%
0.25	178.40	179.02	-0.35%	174.80	175.32	-0.29%	171.20	171.61	-0.24%	167.60	167.91	-0.19%	164.00	164.21	-0.13%
0.3	180.40	180.41	-0.01%	176.80	176.71	0.05%	173.20	173.01	0.11%	169.60	169.31	0.17%	166.00	165.61	0.24%
0.35	182.40	182.07	0.18%	178.80	178.25	0.31%	175.20	174.44	0.44%	171.60	170.62	0.58%	168.00	166.80	0.72%
0.4	184.54	183.40	0.62%	180.54	179.50	0.58%	176.54	175.59	0.54%	172.54	171.69	0.50%	168.54	167.78	0.45%
0.45	184.74	184.70	0.02%	180.74	180.65	0.05%	176.74	176.61	0.07%	172.74	172.56	0.10%	168.74	168.52	0.13%
0.5	184.94	185.55	-0.33%	180.94	181.54	-0.33%	176.94	177.52	-0.33%	172.94	173.51	-0.33%	168.94	169.50	-0.33%
0.55	185.14	186.28	-0.61%	181.14	182.35	-0.66%	177.14	178.43	-0.72%	173.14	174.50	-0.78%	169.14	170.58	-0.84%
0.6	185.34	187.12	-0.95%	181.34	183.13	-0.98%	177.34	179.14	-1.00%	173.34	175.15	-1.03%	169.34	171.16	-1.06%
0.65	185.54	187.89	-1.25%	181.54	183.92	-1.29%	177.54	179.94	-1.34%	173.54	175.97	-1.38%	169.54	172.00	-1.43%
0.7	188.54	188.60	-0.03%	184.54	184.68	-0.08%	180.54	180.76	-0.12%	176.54	176.84	-0.17%	172.54	172.92	-0.22%
0.75	188.94	189.43	-0.26%	184.94	185.49	-0.30%	180.94	181.56	-0.34%	176.94	177.62	-0.39%	172.94	173.69	-0.43%
0.8	189.34	190.09	-0.39%	185.34	186.21	-0.47%	181.34	182.33	-0.54%	177.34	178.45	-0.62%	173.34	174.57	-0.70%
0.85	189.74	190.44	-0.37%	185.74	186.64	-0.48%	181.74	182.85	-0.60%	177.74	179.05	-0.73%	173.74	175.25	-0.86%
0.9	190.14	191.13	-0.52%	186.14	187.29	-0.61%	182.14	183.44	-0.71%	178.14	179.60	-0.81%	174.14	175.76	-0.92%
0.95	190.54	191.69	-0.60%	186.54	187.96	-0.76%	182.54	184.24	-0.92%	178.54	180.51	-1.09%	174.54	176.79	-1.27%
1	190.94	191.69	-0.39%	186.94	187.96	-0.54%	182.94	184.24	-0.70%	178.94	180.51	-0.87%	174.94	176.79	-1.05%

Note: Column Gen. is the data from the generalized curve, and column test is the calculation from the test curve formulae. The error is (Gen.-Test)/Test.

Table A. 3 Second Order Formulae Error Checking for NEON Battery V_terminal - I Curve for the Given SOC

	I=20			*I=40*			*I=60*			*I=80*			*I=100*		
SOC	*Gen.*	*Test*	*%E20*	*Gen.*	*Test*	*%E40*	*Gen.*	*Test*	*%E60*	*Gen.*	*Test*	*%E80*	*Gen.*	*Test*	*%E100*
0.00	180.60	174.55	3.47%	180.60	174.55	3.47%	180.60	174.55	3.47%	180.60	174.55	3.47%	180.60	174.55	3.47%
0.05	186.96	183.40	1.94%	193.84	193.86	-0.01%	201.44	205.91	-2.17%	209.76	219.57	-4.47%	218.80	234.82	-6.82%
0.1	187.16	183.46	2.02%	194.04	193.86	0.09%	201.64	205.91	-2.07%	209.96	219.57	-4.37%	219.00	234.82	-6.74%
0.15	187.36	187.23	0.07%	194.24	193.86	0.20%	201.84	205.91	-1.98%	210.16	219.57	-4.28%	219.20	234.82	-6.65%
0.2	187.56	189.24	-0.89%	194.44	193.86	0.30%	202.04	205.91	-1.88%	210.36	219.57	-4.19%	219.40	234.82	-6.57%
0.25	189.99	189.97	0.01%	195.91	195.87	0.02%	202.31	202.25	0.03%	209.19	209.11	0.04%	216.55	216.45	0.05%
0.3	191.49	191.14	0.18%	197.41	195.87	0.79%	203.81	202.25	0.77%	210.69	209.11	0.76%	218.05	216.45	0.74%
0.35	192.99	193.45	-0.24%	198.91	195.87	1.55%	205.31	202.25	1.51%	212.19	209.11	1.47%	219.55	216.45	1.43%
0.4	194.49	194.78	-0.15%	200.41	195.87	2.32%	206.81	202.25	2.25%	213.69	209.11	2.19%	221.05	216.45	2.13%
0.45	195.99	194.87	0.57%	201.91	195.87	3.08%	208.31	202.25	3.00%	215.19	209.11	2.91%	222.55	216.45	2.82%
0.5	197.49	196.99	0.25%	203.41	195.87	3.85%	209.81	202.25	3.74%	216.69	209.11	3.62%	224.05	216.45	3.51%
0.55	198.99	196.66	1.18%	204.91	195.87	4.62%	211.31	202.25	4.48%	218.19	209.11	4.34%	225.55	216.45	4.20%
0.6	196.02	195.87	0.08%	200.54	200.31	0.11%	205.14	204.83	0.15%	209.82	209.43	0.19%	214.58	214.11	0.22%
0.65	196.22	197.47	-0.63%	200.74	200.31	0.21%	205.34	204.83	0.25%	210.02	209.43	0.28%	214.78	214.11	0.31%
0.7	196.42	197.13	-0.36%	200.94	200.31	0.31%	205.54	204.83	0.35%	210.22	209.43	0.38%	214.98	214.11	0.41%
0.75	195.42	196.24	-0.42%	198.68	199.48	-0.40%	201.78	202.57	-0.39%	204.72	205.49	-0.38%	207.50	208.26	-0.36%
0.8	195.92	196.89	-0.49%	199.18	199.48	-0.15%	202.28	202.57	-0.14%	205.22	205.49	-0.13%	208.00	208.26	-0.12%
0.85	198.44	198.54	-0.05%	202.56	203.07	-0.25%	206.76	208.01	-0.60%	211.04	213.34	-1.08%	215.40	219.08	-1.68%
0.9	199.94	200.80	-0.43%	204.06	203.07	0.49%	208.26	208.01	0.12%	212.54	213.34	-0.38%	216.90	219.08	-1.00%
0.95	201.44	199.78	0.83%	205.56	203.07	1.23%	209.76	208.01	0.84%	214.04	213.34	0.33%	218.40	219.08	-0.31%
1	202.94	199.78	1.58%	207.06	203.07	1.96%	211.26	208.008	1.56%	215.54	213.34	1.03%	219.9	219.08	0.37%

Note: Column Gen. is the data from the generalized curve, and column test is the calculation from the test curve formulae. The error is (Gen.-Test)/Test.

Appendix 4

MATLAB FILE: NEONBAT.M

------battery File for NEON Lead-acid battery simulation with ADVISOR

```
%**** the HEV ADVISOR file on NEONBT_E.M*************************************
%       This m-file loads the variables for an Lead_acid battery model number          *
%       UI DC9 from EXIDE Co. Data  was gathered from the test on battery               *
%       when vehicle is running on  the dynamometer.                                    *
%       Data includes Ah capacity, and open-circuit voltage and internal resistance as  *
%       a  function of SOC.                                                             *
%                                                                                       *
%*****************************************************************************

Peukert_const=62.132;                   % Peukert constant and exponent calculated from
                                                test data
Peukert_exp=-0.5273;
ESS_maxAhcap=25;                        % C/3-rate capacity, capacity to prevent  computing error
                                                when I approaches 0.
ESS_Rint_dis=[0.0112 0.0112 0.0112 0.0112 0.0125 0.0125 0.0125 0.0125 0.0125 0.0125 0.0125];
                                        % Battery resistance of each cell
ESS_Rint_chg=ESS_Rint_dis;
ESS_SOC=[0:.1:1];
ESS_Voc=[10.7500 11.0000 11.2500 11.5000 11.7838 11.8088 11.8338 12.0338 12.0838 12.1337
12.1838];                               % Battery Voc of each cell
ESS_modulemass=9.05;                    % Battery cell mass
ESS_num=16;                             % Battery number in the pack
ESS_Aheta=.93;                          % Estimated--used numbers from Ovonic NiMH%
disp('Data loaded: NEONBT_E battery')
```

Appendix 5

MATLAB FILE: H12N85_E.M

----------NEON Vehicle file for simulation

```
%**** the HEV ADVISOR file H12N85_E.M*****************************************
%       This m-file loads the variables for an Electrosouce Horizon advanced lead      *
%       -acid battery, model number  H12N85.  Data was provided by Electrosource.      *
%       Data includes Ah capacity, and open-circuit voltage and  internal resistance   *
%       as a function of SOC.                                                          *
%*******************************************************************************

Peukert_const=165.7;                    % Peukert constant and exponent calculated from
                                                C,C/2,C3-rate capacities of 70, 76.5, and 85 Ah
Peukert_exp=-0.205;
ESS_maxAhcap=85;                        % C/3-rate capacity
ESS_Rint_dis=[0.00457 0.002686 0.002226 0.001970 0.001843 0.001747 0.001711 0.001685 0.001697
0.001756 0.001769];
ESS_Rint_chg=ESS_Rint_dis;
ESS_SOC=[0:.1:1];
ESS_Voc=[11.406 11.73 11.904 12.096 12.216 12.384 12.492 12.636 12.75 12.918 12.99];
ESS_modulemass=24.9;
ESS_num=15;
ESS_Aheta=.93;                          % estimated--used numbers from Ovonic NiMH
%
disp('Data loaded: H12N85_E battery')
```

Appendix 6

MATLAB FILE: GEO1L_A.M

----------NEON Vehicle file for simulation

```
%**** the revised HEV ADVISOR file GEO1L_A.M************************************
%       This file loads the variables associated with a Geo Metro APU, including                *
%       emissions and certain       operation design points.                                    *
%                                                                                               *
%*******************************************************************************
APU_TPindex=[0 0.025 0.05 0.075 0.1 0.125 0.15 0.175 0.2 0.3 0.4 0.5 0.6 0.7 0.8 0.9 1];
                                        % throttle position in percentage
APU_TQ1_ratio=[0 0.2216 0.4432 0.6648 0.8864 0.9670 0.9684 0.9698 0.9713 0.9770 0.9828 0.9885
0.9942 0.9999 1 1 1];                   % APU torque ratio at certain speed range
APU_TQ2_ratio=[-0.2 0 0.2022 0.4045 0.6067 0.8090 0.8788 0.8843 0.8898 0.9119 0.9339 0.9559 0.9779
1 1 1 1];                               % APU torque ratio at certain speed range
APU_maxtrq=[61.0058    67.6486 73.7492 78.4941 80.9343 77.274   76.1895 73.3425 68.7332];

APU_map_spd=[104.5     149.2   220.9   292.5   364.1   435.7   507.4   552.2   596.9];

APU_map_trq=[6.8       13.6    20.4    27.2    33.8    40.6    47.4    54.2    61      67.8
        74.6    81.4];
APU_idlespd =62.8319;
APU_idletrq=13.5568;
% If APU is used in a series vehicle, the following is the operating point
APU_oppnt_spd=294.9853;                 % rad/s, single operating point for the APU
APU_oppnt_trq=67.8;                             % Nm
APU_sp_power=0.285;                     % kW/kg
APU_omegamax=ones(1,5)*3200*pi/30;

APU_omegamin=ones(1,5)*1500*pi/30;
fuel_mden=737;                          % g/L, RFG

%
CO_tbl =[71.8   71.8    58.8    45.7    32.7    27.5    22.4    82.9    143.3   143.3   143.3
        143.3
104.4   68.3    56.8    45.3    33.9    23.3    25.7    24.2    22.8    268.6   268.6   268.6
48.3    48.3    42.9    37.2    31.8    28.6    25.4    22.2    22.8    152.9   283     283
103.1   82.7    72.2    61.8    41.5    36.9    32.3    27.8    31.1    34.4    178.5   279.9
88.1    88.1    74.2    59.9    46      41.9    37.8    33.7    34.8    35.8    158.8   264.6
96.1    74.5    52.9    51.2    49.5    45.9    42.4    34      117.9   201.8   285.7   285.7
114.6   114.6   92.1    69      46.5    60.7    74.8    129.6   195.5   261.4   277.8   277.8
60.1    63.8    64      64.1    64.3    108.2   130.2   152.2   216.7   281.2   278.1   278.1
51.8    75.2    99.3    122.8   134.9   147.1   159.7   172.2   196.6   286.6   286.6   286.6];
%
COcat_tbl=[0.999        0.999   0.999   0.999   1       0.996   0.992   0.919   0.846   0.846
        0.846   0.846
1       1       1       1       0.999   0.999   0.998   0.988   0.978   0.698   0.698   0.698
1       1       1       1       1       1       1       0.999   0.978   0.835   0.691   0.691
0.999   0.995   0.993   0.991   0.986   0.986   0.985   0.984   0.991   0.997   0.869   0.686
1       1       0.996   0.992   0.988   0.986   0.985   0.983   0.986   0.988   0.808   0.832
1       1       1       1       1       0.999   0.999   0.999   0.936   0.872   0.809   0.809
0.95    0.95    0.963   0.975   0.987   0.924   0.86    0.857   0.842   0.827   0.821   0.821
```

```
0.998   0.999   0.97    0.954   0.938   0.893   0.866   0.839   0.832   0.824   0.824   0.824
0.999   0.956   0.904   0.843   0.841   0.839   0.837   0.834   0.83    0.842   0.842   0.842];
%
fuel_tbl =[635.7 635.7  541.4   447.2   352.9   332.2   311.4   322.4   333.5   333.5   333.5
        333.5
678.4   500.1   443.8   387.4   331.1   301.8   297     283.4   269.8   358     358     358
463.4   463.4   407.6   350.1   294.3   280.8   267.3   253.9   269.8   303.2   336.7   336.7
699.1   567.9   500.3   432.7   301.4   283.9   266.3   248.7   258.8   268.8   271.9   317.9
592.9   592.9   494.6   393.4   295.1   279.4   263.6   247.9   255.2   262.5   295     322.6
667.9   524.8   381.6   351.9   322.2   304.9   287.5   270.8   290.8   310.9   330.9   330.9
630.6   630.6   522.5   411.1   303     304.4   305.8   304.2   314.5   324.8   327.7   327.7
698.4   500.5   428.6   392.7   356.8   337.9   328.4   319     328.8   338.6   333.7   333.7
751.1   637.8   521.1   407.8   393.1   378.4   363.3   348.2   318.8   340.2   340.2   340.2];
%
HC_tbl =[11.5   11.5    9.8     8.2     6.5     5.8     5.1     5.9     6.8     6.8     6.8
        6.8
7.8     7       6.2     5.5     4.7     4.3     4.7     4.6     4.5     4.6     4.6     4.6
5.8     5.8     5.2     4.6     4       4       4       4       4.5     4.6     4.6     4.6
7.1     6       5.4     4.9     3.8     3.7     3.6     3.4     3.2     3       3.4     3.9
5.8     5.8     5       4.3     3.6     3.6     3.6     3.7     3.6     3.6     4       3.9
5.6     4.7     3.7     3.7     3.7     3.4     3.1     3       3.2     3.4     3.5     3.5
8.2     8.2     6.8     5.4     4.1     3.7     3.3     3.1     3.2     3.2     3.3     3.3
5.8     5.2     4.8     4.5     4.3     3.7     3.4     3.2     3.3     3.3     3.3     3.3
5.6     5.8     5.9     6.1     5.7     5.4     5       4.6     3.9     3.9     3.9     3.9];
%
HCcat_tbl=[0.987        0.987   0.991   0.995   0.998   0.981   0.963   0.601   0.24    0.24
        0.24    0.24
0.973   0.979   0.981   0.983   0.985   0.987   0.97    0.94    0.911   0       0       0
0.979   0.979   0.98    0.981   0.982   0.982   0.982   0.981   0.911   0.455   0       0
0.993   0.962   0.946   0.93    0.898   0.897   0.896   0.895   0.936   0.977   0.053   0
0.996   0.996   0.958   0.919   0.881   0.886   0.892   0.897   0.923   0.949   0.383   0.276
0.999   0.998   0.998   0.997   0.997   0.993   0.988   0.974   0.716   0.458   0.2     0.2
0.721   0.721   0.794   0.869   0.942   0.802   0.662   0.488   0.431   0.374   0.401   0.401
0.99    0.983   0.919   0.886   0.854   0.659   0.561   0.463   0.432   0.401   0.431   0.431
0.98    0.868   0.752   0.64    0.594   0.548   0.501   0.454   0.362   0.352   0.352   0.352];
%
NOx_tbl =[5.8   5.8     9.3     12.8    16.3    16.1    15.9    13      10.2    10.2    10.2
        10.2
5.2     8.8     9.2     9.7     10.2    8       8.9     13.2    17.5    4.6     4.6     4.6
8.1     8.1     8.8     9.6     10.4    10.8    11.3    11.7    17.5    11.6    5.7     5.7
4.2     5.6     6.3     7       8.4     8.9     9.5     10.1    13.9    17.7    8.1     3.1
5.8     5.8     7.2     8.7     10.1    11      11.8    12.6    15.9    19.2    9.3     6.8
14.9    16.4    17.8    19.4    21      20.6    20.3    19.1    14.6    10.2    5.7     5.7
28.7    28.7    26.8    25      23.1    22.4    21.7    16.5    12.1    7.8     6.5     6.5
31.1    27.9    26.7    26.2    25.6    20.9    18.6    16.3    12.1    7.8     6.8     6.8
35      31.1    27.1    23.2    21.1    19.1    17      14.9    10.9    7.4     7.4     7.4];
%
NOxcat_tbl=[0.949       0.949   0.966   0.983   1       0.993   0.987   0.993   1       1
        1       1
0.915   0.917   0.917   0.918   0.918   0.939   0.855   0.909   0.963   0.996   0.996   0.996
0.923   0.923   0.917   0.911   0.905   0.888   0.87    0.853   0.963   0.979   0.995   0.995
0.997   0.998   0.998   0.999   1       1       1       1       0.998   0.996   0.996   0.995
0.973   0.973   0.982   0.991   1       1       1       0.999   0.998   0.997   0.995   0.993
0.923   0.904   0.884   0.922   0.96    0.975   0.989   0.983   0.987   0.991   0.995   0.995
```

```
1       1       0.996   0.991   0.986   0.993   1       0.999   0.998   0.998   0.997   0.997
0.72    0.749   0.901   0.95    1       0.999   0.999   0.999   0.998   0.997   0.996   0.996
0.631   0.812   0.922   1       0.999   0.999   0.998   0.998   0.997   0.997   0.997   0.997];
%
disp('Data loaded: GEO1L_A engine')
```

Appendix 7

MATLAB FILE: GUINEON.M

----- for ADVISOR GUI revision for NEON Simulation

```
%****  the HEV ADVISOR file GUINEON.M*****************************************
%       Implements a graphical user interface to allow point-and-click                *
%       selection of components, drive cycles, analyses, and output variables.        *
%                                                                                     *
*************************************************************************************
clear outputs_selected choice
outputs_selected=[];

%%%%% open and size figure window
fleft=200;,fbottom=200;,fwidth=300;,fheight=420;
f1=figure('Resize','off','Position',[fleft fbottom fwidth
fheight],'Name','ADVISOR_NEON','NumberTitle','off');

%%%%% define lists of components, driving cycles, batch analyses, vehicle configurations):

vehicles='neon_v pngv_v subcom_v';
tx_s='neon_t m5spd_t';
motors='sr180p_m dr156s_m solect_m westng_m';
ess_s='neonbt_e h12n85_e gnb_e maxwel_e';
apu_s='geo11_a dodg3l_a';
gens='eta95_g';
cycles='fuds_c busrte_c ftpsok_c fudshi_c hiway_c saetpu_c saetph_c';
configs='conven parallel paraneon series ev';
analyses='none accel_ba mpg_1cyc mpg_2cyc mpg_5cyc mpg10cyc saetp_ba';
outputs='mpha range P_APU P_ESS SOC TP current Vterm E_bty';

%%%%% build matrix of filenames for use in CallBacks
vmat=bldmat(vehicles);
tmat=bldmat(tx_s);
mmat=bldmat(motors);
emat=bldmat(ess_s);
amat=bldmat(apu_s);
gmat=bldmat(gens);
cmat=bldmat(cycles);
con_mat=bldmat(configs);
an_mat=bldmat(analyses);
outmat=bldmat(outputs);

%%%%% build strings for use in uicontrols below
vlist=bldstr(vehicles);
tlist=bldstr(tx_s);
mlist=bldstr(motors);
elist=bldstr(ess_s);
alist=bldstr(apu_s);
glist=bldstr(gens);
clist=bldstr(cycles);
con_list=bldstr(configs);
an_list=bldstr(analyses);
```

```
outlist=bldstr(outputs);
vlabel='Vehicle:';
tlabel='Transmission:';
mlabel='Motor/Controller:';
elabel='Energy Storage:';
alabel='APU:';
glabel='Generator:';
clabel='Driving Cycle:';
con_label='Vehicle Config.:';
an_label='Batch Analyses:';
run_label='Run Simulation';
out_label='Outputs:';

%%%%% define call backs
vcb='choice(1,1:8)=vmat(get(vref,"Value"),:);';
tcb='choice(2,1:8)=tmat(get(tref,"Value"),:);';
mcb='choice(3,1:8)=mmat(get(mref,"Value"),:);';
ecb='choice(4,1:8)=emat(get(eref,"Value"),:);';
acb='choice(5,1:8)=amat(get(aref,"Value"),:);';
gcb='choice(6,1:8)=gmat(get(gref,"Value"),:);';
ccb='choice(7,1:8)=cmat(get(cref,"Value"),:);';
con_cb='choice(8,1:8)=con_mat(get(con_ref,"Value"),:);';
an_cb='choice(9,1:8)=an_mat(get(an_ref,"Value"),:);';
run_cb='eval("neonbat")';
for i=1:size(outmat,1)
  text_i=num2str(i);
  out_cb(i,1:43)=['outputs_selected(',text_i,')=get(outref(',text_i,'),"Value");'];
end

%%%%% set placement variables which define position of the menus
hspacing=10;
vspacing=10;
width=100;
height=40;
% first column of menus (built from the bottom up)
xcounter=hspacing;,ycounter=vspacing;

[xcounter,ycounter,cref]=adv_menu(clabel,clist,ccb,xcounter,ycounter,width,height);
ycounter=ycounter+vspacing;
[xcounter,ycounter,gref]=adv_menu(glabel,glist,gcb,xcounter,ycounter,width,height);
ycounter=ycounter+vspacing;
[xcounter,ycounter,aref]=adv_menu(alabel,alist,acb,xcounter,ycounter,width,height);
ycounter=ycounter+vspacing;
[xcounter,ycounter,eref]=adv_menu(elabel,elist,ecb,xcounter,ycounter,width,height);
ycounter=ycounter+vspacing;
[xcounter,ycounter,mref]=adv_menu(mlabel,mlist,mcb,xcounter,ycounter,width,height);
ycounter=ycounter+vspacing;
[xcounter,ycounter,tref]=adv_menu(tlabel,tlist,tcb,xcounter,ycounter,width,height);
ycounter=ycounter+vspacing;
[xcounter,ycounter,vref]=adv_menu(vlabel,vlist,vcb,xcounter,ycounter,width,height);
ycounter=ycounter+vspacing;
% second column of menus (again, build up from bottom)
xcounter=width+2*hspacing;,ycounter=vspacing;
```

```
% execute button
[xcounter,ycounter,run_ref]=adv_bttn(run_label,run_cb,xcounter,ycounter,width,15);
ycounter=ycounter+vspacing;

% outputfile selection
editfilename=uicontrol('Style','edit','String','out.txt','Position',[xcounter,ycounter,130,15],'BackgroundColor',
[1 1 1]);
ycounter=ycounter+20;
fileselectext=uicontrol('Style','text','Position',[xcounter,ycounter,130,15],'String','Output file
name:','BackgroundColor',[.75 0 0],'ForegroundColor',[1 1 1]);
ycounter=ycounter+15+vspacing;

% output selection
for i=size(outmat,1):-1:1
  [xcounter,ycounter,outref(i)]=adv_cbox(outmat(i,:),out_cb(i,:),xcounter,ycounter,130,15);
end
ycounter=ycounter+5;
outtext=uicontrol('Style','text','String',out_label,'Position',[xcounter,ycounter,130,15],'BackgroundColor',[.7
5 0 0],'ForegroundColor',[1 1 1]);
ycounter=ycounter+vspacing+15;

[xcounter,ycounter,an_ref]=adv_menu(an_label,an_list,an_cb,xcounter,ycounter,width,height);
ycounter=ycounter+vspacing;
[xcounter,ycounter,con_ref]=adv_menu(con_label,con_list,con_cb,xcounter,ycounter,width,height);
ycounter=ycounter+vspacing;

%%%%% set default inputs
choice(1,1:8)=vmat(1,:);
choice(2,1:8)=tmat(1,:);
choice(3,1:8)=mmat(1,:);
choice(4,1:8)=emat(1,:);
choice(5,1:8)=amat(1,:);
choice(6,1:8)=gmat(1,:);
choice(7,1:8)=cmat(1,:);
choice(8,1:8)=con_mat(1,:);
choice(9,1:8)=an_mat(1,:);

%%%%% put logo in upper right corner
lwidth=width;,lheight=lwidth*1/2;,lleft=hspacing+3;,lbottom=fheight-lheight-vspacing;
load adv_logo.mat
colormap(clr),logo=image(data);
set(gca,'Units','Pixels','Position',[lleft lbottom lwidth lheight],'Visible','off');
```

Appendix 8

MATLAB FILE: NEONBAT.M
-------- for simulation of NEON

```
%**** the HEV ADVISOR file on NEONBAT.M*************************************
%       Responds to requests made in the ADVISOR GUI loads data, runs simulation,      *
%       makes plots and writes output file.Called by GUINEON.M.                        *
%*******************************************************************************

%%%%% DEFINE VEHICLE %%%%%%

%%% set defaults
cat1                                % loads temperature dependence of catalyst
Tcatmax=650;                        % deg. C, maximum catalyst temperature
Tcatinit=20;                        % deg. C, initial catalyst temperature
TECss=95;                           % deg. C, maximum engine coolant temperature
TECinit=20;                         % deg. C, initial engine coolant temperature
Tamb=20;                            % deg. C, ambient temperature
SOCinit=0.8;                        % initial state-of-charge
SOChi=0.8;                          % highest desired SOC
SOClo=0.2;                          % lowest desired SOC
dt=1;                               % s, time step for simulation
grade=0.0;                          % grade, for example, 0.06 => constant 6% climb
wheel_inertia=0;                    % kg-m^2, rotational inertia of wheels, axle(s), & anything
else that rotates at                        wheel RPM
tx_inertia=0;                       % kg-m^2, transmission inertia measured at torque input (APU
or motor)
mot_inertia=0;                      % kg-m^2, motor rotational inertia
APU_inertia=0;                      % kg-m^2, APU rotational inertia
APU_spdscale=1;                     % speed scaling for all APU maps.  a value of 2 doubles the
APU maximum                                 speed
APU_trqscale=1;                     % torque scaling for all APU maps.  a value of 2 doubles the
APU max. torque at                          given speed
mot_spdscale=1;                     % speed scaling for motor maps
mot_trqscale=1;                     % torque scaling for motor maps
gen_spdscale=1;                     % speed scaling for generator maps
gen_trqscale=1;                     % torque scaling for generator maps
tx_shiftdelay=1;                    % s, duration of shift.  during this time, no torque can be
                                            tted by transmission
accsry_kW=0.2;                      %kW, accessory load.
MPHinit=0;                          % MPH, speed at t=0 s
tire_mu_static=1;                   % coefficient of static friction at tire/road interface
front_weight_frac=0.6;              % fraction of weight supported by the front wheels while the
car is                                      standing
regeneration=1;                     % regeneration control, 1 for regen., 0 for no regen.
regen_level=1;                      % regenerative braking control from 0~1 of the max_mot_trq

%%%%% LOAD SELECTED FILES %%%%%%
% note that data in these files may override above defaults component files
eval(choice(1,:));
eval(choice(2,:));
eval(choice(3,:));
eval(choice(4,:));
```

```
eval(choice(5,:));
% first letter in model name='s' => series model, load generator
if strcmp(choice(8,1),'s'),eval(choice(6,:));,end
filename=nospaces(choice(8,:));

%%% load/compute data specific to the chosen model
if strcmp(filename,'paraneon')
 motor_to_ICE_gr=1.3;   % ratio of motor speed to APU speed
 idlebool=0;
 HEVbool=1;
 APUbool=1;
 gen_mass=0;
 TP_threshold=0.5*APUbool;              % threshold position of APU for ESS assist
elseif strcmp(filename,'series')
 gen_mass=max(gen_map_spd.*gen_maxtrq)/gen_sp_power/1000;     % kg
elseif strcmp(filename,'conven')
 motor_to_ICE_gr=1.3;
 idlebool=1;
 HEVbool=0;
 APUbool=1;
 gen_mass=0;
 filename='paraneon';
 mot_mass=0;
 mot_inertia=0;
TP_threshold=0.5*APUbool;               % threshold position of APU for ESS assist
elseif strcmp(filename,'ev')
 motor_to_ICE_gr=1.3;                   % ratio of motor speed to APU speed
 idlebool=0;
 HEVbool=1;
 APUbool=0;
 gen_mass=0;
 filename='paraneon';
 mot_mass=0;
 mot_inertia=0;
 TP_threshold=0*APUbool;                % threshold position of APU for EV
end
APU_mass=max(APU_map_spd.*APU_maxtrq)/APU_sp_power/1000;% kg
mot_mass=max(mot_map_spd.*mot_maxtrq)/mot_sp_power/1000;     % kg
ESS_mass=ESS_num*ESS_modulemass;                                        % kg
mass=shell_mass+APU_mass+mot_mass+ESS_mass+gen_mass;                    % kg
if (mot_inertia+wheel_inertia+tx_inertia+APU_inertia==0)
 mipart=0.02*mass;                      % kg, mass equivalent of inertia of rotating parts
end

%%%%% EXECUTE APPROPRIATE MODEL AND SCRIPT %%%%%
disp(['Model used : ',filename])
if (1-strcmp('none   ',choice(9,:)))    % batch analysis chosen
%%% script to compute SOC-corrected MPG
 if strcmp(choice(9,1:3),'mpg')
  eval(choice(7,:));
  numcyc=str2num(choice(9,5));
  if numcyc==0,numcyc=10;,end
  mpg_ba
  disp(['MPG=',num2str(mpg)])
```

```
 else
%%% script to compute maximum effort acceleration
   if strcmp(choice(9,:),'accel_ba')
     dt=0.1;
     tx_shiftdelay=0.2;
% ensure that APU will operate during acceleration
     SOChi=2;
     SOClo=1.9;
% if a series vehicle with single op. pnt., ensure it is highest power point

APU_oppnt_trq=APU_trqscale*APU_maxtrq(find(APU_maxtrq.*APU_map_spd==max(APU_maxtrq.*A
PU_map_spd)));

APU_oppnt_spd=APU_spdscale*APU_map_spd(find(APU_maxtrq.*APU_map_spd==max(APU_maxtrq.
*APU_map_spd)));
% choose max. performance shift points

mot_omegamax=ones(1,gears_num)*mot_spdscale*mot_map_spd(find(mot_maxtrq.*mot_map_spd==max(
mot_maxtrq.*mot_map_spd)));
     APU_omegamax=ones(1,gears_num)*APU_oppnt_spd;
   end
   eval(choice(9,:));
  end
else
%%% no batch analysis chosen
  eval(choice(7,:));                          % load driving cycle
  dur=max(mph(:,1));
  euler(filename,dur,[],[1e-3 dt dt 0 0 2])
end



%%%%% OUTPUTS %%%%%
%%% plot selected variables, and build output strings
nplotted=0;
nplots=sum(outputs_selected);
if nplots
  fplots=figure;
  outputlabels='   time(s) ';
  outputformats='%10.1f';
  for i=1:size(outputs_selected,2);
    if outputs_selected(i)
      nplotted=nplotted+1;
      varname=nospaces(outmat(i,:));
      subplot(nplots,1,nplotted),plot(t,eval(varname)),ylabel(varname)
      outputdata(nplotted+1,1:size(t,1))=[eval(varname)]';
      outputlabels=[outputlabels,filspace(varname,10)];
      if strcmp(varname(1),'P')
        varformat='%10.1f';
      else
        varformat='%10.3f';
      end
      outputformats=[outputformats,' ',varformat];
    end
```

```
 end
 outputlabels=[outputlabels,'\n'];
 outputformats=[outputformats,'\n'];
 subplot(nplots,1,1),title('ADVISOR Simulation Results')
 subplot(nplots,1,nplots),xlabel('time (s)')
 outputdata(1,1:size(t,1))=t';

%%% write output file named outputfilename
 if nplots>0
  outputfilename=get(editfilename,'String');
  fid=fopen(outputfilename,'w');
  fprintf(fid,'ADVISOR_NEON results\n\nYour input files:\n');
  for i=1:size(choice,1),fprintf(fid,choice(i,:));,fprintf(fid,'\n');,end
  fprintf(fid,'\n');
  fprintf(fid,outputlabels);
  fprintf(fid,outputformats,outputdata);
 end
end
fclose('all');
```

Appendix 9

MATLAB FILE: NEON_V.M

----------NEON Vehicle file for simulation

```
%**** the HEV ADVISOR file: NEON_V.M*****************************************
%Defines vehicle and miscellaneous specifications                              *
%for a Neon HEV built by mechanical engineering department of UT.              *
%*******************************************************************************
shell_mass=1360.78;                    % kg
mipart=40.82;                          % kg
rho=1.23;                              % kg/m^3
CD=0.328;
Area=1.9;                              % m^2
gravity=9.807;                         % m/s^2
Crr=0.008;
Crr1=0;                                % s/m
Crr2=0;                                % (s/m)^2
rf=0.5;
rradius=0.274;                         % m
wheel_inertia=0;
disp('Data loaded: NEON_V vehicle specs')
```

Appendix 10

MATLAB FILE: NEON_T.M

----------NEON Vehicle file for simulation

```
%**** the HEV ADVISOR file NEON_T.M*****************************************
%       Loads gearing from NEON transmission                                  *
%       Efficiency map included with SIMPLEV 3.0, from INEL.                  *
%*****************************************************************************
gears_num =5;
gr =[17.70  10.65   6.80   5.15  3.60];
tx_map_spd =[0  8.587   17.174  25.7611 34.3481 43.0398 51.6268 60.2139 68.8009 77.3879 85.9749
        94.5619 103.149 111.736];
tx_map_trq =1000*[-2.4402       -1.3557 -1.2201 -1.0845 -0.949  -0.8134 -0.6778 -0.5423 -0.4067
        -0.2711 -0.1356 0       0.1356  0.2711  0.4067  0.5423  0.6778  0.8134  0.949   1.0845
        1.2201  1.3557  1.4913  1.6268  1.7624  1.898   2.0335  2.1691  2.3047  2.4402];
tx_map_eta =[0.962      0.958   0.956   0.954   0.951   0.946   0.939   0.929   0.913   0.874
        0.766   0.164   0.766   0.874   0.913   0.929   0.939   0.946   0.951   0.954   0.956
        0.958   0.96    0.961   0.961   0.962   0.962   0.962   0.963   0.962
0.963   0.96    0.958   0.956   0.953   0.949   0.942   0.933   0.918   0.885   0.793   0.136
        0.793   0.885   0.918   0.933   0.942   0.949   0.953   0.956   0.958   0.96    0.961
        0.962   0.962   0.963   0.963   0.963   0.963   0.963
0.963   0.961   0.96    0.958   0.955   0.951   0.946   0.937   0.923   0.895   0.82    0.168
        0.82    0.895   0.923   0.937   0.946   0.951   0.955   0.958   0.96    0.961   0.962
        0.963   0.963   0.963   0.963   0.963   0.963   0.963
0.963   0.96    0.959   0.957   0.955   0.951   0.946   0.937   0.924   0.897   0.818   0.17
        0.818   0.897   0.924   0.937   0.946   0.951   0.955   0.957   0.959   0.96    0.961
        0.963   0.963   0.963   0.963   0.963   0.963   0.963
0.963   0.959   0.958   0.956   0.953   0.949   0.943   0.935   0.92    0.892   0.809   0.156
        0.809   0.892   0.92    0.935   0.943   0.949   0.953   0.956   0.958   0.959   0.96
        0.963   0.963   0.963   0.963   0.963   0.963   0.963
0.963   0.959   0.955   0.953   0.95    0.947   0.941   0.932   0.917   0.887   0.803   0.153
        0.803   0.887   0.917   0.932   0.941   0.947   0.95    0.953   0.955   0.959   0.96
        0.963   0.963   0.963   0.963   0.963   0.963   0.963
0.963   0.959   0.955   0.951   0.948   0.944   0.939   0.93    0.916   0.885   0.802   0.147
        0.802   0.885   0.916   0.93    0.939   0.944   0.948   0.951   0.955   0.959   0.96
        0.963   0.963   0.963   0.963   0.963   0.963   0.963
0.963   0.959   0.955   0.951   0.946   0.943   0.937   0.929   0.915   0.887   0.808   0.154
        0.808   0.887   0.915   0.929   0.937   0.943   0.946   0.951   0.955   0.959   0.96
        0.963   0.963   0.963   0.963   0.963   0.963   0.963
0.963   0.959   0.955   0.951   0.946   0.941   0.937   0.929   0.916   0.89    0.816   0.155
        0.816   0.89    0.916   0.929   0.937   0.941   0.946   0.951   0.955   0.959   0.96
        0.963   0.963   0.963   0.963   0.963   0.963   0.963
0.963   0.959   0.955   0.951   0.946   0.941   0.936   0.929   0.917   0.892   0.82    0.16
        0.82    0.892   0.917   0.929   0.936   0.941   0.946   0.951   0.955   0.959   0.96
        0.963   0.963   0.963   0.963   0.963   0.963   0.963
0.963   0.959   0.955   0.951   0.946   0.941   0.935   0.929   0.917   0.892   0.822   0.162
        0.822   0.892   0.917   0.929   0.935   0.941   0.946   0.951   0.955   0.959   0.96
        0.963   0.963   0.963   0.963   0.963   0.963   0.963
0.963   0.959   0.955   0.951   0.946   0.941   0.935   0.929   0.917   0.892   0.821   0.152
        0.821   0.892   0.917   0.929   0.935   0.941   0.946   0.951   0.955   0.959   0.96
        0.963   0.963   0.963   0.963   0.963   0.963   0.963
```

```
0.963   0.959   0.955   0.951   0.946   0.941   0.935   0.929   0.917   0.892   0.821   0.152
        0.821   0.892   0.917   0.929   0.935   0.941   0.946   0.951   0.955   0.959   0.96
        0.963   0.963   0.963   0.963   0.963   0.963   0.963
0.963   0.959   0.955   0.951   0.946   0.941   0.935   0.929   0.917   0.893   0.82    0.151
        0.82    0.893   0.917   0.929   0.935   0.941   0.946   0.951   0.955   0.959   0.96
        0.963   0.963   0.963   0.963   0.963   0.963   0.963];
disp('Data loaded: NEON_T transmission map')
eta_tconverter=1;
tx_inertia=0;                           % unknown
```

Appendix 11

MATLAB FILE: NEONSET.M

----------NEON Vehicle file for simulation

```
% **** the HEV ADVISOR help on NEONSET.M*************************************
%       This file loads all component data necessary to simulate a parallel power-assist      *
%       hybrid NEON     using the PARANEON.M block diagram.                                    *
%*****************************************************************************

% TRANSMISSION
neon_t
eta_tconverter=0.85;                    % torque converter efficiency
tx_shiftdelay=1;  % s

% APU
geo11_a                                 % fuel and emissions maps
APU_trqscale=1;                         % modify the maximum torque and the torque points in the
                                                maps
APU_spdscale=1;                         % modify the maximum speed and the speed points in the
                                                maps
fuel_mden=737;                          % g/L, mass density of fuel

% EMISSIONS CALCS
cat1                                    % temperature dependence of catalyst
Tcatmax=650;                            % deg. C, maximum catalyst temperature
Tcatinit=20;                            % deg. C, initial catalyst temperature
TECss=95;                               % deg. C, maximum engine coolant temperature
TECinit=20;                             % deg. C, initial engine coolant temperature
Tamb=20;                                % deg. C, ambient temperature

% ROAD LOAD & MISCELLANY
shell_mass=1360.78;                     % kg
mipart=40.82;                           % kg
rho=1.23;                               % kg/m^3
CD=0.328;
Area=1.9;                               % m^2
gravity=9.807;                          % m/s^2
Crr=0.008;
Crr1=0;                                 % s/m
Crr2=0;                                 % (s/m)^2
rf=0.5;
rradius=0.274;                          % m
wheel_inertia=0;
accsry_kW=0.5;                          % kW
grade=0;
MPHinit=0;
tire_mu_static=1;
front_weight_frac=0.6;

% MOTOR
sr180p_m                                % efficiency map, torque envelope
```

```
mot_trqscale=1;                 % modify the maximum torque and the torque points in the
                                    map
mot_spdscale=1;                 % modify the maximum speed and the speed points in the
                                    map
motor_to_ICE_gr=1.3;            % ratio of motor speed to APU speed

% ENERGY STORAGE
neonbt_e                        % Battery file for NEON

% CONTROL STRATEGY
APUbool=1;
idlebool=0;
HEVbool=1;
SOCinit=.8;
SOChi=.8;
SOClo=.2;
regeneration=1;                 % Boolean parameter for regeneration scheme control.
                                    1- for SOC sustaining scheme;
                                    0- for SOC depletion scheme.
regen_level=1;                  % parameter for regenerative braking control. Regen_level
                                    value from 0 to 1 continuously.

dt=1;
```

VITA

He, xiaoling was born in The People's Republic of China in Nov.2 ,1963. She attended the Daliain Railway Institute in August, 1981 where she received Bachelor of Science in Mechanical Engineering in August,1985. She started working as an assistant engineer and engineer in mechanical design in Fengtai Bridge Plant of Ministry of Railway, P.R. China from 1985 to 1990. From February, 1990 to 1995, she was a design engineer in mechanical engineering with The Professional Design Institute of Ministry of Railway, P.R. China. She entered the Master Degree program in Mechanical Engineering at The University of Tennessee, Knoxville in August,1995 under the guidance of Dr. Jeffrey W. Hodgson. She officially received her Master Degree in August, 1997.